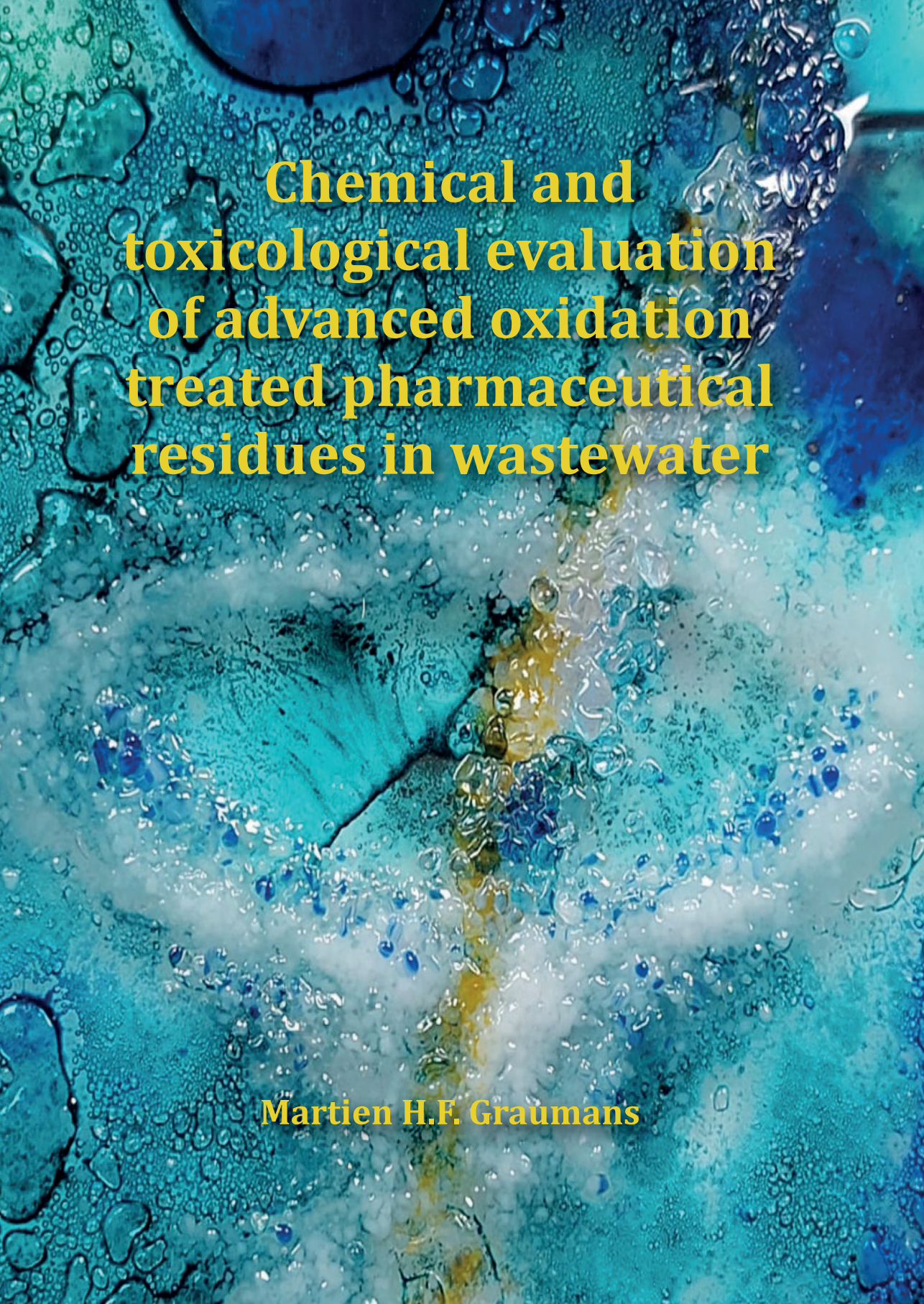

Chemical and toxicological evaluation of advanced oxidation treated pharmaceutical residues in wastewater

Martien H.F. Graumans

Chemical and toxicological evaluation of advanced oxidation treated pharmaceutical residues in wastewater

Martien H.F. Graumans

Author: Martien H.F. Graumans

The work presented in this thesis was done within the Department for Health Evidence, Radboud Institute for health Sciences, Radboud University Medical Centre, Nijmegen, the Netherlands

ISBN: 978-94-6510-219-1

Cover design: Josien J. Jong

Inside design: Ilse Radstaat

Print: Proefschriftmaken | www.proefschriftmaken.nl

Chemical and toxicological evaluation of advanced oxidation treated pharmaceutical residues in wastewater

Proefschrift ter verkrijging van de graad van doctor
aan de Radboud Universiteit Nijmegen
op gezag van rector magnificus prof. dr. J.M. Sanders,
volgens besluit van het college voor promoties
in het openbaar te verdedigen op
dinsdag 19 november 2024
om 16:30 uur precies

door

Martinus Hendrik Franciscus Graumans
geboren op 31 januari 1991
te Tilburg

Promotor:

Prof. dr. F.G.M. Russel

Copromotoren:

Dr. ir. P.T.J. Scheepers

Dr. ir. W.F.L.M. Hoeben (Technische Universiteit Eindhoven)

Manuscriptcommissie:

Prof. dr. B.J.F. van den Bemt (voorzitter)

Prof. dr. A.P. van Wezel (Universiteit van Amsterdam)

Dr. C.T.A. Moermond *(*Rijksinstituut voor Volksgezondheid en Milieu)

“It’s the water pump on Broad Street,” said John Snow (1854, London, United Kingdom). “Ridiculous,” said everyone else. “Water can’t make you sick.”

(Rothman, 2012, Lifeguard Science for Health, 2024)

Table of contents

Terminology and abbreviations

General terminology

(ABS)	Acid buffer solution
(A&E)	Accident and Emergency
(AMR)	Antimicrobial resistance
(AOP)	Active pharmaceutical ingredient
(API)	Advanced oxidation processes
(BOD)	Biochemical oxygen demand
(CEC)	Contaminants of emerging concern
(CCL)	Contaminant Candidate List, United States
(COVID19)	Corona virus disease 2019
(CWA)	Clean Water Act, United States
(DNA)	Deoxyribonucleic acid
(DoA)	Drugs of abuse
(DOM)	Dissolved organic matter
(EC)	European Commission
(ECOSAR)	Ecological Structure Activity Relationships Program
(EMA)	European Medicines Agency, European Union
(EPA)	Environmental protection agency, United States
(ESI)	Electron spray ionisation
(EU)	European Union
(FMO)	Frontier molecular orbitals
(HOMO)	Highest Occupied Molecular Orbital
(HPLC)	High performance liquid chromatography
(HSW)	Hospital sewage water
(ICU)	Intensive care unit
(IPCHEM)	Information Platform for Chemical Monitoring
(JRC)	Joint Research Centre, European Commission
(LC)	Liquid chromatography
(LUMO)	Lowest Occupied Molecular Orbital
(MEC)	Measured environmental concentration
(MO)	Molecular orbitals
(MQ)	Milli-Q water
(MRM)	Multiple reaction monitoring
(MS)	Mass spectrometry
(NHS)	National Health Services, United Kingdom
(NOM)	Natural organic matter
(NSAID)	Non-steroidal anti-inflammatory
(OECD)	Organisation for Economic Co-operation and development
(PAH)	Polycyclic aromatic hydrocarbons
(PAW)	Plasma activated water
(PCD)	Pulsed corona discharges
(PPPs)	Plant protection products
(RIVM)	Rijksinstituut voor Volksgezondheid en Milieu *National Institute for Public Health and the environment*
(RNS)	Reactive nitrogen species
(RONS)	Reactive oxygen and nitrogen species
(ROS)	Reactive oxygen species
(SDWA)	Safe drinking water act, United States
(SSbD)	Safe and sustainable-by-design
(SSW)	Synthetic sewage water
(STP)	Sewage water treatment plant
(UK)	United Kingdom
(US)	United States
(UV)	Ultraviolet
(WHO)	World Health Organization
(WWTP)	Wastewater treatment plant

Pharmaceuticals

(1-CH_3-BIG)	1-Methylbiguanide
(1-OH-IBP)	1-Hydroxyibuprofen
(3-OH-IBP)	3-Hydroxyibuprofen
(3-OH-APAP)	3-Hydroxyacetaminophen
(4-keto-CP)	4-keto-cyclophosphamide
(4-OH-CP)	4-Hydroxycyclophosphamide
(4-OH-DF)	4-Hydroxydiclofenac
(8-OH-CIP)	8-Hydroxyciprofloxacin
(APAP)	Acetaminophen
(CB)	Carbamazepine
(CIP)	Ciprofloxacin
(CIP-Hemi)	Ciprofloxacin-Hemi
(CP)	Cyclophosphamide
(DF)	Diclofenac
(DIA)	Diatrizoic acid
(DOXY)	Doxycycline
(EPX-CB)	Carbamazepine-10,11-epoxide
(FLU)	Fluoxetine
(IBP)	Ibuprofen
(IOM)	Iomeprol
(IOP)	Iopamidol
(KP)	Ketoprofen
(MET)	Metoprolol
(MF)	Metformin
(N-D-DOXY)	n-Desmethyl-doxycycline
(NPX)	Naproxen
(PHE)	Phenazone/antipyrine
(p-OH-PHE)	p-Hydroxyantipyrine
((s)-Nor-FLU)	(s)-Norfluoxetine
(TER)	Terbutaline

Drugs of abuse

(MDMA)	3,4-Methylenedioxy methamphetamine
(THC)	Tetrahydrocannabinol

Chapter 1

Introduction

1.1 Anthropogenic pollution of the hydrosphere

Human activities affect our environment by the usage of chemical compounds for industry, agriculture, healthcare and leisure purposes. Frequently and routinely used compounds are personal care products for life enhancement, pesticides for crops and agricultural protection and pharmaceuticals for prevention or treatment of disease. Next to the manufacturing of these goods, our industrial, agricultural and urbanised activities result in the release of multiple chemicals in the environment, varying from heavy metals, (micro)plastics, polycyclic aromatic hydrocarbons (PAHs), pesticides, detergents, surfactants and pharmaceuticals (Emerging Contaminants in the Environment, 2022; Peake et al., 2016; Geissen et al., 2015; Kümmerer, 2004, 2009; Patel et al., 2019; Stenström et al., 2021; Verlicchi et al., 2012). Also, illegal contaminants, such as non-regulated substances or drugs of abuse (DoA) contribute to the emission (Bijlsma et al., 2012). Despite the attempts to control our waste flows, accidents, improper disposal, illegal dumping, user frequency and runoff from land by manure or landfill will cause introduction of contaminants into the water cycle, see **Fig 1.1** (Geissen et al., 2015; Peake et al., 2016; Žegura et al., 2009). Depending on the geographical location, seasonal and weather influences on the composition and concentration of pollutants emitted into the aquatic environment can vary greatly (Patel et al., 2019; Peake et al., 2016; Verlicchi et al., 2012). Leachate from landfill, illegal dumpsites or accidental spill can contaminate underlying groundwater resources directly (Gray et al., 2017; Melnyk et al., 2014; Patel et al., 2019). Additionally, also plant protection products (PPPs) and veterinary medicines might runoff from agricultural soil or manure into surface waters after heavy rainfall and percolation (Emerging Contaminants in the Environment, 2022; Kümmerer, 2004). In urbanised and industrial regions, wastewater streams are usually passed through a wastewater treatment plant (WWTP). At a WWTP multiple steps are applied for the removal of contaminants so that the water can be released back into the environment. However, during the WWTP process, chemical substances are persistent and are minimally removed, where other compounds are adsorbed onto solid particles of the sewage sludge. When the WWTP sludge is recycled as fertiliser, the adsorbed contaminants can indirectly contaminate nearby surface and ground water (Gray et al., 2017; Patel et al., 2019).

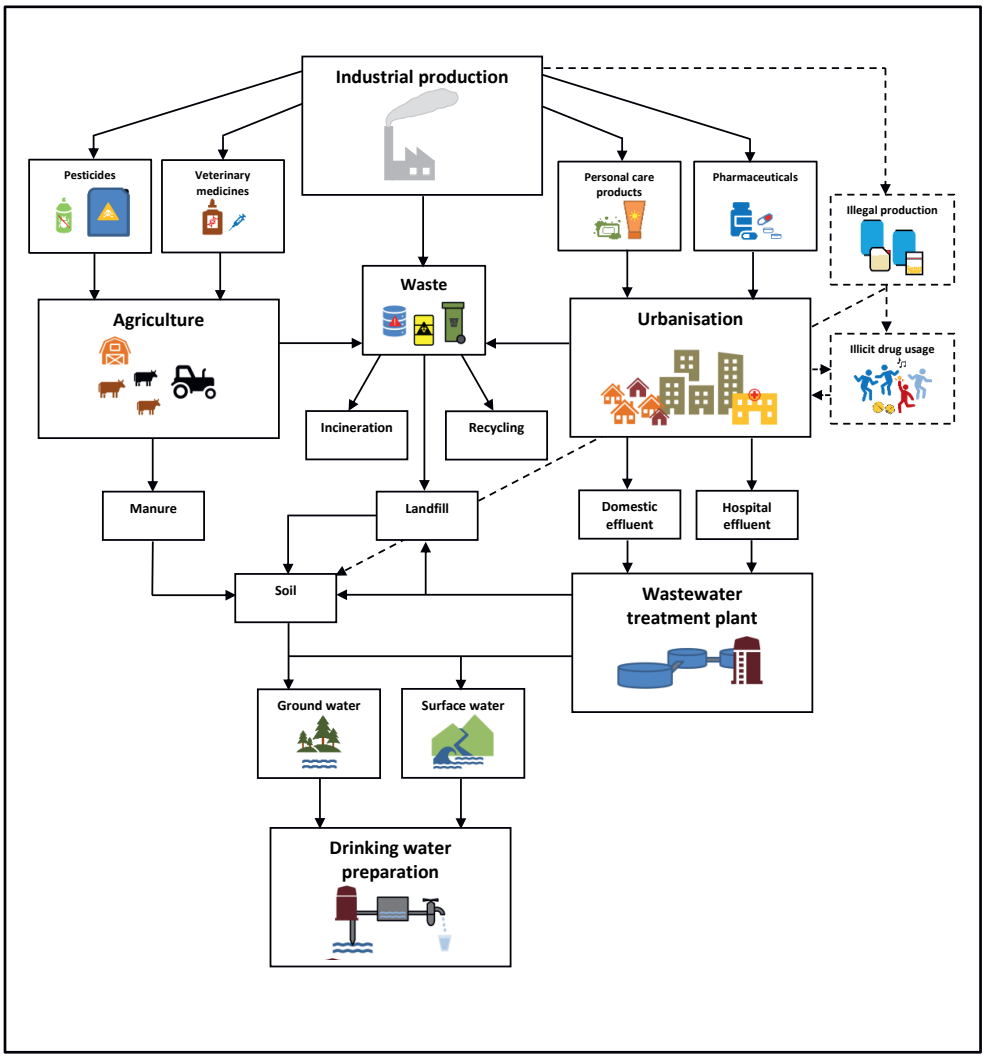

Fig. 1.1 Sources, emissions and transport routes of pharmaceuticals and other anthropogenic pollutants, entering into the aquatic environment. Dotted lines (- -) indicate clandestine pollutant routes. Adapted schematic representation of possible pollutant routes (Kümmerer, 2004; Peake et al., 2016)

1.2 Pharmaceutical residues in the aquatic environment

For many years there is an emerging attention for emission of anthropogenic pollution in the hydrosphere (Kümmerer, 2009; Patel et al., 2019; Verlicchi et al., 2012), but in the last decade the potential risk for aquatic organisms and our drinking water quality has been well recognised by national and international studies (Communication from the Commission to the European Parliament, the Council and the European Economic and Social Committee, 2019; House of Commons Environmental Audit Committee, 2022; Moermond et al., 2020; World Health Organization, 2012). A substantial amount of water pollution is caused by pharmaceuticals, which are specifically designed molecules that initiate a biological interaction in living organisms for therapeutic purposes (Pandit, 2012). Depending on the indication, many different substances are available as over-the-counter medication in drugstores and supermarkets. Pharmaceuticals used for conditions that are best diagnosed and managed by health professionals are prescribed by a physician (Emerging Contaminants in the Environment, 2022; Peake et al., 2016).

The biologically active compound in a therapeutic is the active pharmaceutical ingredient (API). Depending on the administered dose and the physicochemical properties this compound will interact with endogenous proteins to stimulate or inhibit specific biological functions (Pandit, 2012). Within the body pharmaceuticals are completely or partially bio-transformed into metabolites and excreted via urine and faeces. The excrement is discarded via domestic and hospital effluents ending up at the WWTP. During conventional wastewater treatment, gross particles are first removed by filtration and sedimentation, followed by treatment steps where organic matter and other suspended solids are eliminated (Emerging Contaminants in the Environment, 2022; Peake et al., 2016). Activated sludge will eliminate organic compounds by microbial oxidation (Emerging Contaminants in the Environment, 2022; Peake et al., 2016; Nolte et al., 2020; van Bergen et al., 2021). However, conventional WWTPs are not designed for the removal of complex xenobiotic, stable and persistent molecules such as pharmaceuticals or their metabolites. During incomplete removal hydrophilic or non-biodegradable compounds are not, or only partially degraded, where other excreted metabolites might be transformed back into their original APIs (Ajo et al., 2018; Vasiliadou et al., 2013). The continuous supply of certain substances can also overload the WWTP or substances might inhibit the WWTP biofilm, resulting in less efficient elimination levels. Partial or insufficient wastewater treatment thus results in accumulation in surface waters (Álvarez-Torrellas et al., 2017; Patel et al., 2019). The concentrations of pharmaceuticals in environmental compartments, such as surface and groundwater range from ng/L up to µg/L levels. Next to the ecotoxicological risks on aquatic

species, the introduction of untreated antibiotics in the environment has the potential to cause antimicrobial resistance (AMR) (Comber et al., 2018; Emerging Contaminants in the Environment, 2022). Excessive usage of antibiotics in healthcare, livestock or poultry agriculture can result in multi-resistant infectious pathogens that are hard to treat with general available classes of antibiotics (Álvarez-Torrellas et al., 2017). To mitigate the discharge of pharmaceutical residues in wastewater, awareness and behavioural change are needed to improve the hydrosphere. However, next to that, due to the introduction of new therapeutics, population demographics and climate change, it is also insuperable that complementary sustainable wastewater treatment techniques need to be implemented. Research into oxidative treatment technologies will contribute to this and lead to a better understanding of how complex molecules can be effectively removed.

1.2.1 Pharmaceuticals of concern

Due to the occurrence of wide range of chemical substances in the aquatic environment, it is difficult to prioritise the pharmaceuticals of highest concern (Donnachie et al., 2016; Water voor drinkwaterbereiding (RIVM), 2023) According to the 2012 report of the World Health Organization (WHO), several national studies reported the presence of pharmaceuticals in ground, surface and drinking water (World Health Organization, 2012). Many different classes of therapeutics are used, the presence of which in the environment varies greatly depending on the source of effluent and WWTP efficiency. A specific effluent that contributes to the release of pharmaceuticals in the wastewater stream is hospital sewage water (HSW). Hospital effluent contains a concentrated mixture of pharmaceuticals and metabolites derived from a wide variety of drug classes, e.g. analgesics, antibiotics, anticancer compounds, antidepressants, antidiabetics, beta-blockers and contrast agents. Other compounds that are also present in the complex HSW matrix are pathogens, disinfectants, detergents, heavy metals, radioactive markers (radionuclides for diagnosis or therapy), adsorbable organic halides (AOX) and ammonium (Ajo et al., 2018; Álvarez-Torrellas et al., 2017; Emmanuel et al., 2005; Escher et al., 2011; Laquaz et al., 2018; Orias & Perrodin, 2013; Ajala et al., 2022; Barquero et al., 2008). The complex composition of HSW varies over time and is primarily derived from either unaffected products or excreted metabolites. E.g. heavy metals are released via excretion of anticancer drugs containing metals such as platinum (*cis*-platinum or carboplatinum), or contrast agents containing gadolinium. Additionally, metals could also be released from antiseptics, disinfectants or antifungal agents containing organomercury (thiomersal or nitromersol) (Ajala et al., 2022; Kümmerer, 2004). In The Netherlands, water quality standards

are available for biocides, pesticides and a few pharmaceuticals that have the potential of negatively affecting the water quality. The available surface water quality standards are primarily provided for compounds that are frequently detected in the aquatic environment and have been thoroughly assessed (Moermond et al., 2019). The quality standards are specified as maximum allowable concentrations for long-term and short-term ecotoxicity. Examples of pharmaceuticals which are included in the Netherlands national water quality standard policy are carbamazepine, metoprolol and metformin, with respective maximum concentrations for long-term presence of 0.5, 62 and 780 µg/L in fresh surface water (Wet Milieubeheer, 1979; Waterwet, 2009; National Institute for Public Health and the Environment (Rijksinstituut voor Volksgezondheid en Milieu), 2023). Next to the available surface water standards, a standard signalling concentration of 1.0 µg/L for drinking water sources is suggested to maintain the quality (Medicijnen in drinkwater, 2017). At European level there are specific directives and guidelines implemented to protect the aquatic environment and drinking water resources. The Water Framework Directive (WFD) (2000/60/EC) and the Directive on Environmental Quality Standards (EQSD) (2008/105/EC) were amended by the Directive 2013/39/EU, which contains a priority substance list and a specific obligation paragraph to minimise water pollution from pharmaceutical residues. Monitoring data is continuously obtained in all member states and a surface water Watch List is prepared in addition to the priority substance list for monitoring of emerging industrial chemicals, plant protection products and pharmaceutical compounds. With sufficient monitoring data, the environmental risk could be determined. The Watch List is a living document updated every 2 years. Substances are no longer listed than 4 years and are periodically evaluated by the Joint Research Centre (JRC) of the European Commission. Within these technical reports registered compounds are appraised and new emerging substances are shortlisted by specified criteria (Carvalho et al., 2015; Gomez Cortes et al., 2020, 2022; Loos et al., 2018). **Table 1.1.**, provides an overview of the pharmaceuticals placed on the list. Next to pharmaceuticals also pesticides and sunscreens are placed on the Watch List and only the most recent update of this list is in force ((EU) 2015/495, 2015; (EU) 2018/840, 2018; (EU) 2020/1161, 2020; (EU) 2022/1307, 2022).

Table 1.1.
Pharmaceuticals placed on the Watch List of the EU

1st Watchlist (2015)	**2nd Watchlist** (2018)	**3rd Watchlist** (2020)	**4th Watchlist compounds** (2022)
17-alpha-Ethinylestradiol (EE2) *Synthetic estradiol hormone*	17-alpha-Ethinylestradiol (EE2) *Synthetic estradiol hormone*	Amoxicillin *Antibiotic*	Sulfamethoxazole *Antibiotic*
Diclofenac *NSAID*	Azithromycin *Macrolide antibiotic*	Ciprofloxacin *Antibiotic*	Trimethoprim *Antibiotic*
Azithromycin *Macrolide antibiotic*	Clarithromycin *Macrolide antibiotic*	Sulfamethoxazole (Co-trimoxazole) *Antibiotic*	Venlafaxine *Antidepressant*
Clarithromycin *Macrolide antibiotic*	Erythromycin *Macrolide antibiotic*	Trimethoprim (Co-trimoxazole) *Antibiotic*	(O-desmethylvenlafaxine) *Metabolite*
Erythromycin *Macrolide antibiotic*	Amoxicillin *Antibiotic*	Venlafaxine *Antidepressant*	10 Azole compounds *3 Antifungal medicines*[A] *7 Antifungal pesticide*[B]
	Ciprofloxacin *Antibiotic*	(O-desmethylvenlafaxine) *Metabolite*	Clindamycin *Antibiotic*
		10 Azole compounds *3 Antifungal medicines*[A] *7 Antifungal pesticide*[B]	Metformin *Antidiabetic* (Guanylureum) *Degradation product*
			Ofloxacin *Antibiotic*

[A]Pharmaceutical azole compounds: clotrimazole, fluconazole, miconazole.
[B]Pesticide azole compounds: Imazalil, ipconazole, metconazole, penconazole, prochloraz, tebuconazole, tetraconazole.

A similar system is applied in the United States of America (USA) where the Environmental Protection Agency (EPA) adopted the Clean Water Act (CWA) and manages the Safe Drinking Water Act, which is complemented by a Contaminant Candidate List (CCL). To recognise and address potential problems, monitoring programs are used to gather information for policymakers, risk assessors and water managers (Derksen, 2014). In The Netherlands the Watson database of the Ministry of Infrastructure and Water Management contains publicly available influent and effluent monitoring data for many different pharmaceuticals (Derksen, 2014). In addition to the overall effectiveness of WWTPs, also the occurrence of pharmaceutical residues is monitored. More comprehensive data on pharmaceuticals in sediment, soil, surface, ground and sewage water can be found via the European Information Platform for Chemical Monitoring (IPCHEM). With this online platform multiple databases are accessible by using selection criteria, such as chemical substance, country or matrix. The risk assessment of measured pharmaceuticals in the environment is supported by monitoring data and actual toxicity data. According to the determined substances in a selected catchment area, individual risk coefficients per compound reflects the potentially ecotoxicological risk (Kar et

al., 2020; Khan et al., 2019; Reuschenbach et al., 2008; Sanderson et al., 2004). Ecotoxicological input parameters are often derived from specific applied toxicity tests. Bioassays in the form of a bioluminescence parameter on *Vibrio fischeri* is an example of a standardised methodology to detect acute aquatic ecotoxicity (Abbas et al., 2019; Vasiliadou et al., 2018). The *Vibrio fischeri* is a luminescent microorganism; when a toxic substance negatively affects the ambient life condition of this species, the luminescence production will decrease. Lowered luminescence is thus a measure for toxicity. Other aquatic species that could be used in toxicity testing according to the Organization for Economic Cooperation and Development (OECD) standards are fish, water flees and green algae (*Test No. 201: Alga, Growth Inhibition Test*, 2006; *Test No. 202: Daphnia Sp. Acute Immobilisation Test*, 2004; *Test No. 203: Fish, Acute Toxicity Test*, 2019). Despite that bioassays are commonly applied, single aquatic species cannot represent a complex ecosystem (Abbas et al., 2019; Vasiliadou et al., 2018). Certain aquatic species are more vulnerable to specific compounds than others. Therefore, multiple toxicity assays are needed to provide a more comprehensive assessment. Due to the wide variety of substances, continuous discharge, changing composition and concentration, it is difficult to prioritise the most concerning pharmaceuticals. However, with accurate monitoring data and toxicity testing water quality is evaluated and could be managed if needed.

1.2.2 Wastewater as information source

Wastewater monitoring has demonstrated to be a great information source for indicating the presence of specific compounds. During the SARS-CoV-2 (COVID19) pandemic, RNA particles served as a great epidemiological indicator for the number of infections (Picó & Barceló, 2021; Proverbio et al., 2022; Rodríguez Rasero et al., 2022; UK Health Security Agency, 2021; Y. Wang et al., 2022). In addition to the SARS-CoV-2 National Sewage Surveillance programme in the Netherlands, WWTPs in the region of Amsterdam were sampled for the screening on Monkeypox virus DNA (de Jonge et al., 2022). In this established sewage surveillance programme, it is clearly demonstrated that virus particles end up in wastewater via animal or human discharges. Also, other interesting epidemiological information could be retrieved from sewage water, for example on tabaco and alcohol consumption. In this Chinese study it was indicated for tobacco that survey data and sale statistics matched well with wastewater concentrations, where the results for alcohol consumption were lower than WHO survey results (Gao et al., 2020; Kuloglu Genc et al., 2021). Other retrospective information from wastewater monitoring showed for example in Greater London (UK) during the SARS-

Cov-2 pandemic that urban activity and health do have consequences on urban river ecosystems (Egli et al., 2023). During the period of 2019-2021, 390 water samples were analysed on contaminants of emerging concern (CECs) demonstrating that measured environmental concentrations (MECs) in river Thames decreased during the lockdown period (2020) and increased again after lockdown ending (2021). Limited wastewater dilution was found in river branches, as these were impacted by WWTP effluent, because pharmaceutical MECs correlated with National Health Services (NHS) prescription statistics (Egli et al., 2023). Similar methods have been applied to demonstrate illegal drug usage in large European cities, using monitoring data to reveal the consumption and peak intakes. Next to the epidemiological aspect regarding the usage frequency, consumption rate and geographical location, also forensic intelligence could be obtained (Bannwarth et al., 2019; Emke et al., 2018; Greif et al., 2022; Rapp-Wright et al., 2017; Schoenmakers, 2016). Wastewater analysis can provide indicative information to see whether new compounds (legal highs) are used or possibly will demonstrate activity of clandestine drug laboratories (Bannwarth et al., 2019; EMCDDA, 2017; Huizer et al., 2021). Other forensic monitoring information that could support security services and policing is the detection of explosive residues (Rapp-Wright et al., 2017). Screening of explosive traces and their precursors or degradation intermediates can provide intelligence concerning a nearby location whether there is clandestine activity (Rapp-Wright et al., 2017). As well as for drugs of abuse (DoA) the precursors, production intermediates and chemical waste products detected in sewage and surface water could suggest the illegal production. Despite that DoA are illegal, their bioactivity is equal to that of pharmaceuticals. Therefore, these compounds should not be neglected as unwanted residues in the hydrosphere. Their presence in the aquatic environment is however not unnoticed, and specific substances were even considered for the 4th Watch List, but methamphetamine, 3,4-methylenedioxymethamphetamine (MDMA), ephedrine, cannabinol and tetrahydrocannabinol (THC) are not yet placed on the suggested priority list ((EU) 2022/1307, 2022; Gomez Cortes et al., 2022)). According to the National Police of the Netherlands it is estimated that 350,000 up to 700,000 Liter chemical waste is derived for the illegal production of amphetamine (Schoenmakers, 2016). A part of this waste will end up directly in surface water or will pass through the WWTP. For amphetamine, for example, it is well demonstrated that it can lower the WWTP biofilm density, affecting thus the WWTP efficacy (Bijlsma et al., 2012; Emke et al., 2018; Lee et al., 2016). According to wastewater monitoring data it can be concluded that many different substances are present, which all need to be removed by conventional wastewater techniques. According to the National Institute for Public Health and the environment (RIVM) in the Netherlands, approximately 190,000 kg

prescription medicines enter yearly the environment (Moermond, 2020). For this estimate, DoA, and over the counter pharmaceuticals are not included, the actual number of unwanted compounds contributing to aquatic pollution and potential (eco)toxicological effects should therefore be considered as much higher.

1.2.3 Chemical design of pharmaceutical compounds

To better understand the reactivity, stability and potential toxicity of a pharmaceutical, the molecular structure is of great importance. Pharmaceutical products are especially designed to initiate a specific biological response in the body. Their three-dimensional structure is often complementary to a specific molecular target. A pharmaceutical will bind to a receptor so it can provoke a response by increasing or decreasing a biological function. Healthy organs and cells will produce well-functioning proteins, however, a deficient or incorrectly working physiology can lead to ailment or disease (Pandit, 2012; Peake et al., 2016). For the prevention and treatment of disease or pain, many different therapeutic classes are available. Depending on the required therapy, the specific active pharmaceutical ingredient (API) will bind to a receptor, ion channel, enzyme or transporter protein. When a pharmaceutical is administered the endogenous ligand is replaced by a structurally similar API to increase or decrease a certain biological function. Both protein-ligand and protein-API complexes are formed by reversible chemical interactions, such as hydrophobic interactions (Log $P_{octanol/water}$), ionic bonds (Pk_a) or hydrogen bridges. Functional groups of an API will align with complementary groups of the protein, see **Fig 1.2.**

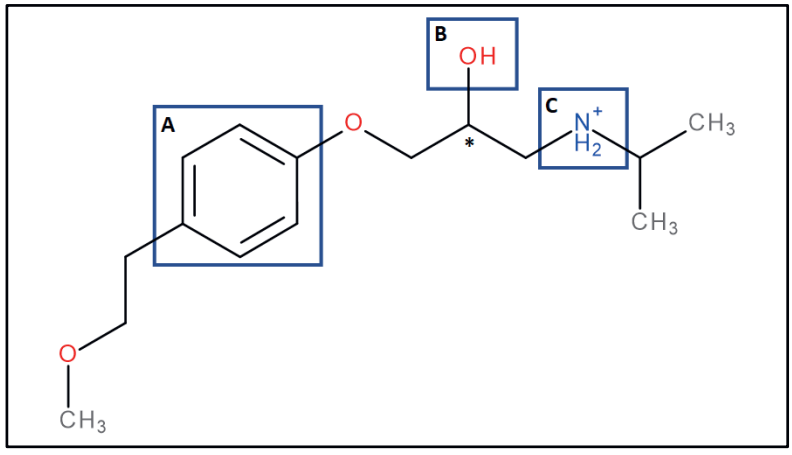

Fig. 1.2. Schematic representation of a protonated metoprolol molecule (NH_2^+; pK_a basic 9.27). The available functional groups can align with complementary structures of a protein having hydrophobic interactions (Log *P*: 1.76) (**A**), hydrogen bonding (**B**) or ionic bonding (**C**). The chiral point is denoted with an asterisk (*****), indicating the enantiomers *R*-(+)-MET and *S*-(-)-MET.

Specific reactive moieties of an API represent the pharmacophore and determine also the physicochemical properties of a molecule. The reactivity and stability of a molecule is determined by electronic structures. Each atom has its own electron configuration, occupying multiple shells filled with 2 electrons. Molecular orbitals (MO) are characterised by the bonding interactions of multiple atoms, where electrons are delocalised throughout the molecule. The electronic density of a molecule is thus involved in chemical bonding and chemical reactions (Wade, 2010). Chemical reactive groups are distinguished by ionic or covalent bonding. Formation of an ionic bond is caused by electron transfer where a positive electron (Na^+) is attracted by the opposite negative charge (Cl^-) to form a compound (NaCl). In organic molecules electrons are usually shared by covalent bond formation. In addition, with the formation of a molecule the nonbonding electrons, lone pair electrons as in oxygen, nitrogen or halogens can determine the reactivity of a substance (Wade, 2010).

1.3 Conventional wastewater treatment

Conventional WWTPs are very efficient systems for the removal of physical and suspended solids, including the removal of organic matter by lowering the biochemical oxygen demand (BOD). The BOD is an indirect measure of the amount of organic carbon, since the quantity of oxygen consumed by aerobic microorganisms indicates the degradation of organic material in wastewater (Peake et al., 2016). Too high levels of BOD after sewage water treatment will have an adverse effect on receiving water environments. The European urban wastewater treatment directive (91/271/EEC) aims to protect the environment from adverse effects of wastewater discharges derived from industry, households and rainwater overflow (Concerning Urban Waste Water Treatment 91/271/EEC, 1991; Peake et al., 2016). Therefore, sewage water is subjected to multiple stages of treatment (**Fig. 1.3.**). During preliminary treatment, solid waste and gross particles are physically removed by a mesh screen. Subsequently, BOD levels are lowered during primary treatment using sedimentation for the settlement of suspended solids. Particulates which are not removed by gravity can be physically eliminated by flotation, filtration, adsorption or by using a combination of coagulation and flocculation steps.

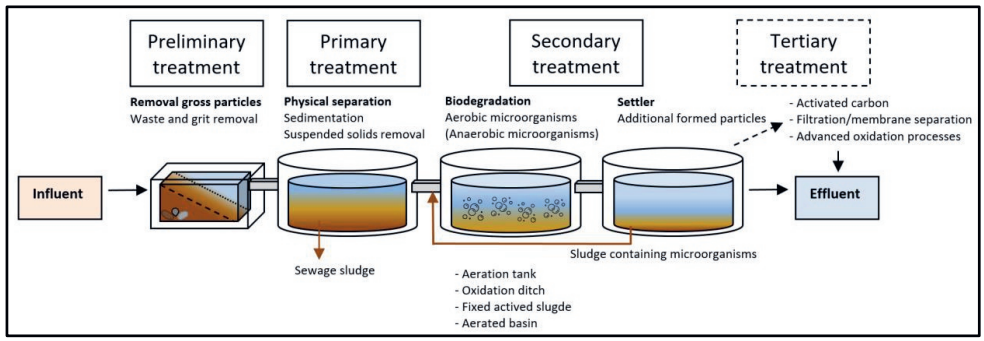

Fig. 1.3. Multiple conventional wastewater treatment stages. The schematic representation is according to the steps presented in (Peake et al., 2016).

During coagulation and flocculation small particles of (poly)ferric or (poly)aluminium chloride ($FeCl_3$ or $AlCl_3$) are added to the sewage water to form flocs and lower the surface charge of colloidal particles (Emerging Contaminants in the Environment, 2022; Rana & Suresh, 2017; STOWA, 2008). During the floc formation, adsorption of organic matter and other impurities occurs. Coagulation/flocculation is a simple and effective application, but factors such as pH, amount of coagulant, mixing speed, temperature and time of retention influence its efficacy. Despite that optimised coagulation/flocculation removes organic micropollutants successfully, a limitation is that high amounts of sludge are formed, which is harmful to human health, and the pH of the treated water needs to be adjusted. Also, the operational costs are relatively high. Secondary treatment is applied for the further reduction of the total organic content (TOC). Aerobic or anaerobic microorganisms present in the activated sludge will use TOC as substrate. TOC includes carbon containing constituents such as sugars (carbohydrates), fats, proteins, soaps, detergents, pharmaceuticals and metabolites (Nolte et al., 2020; Peake et al., 2016). Effective biodegradation will result in further reduced BOD levels.

To achieve effective biodegradation, multiple treatment techniques are possible. A commonly applied technique is the usage of suspended growth-activated sludge deployed in an aeration tank or oxidation ditch. During this biodegradation processes new suspended solids are formed, which are subsequently also removed by settlement. A part of that newly produced sludge is re-used for the biodegradation step, as it still contains the microorganisms. Other applicable treatment techniques are fixed-layer treatment, where the activated sludge is mounted on porous media, or where biodegradation is stimulated by natural influences in aerated basins. Conventional WWTPs are essentially designed for the removal of high concentrations (mg/L) of biodegradable substances containing carbon (C), nitrogen (N) and phosphorous (P) (Alfonso-Muniozguren et al., 2021; Peake et al., 2016; Verlicchi et al., 2012). It is well known that

WWTPs are not designed to remove organic stable or persistent molecules such as pharmaceutical residues. Certain pharmaceuticals are biodegraded, where others remain unaffected (Nolte et al., 2020; Nolte & Ragas, 2017; van Bergen et al., 2021; Vasiliadou et al., 2018; Verlicchi et al., 2012). During pharmaceutical removal in activated sludge, autotrophic and heterotrophic biodegradation occurs. For autotrophic biodegradation bacteria use inorganic carbon as a substrate and in heterotrophic degradation bacteria take organic carbon as their food source (Alfonso-Muniozguren et al., 2021). Because pharmaceuticals enter the WWTP via multiple routes, their composition and concentration vary continuously. For example, too low concentrations of certain residues can pass through the WWTP unaffected (Verlicchi et al., 2012). Dependent on the WWTP influent, microbial communities in the activated sludge tend to have the ability to acclimate, adapting their performance to certain pharmaceuticals (Nolte & Ragas, 2017; Vasiliadou et al., 2018). However, specific toxophores derived from contaminants can negatively affect the microbial activity in sludge. Inhibition of the microbial metabolism or growing activities can result in poor effluent quality (Vasiliadou et al., 2018). Next to the biodegradability and physicochemical properties of individual compounds, the WWTP operational procedures define the removal efficiency (Alfonso-Muniozguren et al., 2021). Relevant operational procedures are temperature, pH and the time interval for biodegradation (hydraulic retention time) (Alfonso-Muniozguren et al., 2021). Regarding the temperature, seasonal effects are responsible for changes in removal efficiency, since lower temperatures will decrease the biological activity of activated sludge (Alfonso-Muniozguren et al., 2021; van Bergen et al., 2021).

1.3.1 Chemical processes during conventional wastewater treatment

In addition to the design of a conventional WWTP, pharmaceutical characteristics have an influence on the degradation efficiency. During conventional treatment processes contaminants undergo multiple physicochemical processes such as photolysis, dissociation, hydrolysis, oxidation and sorption reactions (Alfonso-Muniozguren et al., 2021; Nolte & Ragas, 2017; Peake et al., 2016; Verlicchi et al., 2012). With the presence of suspended solids, particulate matter and sludge, sorption of pharmaceuticals to these matrices will occur. An important physicochemical parameter to determine the absorption is the partition coefficient (Log $P_{\text{octanol/water}}$). Lipophilic compounds will interact via hydrophobic interactions by binding to particulate matter or suspended solids. Absorption levels of hydrophilic compounds will be lower, as these substances have higher affinity to the aqueous phase. In addition, the dissociation constant (p*K*a) is also of importance for the sorption behaviour (Nolte et al., 2020;

Ziylan & Ince, 2011). The protonation of a molecule is defined by the matrix pH. Protonated compounds increase in hydrophilicity making a molecule less bioavailable to microorganisms due to low cellular uptake (Nolte et al., 2020). However, protonated molecules can undergo electrostatic interactions via adsorption to an opposite ionic functional group of sewage sludge (Barron et al., 2009; Sellier et al., 2022). The composition of organic matter in conventional treatment will influence the chemical reactivity. Functional groups of compounds present in sewage sludge have particular p*K*a ranges deriving from microorganism and different humic substances. Depending on the composition are the main specific functional groups derived from humic, fulvic and uronic acids (carboxyl groups R-COOH), phosphoric groups (R-POOH) from bacterial membranes and amine ($R\text{-}NH_2$) or hydroxyl groups (R-OH) derived from polysaccharide and protein structures from the organic fraction of microorganisms (Sellier et al., 2022). Primarily smaller compounds pass through microbial membranes, where lipophilic compound will absorb to the membrane (Nolte et al., 2020). According to the types of microorganisms the biodegradation can result in mineralisation, production of smaller intermediates or in the formation of minor structural changes. The main biochemical transformation processes that occur are oxidation, reduction and lysis reactions (Alfonso-Muniozguren et al., 2021). In a review by Ziylan and Ince (2011), the elimination of anti-inflammatory analgesics was critically evaluated, showing that the secondary treatment of ibuprofen can result in hydroxy or carboxy transformation products (Ziylan & Ince, 2011). Ibuprofen is one of the most consumed non-steroidal anti-inflammatory drugs (NSAIDs) worldwide (Chopra & Kumar, 2020). During aerobic biotransformation, hydroxy-ibuprofen or carboxy-ibuprofen is rapidly formed (Alfonso-Muniozguren et al., 2021; Marchlewicz et al., 2015; Ziylan & Ince, 2011). In contrast, under anaerobic conditions carboxy-ibuprofen could also be produced as well as the hydrophilic intermediate carboxy-hydratropic acid (Alfonso-Muniozguren et al., 2021). WWTP influent will also contain ibuprofen metabolites, such as ibuprofen glucuronide. According to multiple biochemical reactions it is found that ibuprofen glucuronide conjugate can undergo hydrolysis reaction, yielding pristine ibuprofen again (Bendz et al., 2005; Chopra & Kumar, 2020; Marchlewicz et al., 2015; Murdoch & Hay, 2015; Ziylan & Ince, 2011), see **Fig 1.4**. Next to aerobic or anaerobic formed biotransformation products, effluent can also contain pristine ibuprofen. Similar WWTP reactions occur for pharmaceuticals and their metabolites. Removal by secondary wastewater treatment is not always sufficient. To increase the removal efficiency of contaminants, additional tertiary wastewater treatment processes are available. Tertiary treatment steps are applied so that the

discharge of bioactive pharmaceutical products in the aquatic environment are mitigated (Ajo et al., 2018; Beier et al., 2010; Ferrando-Climent et al., 2014; Peake et al., 2016).

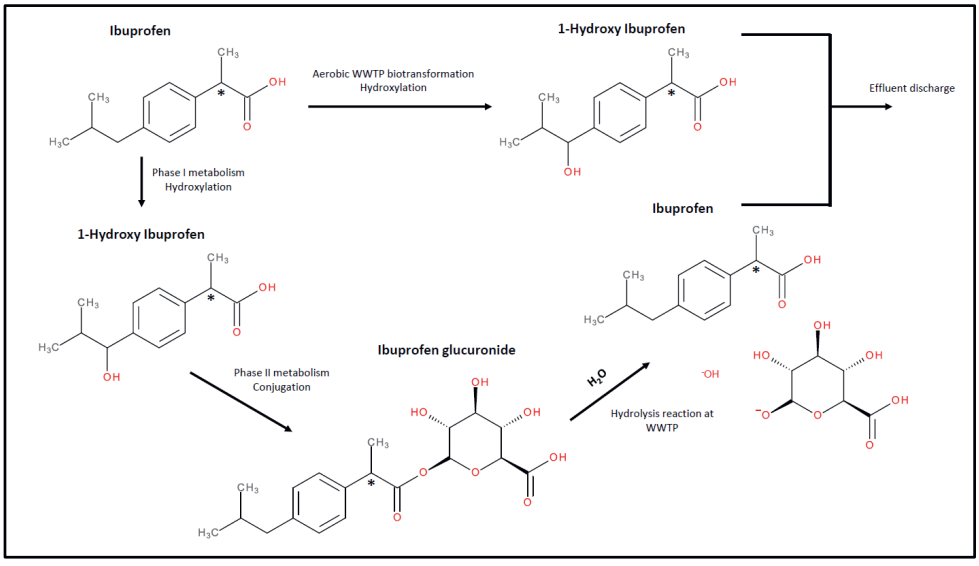

Fig. 1.4. A simplified expectation of ibuprofen reformation during WWTP. Ibuprofen (IBP) is a chiral drug which is used clinically as a racemic mixture present as *R*(-)-IBP or *S*(+)-IBP, which is the pharmacologically active enantiomer. The chiral C atom in IBP is denoted with an asterisk (*). Multiple degradation routes are possible causing the secretion of unmetabolised ibuprofen, isomeric hydroxy-IBP (1-OH-IBP and 3-OH-IBP) and IBP-glucuronide conjugate (Mazaleuskaya et al., 2015). The conjugated metabolite can be back-transformed into the original structure. Unmetabolised ibuprofen is transformed into hydroxy ibuprofen via aerobic biodegradation (Marchlewicz et al., 2015).

1.3.2 Tertiary wastewater treatment

With the increasing burden of pharmaceutical residues in the aquatic environment, conventional WWTPs become deployed with additional treatment steps for micropollutant removal. Tertiary treatment is often applied at WWTPs that discharge the effluent on catchments used for drink water preparation (Emerging Contaminants in the Environment, 2022; Peake et al., 2016; Rizzo, 2022). Processes applied during tertiary treatment rely on physical and chemical processes, using activated carbon, filtration/separation processes or advanced oxidation (Banaschik et al., 2015). When too small contaminant particles remain after secondary sedimentation, physical removal steps are applied using sand filtration or passing the effluent under pressure through a specific membrane filter. With the application of membrane filtration different pore sizes are available. Based on the installed pore size specific contaminants will be eliminated. Sand filtration (100 – 10 µm) is mainly applicable for removal of algae, bacteria and other insoluble particles. Microfiltration (10 – 0.1 µm) will eliminate organic

macromolecules, while ultrafiltration and nanofiltration (0.0005 – 0.1 µm) can remove viruses and smaller organic compounds. For the removal of excess minerals and micropollutants reverse osmosis (>0.0001 µm) is applicable. Within this reverse osmosis treatment step, active (reverse) diffusion occurs under pressure where water molecules are passed through a semipermeable membrane, leaving contaminants, such as pharmaceuticals, in the polluted fraction (Alfonso-Muniozguren et al., 2021; Back et al., 2018).

An alternative to filtration for the removal of micropollutants is the application by sorption using activated carbon. Activated carbon will have a large surface area where dissolved organic compounds will undergo hydrophobic interactions by adsorbing to the activated carbon surface. For the removal of pollutants, secondary effluent is passed through a fixed bed of activated carbon, but activated carbon could also be suspended as powder (Thellmann et al., 2015). A comparable treatment step to coagulation/flocculation is the use of powdered activated carbon in activated sludge (PACAS). With the addition of PACAS directly suspended in activated sludge increases the chemical sorption of organic pollutants onto the additive. PACAS is easily removed by filtration steps. Disadvantages of using fixed carbon columns or PACAS is that the content becomes saturated with adsorbed residues (Man de, 2018). Next to that, primarily hydrophobic compounds will absorb to the carbon surface, and hydrophilic substances might escape from this tertiary treatment step. Usage of membrane filtration and carbon adsorption mainly rely on transferring pollutants to another phase or adsorbent, which result in additional waste-streams. To lower the chemical burden of coagulant/flocculants, alternative bio-coagulants are becoming more interesting since the bio-coagulants are produced from marine shells or plant-based material. (Emerging Contaminants in the Environment, 2022; Hassan et al., 2022; Owodunni & Ismail, 2021). However, to minimise additional waste streams and formation of sludge advanced oxidation techniques are applicable as tertiary treatment. Active generation of reactive oxygen species can degrade organic micropollutants completely by mineralisation.

1.4 Advanced oxidation processes

For the degradation or complete mineralisation of unwanted substances advanced oxidation processes (AOPs) are useful techniques. Reactive oxygen species (ROS) are used for the elimination of organic compounds such as pharmaceuticals. Many different techniques are available, including electrochemical oxidation, Fenton process, UV/H_2O_2, O_3/H_2O_2 and O_3/UV. Techniques under development or better described as emerging technologies are radiolytic degradation (e-beam and gamma radiation) catalytic ozonation, sulphate-based degradation,

cavitation/ultrasonication and plasma treatment (Priyadarshini et al., 2022). Sulphate radicals ($SO_4^{\bullet-}$) are also strong oxidising agents, which are often produced from peroxymonosulfate or peroxydisulfate using heat, microwave, ultrasound, photolysis or Fenton-like processes (Domingues et al., 2022; Giannakis et al., 2021; Qiu et al., 2020). AOP technology is mainly deployed to produce ROS such as hydroxyl radicals ($^{\bullet}OH$), hydroperoxyl ($HO_2^{\bullet}$) and singlet molecular oxygen ($^1O_2$) are produced. During the Fenton process iron will initiate the formation of hydroxyl radicals (**R1**).

$Fe^{2+} + H_2O_2 \rightarrow Fe^{3+} + {}^{\bullet}OH + HO^-$ **R1**

$Fe^{3+} + H_2O_2 \rightarrow Fe^{2+} + HOO^{\bullet} + H^+$ **R2**

$H_2O_2 + {}^{\bullet}OH \rightarrow HOO^{\bullet} + H_2O$ **R3**

In addition to the reaction of Fe^{2+} with H_2O_2, oxygen (O_2) also contributes to the reaction by accepting an extra electron resulting in superoxide radical ($^{\bullet}O_2^-$) formation. $^{\bullet}O_2$ reduces Fe^{3+} into Fe^{2+}, which is the main initiator of the Fenton process, causing rapid formation of $^{\bullet}OH$ radicals (**R2-3**). Formed hydroxyl radicals will cause the degradation of organic molecules (Banaschik et al., 2015, 2018; Giannakis et al., 2021; Magureanu et al., 2015; Qiu et al., 2020). The most widely applied AOPs are combined with UV irradiation. UV deployment for wastewater treatment was previously solely applied for the disinfection of pathogens. UV photons are produced in the range of 100 – 400 nm and are categorised in three UV irradiance bands UV-A (320-400 nm), UV-B (280-315 nm) and UV-C (100-280 nm) (Kowalski, 2009). UV-C wavelengths have the highest photon energy, causing germicidal effects that inactivates bacteria and degrades viruses (Kowalski, 2009). With direct UV irradiation in and on water, photon energy is transformed into chemical energy by producing reactive species such as $^{\bullet}OH$ (Emerging Contaminants in the Environment, 2022). Next to the fact that UV photons can initiate direct molecular degradation of organic compounds, the presence of hydrogen peroxide (H_2O_2), ozone (O_3), titanium oxide (TiO_2) and other oxide containing semiconductors like zinc oxide (ZnO), tungsten trioxide (WO_3) and nickel oxide (NiO), will stimulate the formation of reactive oxygen species (Priyadarshini et al., 2022; (Emerging Contaminants in the Environment, 2022; Zhang et al., 2017). Direct irradiation of H_2O_2 causes homolytic cleavage producing hydroxyl radicals (**R4**). Irradiation of ozone (O_3) will produce oxygen (O_2) and atomic oxygen ($O^{\bullet}$) (**R5**), the latter will react subsequently with water forming hydrogen peroxide (H_2O_2), which is then also rapidly photolytically cleaved into 2 $^{\bullet}OH$ (**R4**). The reaction mechanism of an oxide containing semiconductor such as TiO_2 relies on the excitation of an electron (e^-). This excitation reaction occurs at the surface of a solid photocatalyst in the valance

band (vb), where the electron migrates to the conduction band (cb). The excitation of an electron will leave a hole (h^+) in the valence band (vb). Photoactivated species e^- or h^+ will react with oxygen (O_2) or water (H_2O) producing ROS in the form of $^{\bullet}O_2^-$ and $^{\bullet}OH$ (**R6**).

$H_2O_2 + h\nu \rightarrow 2\ ^{\bullet}OH$ **R4**

$O_3 + h\nu \rightarrow O_2 + O^{\bullet}$ **R5**

$O^{\bullet} + H_2O \rightarrow 2\ ^{\bullet}OH$

$^{\bullet}OH + {}^{\bullet}OH \rightarrow H_2O_2$

$TiO_2 + h\nu \rightarrow e_{cb}^- + h_{vb}^+$ **R6**

$O_2 + e_{cb}^- \rightarrow O_2^{\bullet-}$

$h_{vb}^+ + H_2O \rightarrow {}^{\bullet}OH + H_{aq}^+$

To achieve the best degradation efficiencies of organic micropollutants, an UV source is therefore combined with a photocatalyst. Certain micropollutants are prone to direct photolytic degradation, where other organic compounds are more sensitive to the formed oxidative species. The organic matter present in wastewater might absorb UV irradiation but also acts as a radical scavenger, reducing thus AOP reactivity. Depending on the scavenging properties, the organic matter could also contribute to the formation of transient species, by generating dissolved organic matter radicals ($DOM^{\bullet}$) (Giannakis et al., 2018; Westerhoff et al., 2007). The degradation of micropollutants will depend on the redox potential of the produced oxidative species. With the formation of hydroxyl radicals, it is expected that the oxidative degradation will elapse via H-abstraction, electron transfer or $^{\bullet}OH$ binding to the molecule, its aromatic ring or unsaturated bond (Banaschik et al., 2018; von Sonntag, 2008). Hydroxyl radicals have one of the highest oxidation-reduction potentials (2.8 eV), compared to other oxidiser species such as $SO_4^{\bullet-}$ (2.6 eV), O_3 (2.1 eV), H_2O_2 (1.8 eV) or $KMnO_4$ (1.7 eV). Despite the great degradation efficiencies of these AOPs, their introduction at the WWTP as tertiary treatment step should by carefully considered, based on their removal efficiency, operating costs and waste production (Emerging Contaminants in the Environment, 2022; Mousset et al., 2021). For example, for the Fenton process large quantities of chemical substances are needed, such as ferric and ferrous iron (Fe^{3+}, Fe^{2+}) and hydrogen peroxide, but also chemical substances to adjust the pH since Fenton's treatment effectiveness is the highest in acidified effluent (pH 2 – 4) (Emerging Contaminants in the Environment, 2022). Similar drawbacks are observed for UV sources combined with a photocatalysts. UV-lamps have a limited life and again high quantities of additional chemicals are needed. To overcome these limitations other AOP technologies are available such as electrochemical oxidation, ozonation or plasma treatment. **Table 1.2.**

summarises information of the most prominent available AOP technologies. For each AOP the essential advantages and disadvantages are given (Banaschik et al., 2018; Domingues et al., 2022; Duan et al., 2022; Emerging Contaminants in the Environment, 2022; Feng et al., 2014; Giannakis et al., 2021; Hoeben et al., 2019; Hossain et al., 2018; Khouri et al., 2004; Magureanu et al., 2015; Tay & Madehi, 2015; von Sonntag, 2008; Westerhoff et al., 2007; Yang et al., 2018).

Table 1.2.
Comparison of available advanced oxidation techniques

AOPs	Reactive species	Advantage	Disadvantage
Fenton process	H_2O_2; $^{\bullet}OH$; $HOO^{\bullet}$	• Short reaction time; • No additional energy needed; • Rapid non-selective degradation of organic molecules; • H-abstraction, electrophilic addition	• Chemicals needed: (Fe^{3+}, Fe^{2+}); H_2O_2; • Toxic when high concentrated; • Instable and explosive; • Effluent pH need to be adjusted to 2- 4; • Large quantity of iron containing sludge
Photo-Fenton process	UV; $^{\bullet}OH$; $O_2^{\bullet-}$/ $HO_2^{\bullet}$	• Modified Fenton process with solid catalysts using iron-based minerals; • Improved production of $^{\bullet}OH$ radicals (direct photolysis of H_2O_2)	• Difficult to produce large solid catalysts; • Limited performance due to neutral pH; • High operating cost due to limited life expectancy of UV-lamps
Photocatalytic processes *UV/H_2O_2; O_3/UV (TiO_2; ZnO, WO_3 NiO)*	O_3; $O_2^{\bullet-}$/ $HO_2^{\bullet}$; H_2O_2; $^{\bullet}OH$	• Disinfection properties; • UV-light is used as catalyst to produce reactive species or for the chemical transformation ; • Wide range of organic (micro)pollutants are degraded	• High operating cost due to limited life expectancy of UV-lamps; • Special design needed for photoreactors, challenging for full-scale operation

Table 1.2. *Continued*

Ozonation	O_3; $O_2^{\bullet-}$/ $HO_2^{\bullet}$; H_2O_2; $^{\bullet}OH$	• Reactive species are produced from air or pure oxygen using electrical discharges interaction; • Useful technology for removal of bacteria and water disinfection; • Organic molecule degradation occurs via 2 pathways; ▪ Primary oxidation pathway with O_3 ▪ Secondary reactions with produced $^{\bullet}OH$	• O_3 is an unstable molecule, easily reverted, high concentrations needed; • Difficult to dissolve in water, and therefore partially oxidation of organic molecules occur; • Multiple oxidation pathway cause the formation of different degradation intermediates; • High amounts of energy needed to produce O_3, making the technology expensive
Sulphate – radical oxidation process (SR-AOP)	$SO_4^{\bullet-}$; SO_5^{2-}; $^1O_2$	• Longer active than $^{\bullet}OH$ radical due to increased stability; • Higher selectivity to aromatic ring and unsaturated (C=C) structures; ▪ Single-electron transfer ▪ Electron abstraction ($^1O_2$) ▪ Electrophilic addition • Applicable at wider pH range (2 – 8); • Cheaper than H_2O_2	• SO_4^{2-} increased concentrations; • Toxic by-products • During SR-AOP, heat or UV irradiation is produced; • Additional treatment steps needed, to remove SO_4^{2-}

Table 1.2. *Continued*

Electrochemical oxidation	H_2O_2; $^{\bullet}OH$ (Direct) $Cl^{\bullet}$; Cl_2; $ClO^{\bullet}$	• Wide pH range applicability • Direct oxidation; ▪ $^{\bullet}OH$ radical production without additional chemicals; ▪ Ambient reaction conditions needed; ▪ Short reaction time • Indirect oxidation; ▪ Addition of chemicals such as chlorine (Cl_2) for disinfection and degradation of organic compounds; ▪ Low amount of additional chemicals needed	• Difficulties in scaling up the technique; • Expected high cost due to high electricity; consumption • Expensive electrode material; • Maintenance issues
Cavitation *Ultrasonication* *Hydrodynamic cavitation*	$^{\bullet}OH$; Ultrasonication/ O_3; $O_2^{\bullet-}$/ $HO_2^{\bullet}$ and $^{\bullet}OH$	• Water molecules are rapidly split into hydroxyl radicals for the degradation of organic molecules; • Production of microbubbles that are implosive releasing energy that can degrade contaminants; • Low maintenance, easy and flexible operation	• Additional chemicals needed, such as O_3 and H_2O_2; • Wastewater absorbs ultrasonic waves; • Ultrasonic cavitation has higher efficiency at acidic pH; • Spreading of cavitation effects is limited; • Hydrodynamic cavitation need expensive pumps

Table 1.2. *Continued*

Radiolytic AOPs *Gamma radiation* *Electron beam*	$^{\bullet}OH$; e^-_{aq} and $H^{\bullet}$ ions	• No additives or additional chemicals are needed (Eco-friendly); • Strong disinfection properties; • Radiation enters into the contaminant (High penetration rate); • Radiation contains extremely high energy that can removes electrons. • *keV/MeV* ionise, dissociate and excite molecules.	• High costs expected due to; ▪ High energy demand ▪ Trained operators needed, that need to wear protective gear
Plasma treatment *Thermal plasma* *Non-thermal plasma*	H_2O_2 ; $^{\bullet}OH$; $O_2^{\bullet-}$ / $HO_2^{\bullet}$; ONOOH and NO_X	• Many different reactive species ($H_aN_bO_C$) are produced for the degradation of organic contaminants • Near to complete degradation possible • No additional chemicals are needed • Difference in applied energy density for *Thermal plasma* and *Non-thermal plasma* to produce reactive species • Non – thermal plasma requires lower power	• Safety hazards expected from produced toxic by-products • High energy costs expected • Electrical energy optimisation needed • Skilled labour required to operate the technique

1.4.1 Plasma oxidation

Efficient production of ROS without using additional chemicals is stimulated by creating a plasma in oxygen, atmosphere or water. To ionise a medium, heat or an active electrical current is needed to generate energetic particles. With direct application of electrical discharge in the atmosphere (the conductor), energetic particles in the form of electrons (e^-), ions (O_2^-, $N^{\bullet}$, $^1O_2$, $NO^{\bullet}$) and photons (Y) are formed. The produced electrical flow will move from the cathode (-) to an anode (+), within their movement they will collide with atoms and molecules present in the gas or liquid phase. Upon collision complete and partial ionisation occurs. During the ionisation process more energetic electrons become available which will initiate subsequently similar reaction mechanisms producing a plasma. A plasma is defined as quasineutral energetic gaseous medium, containing energetic electrons, photons, molecular and atomic species which

are ionised, radicals or excited states (Go, 2018; Gomez et al., 2009; Priyadarshini et al., 2022; Samal, 2017). Complementary to solid, liquid and gas state, plasma is referred as the 'fourth state of matter'. The energy input defines the degree of ionisation featuring a non-thermodynamical equilibrium of the energetic electrons and neutral species. Thermal plasmas comprise of a high ionisation degree, having highly excited non-molecular states including species with temperatures close to thermodynamical equilibrium (Chen, 1995; Lieberman & Lichtenberg, 2005; Meichsner et al., 2012). Plasma technology has major applications in semiconductor industry (deposition, etching, ashing), formerly but declining in lighting technology as light emitting medium, in textile industry for improving surface wettability, in flue- and waste gas treatment and not at last - future nuclear fusion technology (Deng et al., 2022; Hoeben et al., 2000, 2019; Scholtz et al., 2015). Additionally, plasma technology is also proposed as a promising technology within the healthcare sector for wound cleaning, dental practice, control of apoptosis or tumour treatment (Go, 2018; Scholtz et al., 2015). As previously described, the gas discharge is theoretically divided into different types of fragments (Go, 2018). The neutral charged elements are a specific ambient gas (or atmosphere N_2, O_2, Ar), including excited gas particles (photons). Positive and negative ions comprehend ionised gas elements and electrons (e^-). All these elements have a kinetic energy (eV) and the produced energy equilibrium of these particles within a gas discharge determines whether a plasma is either thermal or non-thermal (Go, 2018). Non-thermal plasma has a low ionisation degree (typically 10^{-7}-10^{-4}), and comprises energetic electrons and excited states, where the neutral and ion species energy is not pronounced ($T_{e^-} >> T_{gas} \sim T_{ions}$) (Go, 2018; Hoeben et al., 2000, 2019). On the contrary, thermal plasmas exhibit a high ionisation degree and plasma species are in near thermodynamical equilibrium, i.e. electrons, ions and neutrals having similar energies ($T_{e^-} \sim T_{gas} \sim T_{ions}$) (Go, 2018; Hoeben et al., 2000). Examples of thermal plasma are lightning and hot electrical arcs; St. Elmo's fire, Northern Light, fluorescent lamps, comprise non-thermal electrical discharges (Fridman, 2008, Go, 2018; Hoeben et al., 2000; Scholtz et al., 2015). Both thermal and non-thermal plasmas can generate reactive oxygen and nitrogen species (RONS). In the current study thermal plasma activation was used with an electrical discharge in air-over-water, see **Fig. 1.5**. The plasma in direct contact with the water surface leads to atmospherically produced RONS that dissolve into the water phase. Also, plasma energetic particles bombardment of the water generates hydroxyl radicals. Plasma-activated water (PAW) contains many reactive species enabling oxidative degradation reactions (Banaschik et al., 2015, 2018; Magureanu et al., 2015).

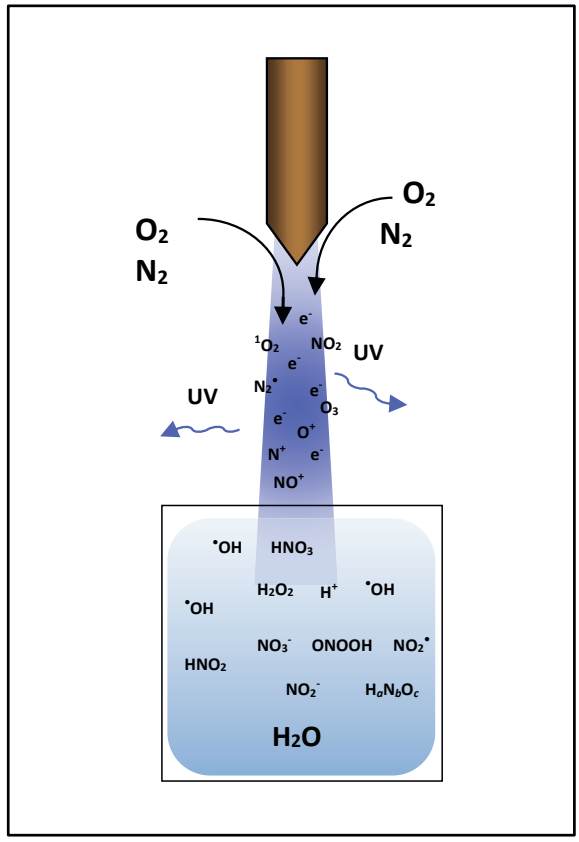

Fig. 1.5. During thermal plasma operation in air-over-water, oxygen (O_2) and nitrogen (N_2) are converted into oxides of nitrogen, which dissolve in water. Many different reactive oxygen and nitrogen species are formed in the liquid matrix ($H_aN_bO_c$ comprises multiple transient RONS).

1.5 Overall objective

It is well documented that our aquatic environment and drinking water quality is threatened due to chemical pollution. Increasing anthropogenic pollution, climate change, population growth and increased life expectancy of the aging population will raise the burden of contaminants in fresh water. Via multiple emission routes, anthropogenic contaminants end up in the aquatic environment. The group of pharmaceuticals represent one of the most emerging pollutants present in the hydrosphere as their consumption intensifies worldwide. With the wastewater from municipal and hospital sewage, pharmaceutical residues reach the WWTPs. As demonstrated in the introduction, conventional wastewater treatment techniques are not designed to remove low levels of organics like pharmaceutical residues, leading to partially altered or direct discharge of bioactive substances in receiving waters. Certain high concentrations of contaminants can damage or inhibit the activated sludge of WWTPs.

Difficulties in the removal of pharmaceuticals and their metabolites are caused by their continuous load, varying composition, diluted concentration and poor biodegradability.

Usage of tertiary treatment steps, such as membrane filtration or advanced oxidation could contribute to reduce the micropollutant load. However, too short reaction times, necessity of additional chemicals (activated carbon, Fe^{3+}, H_2O_2 or SO_x^{n-}), UV sources or filtration beds will generate extra waste and might increase wastewater treatment costs. Next to that, also the selection and deployment of an appropriate removal technique is of importance to achieve the desired removal efficiency.

The highest medicinal load is discharged from pharmaceutical industry and from municipal and hospital effluents (Emerging Contaminants in the Environment, 2022; Kümmerer, 2004; K. Samal et al., 2022). Additionally, also the emissions of illicit drug activities should not be neglected. To increase the effectiveness of additional wastewater treatment techniques, it is expected that with the deployment of AOPs at the contamination source could complement conventional WWTPs. This study was part of the MEDUWA (Medicine Unwanted in Water) project funded by Interreg of the EU. The MEDUWA project increased public awareness of pharmaceuticals in water and also provides solutions for sustainable changes (European Union, 2016). Our contribution focused on the mitigation of pharmaceutical emission by testing the possibility of pre-treatment at the contamination source. Simulation matrices and hospital sewage were used to determine the degradation kinetics of 14 prioritised pharmaceuticals.

1.5.1 Research objective

This thesis aimed at evaluating thermal plasma treatment technology for the removal of pharmaceutical residues from hospital sewage water. The suitability of the plasma technology was studied on laboratory scale. Oxidative treatment was applied to reconstituted simulations of real-life matrices and raw hospital sewage water to determine the degradation kinetics. To explore whether plasma treatment could be useful as a pre-treatment step preceding conventional wastewater processing steps, cytotoxicity assays were applied on untreaded and oxidatively treated water matrices. In addition, the ecotoxicological risk was also estimated by extrapolation of the previously obtained degradation kinetics. This thesis consists of four experimental chapters (**2**-**5**) including a chemical supporting chapter (**6**) addressing the following specific research questions:

Does plasma activation of water degrade pharmaceuticals in (waste)-water?

The antineoplastic agent cyclophosphamide was selected to investigate whether plasma activation is capable to degrade a cytotoxic and environmental persistent compound. Hospital sewage water effluents will contain multiple different pharmaceutical classes, including the harmful antineoplastic agents. **Chapter 2** presents a technical study, showing the optimisation of laboratory-scale plasma treatment. Different plasma energy densities were applied to produce reactive species for the degradation of a known concentration of cyclophosphamide (CP). Simultaneously UV-C/H_2O_2 advanced oxidation was applied as a reference.

What is the effect of plasma treatment on complex water matrices containing multiple pharmaceutical residues?

As a follow-up to the optimisation study, laboratory-scale plasma technology was further examined by direct oxidative treatment in complex water matrices. Relevant pharmaceuticals were selected according to the MEDUWA compound shortlist combined with prioritised substances often found in HSW emissions. In **Chapter 3** chemical degradation kinetics of 14 different pharmaceuticals were determined, by spiking relevant simulated matrices with a known concentration in Milli-Q, tap-water, synthetic urine, diluted human urine and synthetic sewage water (SSW). Additionally, an end-of-pipe grab sample of hospital sewage water (HSW) was analysed and subsequently treated with plasma and UV-C/H_2O_2 technology.

Does plasma-induced oxidative degradation decrease the toxicity of treated water matrices?

In **Chapter 4** a cytotoxicity assay was applied to measure the potential toxicity of untreated and oxidatively treated water matrices. Thermal plasma and UV-C/H_2O_2 oxidation were directly applied in Milli-Q, SSW and end-of-pipe HSW matrices. Insufficient advanced oxidation could result in toxic degradation products. With direct cellular exposure of untreated and oxidatively treated pharmaceutical matrices, the overall viability and oxidative stress of HeLa cells were evaluated.

Are predictive models applicable in providing indicative (eco)toxicity data by complementing actual measured results?

In order to quickly retrieve indicative ecotoxicity results, quantitative structural analysis (QSAR) tools are available. **Chapter 5** describes the use of a software application to complement actual measured (cyto)toxicity results and to perform a preliminary and rapid *in silico* environmental risk assessment. This *in silico* approach was used to complement measured pharmaceutical data. Measured results and toxicity predictions were combined in an

environmental risk assessment comparing untreated and oxidative treated hospital sewage water.

How can quantum chemical calculations support the understanding of oxidative chemical degradation?

In **Chapter 6** the usage of quantum chemical software was demonstrated. With applied quantum chemical calculations, the most reactive molecular moieties and the highest occupied molecular orbitals (HOMO) of the tested pharmaceuticals were localised. Designated HOMO positions indicate a molecule's nucleophilicity. These nucleophilic positions are expected to react easily with electrophiles such as the oxidatively formed reactive species (ROS and RNS). The quantum chemical calculated parameters were therefore compared with our previously measured chemical abatement kinetics, to understand the observed oxidative degradation. Additionally, the HOMO-LUMO gap energy (ΔE) was determined, providing a simple approximate to determine a molecule's stability.

Literature

Abbas, A., Schneider, I., Bollmann, A., Funke, J., Oehlmann, J., Prasse, C., Schulte-Oehlmann, U., Seitz, W., Ternes, T., Weber, M., Wesely, H., & Wagner, M. (2019). What you extract is what you see: Optimising the preparation of water and wastewater samples for in vitro bioassays. *Water Research*, *152*, 47–60. https://doi.org/10.1016/j.watres.2018.12.049

Ajala, O. J., Tijani, J. O., Salau, R. B., Abdulkareem, A. S., & Aremu, O. S. (2022). A review of emerging micro-pollutants in hospital wastewater: Environmental fate and remediation options. *Results in Engineering*, *16*, 100671. https://doi.org/10.1016/j.rineng.2022.100671

Ajo, P., Preis, S., Vornamo, T., Mänttäri, M., Kallioinen, M., & Louhi-Kultanen, M. (2018). Hospital wastewater treatment with pilot-scale pulsed corona discharge for removal of pharmaceutical residues. *Journal of Environmental Chemical Engineering*, *6*(2), 1569–1577. https://doi.org/10.1016/j.jece.2018.02.007

Alfonso-Muniozguren, P., Serna-Galvis, E. A., Bussemaker, M., Torres-Palma, R. A., & Lee, J. (2021). A review on pharmaceuticals removal from waters by single and combined biological, membrane filtration and ultrasound systems. *Ultrasonics Sonochemistry*, *76*, 105656. https://doi.org/10.1016/j.ultsonch.2021.105656

Álvarez-Torrellas, S., Peres, J. A., Gil-Álvarez, V., Ovejero, G., & García, J. (2017). Effective adsorption of non-biodegradable pharmaceuticals from hospital wastewater with different carbon materials. *Chemical Engineering Journal*, *320*, 319–329. https://doi.org/10.1016/j.cej.2017.03.077

Back, J. O., Obholzer, T., Winkler, K., Jabornig, S., & Rupprich, M. (2018). Combining ultrafiltration and non-thermal plasma for low energy degradation of pharmaceuticals from conventionally treated wastewater. *Journal of Environmental Chemical Engineering*, *6*(6), 7377–7385. https://doi.org/10.1016/j.jece.2018.07.047

Banaschik, R., Lukes, P., Jablonowski, H., Hammer, M. U., Weltmann, K.-D., & Kolb, J. F. (2015). Potential of pulsed corona discharges generated in water for the degradation of persistent pharmaceutical residues. *Water Research*, *84*, 127–135. https://doi.org/10.1016/j.watres.2015.07.018

Banaschik, R., Jablonowski, H., Bednarski, P. J., & Kolb, J. F. (2018). Degradation and intermediates of diclofenac as instructive example for decomposition of recalcitrant pharmaceuticals by hydroxyl radicals generated with pulsed corona plasma in water. *Journal of Hazardous Materials*, *342*, 651–660. https://doi.org/10.1016/j.jhazmat.2017.08.058

Bannwarth, A., Morelato, M., Benaglia, L., Been, F., Esseiva, P., Delemont, O., & Roux, C. (2019). The use of wastewater analysis in forensic intelligence: drug consumption comparison between Sydney and different European cities. *Forensic Sciences Research*, *4*(2), 141–151. https://doi.org/10.1080/20961790.2018.1500082

Barquero, R., Agulla, M. M., & Ruiz, A. (2008). Liquid discharges from the use of radionuclides in medicine (diagnosis). *Journal of Environmental Radioactivity*, *99*(10), 1535–1538. https://doi.org/10.1016/j.jenvrad.2007.12.009

Bendz, D., Paxéus, N. A., Ginn, T. R., & Loge, F. J. (2005). Occurrence and fate of pharmaceutically active compounds in the environment, a case study: Höje River in Sweden. *Journal of Hazardous Materials*, *122*(3), 195–204. https://doi.org/10.1016/j.jhazmat.2005.03.012

Bijlsma, L., Emke, E., Hernández, F., & de Voogt, P. (2012). Investigation of drugs of abuse and relevant metabolites in Dutch sewage water by liquid chromatography coupled to high resolution mass spectrometry. *Chemosphere*, *89*(11), 1399–1406. https://doi.org/10.1016/j.chemosphere.2012.05.110

Carvalho, R. N. , Ceriani, L., Ippolito, A., & Lettieri, T. (2015). *Development of the First Watch List under the Environmental Quality Standards Directive*. *LB-NA-27142-EN-N*. https://doi.org/10.2788/101376

Chen, F. F. (1995). *Introduction to Plasma Physics*. Springer US. https://doi.org/10.1007/978-1-4757-0459-4

Chopra, S., & Kumar, D. (2020). Ibuprofen as an emerging organic contaminant in environment, distribution and remediation. *Heliyon*, *6*(6), e04087. https://doi.org/10.1016/j.heliyon.2020.e04087

Comber, S., Gardner, M., Sörme, P., Leverett, D., & Ellor, B. (2018). Active pharmaceutical ingredients entering the aquatic environment from wastewater treatment works: A cause for concern? *Science of The Total Environment*, *613–614*, 538–547. https://doi.org/10.1016/j.scitotenv.2017.09.101

de Jonge, E. F., Peterse, C. M., Koelewijn, J. M., van der Drift, A.-M. R., van der Beek, R. F. H. J., Nagelkerke, E., & Lodder, W. J. (2022). The detection of monkeypox virus DNA in wastewater samples in the Netherlands. *Science of The Total Environment*, *852*, 158265. https://doi.org/10.1016/j.scitotenv.2022.158265

Deng, L., Hu, H., Wang, Y., Wu, C., He, H., Li, J., Luo, X., Zhang, F., & Guo, D. (2022). Surface plasma treatment reduces oxygen vacancies defects states to control photogenerated carriers transportation for enhanced self-powered deep UV photoelectric characteristics. *Applied Surface Science*, *604*, 154459. https://doi.org/10.1016/j.apsusc.2022.154459

Derksen, A. , Jansen. S. , Rijk. de, S. , Duijnhoven. N. , Roex. E. , Palsma. B. , Berbee. R. , Pieters. B. , Kools. S. (2014). *Wat zit er in ons afvalwater?: Watson geeft antwoord!*

Domingues, E., Silva, M. J., Vaz, T., Gomes, J., & Martins, R. C. (2022). Sulfate radical based advanced oxidation processes for agro-industrial effluents treatment: A comparative review with Fenton's peroxidation. *Science of The Total Environment*, *832*, 155029. https://doi.org/10.1016/j.scitotenv.2022.155029

Donnachie, R. L., Johnson, A. C., & Sumpter, J. P. (2016). A rational approach to selecting and ranking some pharmaceuticals of concern for the aquatic environment and their relative importance compared with other chemicals. *Environmental Toxicology and Chemistry*, *35*(4), 1021–1027. https://doi.org/10.1002/etc.3165

Duan, X., Niu, X., Gao, J., Wacławek, S., Tang, L., & Dionysiou, D. D. (2022). Comparison of sulfate radical with other reactive species. *Current Opinion in Chemical Engineering*, *38*, 100867. https://doi.org/10.1016/j.coche.2022.100867

Egli, M., Rapp-Wright, H., Oloyede, O., Francis, W., Preston-Allen, R., Friedman, S., Woodward, G., Piel, F. B., & Barron, L. P. (2023). A One-Health environmental risk assessment of contaminants of emerging concern in London's waterways throughout the SARS-CoV-2 pandemic. *Environment International*, *180*, 108210. https://doi.org/10.1016/j.envint.2023.108210

EMCDDA. (2017). *European Drug Report 2017: Trends and Developments*.

Emerging Contaminants in the Environment. (2022). Elsevier. https://doi.org/10.1016/C2020-0-02013-X

Emke, E., Vughs, D., Kolkman, A., & de Voogt, P. (2018). Wastewater-based epidemiology generated forensic information: Amphetamine synthesis waste and its impact on a small sewage treatment plant. *Forensic Science International*, *286*, e1–e7. https://doi.org/10.1016/j.forsciint.2018.03.019

Emmanuel, E., Perrodin, Y., Keck, G., Blanchard, J.-M., & Vermande, P. (2005). Ecotoxicological risk assessment of hospital wastewater: a proposed framework for raw effluents discharging into urban sewer network. *Journal of Hazardous Materials*, *117*(1), 1–11. https://doi.org/10.1016/j.jhazmat.2004.08.032

Escher, B. I., Baumgartner, R., Koller, M., Treyer, K., Lienert, J., & McArdell, C. S. (2011). Environmental toxicology and risk assessment of pharmaceuticals from hospital wastewater. *Water Research*, *45*(1), 75–92. https://doi.org/10.1016/j.watres.2010.08.019

Directive 2000/60/EC, Pub. L. No. Directive 2000/60/EC (2000).

Concerning urban waste water treatment 91/271/EEC, Pub. L. No. 91/271/EEC, Council Directive (1991).

Commission Implementing Decision (EU) 2015/495, Pub. L. No. C(2015) 1756 (2015).

Commission Implementing Decision (EU) 2018/840, Pub. L. No. C(2018) 3362 (2018).

Communication from the Commission to the European Parliament, the Council and the European Economic and Social Committee, Pub. L. No. COM(2019) 128 final (2019).

Commission Implementing Decision (EU) 2020/1161, Pub. L. No. C(2020) 5205 (2020).

Commission Implementing Decision (EU) 2022/1307, Pub. L. No. C(2022) 5098 (2022).

Feng, L., Oturan, N., van Hullebusch, E. D., Esposito, G., & Oturan, M. A. (2014). Degradation of anti-inflammatory drug ketoprofen by electro-oxidation: comparison of electro-Fenton and anodic oxidation processes. *Environmental Science and Pollution Research*, *21*(14), 8406–8416. https://doi.org/10.1007/s11356-014-2774-2

Ferrando-Climent, L., Rodriguez-Mozaz, S., & Barceló, D. (2014). Incidence of anticancer drugs in an aquatic urban system: From hospital effluents through urban wastewater to natural environment. *Environmental Pollution*, *193*, 216–223. https://doi.org/10.1016/j.envpol.2014.07.002

Fridman, A. (2008). *Plasma Chemistry*. Cambridge University Press. https://doi.org/10.1017/CBO9780511546075

Gao, J., Zheng, Q., Lai, F. Y., Gartner, C., Du, P., Ren, Y., Li, X., Wang, D., Mueller, J. F., & Thai, P. K. (2020). Using wastewater-based epidemiology to estimate consumption of alcohol and nicotine in major cities of China in 2014 and 2016. *Environment International*, *136*, 105492. https://doi.org/10.1016/j.envint.2020.105492

Geissen, V., Mol, H., Klumpp, E., Umlauf, G., Nadal, M., van der Ploeg, M., van de Zee, S. E. A. T. M., & Ritsema, C. J. (2015). Emerging pollutants in the environment: A challenge for water resource management. *International Soil and Water Conservation Research*, *3*(1), 57–65. https://doi.org/10.1016/j.iswcr.2015.03.002

Giannakis, S., Androulaki, B., Comninellis, C., & Pulgarin, C. (2018). Wastewater and urine treatment by UVC-based advanced oxidation processes: Implications from the interactions of bacteria, viruses, and chemical contaminants. *Chemical Engineering Journal*, *343*, 270–282. https://doi.org/10.1016/j.cej.2018.03.019

Go, D. B. (2018). *Ionization and Ion Transport*. Morgan & Claypool Publishers. https://doi.org/10.1088/978-1-6817-4601-2

Gomez Cortes, L., Marinov, D., Sanseverino, I., Navarro Cuenca, A., Niegowska Conforti, M., Porcel Rodriguez, E., Stefanelli, F., & Lettieri, T. (2022). *Selection of substances for the 4th Watch List under the Water Framework Directive*. *KJ-NA-31-148-EN-N (online),KJ-NA-31-148-EN-C (print)*. https://doi.org/10.2760/01939 (online),10.2760/909608 (print)

Gomez Cortes, L., Marinov, D., Sanseverino, I., Navarro Cuenca, A., Niegowska, M., Porcel Rodriguez, E., & Lettieri, T. (2020). *Selection of substances for the 3rd Watch List under the Water Framework Directive . KJ-NA-30297-EN-N (online),KJ-NA-30297-EN-C (print)*. https://doi.org/10.2760/194067 (online),10.2760/240926 (print)

Gomez, E., Rani, D. A., Cheeseman, C. R., Deegan, D., Wise, M., & Boccaccini, A. R. (2009). Thermal plasma technology for the treatment of wastes: A critical review. *Journal of Hazardous Materials*, *161*(2–3), 614–626. https://doi.org/10.1016/j.jhazmat.2008.04.017

Gray, J. L., Borch, T., Furlong, E. T., Davis, J. G., Yager, T. J., Yang, Y.-Y., & Kolpin, D. W. (2017). Rainfall-runoff of anthropogenic waste indicators from agricultural fields applied with municipal biosolids. *Science of The Total Environment*, *580*, 83–89. https://doi.org/10.1016/j.scitotenv.2016.03.033

Greif, M., Köke, N., Pütz, M., Rößler, T., Knepper, T. P., & Frömel, T. (2022). Nontarget screening of production waste samples from Leuckart amphetamine synthesis using liquid chromatography - high-resolution mass spectrometry as a complementary method to GC-MS impurity profiling. *Drug Testing and Analysis*, *14*(3), 450–461. https://doi.org/10.1002/dta.3224

Hassan, L. S., Abdullah, N., Abdullah, S., Ghazali, S. R., Sobri, N. A. M., Hashim, N., Yahya, N. A. M., & Muslim, W. M. N. (2022). The Effectiveness of Chitosan Extraction from Crustaceans' Shells as a natural coagulant. *Journal of Physics: Conference Series*, *2266*(1), 012002. https://doi.org/10.1088/1742-6596/2266/1/012002

Hoeben, W. F. L. M. (2000). *Pulsed corona-induced degradation of organic materials in water*. Technische Universiteit Eindhoven.

Hoeben, W. F. L. M., van Ooij, P. P., Schram, D. C., Huiskamp, T., Pemen, A. J. M., & Lukeš, P. (2019). On the Possibilities of Straightforward Characterization of Plasma Activated Water. *Plasma Chemistry and Plasma Processing*, *39*(3), 597–626. https://doi.org/10.1007/s11090-019-09976-7

House of Commons Environmental Audit Committee. (2022). *Water quality in rivers*.

Huizer, M., ter Laak, T. L., de Voogt, P., & van Wezel, A. P. (2021). Wastewater-based epidemiology for illicit drugs: A critical review on global data. *Water Research*, *207*, 117789. https://doi.org/10.1016/j.watres.2021.117789

Kar, S., Sanderson, H., Roy, K., Benfenati, E., & Leszczynski, J. (2020). Ecotoxicological assessment of pharmaceuticals and personal care products using predictive toxicology approaches. *Green Chemistry*, *22*(5), 1458–1516. https://doi.org/10.1039/C9GC03265G

Khan, K., Baderna, D., Cappelli, C., Toma, C., Lombardo, A., Roy, K., & Benfenati, E. (2019). Ecotoxicological QSAR modeling of organic compounds against fish: Application of fragment based descriptors in feature analysis. *Aquatic Toxicology*, *212*, 162–174. https://doi.org/10.1016/j.aquatox.2019.05.011

Khouri, H., Collin, F., Bonnefont-Rousselot, D., Legrand, A., Jore, D., & Gardès-Albert, M. (2004). Radical-induced oxidation of metformin. *European Journal of Biochemistry*, *271*(23–24), 4745–4752. https://doi.org/10.1111/j.1432-1033.2004.04438.x

Kowalski, W. (2009). *Ultraviolet Germicidal Irradiation Handbook*. Springer Berlin Heidelberg. https://doi.org/10.1007/978-3-642-01999-9

Kuloglu Genc, M., Mercan, S., Yayla, M., Tekin Bulbul, T., Adioren, C., Simsek, S. Z., & Asicioglu, F. (2021). Monitoring geographical differences in illicit drugs, alcohol, and tobacco consumption via wastewater-based epidemiology: Six major cities in Turkey. *Science of The Total Environment*, *797*, 149156. https://doi.org/10.1016/j.scitotenv.2021.149156

Kümmerer, K. (Ed.). (2004). *Pharmaceuticals in the Environment*. Springer Berlin Heidelberg. https://doi.org/10.1007/978-3-662-09259-0

Kümmerer, K. (2009). The presence of pharmaceuticals in the environment due to human use – present knowledge and future challenges. *Journal of Environmental Management*, *90*(8), 2354–2366. https://doi.org/10.1016/j.jenvman.2009.01.023

Laquaz, M., Dagot, C., Bazin, C., Bastide, T., Gaschet, M., Ploy, M.-C., & Perrodin, Y. (2018). Ecotoxicity and antibiotic resistance of a mixture of hospital and urban sewage in a wastewater treatment plant. *Environmental Science and Pollution Research*, *25*(10), 9243–9253. https://doi.org/10.1007/s11356-017-9957-6

Lee, S. S., Paspalof, A. M., Snow, D. D., Richmond, E. K., Rosi-Marshall, E. J., & Kelly, J. J. (2016). Occurrence and Potential Biological Effects of Amphetamine on Stream Communities. *Environmental Science & Technology*, *50*(17), 9727–9735. https://doi.org/10.1021/acs.est.6b03717

Leon Barron, Martha Purcell, Josef Havel, Kevin Thomas, John Tobin, & Brett Paull. (2009). *Occurrence and Fate of Pharmaceuticals and Personal Care Products within Sewage Sludge and Sludge-Enriched Soils*.

Lieberman, M. A., & Lichtenberg, A. J. (2005). *Principles of Plasma Discharges and Materials Processing*. Wiley. https://doi.org/10.1002/0471724254

Loos, R., Marinov, D., Sanseverino, I., Napierska, D., & Lettieri, T. (2018). *Review of the 1st Watch List under the Water Framework Directive and recommendations for the 2nd Watch List*. *KJ-NA-29173-EN-C (print),KJ-NA-29173-EN-N (online)*. https://doi.org/10.2760/614367 (online),10.2760/701879 (print)

Magureanu, M., Mandache, N. B., & Parvulescu, V. I. (2015). Degradation of pharmaceutical compounds in water by non-thermal plasma treatment. *Water Research*, *81*, 124–136. https://doi.org/10.1016/j.watres.2015.05.037

Man de, A., Mulder, M., Gerritse, W., Scherrenberg, S., Bechger, M., Vingerhoeds, R., Verberkt, B., Lekkerkerker, K., Rijs, G., Dikkenberg van den, J. (2018). *PACAS - POEDERKOOLDOSERING IN ACTIEFSLIB VOOR VERWIJDERING VAN MICROVERONTREINIGINGEN*.

Marchlewicz, A., Guzik, U., & Wojcieszyńska, D. (2015). Over-the-Counter Monocyclic Non-Steroidal Anti-Inflammatory Drugs in Environment—Sources, Risks, Biodegradation. *Water, Air, & Soil Pollution*, *226*(10), 355. https://doi.org/10.1007/s11270-015-2622-0

Meichsner, J., Schmidt, M., Schneider, R., & Wagner, H.-E. (Eds.). (2012). *Nonthermal Plasma Chemistry and Physics*. CRC Press. https://doi.org/10.1201/b12956

Melnyk, A., Kuklińska, K., Wolska, L., & Namieśnik, J. (2014). Chemical pollution and toxicity of water samples from stream receiving leachate from controlled municipal solid waste (MSW) landfill. *Environmental Research*, *135*, 253–261. https://doi.org/10.1016/j.envres.2014.09.010

Moermond, C., Montforts, M. , Smit. E. (2019). *Informatieblad nut en noodzaak van normen voor medicijnresten in oppervlaktewater*.

Moermond C.T.A., Montforts, M.H.M.M., Roex, E.W.M., Venhuis, B.J. (2020). *Pharmaceutical residues and water quality: an update*.

Murdoch, R. W., & Hay, A. G. (2015). The biotransformation of ibuprofen to trihydroxyibuprofen in activated sludge and by Variovorax Ibu-1. *Biodegradation*, *26*(2), 105–113. https://doi.org/10.1007/s10532-015-9719-4

National Institute for Public Health and the Environment (Rijksinstituut voor Volksgezondheid en Milieu). (2023, October 18). *Water voor drinkwaterbereiding*. https://rvs.rivm.nl/onderwerpen/normen/milieu/water-voor-drinkwaterbereiding

Nolte, T. M., Chen, G., van Schayk, C. S., Pinto-Gil, K., Hendriks, A. J., Peijnenburg, W. J. G. M., & Ragas, A. M. J. (2020). Disentanglement of the chemical, physical, and biological processes aids the development of quantitative structure-biodegradation relationships for aerobic wastewater treatment. *Science of The Total Environment*, *708*, 133863. https://doi.org/10.1016/j.scitotenv.2019.133863

Nolte, T. M., & Ragas, A. M. J. (2017). A review of quantitative structure–property relationships for the fate of ionizable organic chemicals in water matrices and identification of knowledge gaps. *Environmental Science: Processes & Impacts*, *19*(3), 221–246. https://doi.org/10.1039/C7EM00034K

Orias, F., & Perrodin, Y. (2013). Characterisation of the ecotoxicity of hospital effluents: A review. *Science of The Total Environment*, *454–455*, 250–276. https://doi.org/10.1016/j.scitotenv.2013.02.064

Wet milieubeheer, (1979).

Waterwet, Pub. L. No. BWBR0025458 (2009).

Owodunni, A. A., & Ismail, S. (2021). Revolutionary technique for sustainable plant-based green coagulants in industrial wastewater treatment—A review. *Journal of Water Process Engineering*, *42*, 102096. https://doi.org/10.1016/j.jwpe.2021.102096

Pandit, N. K. , S. R. , P. B. S. (2012). *Introduction to the pharmaceutical sciences: an integrated Approach* (2nd edtion). Lippincott Williams & Wilkins, a Wolters Kluwer business.

Patel, M., Kumar, R., Kishor, K., Mlsna, T., Pittman, C. U., & Mohan, D. (2019). Pharmaceuticals of Emerging Concern in Aquatic Systems: Chemistry, Occurrence, Effects, and Removal Methods. *Chemical Reviews*, *119*(6), 3510–3673. https://doi.org/10.1021/acs.chemrev.8b00299

Peake, B. M., Braund, R., Tong, A. Y. C., & Tremblay, L. A. (2016). *The Life-cylce of pharmaceuticals in the environment*. Woodhead Publishin, Elsevier.

Picó, Y., & Barceló, D. (2021). Identification of biomarkers in wastewater-based epidemiology: Main approaches and analytical methods. *TrAC Trends in Analytical Chemistry*, *145*, 116465. https://doi.org/10.1016/j.trac.2021.116465

Priyadarshini, M., Das, I., Ghangrekar, M. M., & Blaney, L. (2022). Advanced oxidation processes: Performance, advantages, and scale-up of emerging technologies. *Journal of Environmental Management*, *316*, 115295. https://doi.org/10.1016/j.jenvman.2022.115295

Proverbio, D., Kemp, F., Magni, S., Ogorzaly, L., Cauchie, H.-M., Gonçalves, J., Skupin, A., & Aalto, A. (2022). Model-based assessment of COVID-19 epidemic dynamics by wastewater analysis. *Science of The Total Environment*, *827*, 154235. https://doi.org/10.1016/j.scitotenv.2022.154235

Qiu, Q., Li, G., Dai, Y., Xu, Y., & Bao, P. (2020). Removal of antibiotic resistant microbes by Fe(II)-activated persulfate oxidation. *Journal of Hazardous Materials*, *396*, 122733. https://doi.org/10.1016/j.jhazmat.2020.122733

Rana, S., & Suresh, S. (2017). Comparison of different Coagulants for Reduction of COD from Textile industry wastewater. *Materials Today: Proceedings*, *4*(2), 567–574. https://doi.org/10.1016/j.matpr.2017.01.058

Rapp-Wright, H., McEneff, G., Murphy, B., Gamble, S., Morgan, R., Beardah, M., & Barron, L. (2017). Suspect screening and quantification of trace organic explosives in wastewater using solid phase extraction and liquid chromatography-high resolution accurate mass

spectrometry. *Journal of Hazardous Materials*, *329*, 11–21. https://doi.org/10.1016/j.jhazmat.2017.01.008

Reuschenbach, P., Silvani, M., Dammann, M., Warnecke, D., & Knacker, T. (2008). ECOSAR model performance with a large test set of industrial chemicals. *Chemosphere*, *71*(10), 1986–1995. https://doi.org/10.1016/j.chemosphere.2007.12.006

Rizzo, L. (2022). Addressing main challenges in the tertiary treatment of urban wastewater: are homogeneous photodriven AOPs the answer? *Environmental Science: Water Research & Technology*, *8*(10), 2145–2169. https://doi.org/10.1039/D2EW00146B

Rodríguez Rasero, F. J., Moya Ruano, L. A., Rasero Del Real, P., Cuberos Gómez, L., & Lorusso, N. (2022). Associations between SARS-CoV-2 RNA concentrations in wastewater and COVID-19 rates in days after sampling in small urban areas of Seville: A time series study. *Science of The Total Environment*, *806*, 150573. https://doi.org/10.1016/j.scitotenv.2021.150573

Rothman, K. J. (2012). *Epidemiology An Introduction* (2nd ed.). Oxford University Press.

Rydh Stenström, J., Kreuger, J., & Goedkoop, W. (2021). Pesticide mixture toxicity to algae in agricultural streams – Field observations and laboratory studies with in situ samples and reconstituted water. *Ecotoxicology and Environmental Safety*, *215*, 112153. https://doi.org/10.1016/j.ecoenv.2021.112153

Samal, K., Mahapatra, S., & Hibzur Ali, M. (2022). Pharmaceutical wastewater as Emerging Contaminants (EC): Treatment technologies, impact on environment and human health. *Energy Nexus*, *6*, 100076. https://doi.org/10.1016/j.nexus.2022.100076

Samal, S. (2017). Thermal plasma technology: The prospective future in material processing. *Journal of Cleaner Production*, *142*, 3131–3150. https://doi.org/10.1016/j.jclepro.2016.10.154

Sanderson, H., Johnson, D. J., Reitsma, T., Brain, R. A., Wilson, C. J., & Solomon, K. R. (2004). Ranking and prioritization of environmental risks of pharmaceuticals in surface waters. *Regulatory Toxicology and Pharmacology*, *39*(2), 158–183. https://doi.org/10.1016/j.yrtph.2003.12.006

Schoenmakers, Y. , M. S. , E. M. , P. C. (2016). *Elke dump is een plaats delict: Dumping en lozing van synthetisch drugsafval: verschijningsvormen en politieaanpak*. Reed Business, Amsterdam.

Scholtz, V., Pazlarova, J., Souskova, H., Khun, J., & Julak, J. (2015). Nonthermal plasma — A tool for decontamination and disinfection. *Biotechnology Advances*, *33*(6), 1108–1119. https://doi.org/10.1016/j.biotechadv.2015.01.002

Sellier, A., Khaska, S., & Le Gal La Salle, C. (2022). Assessment of the occurrence of 455 pharmaceutical compounds in sludge according to their physical and chemical properties: A review. *Journal of Hazardous Materials*, *426*, 128104. https://doi.org/10.1016/j.jhazmat.2021.128104

STOWA. (2008). *Demonstratieonderzoek vergaande zuiveringstechnieken op de RWZI Leiden Zuid-West*.

Tay, K. S., & Madehi, N. (2015). Ozonation of ofloxacin in water: By-products, degradation pathway and ecotoxicity assessment. *Science of The Total Environment*, *520*, 23–31. https://doi.org/10.1016/j.scitotenv.2015.03.033

Test No. 201: Alga, Growth Inhibition Test. (2006). OECD Publishing. https://doi.org/10.1787/9789264069923-en

Test No. 202: Daphnia sp. Acute Immobilisation Test. (2004). OECD. https://doi.org/10.1787/9789264069947-en

Test No. 203: Fish, Acute Toxicity Test. (2019). OECD. https://doi.org/10.1787/9789264069961-en

Thellmann, P., Köhler, H.-R., Rößler, A., Scheurer, M., Schwarz, S., Vogel, H.-J., & Triebskorn, R. (2015). Fish embryo tests with Danio rerio as a tool to evaluate surface water and sediment quality in rivers influenced by wastewater treatment plants using different treatment technologies. *Environmental Science and Pollution Research*, *22*(21), 16405–16416. https://doi.org/10.1007/s11356-014-3785-8

UK Health Security Agency. (2021, June 10). *Wastewater testing coverage data for the Environmental Monitoring for Health Protection (EMHP) programme*. Https://Www.Gov.Uk/Government/Publications/Wastewater-Testing-Coverage-Data-for-19-May-2021-Emhp-Programme/Wastewater-Testing-Coverage-Data-for-the-Environmental-Monitoring-for-Health-Protection-Emhp-Programme.

van Bergen, T. J. H. M., Rios-Miguel, A. B., Nolte, T. M., Ragas, A. M. J., van Zelm, R., Graumans, M., Scheepers, P. T. J., Jetten, M. S. M., Hendriks, A. J., & Welte, C. U. (2021). Do initial concentration and activated sludge seasonality affect pharmaceutical biotransformation rate constants? *Applied Microbiology and Biotechnology*, *105*(16–17). https://doi.org/10.1007/s00253-021-11475-9

Vasiliadou, I. A., Molina, R., Martínez, F., & Melero, J. A. (2013). Biological removal of pharmaceutical and personal care products by a mixed microbial culture: Sorption, desorption and biodegradation. *Biochemical Engineering Journal*, *81*, 108–119. https://doi.org/10.1016/j.bej.2013.10.010

Vasiliadou, I. A., Molina, R., Martinez, F., Melero, J. A., Stathopoulou, P. M., & Tsiamis, G. (2018). Toxicity assessment of pharmaceutical compounds on mixed culture from activated sludge using respirometric technique: The role of microbial community structure. *Science of The Total Environment*, *630*, 809–819. https://doi.org/10.1016/j.scitotenv.2018.02.095

Verlicchi, P., Al Aukidy, M., & Zambello, E. (2012). Occurrence of pharmaceutical compounds in urban wastewater: Removal, mass load and environmental risk after a secondary treatment—A review. *Science of The Total Environment*, *429*, 123–155. https://doi.org/10.1016/j.scitotenv.2012.04.028

von Sonntag, C. (2008). Advanced oxidation processes: mechanistic aspects. *Water Science and Technology*, *58*(5), 1015–1021. https://doi.org/10.2166/wst.2008.467

Wade, L. G. (2010). *Organic chemistry* (7th ed.). Pearson Prentice Hall.

Wang, Y., Liu, P., Zhang, H., Ibaraki, M., VanTassell, J., Geith, K., Cavallo, M., Kann, R., Saber, L., Kraft, C. S., Lane, M., Shartar, S., & Moe, C. (2022). Early warning of a COVID-19 surge on a university campus based on wastewater surveillance for SARS-CoV-2 at residence halls. *Science of The Total Environment*, *821*, 153291. https://doi.org/10.1016/j.scitotenv.2022.153291

Westerhoff, P., Mezyk, S. P., Cooper, W. J., & Minakata, D. (2007). Electron Pulse Radiolysis Determination of Hydroxyl Radical Rate Constants with Suwannee River Fulvic Acid and Other Dissolved Organic Matter Isolates. *Environmental Science & Technology*, *41*(13), 4640–4646. https://doi.org/10.1021/es062529n

World Health Organization. (2012). *Pharmaceuticals in drinking-water*.

Yang, B., Wei, T., Xiao, K., Deng, J., Yu, G., Deng, S., Li, J., Zhu, C., Duan, H., & Zhuo, Q. (2018). Effective mineralization of anti-epilepsy drug carbamazepine in aqueous solution by simultaneously electro-generated H2O2/O3 process. *Electrochimica Acta*, *290*, 203–210. https://doi.org/10.1016/j.electacta.2018.09.067

Žegura, B., Heath, E., Černoša, A., & Filipič, M. (2009). Combination of in vitro bioassays for the determination of cytotoxic and genotoxic potential of wastewater, surface water and drinking water samples. *Chemosphere*, *75*(11), 1453–1460. https://doi.org/10.1016/j.chemosphere.2009.02.041

Zhang, G., Sun, Y., Zhang, C., & Yu, Z. (2017). Decomposition of acetaminophen in water by a gas phase dielectric barrier discharge plasma combined with TiO2-rGO nanocomposite: Mechanism and degradation pathway. *Journal of Hazardous Materials*, *323*, 719–729. https://doi.org/10.1016/j.jhazmat.2016.10.008

Ziylan, A., & Ince, N. H. (2011). The occurrence and fate of anti-inflammatory and analgesic pharmaceuticals in sewage and fresh water: Treatability by conventional and non-conventional processes. *Journal of Hazardous Materials*, *187*(1–3), 24–36. https://doi.org/10.1016/j.jhazmat.2011.01.057

Chapter 2

Oxidative degradation of cyclophosphamide using thermal plasma activation and UV/H_2O_2 treatment in tap water

Martien H. F. Graumans, Wilfred F. L. M. Hoeben,
Frans G. M. Russel, Paul T. J. Scheepers

Published in:
Environmental Research 182, March 2020

Abstract

There is a growing concern about pharmaceuticals entering the aquatic environment. Many of these compounds cannot be removed completely in sewage treatment plants. To remove these unwanted medicines from water, oxidative degradation techniques may complement the current purification steps. In this paper we studied the effect of advanced oxidation on the cytostatic drug cyclophosphamide (CP) by comparing thermal plasma activation with UV/H_2O_2 treatment. Plasma activated water (PAW) contains highly reactive oxygen and nitrogen species (RONS) as a result of electric gas discharges in air over water. CP solutions in tap water were oxidised over a period of 120 min and subsequently analysed by LC-MS/MS to measure the compound degradation. Plasma activation was applied at 50, 100, or 150 W electric power input and UV/H_2O_2 treatment was carried out by the addition of H_2O_2 and placing an UV-C source above the test solution for immediate irradiation. The oxidative degradation of CP in PAW resulted in a complete degradation within 80 min at 150 W. CP was also completely degraded within 60 min applying UV/H_2O_2 oxidation. Both treatment techniques do induce different structural changes, demonstrating that CP is completely degraded in tap water.

2.1 Introduction

The widespread usage of pharmaceuticals in human healthcare and veterinary applications causes emission of anthropogenic pollutants to the environment. Via direct and indirect routes, pharmaceuticals end up in the aquatic environment causing a potential risk for the ecosystem (Magureanu et al., 2015; Zhang et al., 2013). To keep our drinking water safe, it is important to minimise the contamination of pharmaceuticals via the waste water stream. The European Union (EU) protects human health and the aquatic environment by using recommended guidelines, such as the Environmental Quality Standards Directive (2013/39/EU) and the Water Framework Directive (2000/60/EC) (ECUnion, 2000; ECUnion, 2013; Carvalho et al., 2015). The aim is to keep watercourses safe and provide guidance for monitoring of priority substances and pollutants. To complement the directives, EU prepares an up-to-date watchlist of emerging pollutants (Loos et al., 2018). In addition to these precautionary documents, the association of European waterworks advised in a memorandum to adopt a threshold of 0.1 µg/L (0.1 ng/mL) for anthropogenic pharmaceuticals in rivers and watercourses so that the contamination could be minimised (IAWR, 2013). The United States Environmental Protection Agency (EPA) has the authority to implement the Clean Water Act (CWA) and the Safe Drinking Water Act (SDWA) (Clean water act, 1972; Safe Drinking Water Act., 1974). The CWA is established to maintain surface water quality standards, where the SDWA protects public drinking water. Regarding pharmaceuticals in water, the US EPA refers to guidelines for evaluation of the risk of emerging contaminants to aquatic organisms (Stephen et al., 1985). With the continuous development of new therapeutics, aging of the population and increased global cancer burden, it is expected that the discharge of pharmaceuticals in waste water will increase in the coming years (Zhang et al., 2013; Banaschik et al., 2015; Moermond et al., 2016; Pieczynska et al., 2017). Conventional sewage treatment plant (STP) technology is based on filtration and biodegradation. Waste water effluents are treated in such a manner to prepare it for return into the environment. Hydrophilic compounds can withstand these purification steps and end up in natural waterbodies (Magureanu et al., 2015; Pieczynska et al., 2017; Ivančev-Tumbas, 2014). Previous studies analysed and detected persistent pharmaceuticals in waste water, surface water and ground water, by showing the presence of antiepileptics, contrast agents, analgesics, antibiotics and cytostatic drugs (Magureanu et al., 2015; Banaschik et al., 2015, 2018; Moermond et al., 2016; Ambuludi et al., 2013; Feng et al., 2014; Wols et al., 2013). Regarding hydrophilic cytotoxic cytostatic compounds it has become clear that detectable concentrations are found in the ng/L range both in influent and effluent of STPs (Pieczynska et al., 2017). Hospital effluents are the major contributors of cytostatic contamination, primarily due to the

emission of partially metabolised compounds excreted by treated patients (Zhang et al., 2013; Pieczynska et al., 2017; Ambuludi et al., 2013; Česen et al., 2016; Ferrando-Climent et al., 2014; Isidori et al., 2016; Moermond et al., 2018; Steger-Hartmann et al., 1996; Yin et al., 2010). One of the frequently used chemotherapeutics is cyclophosphamide (CP), which is administered for the treatment of different cancers, autoimmune diseases or as immunosuppressant after organ transplantations. Approximately 20% of the administered dose is excreted unchanged via urine and faeces, causing emission of CP into the wastewater stream (Buerge et al., 2006; Fernández et al., 2010; Steger-Hartmann et al., 1997). CP is not readily biodegradable, making the compound difficult to remove from waste water (Zhang et al., 2013; Ferrando-Climent et al., 2014; Moermond et al., 2018; Steger-Hartmann et al., 1997). Studies performed in Germany, China and Spain detected CP in hospital effluents in concentration ranges of 6–2000, 19 up to > 4500, and 5730 ng/L respectively (Zhang et al., 2013). If anthropogenic pollution exceeds water quality thresholds, oxidative degradation techniques may complement the current STP technology. Several studies have outlined advanced oxidation processes (AOPs) as an alternative treatment step to remove pharmaceuticals from (waste) water (Magureanu et al., 2015; Zhang et al., 2013; Banaschik et al., 2015; Pieczynska et al., 2017). The currently available techniques are primarily based on ozone degradation, photolytic or electrochemical processes, which generate reactive oxygen species (ROS), such as hydroxyl (radical $^{\bullet}OH$) radicals, hydroperoxyl ($HO_2^{\bullet}$) and singlet molecular oxygen ($^1O_2$) (Magureanu et al., 2010; Garcia-Ac et al., 2010). For the efficient production of reactive oxygen species, plasma technology is proposed as alternative AOP treatment. Electrical discharges in air over water result in the formation of, reactive oxygen and nitrogen species (RONS), including nitric oxide (NO), nitrogen dioxide (NO_2), nitrous acid (HNO_2), nitric acid (HNO_3) and transient nitrogen oxyacids like e.g. peroxynitrous acid (ONOOH) and peroxynitric acid (O_2NOOH) (Hoeben et al., 2019). An electric gas discharge is generated directly at the water surface, causing excitation, dissociation and ionisation of oxygen and nitrogen from the atmosphere. The gas phase produced RONS then diffuse into the liquid phase, producing plasma activated water (PAW) with a low pH (<3) and oxidative degradation potential (Magureanu et al., 2015; Banaschik et al., 2015; Ambuludi et al., 2013; Hoeben et al., 2019; Joshi and Thagard, 2013a, 2013b; Sun et al., 2006) The aim of this study was to observe the oxidative degradation efficiency and formation of transformation products by evaluating the effectiveness of bench-scale PAW technology compared to stationary UV/H_2O_2 applied to tap water dilutions spiked with CP. Additionally, is the oxidative degradation chemistry and applicability studied to observe the production of reaction intermediates.

2.2 Materials and methods

2.2.1 Chemicals and reagents

The used chemicals were all analytical grade or higher. All solutions were freshly prepared in ultrapure Milli-Q water using a Milli-Q Academic A10 system with a resistivity of 18 MΩ•cm (Millipore, Amsterdam the Netherlands). Endoxan from Baxter (Utrecht, the Netherlands) was used to prepare a 1 mg/mL (3.83 mM) CP (Cyclophosphamide, $C_7H_{15}Cl_2N_2O_2P$) stock standard solution. In Milli-Q water and diluted in aliquots of 10 µg/mL and 100 ng/mL. CP calibration standards were freshly prepared prior to the oxidative degradation studies. The derivates 4-ketocyclophosphamide (4-keto-CP), 4-hydroperoxycyclophosphamide (4-hydroperoxy-CP) and carboxyphosphamide were obtained from ASTA Medica GmbH (Essen, Germany). Calibration standards for the derivatives 4-keto-CP and 4-hydroperoxy-CP ranged from 0.5 to 50 ng/mL, and carboxyphosphamide was prepared in the range of 0.01 up to 50 ng/mL (n = 10).

2.2.2 Tap water matrix spiked with CP

To simulate a chemotherapeutic contaminated water matrix, 500 mL of Vitens tap water (Nijmegen, the Netherlands) was spiked with CP. For calibration a very wide range was required. For that we prepared calibration curves in two different ranges (C1 and C2). Prior to preparation of test solution 1 (TS1), with a CP concentration of 4 ng/mL (0.015 µM), a calibration curve 1 (C1) ranging from 0.01 to 10 ng/mL (n = 8) was prepared. Test solution 2 (TS2) was used for the characterisation and identification of possibly formed reaction intermediates and was therefore spiked with a relatively high CP concentration of 1000 ng/mL (3.83 µM). A corresponding calibration curve (C2) ranging from 200 up to 5000 ng/mL (n = 8) was prepared. The average physicochemical characteristics of the used Vitens tap water were taken from a publicly available quality standards report over the period of January 2018 to September 2018. Used tap water had an average pH of 7.71, a total organic carbon concentration (TOC) of <500 ng/mL (0.5 mg/L), and a turbidity of 0.24 NTU. Further details about the tap water matrix are provided in the supplemental data (SI **Table S1**). To quantify the CP oxidation in either TS1 or TS2, the corresponding concentration range C1 or C2 was selected.

2.2.3 Advanced oxidation processes

2.2.3.1 PAW

Plasma activation of water was performed by use of a PAW Lab Unit from VitalFluid (Eindhoven, the Netherlands), generating a thermal arc in air over water with voltages up to 40 kV. To activate test solutions, the power and time of the electric gas discharge was manually

selected in a closed cup system with ambient air, using either 50, 100 or 150 Watt (W). Throughout plasma activation for 120 min, the solution was magnetically stirred. CP oxidative degradation was directly determined by collecting samples at selected time intervals after plasma ignition (2, 4, 5, 7, 10, 15, 20, 25, 30, 40, 50, 60, 80, 100, 120 min).

2.2.3.2 UV/H_2O_2

An Aetaire UV air disinfection unit was modified to create a vent (28 cm × 7 cm) for stationary UV-C irradiation (Philips PL-L 60W/4P HO UV-C lamp, Eindhoven, the Netherlands) using 253.7 nm radiation from a low-pressure Hg lamp. A solution of 30% w/w hydrogen peroxide (H_2O_2) was purchased at Avantor Performance Materials (Deventer, the Netherlands) and added to the test solutions in three different concentrations, 970 mM (~3300 mg/L), 0.11 mM (~5 mg/L) and 0.22 mM (~10 mg/L). Immediately after adding the H_2O_2 solution, the UV source was switched on and placed ~20 cm above the glass beaker for direct irradiation (Wols et al., 2013; Bolton and Linden, 2003; Heringa et al., 2011). The UV irradiance at the tap water surface was predicted using a mathematical model proposed by Kowalski (2009) (SI paragraph **S4**). To standardise the oxidation process, treatment was performed simultaneously with plasma water activation for 120 min. The aqueous solution was magnetically stirred, and the degradation was directly measured by collecting samples at pre-selected time points corresponding to the chosen activation intervals.

2.2.4 Liquid chromatography tandem mass spectrometry analysis

Reaction intermediates and the conversion rate of CP were measured on a Acquity UPLC system from Waters Corporation (Milford, USA). The LC unit consists of a solvent degasser, quaternary solvent manager, seal wash pump, column oven and an auto-sampler. Chromatographic separation was performed on an Acquity UPLC BEH C_{18} (2.1 mm × 100 mm, 1.7 μm) reversed phase column. The auto-sampler temperature was maintained at 10 °C throughout the analysis. Gradient LC conditions were applied at a flow of 0.4 mL/min, using 2.5 μL injection volume and a column oven temperature set at 40 °C. Eluent (A) consisted of 0.1% v/v formic acid (FA, 98–100%) in 5 mM ammonium formate (NH_4HCO_2, ≥99% HPLC grade salt) in combination with eluent (B) 100% v/v acetonitrile (ACN, UHPLC-MS). These chemicals were acquired from Merck group (Darmstadt, Germany), Sigma Aldrich/Fluka Analytical (Zwijndrecht, the Netherlands) and Boom (Meppel, the Netherlands), respectively. Initial condition of 95% for eluent A was selected until 0.20 min, the fraction of 95% A was quickly decreased from 95% to 5% of A at 2.5 min 5% of mobile phase A was maintained until 4 min and subsequently ramped to 95% again at 4.5 min. The gradient program was stopped at

5 min. The LC system was online coupled to a Xevo TQ-S micro quadrupole mass spectrometer, where ionisation was achieved by electro spray ionisation (ESI). ESI was operated in positive ion mode, applying nitrogen gas at 50 L/h in the cone and 1100 L/h for desolvation. The desolvation temperature was set at 600 °C, and argon was used as collision gas during tandem mass spectrometry. The voltages selected for the capillary and cone were 2 kV and 20 V, respectively. Direct infusion of 1 µg/mL CP, 4-hydroperoxy-CP, 4-keto-CP, carboxyphosphamide or phosphoramide mustard (Niomech - IIT GmbH, Bielefeld, Germany) was performed to determine the ion transitions. Compounds were individually infused via the fluidics interface, using a flow rate of 10 µL/min, to optimise the multiple reaction monitoring (MRM) transitions with a precursor ion $[M+H]^+$ combined with the corresponding fragmented daughter ion. The optimised results for the chromatographic separation of CP and its derivates are presented in the supplemental data (SI **Table S2**).

2.2.5 Data analysis

Oxidation kinetics for both tested AOPs were analysed by use of logistic regression and first-order exponential decay. Curve fitting was applied using GraphPad Prism 5.03 statistical software (Graphpad Inc., CA, USA) to calculate the rate constants and half-lives of the observed degradation processes. Optimisation of the analytical procedure was carried out by using Intellistart direct infusion software and TargetLynx software for quantitative analyte calculation (Waters Corporation Milford, USA).

2.3 Results and discussion

2.3.1 Degradation of CP in plasma activated water

The removal rate of CP in tap water was determined as a function of the applied plasma power within the treatment time of 120 min (**Table 2.1**). At a discharge power of 50 W, no compound removal was observed. At 100 W and 150 W, 4 ng/mL CP, was removed for 94.6% within 120 min and complete removal of the parent compound was observed within 80 min, respectively. CP was also be removed within 120 min, using 150 W at a concentration of 1000 ng/mL. During thermal plasma treatment, reactive oxygen and nitrogen species are formed in time, which is well represented by a curve fit of the data to a logistic model. Using the equation $y = c/1 + a \bullet e^{(-b \bullet x)}$, the rate constant and half-life values were determined, where b is the rate constant given as k.

Table 2.1
Cyclophosphamide degradation in PAW

Start conc. (g/L)	**Discharge power** (Watt)	**Treatment time** (min)	**Conversion level** $(\%)_{(time)}$	**Energy yield** (g/kWh)	**Energy yield** (mol/J)	**Rate constant**[A] k (min^{-1})	**Half life**[B] $t_{1/2}$ (min)
$3.59 \cdot 10^{-6}$ ($n = 2$)	50	120	0 (120 min)	n/a	n/a	n/a	n/a
$4.04 \cdot 10^{-6}$ ($n = 3$)	100	120	94.6 (120 min)	$9.55 \cdot 10^{-6}$	$1.02 \cdot 10^{-14}$	0.02	69.4
$3.99 \cdot 10^{-6}$ ($n = 3$)	150	120	100 (80 min)	$9.98 \cdot 10^{-6}$	$1.06 \cdot 10^{-14}$	0.15	29.1
$9.86 \cdot 10^{-4}$ ($n = 4$)	150	120	100 (120 min)	$1.64 \cdot 10^{-3}$	$1.74 \cdot 10^{-12}$	0.07	40.1

[A] Data were fitted to the equation: $y=c/1+a \cdot e^{(-b \cdot x)}$, b = the constant determined by growth which is presented as = k
[B] ln (a)/b: Equals point of maximum growth which is given as the half-life $t_{1/2}$

To measure the degradation efficiency of the currently applied thermal plasma technology, equations (**1**), (**2**) were used according to literature (Magureanu et al., 2010, 2015). In these papers the degradation effectiveness was compared for pharmaceuticals treated under different non-thermal plasma conditions. For the present study, the given energy yield (mol/J) is a measure of the CP conversion per unit energy and implicates the degradation efficiency of the applied plasma technique. According to the results displayed in **Table 2.1**, the degradation efficiency appears to be dependent on multiple factors, such as the initial concentration, the power of discharge, reducing pH and how the plasma is generated. However, it should be noted that the electric power input is not exclusively spent on the plasma formation, but is also unavoidably lost to resistive heating of the gas phase and aqueous solution. Sun et al. (2006) demonstrated that submerged 50 kV plasma discharges in water convert only 1% of the electric energy input into UV irradiation energy (Sun et al., 2006). With the currently applied thermal plasma technology, using electric gas discharges in air over water with voltages up to 40 kV, it is expected that less than 1% of the electric power is converted into UV irradiation (Sun et al., 2006; Lukes et al., 2008; Thirumdas et al., 2018).

$$R = (1 - C_t/C_0) \cdot 100 \quad (\mathbf{1})$$

R = Conversion level (%)
C_t = Concentration of the test substance at treatment time t (g/L)
C_0 = Initial compound concentration (g/L)

$$Y = (C_0 \cdot V \cdot R)/ (P \cdot t) \cdot 1/100 = \text{Energy yield (g/kWh)} \quad (\mathbf{2})$$

V = Volume (L)
P = Discharge power (kW)
t = Treatment time (h)

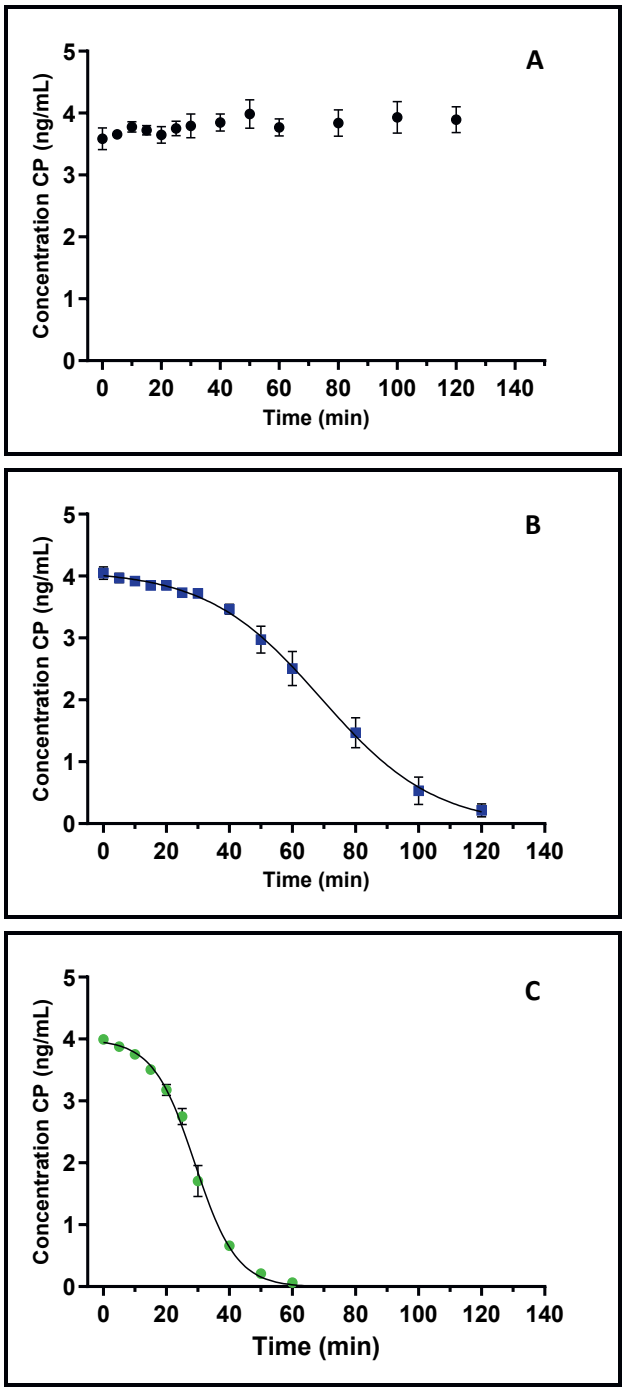

Fig. 2.1. Degradation curves for TS1 4 ng/mL CP. Dissimilar degradation patterns were observed by the application of different discharge powers. No actual degradation was observed at 50 W (**A**), indicating that time-dependent CP removal can be achieved by increasing the power gradually to 100 W (**B**) and 150 W (**C**), respectively.

CP was fairly efficiently degraded by use of plasma activation in a relative large volume of tap water (500 mL). The degradation patterns were accelerated at increasing discharge power (50 < 100 < 150 W), showing the rapid increase of RONS overtime (**Fig. 2.1**). A logistic curve was observed in **Fig. 2.1B** and **C**, with rate constants of 0.02 min^{-1} and 0.15 min^{-1}, respectively. Applying 50 W discharge, the power was either insufficient to produce reactive species for oxidative degradation, or the reaction kinetics were too slow to observe the changes in the period of activation. Another ancillary of increased thermal plasma discharge is the ascending water temperature over time (SI **Fig. S5**). It is expected that temperature increases pharmaceutical degradation (Loftsson, 2014a). Additionally, Johsi and Thagard (Joshi and Thagard, 2013a, 2013b) suggested that apart from production of RONS also thermal dissociation of water may occur. Having thus a thermal plasma arc warmer than >2000 K will cause dissociation of water molecules at the surface interface with the water.

Evaluation of non-thermal plasma techniques like thin liquid film, liquid droplet plasma and dielectric barrier discharges (DBD) demonstrated that the energy demand is low if the non-thermal plasma discharge is applied in the gas phase, in contrast to a liquid phase (Magureanu et al., 2015). In relation to previously described non-thermal plasma reactors (Magureanu et al., 2015), our current bench-scale PAW process appeared to be a feasible laboratory application, though further optimisation is needed to improve its efficacy. In addition, rapid mass transfer is expected from plasma discharges performed on a thin layer of water, suggesting that this configuration has an increased surface-to-volume ratio. Such an increased ratio might be explained by the more rapid production of reactive species in a relative smaller water volume, compared to our thermal plasma activation in 500 mL of tap water. Gas-phase pulsed corona discharges (PCD) is such a technique (Ajo et al., 2018). The PCD system is a vertical reactor in which pharmaceutical contaminated water is showered through the non-thermal plasma, that produced efficient conversion rates ranging from 19% up to 100% for 24 different compounds (Ajo et al., 2018). For paracetamol (580 ng/mL), a 89% conversion rate was obtained in this pilot study with an energy yield of 0.52 g/kWh using 30 W power discharge (Ajo et al., 2018). It is difficult to compare different AOPs due to a large variation in experimental conditions, particularly if the selected pharmaceutical, initial concentration and performed plasma treatment conditions all differ. We have shown that with our PAW application different concentrations of CP at 150 W could be removed, suggesting that this application also may have oxidative potential for other persistent pharmaceuticals.

2.3.2 Degradation of CP in UV/H_2O_2 treated water

To evaluate the oxidative photo-degradation kinetics of CP, a stationary UV/H_2O_2 experiment was carried out for comparison to thermal plasma activation. During the photolytic process, hydroxyl radicals are formed through UV irradiation of hydrogen peroxide ($H_2O_2 + h\nu \rightarrow 2\ ^{\bullet}OH$). The optimal H_2O_2 concentration was determined in a series of exploratory measurements using concentrations of 970 mM (~3300 mg/L), 0.11 mM (~5 mg/L) and 0.22 mM (~10 mg/L). Other researchers used 10 mg/L H_2O_2 for UV/H_2O_2 treatment (Wols et al., 2013; Heringa et al., 2011). From the results presented in **Fig. 2.2**, a time-dependent exponential decay of the CP concentration was observed. These data were subsequently log-normally transformed to obtain a linear relationship. To determine the rate constant and half-life values, first-order reaction kinetics $-d[A]/dt = k_1\,[A]$ was used. The slope of the fitted line represents the rate constant k. Conversion levels of treated TS1 and TS2 showed that 100% of CP can be removed within 60 min using 0.22 mM (~10 mg/L) of H_2O_2 combined with an UV-C lamp, see **Table 2.2**.

Table 2.2
Rate constant using UV light with H_2O_2 (after Log-normal transformation)

Start conc. CP (ng/mL) H_2O_2 Treatment (Conc.)	**Conversion level** (%)(time)	**Rate constant**[A] k (min^{-1})	**Half life**[B] $t_{1/2}$ (min)	**Correlation coefficient** (R^2)[C]
4 ng/mL UV-C H_2O_2 (970 mM) **(*n* = 2)**	92.7 **(120 min)**	0.05	14.1	0.85
4 ng/mL UV-C H_2O_2 (0.11 mM) **(*n* = 1)**	100 **(100 min)**	0.06	11.2	0.98
4 ng/mL UV-C H_2O_2 (0.22 mM) **(*n* = 1)**	100 **(40 min)**	0.22	3.14	0.87
1000 ng/mL UV-C H_2O_2 (0.22 mM) **(*n* = 3)**	100 **(40 min)**	0.17	4.15	0.83

[A] Rate constant is based on the first-order reaction rate using the equation: **$-d[A]/dt = k_1\,[A]$**. Actual CP concentrations are lognormal transformed to obtain a linear equation.

[B] Half-life of the first order reaction was calculated using: **$t_{1/2} = \ln 2 / k$**

[C] Linear correlation coefficient obtained from the log-normal transformed data

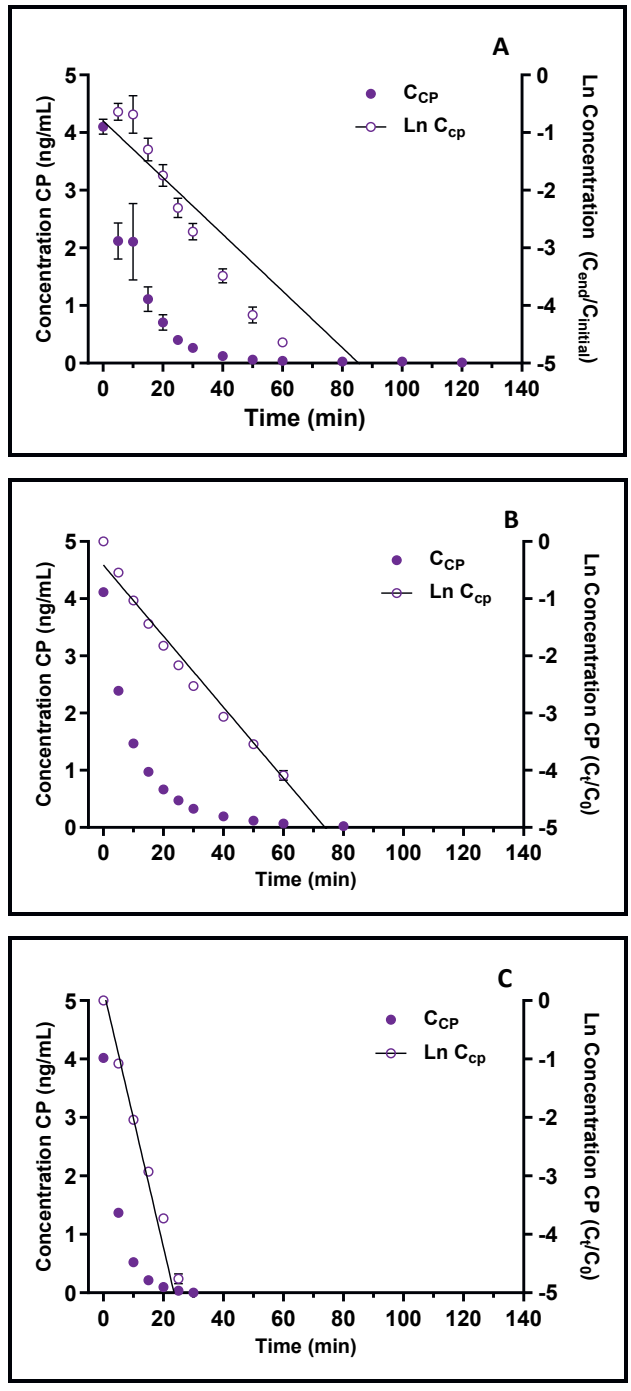

Fig. 2.2. Degradation rate of 4 ng/mL CP applied on TS1 in water at different hydrogen peroxide concentrations in combination with an UV-C source. With UV-C/H_2O_2 (970 mM) treatment no complete CP removal was obtained within 120 min (**A**), in contrast with H_2O_2 concentrations 0.11 (**B**) or 0.22 mM (**C**), which showed complete and rapid CP removal rates.

A similar UV/H_2O_2 degradation experiment was performed on 20,000 ng/mL CP by Lutterbeck et al. (2015) In that study the optimal hydrogen peroxide concentration was determined by testing 9.8 mM, 14.7 mM and 19.6 mM H_2O_2. The best mineralisation was achieved using 9.8 mM of H_2O_2, resulting in 72.5% mineralisation within 256 min (Lutterbeck et al., 2015). Actual mineralisation was determined by measurement of dissolved organic carbon (DOC). Our results were based on the degradation of CP. Inhibited reaction kinetics was observed with 970 mM H_2O_2 (**Fig. 2.2A**), whereas no complete CP removal was observed within 120 min. An excess amount of H_2O_2 will cause retardation of the oxidation kinetics by recombination of hydroxyl radicals and the conversion of H_2O_2 to less reactive perhydroxyl radicals ($HO_2^{\bullet}$) by the hydroxyl radicals ($^{\bullet}OH$) (Pieczynska et al., 2017; Lutterbeck et al., 2015). Similar results were reported by Lutterbeck et al. (2015) who attributed also the loss in mineralisation efficiency to too high concentrations of H_2O_2. In addition, it is important to note that removal efficiency of pharmaceuticals using UV/H_2O_2 treatment is dependent on multiple factors, since also non-priority organic compounds present in a water matrix can act as potential radical scavengers (Wols et al., 2013). Certain pharmaceuticals tend to be sensitive to UV and hydroxyl radicals, but other compounds are degraded by only one of them (Wols et al., 2013; Heringa et al., 2011). Aqueous CP was also moderately degraded by direct photolysis using short-wavelength UV (253.7 nm). A treatment duration of 120 min with UV-C resulted in a conversion of approximately 33% of the 4 ng/mL CP (**Fig. S4**). These results indicate that the photolytic degradation pathway is dependent on the UV source used. As presented in the literature, UV-C irradiation is often produced with wavelengths ranging from 200 to 280 nm, having thus the capability to excite molecular oxygen (O_2) to singlet oxygen ($^1O_2$) and to dissociate molecular oxygen and water into reactive oxygen species such as ozone (O_3) or hydroxyl radicals ($^{\bullet}OH$), respectively (Wols et al., 2013; Kowalski, 2009). The UV-C irradiation applied in this paper was theoretically determined to be ~114 W/m^2 at the tap water surface (Kowalski, 2009). This irradiation level suggests that the currently applied laboratory setup is less efficient than actual UV reactors where (waste)water is actively flushed along multiple UV lamps (Heringa et al., 2011). The applied UV-C lamp surface irradiance is determined to be ~862 W/m^2, indicating that the irradiance decreases when the distance is increasing. Kowalski (2009) described an irradiance prediction model which was used in the absence of an UV-dose radiometer (SI paragraph **S4** for the UV irradiance and dose calculation).

2.3.3 Formation of oxidative degradation products

In addition to the analysis of CP, a LC-MS/MS method was developed for the detection of oxidative degradation products. The reaction products 4-keto-CP, 4-hydroperoxy-CP and carboxyphosphamide were all identified (**Fig. 2.3**). The transformation product concentration at a certain time point (C_t) was quantified and plotted against the initial CP concentration (C_0) and expressed as a percentage (C_t/C_0 •100%). 4-Hydroperoxy-CP was semi-quantitatively quantified to 4-keto-CP, and was selectively detected with LC-MS/MS by using the corresponding and optimised MRM transition. 1000 ng/mL CP was moderately degraded using plasma activation, whereas UV/H_2O_2 treatment appeared to be an immediate removal process, with rate constants of 0.07 min−1 ($t_{1/2}$: 40 min) and 0.17 min−1 ($t_{1/2}$: 4 min), respectively. During the plasma activation process, first the RONS need to be formed, whereas UV/H_2O_2 oxidation starts immediately by both hydroxyl radical reactions and UV photon energy. That the degradation kinetics of both AOPs are distinct is further demonstrated by the transformation product formation. The inactive metabolite 4-keto-CP is the only intermediate observed after PAW treatment, with a maximum of (±SD) (3.2% ± 1.6) formed at 60 min, **Fig. 2.3A/B**.

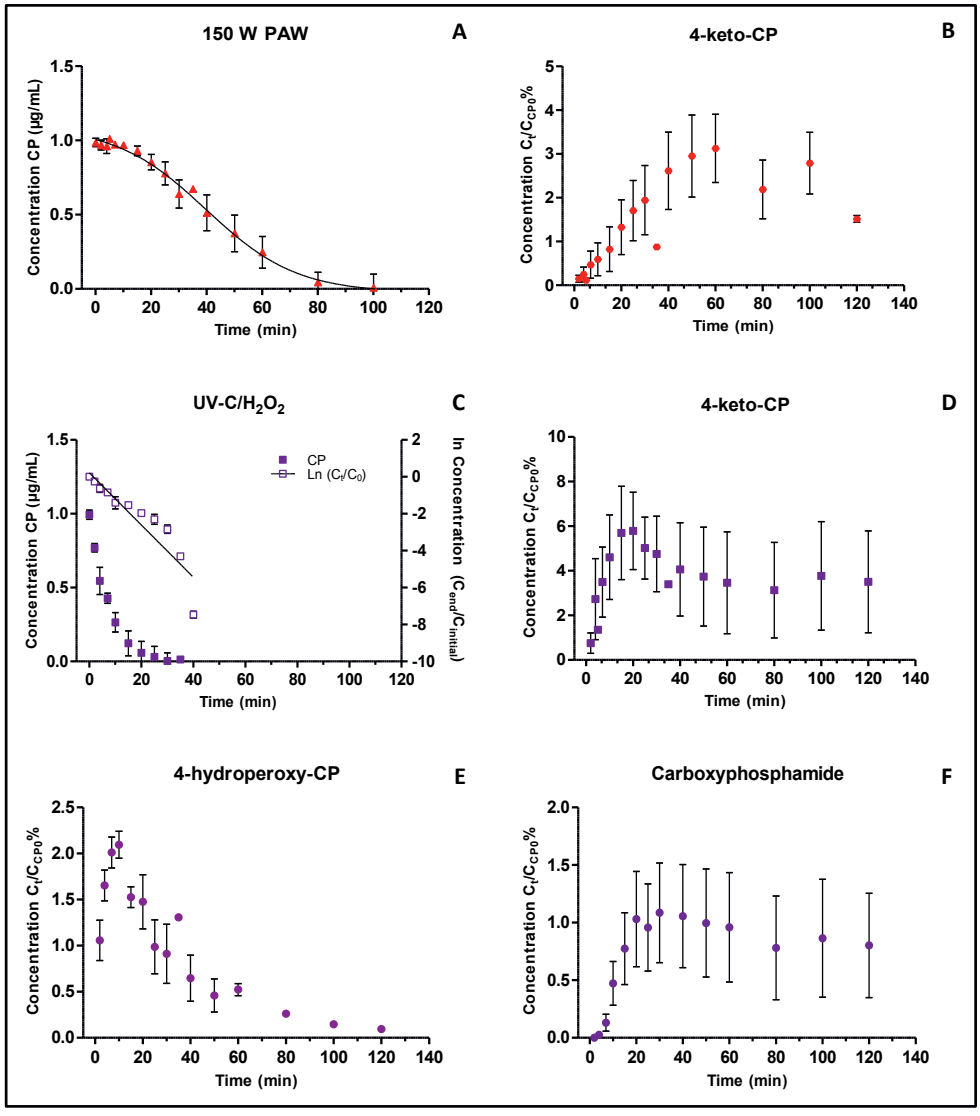

Fig. 2.3. Degradation curves of 1000 ng/mL CP spiked in tap water, either treated with plasma activation at 150 W of PAW (**A**) or UV/H_2O_2 (**C**). Directly after treatment for both techniques the products of oxidative degradation were observed, showing that 4-keto-CP (**B**/**D**) was formed with both UV/H_2O_2 and plasma activation. Reaction intermediates 4-hydroperoxy-CP (**E**) and carboxyphosphamide (**F**) were characteristic intermediates formed during UV/H_2O_2 treatment.

The oxidative degradation products 4-keto-CP, 4-hydroperoxy-CP and carboxyphosphamide were detected during UV/H_2O_2 treatment (**Fig. 2.4**), and the maximum formation of these compounds was rapidly seen at 20 min (5.8% ± 3.5), 10 min (1.68% ± 0.10) and 30 min (1.1% ± 1.0), respectively. In contrast, no phosphoramide mustard was found, indicating that this CP metabolite might not be stable enough in this strongly oxidative aqueous environment. This observation is in line with the literature where it was explained that the reactive aziridinium ring, derived from nitrogen mustards (bis-(2-chloroethyl)methylamine), will react with water molecules to form an inactive hydrolysis product, bis-(2-hydroxyethyl)methylamine (SI **Fig. S6**) (Loftsson, 2014b). Probably more reaction intermediates are formed during the oxidative degradation, but the current quantification method was not optimised to measure any other products. Additionally, **Fig. 2.3** (**B**, **D-F**) suggests that the oxidative degradation intermediates formed are most likely further degraded. This observation is in line with Lutterbeck et al. (2015), who demonstrated that CP is for 72.5% mineralised within 256 min. That no complete mineralisation was observed in PAW, is probably due to the two steps of the degradation process, first the parent molecule is completely converted into intermediate products, which are than subsequently further degraded (Zhang et al., 2016; Lutterbeck et al., 2015).

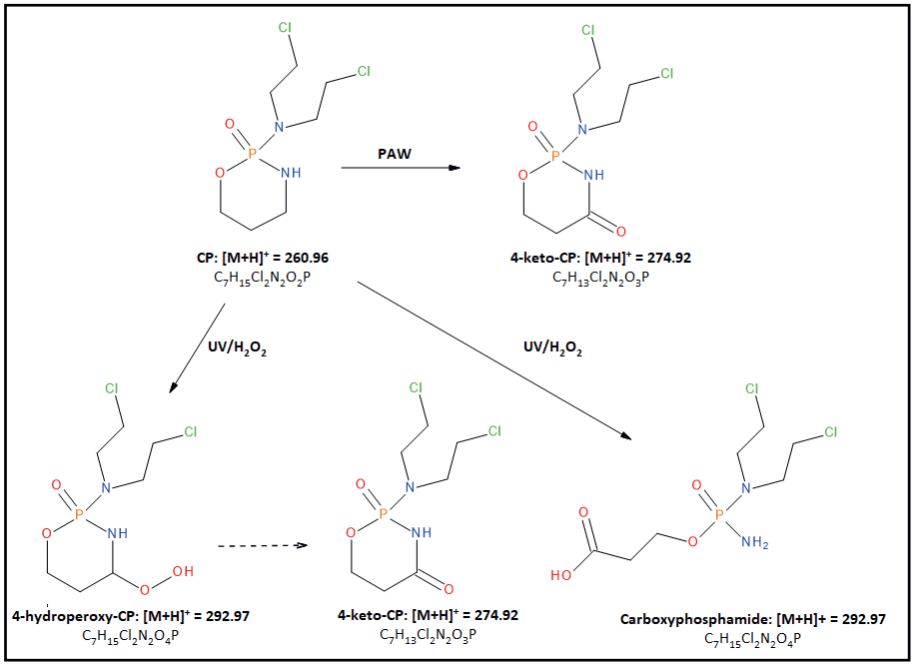

Fig. 2.4. Molecular structures of the precursor ions formed during LC-MS/MS detection. The dotted arrow represents reactivity of 4-hydroperoxy-CP, suggesting that this compound is first transformed to 4-hydroxy-CP before being converted to 4-keto-CP.

2.3.4 Implications of toxicity and risk assessment

Thermal plasma activation applied in the current study produced RONS, which might attribute to the formation of less aggressive oxidation byproducts compared to ozonation, hydroxyl degradation and non-thermal plasma treatment. Further analysis should reveal whether RONS are capable of gradual formation of more stable and less toxic transformation products. In an ecotoxicological assay performed by Lutterbeck et al. (2015), no significant luminescence inhibition of the bacterium *V. Fischeri* was observed after exposure of UV/H_2O_2 treated aqueous CP solution. Toxicity testing of the parent compound gave a lowest observed effect concentration (LOEC) of 120 mg/L, indicating that a relatively high concentration of CP is needed to produce an inhibitory effect in *V. Fischeri*. An explanation for this high LOEC might be that CP is a prodrug, and needs to be metabolically activated to become cytotoxic. (Buerge et al., 2006; Lutterbeck et al., 2015; Busse et al., 1997; de Jonge et al., 2006). Besides the efficient and complete degradation of CP in the present study, 4-hydroperoxy-CP was identified during UV/H_2O_2 treatment. 4-Hydroperoxy-CP is a very potent toxic compound capable of alkylating DNA strands. (National Cancer Institute thesaraus Website). The formation of such reaction intermediate is in line with the literature suggesting, that toxic byproducts may arise during treatment with hydroxyl radicals (Moermond et al., 2016; Wols et al., 2013; Fernández et al., 2010; Heringa et al., 2011; Lutterbeck et al., 2015). Active carbon filtration or membrane filtration are therefore often used as an extra treatment step to remove residual active compounds (Heringa et al., 2011; Ajo et al., 2018). Furthermore, it must be taken into account that additional unidentified reaction intermediates may be formed during oxidative degradation, since metabolic activation also produces byproducts such as acrolein and chloroacetaldehyde (Busse et al., 1997; de Jonge et al., 2006). Chloroacetaldehyde is formed in small quantities since only 10% of the CP dosage is dechloroethylated (MacAllister et al., 2013). During advanced oxidation the yield of these smaller molecules can become higher since no enzymatic oxidation is involved. Both compounds cause adverse effects in humans at concentrations above 300 µM, where chloroacetaldehyde is neurotoxic and nephrotoxic and acrolein is held responsible for inflammation of the bladder (MacAllister et al., 2013). Although, previous toxicity testing of only CP poses a minimal risk to *V. Fischeri*, it must be noted that antineoplastic agents and their transformation products are unwanted in aquatic sources used for drinking water preparation. This observation is in line with the US EPA Clean Water Act and the European Water Framework Directive.

2.3.5 Strengths and limitations of the advanced oxidation laboratory experiments

A strength of our study was the efficacy testing of thermal plasma technology in comparison to the existing and much studied UV/H_2O_2 treatment. Our well-defined laboratory set-up allowed the study of the PAW application at multiple energy inputs compared to UV/H_2O_2 treatment using different concentrations of hydrogen peroxide. This design clearly showed that oxidative degradation for both AOPs are distinct and depend on different parameters such as plasma power input or hydrogen peroxide amount added. In this experimental setting both AOPs were extensively evaluated reflecting similar kinetics also reported by other researchers (Ajo et al., 2018, Fernández et al., 2010, Lutterbeck et al., 2015, Wols et al., 2013, Zhang et al., 2016). The use of tap water as a well standardised and simple test matrix is a clear limitation in the light of the value of this technology for wastewater treatment. A further limitation of our study is that the tests were performed at laboratory scale and should be interpreted with caution regarding extrapolation to real-life. Furthermore, our study reports on degradation of one pharmaceutical product, and the results cannot be readily extrapolated to other medicine residues or their metabolites.

2.4 Conclusions

Our laboratory study showed the performance of thermal plasma compared to UV/H_2O_2 treatment by oxidative degradation of CP. The used techniques do have distinct chemical kinetics, which was confirmed by decay of the parent compound and the formation of degradation intermediates. Further research into AOPs should reveal whether PAW might be a suitable application for the removal of other persistent pharmaceuticals from water as well. More complex (waste) water matrices should be tested, and toxicity assays must be used to evaluate the toxicity before and after oxidative treatment. Further method development will reveal whether plasma treatment may complement current sewage water processes for the elimination of persistent pharmaceuticals. To reduce also the formation of toxic by-products, longer treatment times can achieve a more complete mineralisation. Alternatively, the combination of multiple sustainable water treatment technologies might complement the conventional water purification process.

Declaration of competing interest

None.

Acknowledgement

This work was supported by the INTERREG Deutschland-Nederland program [grant number 142118]. The authors would like to thank R. Anzion and M. van Dael for their technical advice

and support in the laboratory. We also would like to thank Vitalfluid, who provided the PAW lab unit and the UV-C source.

Supplementary data

The supporting information contains the metabolic pathway of CP, physicochemical parameters of the used tap water, the LC-MS/MS method optimisation study, the Kowalski irradiance prediction model, a demonstration of water temperature increase during thermal plasma activation and a modified figure to demonstrate the instability of phosphoramide mustard in water.

Literature

Ajo, P., Preis, S., Vornamo, T., Mänttäri, M., Kallioinen, M., & Louhi-Kultanen, M. (2018). Hospital wastewater treatment with pilot-scale pulsed corona discharge for removal of pharmaceutical residues. *Journal of Environmental Chemical Engineering*, *6*(2), 1569–1577. https://doi.org/10.1016/j.jece.2018.02.007

Ambuludi, S. L., Panizza, M., Oturan, N., Özcan, A., & Oturan, M. A. (2013). Kinetic behavior of anti-inflammatory drug ibuprofen in aqueous medium during its degradation by electrochemical advanced oxidation. *Environmental Science and Pollution Research*, *20*(4), 2381–2389. https://doi.org/10.1007/s11356-012-1123-6

Banaschik, R., Jablonowski, H., Bednarski, P. J., & Kolb, J. F. (2018). Degradation and intermediates of diclofenac as instructive example for decomposition of recalcitrant pharmaceuticals by hydroxyl radicals generated with pulsed corona plasma in water. *Journal of Hazardous Materials*, *342*, 651–660. https://doi.org/10.1016/j.jhazmat.2017.08.058

Banaschik, R., Lukes, P., Jablonowski, H., Hammer, M. U., Weltmann, K.-D., & Kolb, J. F. (2015). Potential of pulsed corona discharges generated in water for the degradation of persistent pharmaceutical residues. *Water Research*, *84*, 127–135. https://doi.org/10.1016/j.watres.2015.07.018

Bolton, J. R., & Linden, K. G. (2003). Standardization of Methods for Fluence (UV Dose) Determination in Bench-Scale UV Experiments. *Journal of Environmental Engineering*, *129*(3), 209–215. https://doi.org/10.1061/(ASCE)0733-9372(2003)129:3(209)

Buerge, I. J., Buser, H.-R., Poiger, T., & Müller, M. D. (2006). Occurrence and Fate of the Cytostatic Drugs Cyclophosphamide and Ifosfamide in Wastewater and Surface Waters. *Environmental Science & Technology*, *40*(23), 7242–7250. https://doi.org/10.1021/es0609405

Busse, D., Busch, F. W., Bohnenstengel, F., Eichelbaum, M., Fischer, P., Opalinska, J., Schumacher, K., Schweizer, E., & Kroemer, H. K. (1997). Dose escalation of cyclophosphamide in patients with breast cancer: consequences for pharmacokinetics and metabolism. *Journal of Clinical Oncology*, *15*(5), 1885–1896. https://doi.org/10.1200/JCO.1997.15.5.1885

Carvalho, R. N. , Ceriani, L., Ippolito, A., & Lettieri, T. (2015). *Development of the First Watch List under the Environmental Quality Standards Directive*. *LB-NA-27142-EN-N*. https://doi.org/10.2788/101376

Česen, M., Kosjek, T., Busetti, F., Kompare, B., & Heath, E. (2016). Human metabolites and transformation products of cyclophosphamide and ifosfamide: analysis, occurrence and formation during abiotic treatments. *Environmental Science and Pollution Research*, *23*(11), 11209–11223. https://doi.org/10.1007/s11356-016-6321-1

Clean Water Act, Pub. L. No. 92–500, the 92nd United States Congress (1972).

de Jonge, M. E., Huitema, A. D. R., Beijnen, J. H., & Rodenhuis, S. (2006). High exposures to bioactivated cyclophosphamide are related to the occurrence of veno-occlusive disease

of the liver following high-dose chemotherapy. *British Journal of Cancer*, *94*(9), 1226–1230. https://doi.org/10.1038/sj.bjc.6603097

Directive 2000/60/EC of the European Parliament and of the Council of 23 October 2000 Establishing a Framework for Community Action in the Field of Water Policy. Union, E., Ed. EUR-Lex: Access to European Union law: 2000; pp p. 1–73.

Directive 2013/39/EU of the European Parliament and of the Council of 12 August 2013 Amending Directives 2000/60/EC and 2008/105/EC as Regards Priority Substances in the Field of Water Policy, Pub. L. No. 2013/39/EU (2013).

Feng, L., Oturan, N., van Hullebusch, E. D., Esposito, G., & Oturan, M. A. (2014). Degradation of anti-inflammatory drug ketoprofen by electro-oxidation: comparison of electro-Fenton and anodic oxidation processes. *Environmental Science and Pollution Research*, *21*(14), 8406–8416. https://doi.org/10.1007/s11356-014-2774-2

Fernández, L. A., Hernández, C., Bataller, M., Véliz, E., López, A., Ledea, O., & Padrón, S. (2010). Cyclophosphamide degradation by advanced oxidation processes. *Water and Environment Journal*, *24*(3), 174–180. https://doi.org/10.1111/j.1747-6593.2009.00169.x

Ferrando-Climent, L., Rodriguez-Mozaz, S., & Barceló, D. (2014). Incidence of anticancer drugs in an aquatic urban system: From hospital effluents through urban wastewater to natural environment. *Environmental Pollution*, *193*, 216–223. https://doi.org/10.1016/j.envpol.2014.07.002

Garcia-Ac, A., Broséus, R., Vincent, S., Barbeau, B., Prévost, M., & Sauvé, S. (2010). Oxidation kinetics of cyclophosphamide and methotrexate by ozone in drinking water. *Chemosphere*, *79*(11), 1056–1063. https://doi.org/10.1016/j.chemosphere.2010.03.032

Heringa, M. B., Harmsen, D. J. H., Beerendonk, E. F., Reus, A. A., Krul, C. A. M., Metz, D. H., & IJpelaar, G. F. (2011). Formation and removal of genotoxic activity during UV/H2O2–GAC treatment of drinking water. *Water Research*, *45*(1), 366–374. https://doi.org/10.1016/j.watres.2010.08.008

Hoeben, W. F. L. M., van Ooij, P. P., Schram, D. C., Huiskamp, T., Pemen, A. J. M., & Lukeš, P. (2019). On the Possibilities of Straightforward Characterization of Plasma Activated Water. *Plasma Chemistry and Plasma Processing*, *39*(3), 597–626. https://doi.org/10.1007/s11090-019-09976-7

IAWR. (2013). *Memorandum regarding the protection of European rivers and watercourses in order to protect the provision of drinking water.*

Isidori, M., Lavorgna, M., Russo, C., Kundi, M., Žegura, B., Novak, M., Filipič, M., Mišík, M., Knasmueller, S., de Alda, M. L., Barceló, D., Žonja, B., Česen, M., Ščančar, J., Kosjek, T., & Heath, E. (2016). Chemical and toxicological characterisation of anticancer drugs in hospital and municipal wastewaters from Slovenia and Spain. *Environmental Pollution*, *219*, 275–287. https://doi.org/10.1016/j.envpol.2016.10.039

Ivančev-Tumbas, I. (2014). The fate and importance of organics in drinking water treatment: a review. *Environmental Science and Pollution Research*, *21*(20), 11794–11810. https://doi.org/10.1007/s11356-014-2894-8

Joshi, R. P., & Thagard, S. M. (2013a). Streamer-Like Electrical Discharges in Water: Part I. Fundamental Mechanisms. *Plasma Chemistry and Plasma Processing*, *33*(1), 1–15. https://doi.org/10.1007/s11090-012-9425-5

Joshi, R. P., & Thagard, S. M. (2013b). Streamer-Like Electrical Discharges in Water: Part II. Environmental Applications. *Plasma Chemistry and Plasma Processing*, *33*(1), 17–49. https://doi.org/10.1007/s11090-013-9436-x

Kowalski, W. (2009). *Ultraviolet Germicidal Irradiation Handbook*. Springer Berlin Heidelberg. https://doi.org/10.1007/978-3-642-01999-9

Loftsson, T., Effect of Temperature. In Drug Stability for Pharmaceutical Scientists. Academic Press: Oxford, 2014; pp 31-40.

Loftsson, T., Nitrogen Mustards. In Drug Stability for Pharmaceutical Scientists. Academic Press: Oxford, 2014; pp 75-76.

Loos, R., Marinov, D., Sanseverino, I., Napierska, D., & Lettieri, T. (2018). *Review of the 1st Watch List under the Water Framework Directive and recommendations for the 2nd Watch List*. *KJ-NA-29173-EN-C (print),KJ-NA-29173-EN-N (online)*. https://doi.org/10.2760/614367 (online),10.2760/701879 (print)

Lukes, P., Clupek, M., Babicky, V., & Sunka, P. (2008). Ultraviolet radiation from the pulsed corona discharge in water. *Plasma Sources Science and Technology*, *17*(2), 024012. https://doi.org/10.1088/0963-0252/17/2/024012

Lutterbeck, C. A., Machado, Ê. L., & Kümmerer, K. (2015). Photodegradation of the antineoplastic cyclophosphamide: A comparative study of the efficiencies of UV/H2O2, UV/Fe2+/H2O2 and UV/TiO2 processes. *Chemosphere*, *120*, 538–546. https://doi.org/10.1016/j.chemosphere.2014.08.076

MacAllister, S. L., Martin-Brisac, N., Lau, V., Yang, K., & O'Brien, P. J. (2013). Acrolein and chloroacetaldehyde: An examination of the cell and cell-free biomarkers of toxicity. *Chemico-Biological Interactions*, *202*(1–3), 259–266. https://doi.org/10.1016/j.cbi.2012.11.017

Magureanu, M., Mandache, N. B., & Parvulescu, V. I. (2015). Degradation of pharmaceutical compounds in water by non-thermal plasma treatment. *Water Research*, *81*, 124–136. https://doi.org/10.1016/j.watres.2015.05.037

Magureanu, M., Piroi, D., Mandache, N. B., David, V., Medvedovici, A., & Parvulescu, V. I. (2010). Degradation of pharmaceutical compound pentoxifylline in water by non-thermal plasma treatment. *Water Research*, *44*(11), 3445–3453. https://doi.org/10.1016/j.watres.2010.03.020

Moermond C.T.A., Smit. C. E., van Leerdam R.C., van der Aa, N.G.F.M., Montforts M.H.M.M. (2016) Geneesmiddelen en waterkwaliteit; Rijksinstituut voor Volksgezondheid en Mileu, Ministerie van Volksgezondheid, Welzijn en Sport: Bilthoven

Moermond C., Venhuis. B. , van elk M. , O. A. , van V. P. , M. M. , van D. J. (2018). *Cytostatics in Dutch surface water: Use, presence and risks to the aquatic environment*.

National Cancer Institute thesaurus Website; https://ncit.nci.nih.gov/ncitbrowser/

Pieczyńska, A., Fiszka Borzyszkowska, A., Ofiarska, A., & Siedlecka, E. M. (2017). Removal of cytostatic drugs by AOPs: A review of applied processes in the context of green technology. *Critical Reviews in Environmental Science and Technology*, *47*(14), 1282–1335. https://doi.org/10.1080/10643389.2017.1370990

Safe Drinking Water Act, Pub. L. No. 93–523, the 93rd United States Congress (1974).

Steger-Hartmann, T., Kümmerer, K., & Hartmann, A. (1997). Biological Degradation of Cyclophosphamide and Its Occurrence in Sewage Water. *Ecotoxicology and Environmental Safety*, *36*(2), 174–179. https://doi.org/10.1006/eesa.1996.1506

Steger-Hartmann, T., Kümmerer, K., & Schecker, J. (1996). Trace analysis of the antineoplastics ifosfamide and cyclophosphamide in sewage water by twostep solid-phase extraction and gas chromatography-mass spectrometry. *Journal of Chromatography A*, *726*(1–2), 179–184. https://doi.org/10.1016/0021-9673(95)01063-7

Stephen, C. E., Mount, D.I., Hansen, D. J., Gentile, J.R., Chapman, G. A., Brungs, W. A., (1985). *Guidelines for Deriving numerical national Water Quality Criteria for the Protection Of Aquatic organisms and Their Uses*.

Sun, B., Kunitomo, S., & Igarashi, C. (2006). Characteristics of ultraviolet light and radicals formed by pulsed discharge in water. *Journal of Physics D: Applied Physics*, *39*(17), 3814–3820. https://doi.org/10.1088/0022-3727/39/17/016

Thirumdas, R., Kothakota, A., Annapure, U., Siliveru, K., Blundell, R., Gatt, R., & Valdramidis, V. P. (2018). Plasma activated water (PAW): Chemistry, physico-chemical properties, applications in food and agriculture. *Trends in Food Science & Technology*, *77*, 21–31. https://doi.org/10.1016/j.tifs.2018.05.007

Wols, B. A., Hofman-Caris, C. H. M., Harmsen, D. J. H., & Beerendonk, E. F. (2013). Degradation of 40 selected pharmaceuticals by UV/H2O2. *Water Research*, *47*(15), 5876–5888. https://doi.org/10.1016/j.watres.2013.07.008

Yin, J., Yang, Y., Li, K., Zhang, J., & Shao, B. (2010). Analysis of Anticancer Drugs in Sewage Water By Selective SPE and UPLC-ESI-MS-MS. *Journal of Chromatographic Science*, *48*(10), 781–789. https://doi.org/10.1093/chromsci/48.10.781

Zhang, J., Chang, V. W. C., Giannis, A., & Wang, J.-Y. (2013). Removal of cytostatic drugs from aquatic environment: A review. *Science of The Total Environment*, *445–446*, 281–298. https://doi.org/10.1016/j.scitotenv.2012.12.061

Zhang, Y., Yu, T., Han, W., Sun, X., Li, J., Shen, J., & Wang, L. (2016). Electrochemical treatment of anticancer drugs wastewater containing 5-Fluoro-2-Methoxypyrimidine using a tubular porous electrode electrocatalytic reactor. *Electrochimica Acta*, *220*, 211–221. https://doi.org/10.1016/j.electacta.2016.10.104

Supplemental Information for Chapter 2

This document provides additional information to support the main text of **Chapter 2**. **Paragraph S.2.1** describes the metabolic pathway of cyclophosphamide, illustrating this in **Fig. S1**. **Paragraph S.2.2** consists of **Table S1** which summarises the physicochemical parameters of the tap water used during the oxidative degradation experiments. **Paragraph S.2.3** describes the optimisation study to measure CP reduction and characterises the degradation intermediates. This section is supported by **Table S2**, which contains the LC-MS/MS data acquisition parameters. **Paragraph S.2.4** explains Kowalski's irradiance prediction model. This section includes **Table S3, S4** and corresponding **Fig. S2**, **S3** and **S4**. **Fig. S5** demonstrates the increase in water temperature during thermal plasma treatment. **Fig. S6** is a modified reaction scheme from Loftsson, showing the instability of phosphoramide mustard in water.

S.2.1 Metabolic pathway cyclophosphamide

As shown in **Fig. S1**. CP is a prodrug which is partly activated by different metabolic pathways (Buerge et al., 2006; Busse et al., 1997; de Jonge et al., 2006). The most evident route is via cytochrome CYP450, causing 4-hydroxylation, where the parent compound is converted into 4-hydroxy-clyclophosphamide (4-hydroxy-CP) in equilibrium with its tautomer aldophosphamide (Hales, 1982). The produced intermediates, 4-hydroxy-CP and aldophosphamide are unstable and thus rapidly further transformed. 4-Hydroxy-CP is defused into the inactive metabolite 4-keto-cyclophosphamide (4-keto-CP), whereas aldophosphamide is enzymatically metabolised into carboxyphosphamide, which leads to the formation of nornitrogen mustard. The non-enzymatic conversion of aldophosphamide results in formation of phosphoramide mustard and acrolein (Giorgianni et al., 2000). Acrolein is held responsible for adverse side effects in the urinary tract (Busse et al., 1997). Phosphoramide mustard and nornitrogen mustard are alkylating agents, involved in formation of DNA adducts (de Jonge et al., 2006; Giorgianni et al., 2000; Hales, 1982, 1983; Mirkes, 1985; Thomson & Colvin, 1974).

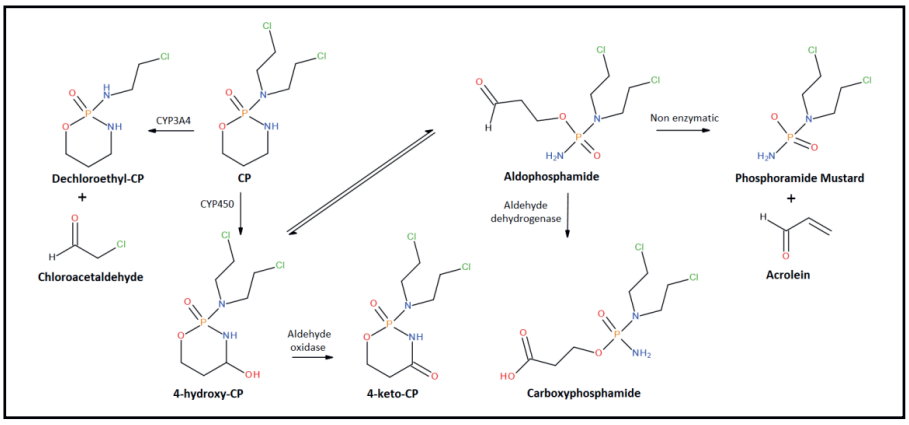

Fig. S1. The metabolic conversion of cyclophosphamide in the human body. The alternative biotransformation pathway for CP is oxidation via cytochrome P450 3A4, oxidising the parent molecule at the 2-chloroethyl amino side chain, forming dechloroethylcyclophosphamide and the by-product chloroacetaldehyde. Although carboxyphosphamide is a stable intermediate (in addition to 4-keto-CP), it can be further oxdatively degraded to a phosphonic acid ester and nornitrogen mustard ($NH(CH_2CH_2Cl)_2$), which also is an alkylating agent. Adapted from de Jonge et al (de Jonge et al., 2006).

S.2.2 Physicochemical characteristics tap water

The drinking water company Vitens is the largest supplier of fresh water for consumer use in the Netherlands, providing tap water in the region of Nijmegen. According to the public available website the physicochemical characteristics are all reported per water extraction location. Extraction point Heumensoord is the water source for the tap water delivered at the Radboud university medical center. According to the Vitens report (Vitens, 2019), the average parameters are given including the minimum and maxium values of n = 39 measurements.

Table S1.
Adopted physicochemical water properties from water extraction point Heumensoord

Measured parameter	Unit	Average (minimum, maximum)
Turbidity	NTU[A]	0.24 (0.11; 0.55)
Total Organic Carbon (TOC)	mg/L	< 0.5 (<0.5; 0.6)
Acidity	pH	7.71 (7.42; 7.93)
Minerals	mg/L	-
Cl_2		26 (25; 26)
PO_4		< 0.03 (<0.03; 0.03)
Si		6.16
SO_4		46 (44; 47)
Nitrogen compounds	mg/L	-
NH_4		< 0.03 (<0.03; 0.03)
NO_2		< 0.01 (<0.01; 0.01)
NO_3		14.8 (13.4; 17)

[A]: Nephelometric Turbidity Unit

S.2.3 Optimising parameters of the analytical method

Compound selectivity was obtained by using two MRM transitions selecting a quantification and a target ion, see **Table S2**. Repeatability was determined by $n = 10$ injections of the highest standard for CP, showing that the retention time was $t_{r\,(min)}$ 2.51. On the other hand, optimisation of the analysis of the CP derivatives carboxyphosphamide, 4-keto-CP and 4-hydroperoxy-CP posed a challenge, primarily for the analyte 4-hydroperoxy-CP, due to its instability when prepared in Milli-Q. Good chromatographic separation was observed for 4-hydroperoxy-CP ($t_{r\,(min)}$ 2.46), however no actual repeatable result and steady linearity could be achieved when injecting a series of calibration standards (0.01 – 100 ng/mL). During the LC-MS/MS data acquisition, also a peak for 4-keto-CP ($t_{r\,(min)}$ 2.31) was obtained, indicating that 4-hydroperoxy-CP transforms into a more stable derivate when prepared in Milli-Q. This is confirmed in the early paper of Kodo et al (Kodo et al., 1985). showing that 4-hydroperoxy-CP dissolved in aqueous solution will rapidly convert into to 4-hydroxy-CP, the major metabolite of CP formed by cytochrome P450 enzymes. 4-Hydroxy-CP is by aldehyde oxidase transformed into the stable derivate 4-keto-CP (Busse et al., 1997; de Jonge et al., 2006). Since it is suggested that 4-keto-CP is a stable derivate of 4-hydroperoxy-CP, 4-keto-CP is selected for the semi-quantitative quantification of 4-hydroperoxy-CP. Limits of detection (LOD) and quantification (LOQ) for all prepared analytes were determined according to the Q2B document of the FDA, using the slope of the calibration curve and the standard deviation for the system response of the blank (FDA, 1996). During the injection of C2 standards (0.02 – 5 µg/mL ($n = 8$), CP quantification was based on a quadratic curve fitting.

Table S2.
LC-MS/MS method optimisation parameters

Compound	**Retention time** t_r(min)	**MRM Transitions** *Quantification ion* *Target ion* (*m/z*)	**Cone Voltage** (V)	**Collision Energy** (V)	**LOD**[A] (ng/mL)	**LOQ**[B] (ng/mL)	**Correlation coefficient** R^2 **Linear range** (ng/mL)
CP	2.51	260.96 > 139.93	44	18	0.01	0.03	0.9996
		260.96 > 105.62	44	24			0.01-10
D4-CP (IS)	2.51	265 > 109.94	52	18	ND	ND	ND
		265 > 143.69	52	22			
Carboxy-phosphamide	2.25	292.97 > 220.98	14	24	0.01	0.02	0.9565
		292.97 > 54.87	14	18			0.1-100
4-keto-CP	2.31	274.97 > 54.81	62	36	0.94	2.86	0.9991
		274.97 > 62.86	62	28			0.1-100

Table S2. *Continued*

4-hydroperoxy-CP	2.46	292.97 > 259.01	24	6	ND	ND	ND
		292.97 > 55.90	24	24			ND
Phosphoramide mustard[C]	1.81	220.97 > 141.86	38	14	ND	ND	ND
		220.97 > 62.91	38	28			ND

[A] **LOD** = 3.3 * SD / *b*, where SD is the standard deviation of the response of the blank and b the slope of the linear range.

[B] **LOQ** = 10 * SD / *b*, where SD is the standard deviation of the response of the blank and b the slope of the linear range.

[C] Phosphoramide mustard, is only included in the LC-MS / MS methodology to screen for this analyte after oxidative treatment of CP.

S.2.4 UV-C irradiance prediction

In the absence of an UV-dose radiometer the UV irradiance at the tap water surface is predicted according to a mathematical model described by Kowalski, see equation **A1** and **A2** (Kowalski, 2009). Equation **A1** determines the view factor (F), which is used to compute the irradiance at any differential area coming from the cylindrical lamp structure, see **Fig. S2**. The values used in equation **A1** are derived from the UV source parameters and distance from the lamp to the (water) surface, see **Fig. S2**. *Specifications* of the used Philips PL-L 60W/4P HO UV-C source, were taken from the Aetaire UV air disinfection unit manual, see **Table S3**. Equation **A2** is used to estimate the irradiance at the surface of interest. The UV power output (W) is dived by the lamp surface (cm^2) and is multiplied by the view factor (F). With the current laboratory setup the actual distance between the lamp and the water surface is 23.5 cm, showing that the predicted irradiance is ~114 W/m^2. **Fig. S3** demonstrates irradiance differences of two similar UV-C lamps. It is found that not only the distance is of great influence but that also the lamp specifications do affect the UV irradiance. To compute the UV dose from the irradiance level, equation **A3** can be used. **Table S4** demonstrate the UV dose for certain exposure times.

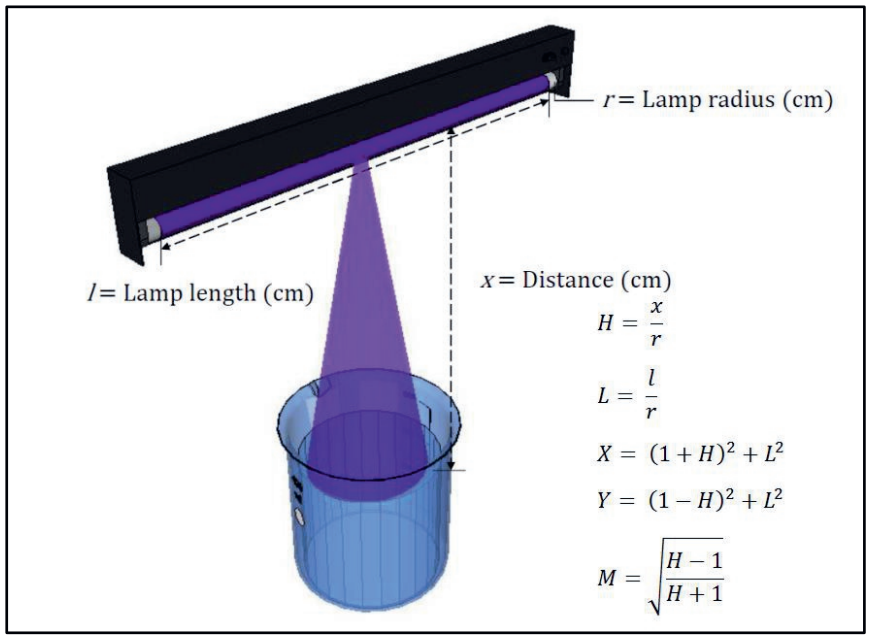

Fig. S2. A schematic representation of the UV/H_2O_2 laboratory setup, including the lamp parameters needed for the view factor calculation in equation **A1**. Line source UV is irradiated from a cylindrical lamp structure.

$$F = \frac{L}{\pi \bullet H} \bullet \left[\frac{1}{L} \bullet \tan^{-1}\left(\frac{L}{\sqrt{H^2-1}}\right) - \tan^{-1}(M) + \frac{X-2\bullet H}{\sqrt{X \bullet Y}} \bullet \tan^{-1}\left(M \bullet \sqrt{\frac{X}{Y}}\right) \right] \quad \textbf{(A1)}$$

$$I = \frac{E_{uv}}{2 \bullet \pi \bullet r \bullet l} \bullet F \quad \textbf{(A2)}$$

$$I = Irradiance\ (W/m^2)$$

$$E_{uv} = UV\ power\ output$$

$$UV\ dose\ \left(\frac{J}{m^2}\right) = Irradiance\ (W/m^2) \bullet Exposure\ time\ (s) \quad \textbf{(A3)}$$

Table S3.
Predicted irradiance levels using the UV-C lamp product sheet specifications

Lamp	UV-C wavelength (nm)	UV-C_{output} (W)	Length (cm)	Radius (cm)	Distance (cm)	Lamp Surface Irradiance (W/m^2)	View factor (F)	Predicted irradiance at water surface (W/m^2)
Philips PL-L60W/TUV[A]	253.7	17.5	41.75	0.45	23.3	1482.48	0.049	73.69
Philips PL-L60/4P HO[B]	253.7	19.0	39.0	0.9	23.3	861.52	0.13	114.29

[A]: UV-C source parameters of the Philips PL-L60W/TUV (Kowalski 2009).

[B]: UV-C source parameters according of the Philips PL-L 60W/4P HO product sheet (Philips UVC Technology).

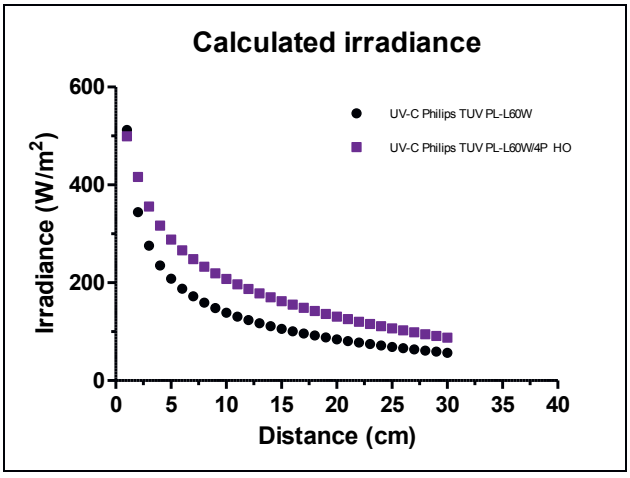

Fig. S3. Predicted irradiance levels of the used Philips PL-L 60W/4P HO (■) compared to a similar UV-C source (●). It is estimated in the range of 1 to 30 cm that the irradiance decreases when the distance from source is increased.

Table S4.
Predicted UV dose by multiplying the irradiance level with the exposure time

	Predicted irradiance at water surface (W/m^2)	Exposure time (s)	Predicted UV dose at water surface (J/m^2)
Philips PL-L 60/4P HO	114.29	1	114.29
		10	1142.9
		100	11429
		1000	114290

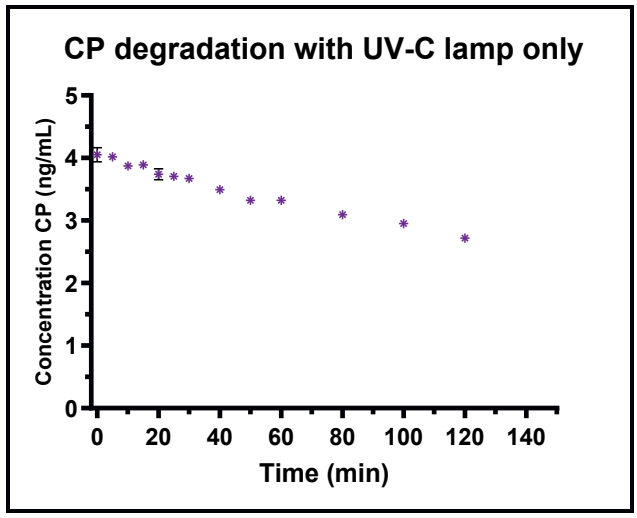

Fig. S4. Degradation data of CP (*) exposed to UV-C only. This experiment is carried out as a control to observe the reactivity of UV-C irradiance only.

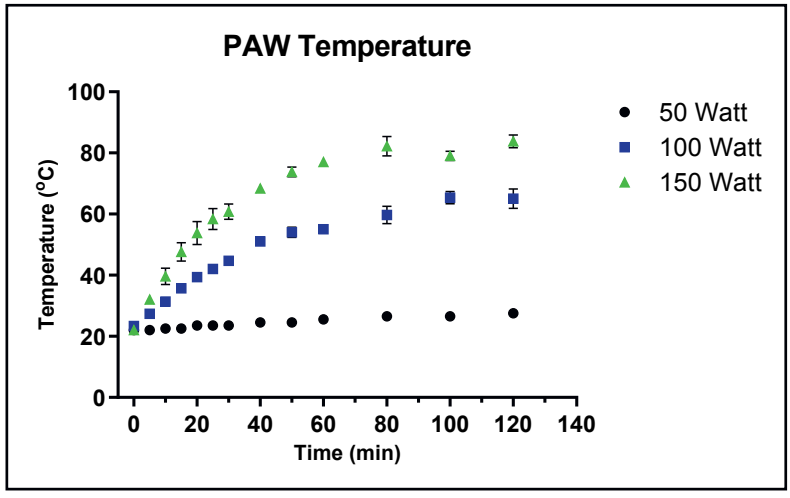

Fig. S5. The increase in water temperature is proportional to the plasma power that is applied, showing that the quickest rise is observed applying 150 W > 100 W > 50 W.

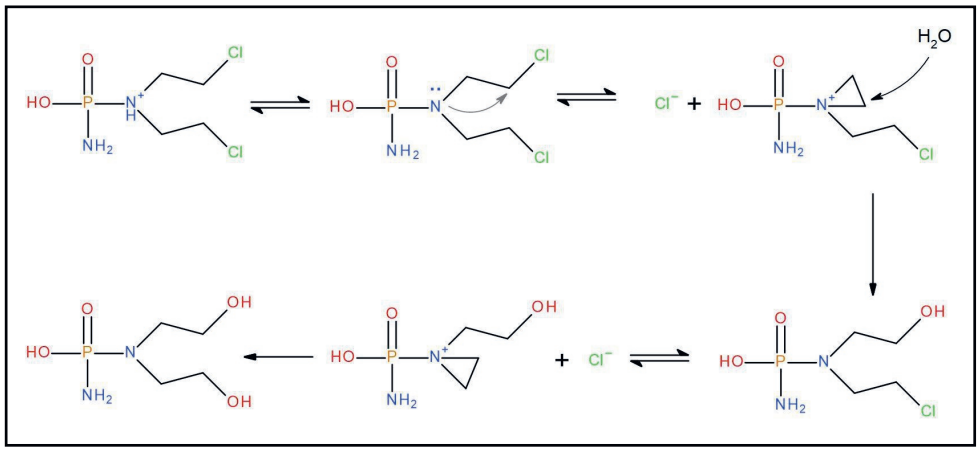

Fig. S6. Chemical reaction of the of phospharmide mustard in water. This figure is adapted from Loftsson demonstrating that the reactive aziridinium ring reacts with water to form an inactive *bis*-(2-hydroxyethyl) methylamine chain (Loftsson, 2014).

Literature

Buerge, I. J., Buser, H.-R., Poiger, T., & Müller, M. D. (2006). Occurrence and Fate of the Cytostatic Drugs Cyclophosphamide and Ifosfamide in Wastewater and Surface Waters. *Environmental Science & Technology*, *40*(23), 7242–7250. https://doi.org/10.1021/es0609405

Busse, D., Busch, F. W., Bohnenstengel, F., Eichelbaum, M., Fischer, P., Opalinska, J., Schumacher, K., Schweizer, E., & Kroemer, H. K. (1997). Dose escalation of cyclophosphamide in patients with breast cancer: consequences for pharmacokinetics and metabolism. *Journal of Clinical Oncology*, *15*(5), 1885–1896. https://doi.org/10.1200/JCO.1997.15.5.1885

de Jonge, M. E., Huitema, A. D. R., Beijnen, J. H., & Rodenhuis, S. (2006). High exposures to bioactivated cyclophosphamide are related to the occurrence of veno-occlusive disease of the liver following high-dose chemotherapy. *British Journal of Cancer*, *94*(9), 1226–1230. https://doi.org/10.1038/sj.bjc.6603097

Drink water company Vitens Website; https://www.vitens.nl/service/waterkwaliteit/waterkwaliteitsoverzichten

FDA. 1996. Q2b validation of analytical procedures: Methodology. U. S. FDA https://www.fda.gov/downloads/drugs/guidances/ucm073384.pdf

Giorgianni, F., Bridson, P. K., Sorrentino, B. P., Pohl, J., & Blakley, R. L. (2000). Inactivation of aldophosphamide by human aldehyde dehydrogenase isozyme 3. *Biochemical Pharmacology*, *60*(3), 325–338. https://doi.org/10.1016/S0006-2952(00)00344-0

Hales, B. F. (1982). Comparison of the mutagenicity and teratogenicity of cyclophosphamide and its active metabolites, 4-hydroxycyclophosphamide, phosphoramide mustard, and acrolein. *Cancer Research*, *42*(8), 3016–3021.

Hales, B. F. (1983). Relative mutagenicity and teratogenicity of cyclophosphamide and two of its structural analogs. *Biochemical Pharmacology*, *32*(24), 3791–3795. https://doi.org/10.1016/0006-2952(83)90151-X

Kodo, H., Bonavida, B., Colvin, M., & Gale, R. P. (1985). Dose —Response effects of 4-hydroperoxycyclophosphamide on human T and B cell function in vitro. *International Journal of Immunopharmacology*, *7*(4), 555–560. https://doi.org/10.1016/0192-0561(85)90076-1

Kowalski, W. (2009). *Ultraviolet Germicidal Irradiation Handbook*. Springer Berlin Heidelberg. https://doi.org/10.1007/978-3-642-01999-9

Loftsson, T., Nitrogen Mustards. In *Drug Stability for Pharmaceutical Scientists*. Academic Press: Oxford, 2014; pp 75-76.

Mirkes, P. E. (1985). Cyclophosphamide teratogenesis: A review. *Teratogenesis, Carcinogenesis, and Mutagenesis*, *5*(2), 75–88. https://doi.org/10.1002/tcm.1770050202

Philips PL-L 60W/4P HO product leaflet Website; https://www.assets.lighting.philips.com/is/content/PhilipsLighting/fp927909004007-pss-global

Philips TUV PL-L- Compact solution for professional applications Website; https://www.assets.lighting.philips.com/is/content/PhilipsLighting/comf2779-pss-en_us

Thomson, M., & Colvin, M. (1974). Chemical oxidation of cyclophosphamide and 4-methylcyclophosphamide. *Cancer Research*, *34*(5), 981–985.

Chapter 3

Thermal plasma activation and UV/H_2O_2 oxidative degradation of pharmaceutical residues

Martien H. F. Graumans, Wilfred F. L. M. Hoeben,
Maurice F. P. van Dael, Rob B. M. Anzion,
Frans G. M. Russel, Paul T. J. Scheepers

Published in:
Environmental Research 195, April 2021

Abstract

The aquatic environment becomes increasingly contaminated by anthropogenic pollutants such as pharmaceutical residues. Due to poor biodegradation and continuous discharge of persistent compounds in sewage water samples, pharmaceutical residues might end up in surface waters when not removed. To minimise this pollution, onsite wastewater treatment techniques might complement conventional waste water treatment plants (WWTPs). Advanced oxidation processes are useful techniques, since reactive oxygen species (ROS) are used for the degradation of unwanted medicine residues. In this paper we have studied the advanced oxidation in a controlled laboratory setting using thermal plasma and UV/H_2O_2 treatment. Five different matrices, Milli-Q water, tap water, synthetic urine, diluted urine and synthetic sewage water were spiked with 14 pharmaceuticals with a concentration of 5µg/L. All compounds were reduced or completely decomposed by both 150 W thermal plasma and UV/H_2O_2 treatment. Additionally, also hospital sewage water was tested. First the concentrations of 10 pharmaceutical residues were determined by liquid chromatography mass spectrometry (LC-MS/MS). The pharmaceutical concentration ranged from 0.08 up to 2400 µg/L. With the application of 150 W thermal plasma or UV/H_2O_2, it was found that overall pharmaceutical degradation in hospital sewage water were nearly equivalent to the results obtained in the synthetic sewage water. However, based on the chemical abatement kinetics it was demonstrated that the degree of degradation decreases with increasing matrix complexity. Since reactive oxygen and nitrogen species (RONS) are continuously produced, thermal plasma treatment has the advantage over UV/H_2O_2 treatment.

3.1 Introduction

Aquatic ecosystems are increasingly polluted with anthropogenic compounds such as industrial waste, personal care products, microplastics, pesticides and pharmaceutical residues. Pharmaceutical pollution has received more attention in recent years, due to their effect on the aquatic ecosystem and potential risk for the drinking water quality (Peake et al. 2016; Petrie et al. 2016; Banaschik et al. 2018). Improper disposal, runoff from manure and the continuous excretion from users cause the introduction of pharmaceuticals into the hydrosphere (Magureanu et al. 2015; Souza and Feris 2016; Li et al. 2019). Complete or partially metabolised pharmaceuticals are discharged via domestic and hospital effluents. These effluents are often complex chemical mixtures where pharmaceuticals and metabolites mix with other wastewater ingredients such as soap or other detergents (Beier et al. 2010; Ferrando-Climent et al. 2014; Peake et al. 2016; Ajo et al. 2018). Excreted pharmaceuticals may be metabolised to more bioactive compounds than the administered parent drug. Conventional wastewater treatment plants (WWTPs) cannot completely remove all pharmaceutical residues. Due to continuous discharge and various wastewater treatment technologies, the degradation efficiency for each individual compound will differ from region to region (Peake et al. 2016). Certain WWTPs do convert glucuronide metabolites back into their pristine structure by enzymatic processes (Ajo et al. 2018; Li et al. 2019). Antiepileptics, contrast agents, analgesics, antibiotics and cytostatic drugs are pharmaceutical classes often identified in raw hospital effluents (Beier et al. 2010; Ferrando-Climent et al. 2014; Ajo et al. 2018). To complement and ease conventional WWTPs, onsite wastewater treatment techniques are proposed (Gerrity et al. 2010; Banaschik et al. 2015; Ajo et al. 2018). Different techniques such as coagulation-flocculation (Suarez et al. 2009), reverse osmosis (Beier et al. 2010) or advanced oxidation processes (AOPs) (Kohler et al. 2012; Ajo et al. 2018) are studied on pilot-scale to treat hospital wastewater. However, further development of a fully operational on-site treatment technique is often economically too expensive for hospitals to realise (Banaschik et al. 2015; Ajo et al. 2018). AOPs covers the principles of using ROS for the degradation of contaminants by ozone, hydrogen peroxide, peroxone (O_3/H_2O_2) Fenton reaction (Fe^{2+}/H_2O_2), UV, photocatalytic supercritical and non-thermal gas discharges based oxidative degradation technology (Banaschik et al. 2015; Magureanu et al. 2015; Marković et al. 2015). According to Ajo et al. 2018, plasma treatment is the most efficient technique to produce ROS. In previous studies high degradation efficiencies were observed for pharmaceuticals treated with non-thermal plasma (Banaschik et al. 2018) or the combination of non-thermal plasma with iron as a catalyst (Marković et al. 2015). Plasma-driven activation of water is a new AOP that uses a hot arc

(thermal plasma) in air over water to increase both reactive oxygen and nitrogen species (RONS) in water (Hoeben et al. 2019; Graumans et al. 2020). In a previous optimisation laboratory-scale experiment we demonstrated that a thermal arc discharged in air over water is capable of the degradation of cyclophosphamide in tap water (Graumans et al. 2020). The aim of the present study was to determine the applicability of thermal plasma to complex matrices. Pharmaceuticals were added to different aquatic matrices, see **Fig. 3.1**. Subsequently a generic extraction technique was developed to determine 14 selected compounds. This method was used to analyse pharmaceutical residues in synthetic and real wastewater matrices such as hospital and domestic sewage water. After analytical determination and characterisation of the pharmaceutical residues the hospital effluent was also plasma-treated, to determine the efficacy on real wastewater samples. Due to the wide variety in physicochemical properties of the selected pharmaceuticals, in addition to solid phase extraction, a novel liquid-liquid extraction method for the polar component metformin was developed.

3.2 Materials and Methods

3.2.1 Chemicals and reagents

Pharmaceutical standards, iopamidol (IOP), diatrizoic acid (DIA), fluoxetine (FLU), diclofenac (DF), metoprolol (MET), carbamazepine (CB), terbutaline (TER), phenazone (PHE), acetaminophen (APAP), ciprofloxacin (CIP), doxycycline (DOX) and metformin (MF), all with >98% purity were retrieved from either Sigma Aldrich/Fluka Analytical (Zwijndrecht, the Netherlands) or Merck Group (Darmstadt, Germany). Endoxan and Iomeron were obtained from Baxter (Utrecht, the Netherlands) and Bracco (Konstanz, Germany) respectively used to prepare a stock solution for cyclophosphamide (CP) and iomeprol (IOM). Mobile phase and buffer solutions were freshly prepared in ultrapure water using a Milli-Q Academic A10 system with a resistivity of 18 MΩ•cm (Millipore, Amsterdam the Netherlands). Pharmaceutical stock solutions, with a concentration of 1.0 mg/mL were prepared in 50:50 (v/v) methanol water. Single aliquots of 10.0 µg/mL were subsequently prepared in Milli-Q water and further diluted together to have a pharmaceutical mixture (n = 14) with a concentration of 100.0 µg/L. Prior to analysis and solid phase extraction calibration standards were freshly prepared, ranging from 0.5 up to 100.0 µg/L (n = 6). Deuterated internal standards (dIS) were all obtained from Toronto Research Chemicals (North York, Canada) and prepared as single stock solutions (1.0 mg/mL) in methanol (SI **paragraph S.3.4**). Compounds needed for the preparation of buffers and simulation matrices included NH_4HCO_2, NaCl, Na_2SO_4, KCl, KH_2PO_4, $CaCl_2 \bullet 2H_2O$, NH_4Cl, K_2HPO_4, $MgSO_4$, sodium dodecyl sulfate, creatine, urea, peptone and meat extract. These

chemicals were either acquired from Sigma Aldrich/Fluka Analytical (Zwijndrecht, the Netherlands) or Merck Group (Darmstadt, Germany). UPLC-MS analytical grade chemicals formic acid (FA), methanol (MeOH) and acetonitrile (ACN) were purchased at Merck Group (Darmstadt, Germany) and Boom B.V. (Meppel, the Netherlands) respectively.

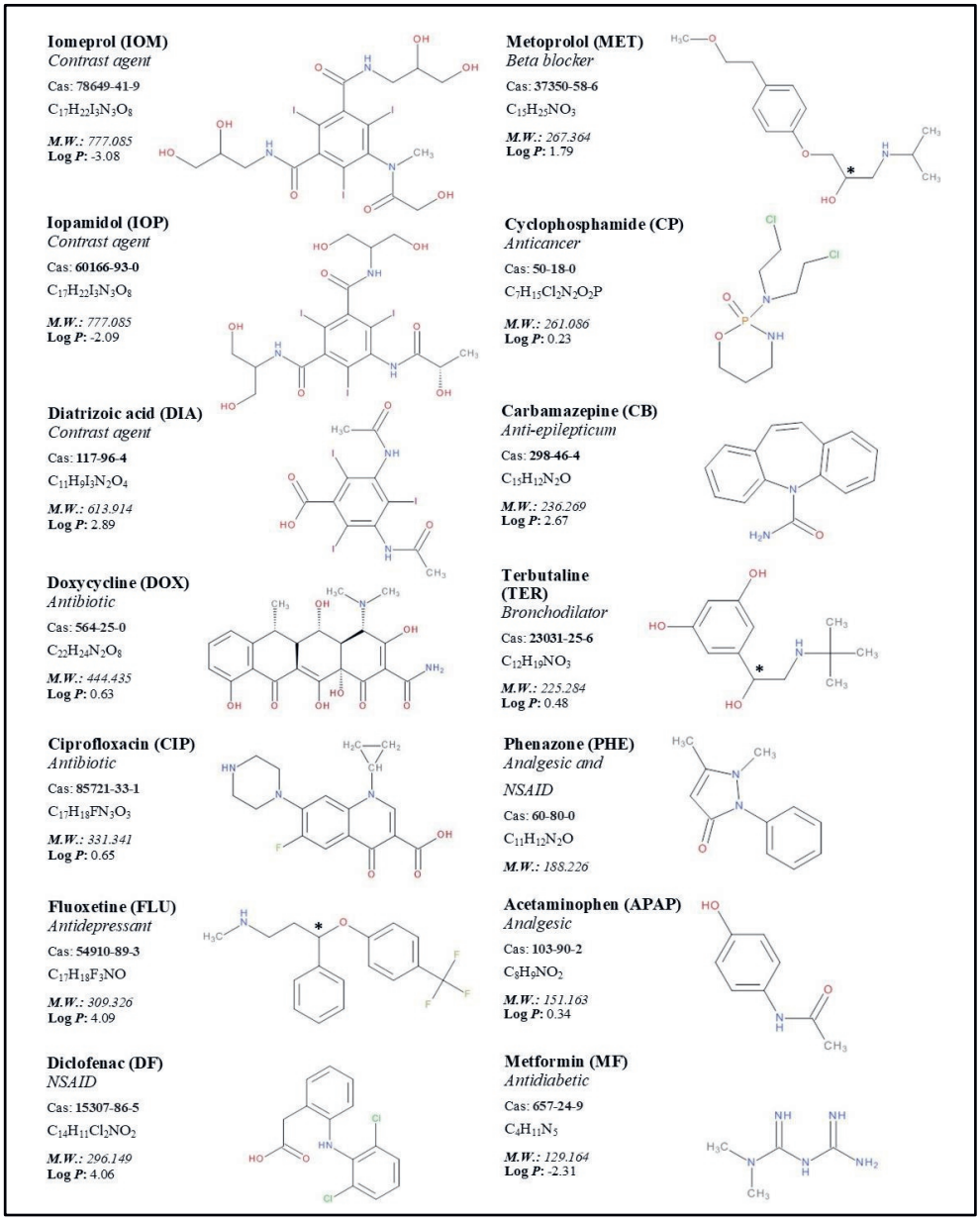

Fig. 3.1. The 14 selected pharmaceutical compounds, including their classifications and physicochemical properties. Chiral points for FLU, MET and TER are marked with an asterisk (*).

3.2.2 Advanced oxidation processes

3.2.2.1 Plasma-driven water activation

Thermal plasma discharge was performed using a laboratory-scale plasma activation unit from VitalFluid (Eindhoven, the Netherlands), comprising a 150 W, 1 MHz dual resonant power modulator with 8 kV arc operation voltage, creating a hot arc in air over water (Pemen et al. 2017; Hoeben et al. 2019). A thermal electric discharge with voltages up to 40 kV was generated in air over water. Thermal arc operation was performed in ambient air with a power output of 150 Watt (W). To maintain the temperature of the water during activation between 20 – 35 ºC, the plasma unit was equipped with an active Peltier cooler.

3.2.2.2 UV-C/H_2O_2

Stationary UV-C irradiation was performed by using a modified Aetaire UV air disinfection unit. To irradiate UV-C (Philips PL-L 60W/4P HO UV-C lamp, Eindhoven, the Netherlands) at 253.7 nm, an opening of 28 cm x 7 cm was used. The distance between the lamp and aqueous matrix surface was approximately 20 cm. At the start of the advanced oxidation process, 0.22 mM (~ 10 mg/L) hydrogen peroxide (H_2O_2) from J.T. Baker, Avantor Performance Materials (Deventer, the Netherlands) was added. To minimise UV scattering and reflection, a container with an appropriate aperture (12 cm, wide) was placed over the glass beaker. The UV-C irradiance at the aqueous matrix surface was extended and derived from our previous oxidation study (Graumans et al. 2020), (SI **paragraph S3.1**).

3.2.3 Simulated aqueous matrices

Thermal plasma and UV-C/H_2O_2 oxidation was applied in Milli-Q, tap water, synthetic urine, diluted urine and synthetic sewage water matrix. All tested aqueous solutions were freshly prepared at the start of the experiment. Milli-Q water was individually tested but also used for the preparation of synthetic urine and synthetic sewage water. A healthy male volunteer consented to provide urine. This urine was diluted to a 20% v/v ratio, in Milli-Q water, to simulate sewer dilution of flushed urine. Physicochemical characteristics of the tap water matrix were adopted from the freely available January – December 2019 quality standard report (Vitens, Arnhem). An average pH of 7.73 was reported, with a total organic carbon (TOC) concentration of <0.5 mg/L and turbidity of 0.24 NTU, detailed information is given in the supplemental data (**Table S3**). To standardise the advanced oxidation processes, both techniques were used in 500 mL aqueous matrix and during treatment magnetically stirred. The initial pharmaceutical concentration (n = 14) was 5 µg/L. The oxidative pharmaceutical degradation was determined by collecting samples at time intervals of 5, 10, 15, 30, 45, 60, 90 and 120 min. Prior to and after oxidative treatment the temperature and pH were measured.

Direct LC-MS/MS injection was applied on the matrices, Milli-Q water, tap water and synthetic urine. Sample pre-treatment was applied on diluted urine, synthetic sewage water and actual wastewater samples prior to LC-MS/MS analysis. Centrifugal filtration was used for the urine samples, where solid phase extraction and liquid-liquid extraction were used to pretreat wastewater matrixes.

3.2.3.1 Synthetic Urine

For the preparation of synthetic urine, all needed analytes were dissolved separately in 100 mL Milli-Q, to minimise the formation of precipitation or undissolved constituents. The final product comprises; 25.0 g urea, 2.9 g NaCl, 2.3 g Na_2SO_4, 1.6 g KCl, 1.4 g KH_2PO_4, 1.1 g $CaCl_2 \bullet 2H_2O$, 1.1 g creatinine and 1.0 g NH_4Cl in 1000 mL Milli-Q, simulating human urine composition (Giannakis et al. 2018).

3.2.3.2 Synthetic Sewage

To simulate the composition of sewage water, a standardised protocol from the Organization for Economic Co-operation and Development (OECD) was used. Similar to the preparation of artificial urine, all analytes were prepared separately in 100 mL of Milli-Q. The final synthetic sewage water solution contained; 160.0 mg Peptone, 110.0 mg Meat Extract, 30.0 mg Urea, 28.0 mg K_2HPO_4, 7.0 mg NaCl, 3.0 mg $CaCl_2 \bullet 2H_2O$ and 0.5 mg $MgSO_4$ in 1000 mL Milli-Q water (OECD, 2001).

3.2.4 Sewage Water sample collection

End-of-pipe hospital sewage water (HSW) samples were periodically collected for one week in September 2019 (composite sample). The HSW samples were collected in two separate jerry cans to obtain a sample including the weekend (Thursday – Monday 12 - 16 Sep 2019) compared to working days sample (Monday – Thursday 16 - 19 Sep 2019). In addition to compare the pharmaceutical concentration present in HSW, also domestic sewage water (DSW) was sampled on 31 Oct 2019 (as a grab sample). These samples were taken from a residential area with no supply of HSW. Upon arrival in the laboratory the wastewater samples were directly centrifuged and vacuum-filtered using a Whatman Filter grade 1 (Maidstone, United Kingdom). The filtered wastewater samples were distributed in separate clean plastic aliquots, labelled and stored in the fridge (4°C) or freezer (-20 °C). Samples stored in the fridge were analysed within 72 hours to maintain the approximate pharmaceutical shelf life.

3.2.5 Centrifugal filtration

To analyse the pharmaceutical oxidative degradation in diluted urine matrix, 0.5 mL urine sample was placed into a Spin-X centrifugal tube from Costar (Salt Lake City, USA). This Spin-

X tube is equipped with a 0.22 µm cellulose acetate filter and placed on top of a 2.0 mL tube. To filter the urine sample, an Eppendorf MiniSpin (Nijmegen, the Netherlands) centrifuge is used for 5 min at maximum speed (134000 rpm). After spinning, a clear urine sample was transferred to a LC-MS/MS vial for analysis.

3.2.6 Solid phase extraction

Acidic buffer solution (ABS) was prepared by dissolving 10 mM of ammonium formate (NH_4HCO_2, ≥ 99% HPLC grade salt) and 3.25 mL of formic acid (FA, 98-100%) in Milli-Q to obtain a pH of ~2.2. Oasis HLB 3cc (cm^3) solid phase extraction (SPE) cartridges with 60 mg of solid sorbent from Waters Corporation (Milford, USA), were selected for the extraction. SPE cartridges were conditioned with 2.0 mL of methanol and 2.0 mL of ABS. Prior to analysis, either 1.0 mL of analyte mixture, including 100 µL dIS, HSW or DSW was diluted in 4 mL of ABS. Vacuum extraction was performed using an SPE manifold from Analytichem international (Bay Meadows Ln, USA). An aliquot of 5.0 mL aqueous pharmaceutical matrix was loaded on the SPE cartridge and subsequently washed with 1.0 mL ABS to remove impurities. After sample loading, the retained pharmaceuticals were extracted using 5.0 mL of methanol. Next, the extracts were vaporised under a gentle stream of nitrogen using a sample concentrator (Stuart, Stone, United Kingdom) at 40 ºC. The vaporised samples were reconstituted in mobile phase A (0.1% formic acid) prior to LC-MS/MS analysis. To develop an extraction method for pharmaceuticals in a complex matrix in a broad concentration range, the recovery of the selected pharmaceuticals was determined in Milli-Q and synthetic sewage water by using three controlled concentrations, 1.0, 10.0 and 50.0 µg/L.

3.2.7 Liquid- liquid extraction of metformin

Due to the high hydrophilicity of metformin, no satisfactory recovery was obtained with SPE. To improve the recovery for metformin, a liquid-liquid extraction with acetonitrile at subzero temperatures was performed according to a previously described method (Yoshida and Akane 1999). An aliquot of 0.5 mL of a solution with a known metformin concentration was extracted by adding 0.1 mL of 2.0 mM sodium dodecyl sulfate (SDS) including 0.5 mL of acetonitrile. Sample aliquots were vortexed and centrifuged at maximum speed for 5 min. By placing the tubes for 30 min. at –20 ºC, the aqueous phase was separated from the acetonitrile phase. Compounds with affinity for the organic layer were retrieved from the acetonitrile phase. The acetonitrile layer was directly transferred to an LC-MS/MS vial for analysis. For the extraction from actual sewage water, the dimensions were increased by a tenfold, using the ratio 5:1:5 mL (Sewage Water: SDS: Acetonitrile).

3.2.8 Liquid chromatography tandem mass spectrometry analysis

An Acquity UPLC system from Waters Corporation (Milford, USA) was used for the analytical separation of pharmaceuticals and deuterated internal standards. The LC system was online coupled to a Xevo TQ-S micro quadrupole mass spectrometer, with electro spray ionisation (ESI), operated in positive ion mode for all selected compounds. Nitrogen gas was applied at 50 L/h in the cone and at 1,100 L/h for desolvation. The desolvation temperature was set at 600 ^{o}C, and argon was used as collision gas during MS/MS. The voltages selected for the capillary and cone were 2 kV and 20 V, respectively. Multiple reaction monitoring (MRM) transitions for all pharmaceuticals were determined by direct infusion to the MS/MS. These transitions are presented as a precursor ion $[M+H]^+$ combined with the corresponding fragmented daughter ion. The compounds were all individually infused via the fluidics interface by using a flow rate of 10 µL/min. The optimised results are given in **Table S4** (SI **paragraph S.3.4**). The LC unit consists of a solvent degasser, quaternary solvent manager, seal wash pump, column oven and auto-sampler. Gradient LC conditions were applied at a flow of 0.5 mL/min, using 2.5 µL of injection volume and a column oven temperature set at 40 ^{o}C. Eluent (A) consisted of 0.1 % v/v formic acid (FA, 98-100%) in Milli-Q water in combination with eluent (B) 100% v/v acetonitrile (ACN, UHPLC-MS). An Acquity UPLC BEH C_{18} (2.1 mm x 100 mm, 1.7 µm) reversed phase column was used for the chromatographic separation. The LC gradient program was started with 100% eluent A until 0.20 min, and quickly changed to 100% B within 2.0 min. This 100% B was maintained until 4.3 min and subsequently ramped to 100% A at 4.5 min. The gradient program was stopped at 8 min.

3.2.9 Data analysis

For all pharmaceutical compounds the method selectivity was obtained by using two MRM transitions per analyte. For each deuterated internal standard only one MRM transition was selected. Linear curve fitting ($y = ax + b$) was applied using TargetLynx LC-MS/MS data acquisition software (Waters Corporation Milford, USA). Data quantification for metformin (MF) was done by using a quadratic curve fitting ($y = ax^2 + bx + c$). To minimise the y-value error of the low analyte concentrations, all calibration points were equally weighted by using a weighting factor 1/X (Almeida et al. 2002, Gu et al. 2014). The pharmaceutical oxidative degradation kinetics were plotted using GraphPad Prism 5.03 statistical software (Graphpad Inc., CA, USA) and the conversion level was determined using **eq. 1** (Graumans et al. 2020). SPE recovery data was determined by dividing the extract concentration through the original concentration, see **eq. 2**. A *two-sided t*-test was applied to test for statistical significance of degradation over time **eq. 3**, assuming first-order kinetics (Miller and Miller 2010).

$$\bar{R} = (1 - C_t/C_0) \cdot 100\ \% \quad (1)$$

$\bar{R}$ = Conversion level (%) ($n = 4$)

C_t = Concentration of the test substance at the end of treatment (µg/L)

C_0 = Initial compound concentration (µg/L)

$$Recovery\ (S\%) = \frac{Concentration\ (Extract)}{Concentration\ (original)} \cdot 100\ \% \quad (2)$$

$$t = \frac{r \bullet \sqrt{n-2}}{\sqrt{1-r^2}} \quad (3)$$

t = t-calculated

r^2 = Correlation coefficient of the log-normal transformed line

3.3 Results and Discussion

3.3.1 Pharmaceutical degradation using thermal plasma activation

The oxidative conversion levels of 14 analytes, spiked in five different matrices, were evaluated in a controlled setting. Selected pharmaceuticals at given initial concentrations were degraded by oxidation to an energy density and compound dependent extent using 150 W thermal plasma treatment, (**Table 3.1**). Milli-Q was used as ultra-pure water matrix where all molecules are solely oxidised by plasma-generated RONS. A time-based decomposition plot demonstrates that the chemical degradation kinetics are distinct for all analytes tested, see **Fig. 3.2**. DOX, DF, CP, PHE and APAP were all rapidly 100% decomposed, with similar abatement kinetics. The compounds CIP, FLU, CB and TER were converted for at least >90% within 120 min. The slowest degradation was observed for MET (72.3%), IOM (66.9%), IOP (63.0%), DIA (41.3%) and MF (17.6%) after 120 min treatment. Although the chemical degradation kinetics differ between compounds and matrices, during thermal plasma treatment the analytes were observed to be subjected to exponential decay. Log-normal transformation of this concentration data resulted in linear time-based decomposition plots, see **Fig. S5** (SI **paragraph S.3.5**). The slope of this linear decay represents the first-order rate constant (k) where $r^2 > 0.50$ demonstrates significant correlation for first-order degradation kinetics (SI **paragraph S.3.5**).

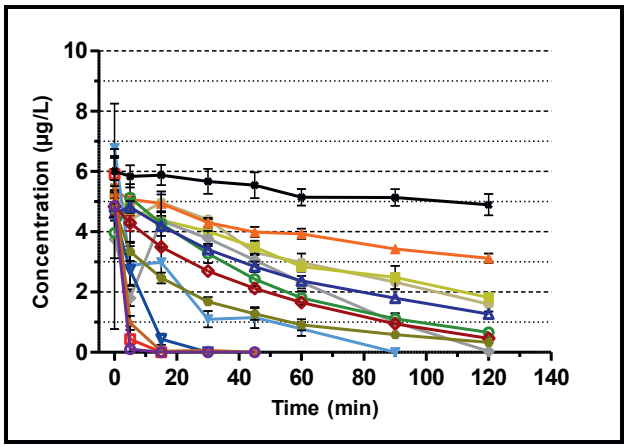

Fig. 3.2. The time-based decomposition plot for the pharmaceuticals **IOM** (●), **IOP** (■), **DIA** (▲), **CIP**(◆), **DOX**(▼), **FLU**(○), **DF**(□), **MET**(△), **CP**(▽), **CB**(◇), **TER**(●), **PHE**(★), **APAP**(○) and **MF**(✖), treated in Milli-Q water with 150 W thermal plasma.

Table 3.1.

Pharmaceutical removal by thermal plasma treatment in different matrices

Comp.	Milli-Q Water			Tap Water			Synthetic Urine			Urine			Synthetic Sewage		
	$\bar{R}$(%)	$k_{(min^{-1})}$[A]	$t_{1/2}$	$\bar{R}$(%)	$k_{(min^{-1})}$	$t_{1/2}$	$\bar{R}$(%)	$k_{(min^{-1})}$	$t_{1/2}$	$\bar{R}$(%)	$k_{(min^{-1})}$	$t_{1/2}$	$\bar{R}$(%)	$k_{(min^{-1})}$	$t_{1/2}$
	$C_{t(min)}$		(min)	$C_{t(min)}$		(min)	$C_{t(min)}$		(min)	$C_{t(min)}$		(min)	$C_{t(min)}$		(min)
IOM	66.9	0.009	77.0	62.2	0.007	99.0	43.1	0.005	138.6	25.1	0.002	346.6	56.3	0.008	86.6
	120	*0.96 r^2*		*120*	*0.84 r^2*		*120*	*0.93 r^2*		*120*	*0.73 r^2*		*120*	*0.93 r^2*	
IOP	63.0	0.008	86.6	47.1	0.005	138.6	0.0	-	-	35.5	0.003	231.1	33.1	0.007	99.0
	120	*0.99 r^2*		*120*	*0.89 r^2*		-	-		*120*	*0.48 r^{2*}*		*120*	*0.75 r^2*	
DIA	41.3	0.004	173.3	31.8	0.003	231.1	30.7	0.003	231.1	5.9	<0.001	>693.2	15.3	0.002	346.6
	120	*0.97 r^2*		*120*	*0.89 r^2*		*120*	*0.91 r^2*		*120*	*0.02 r^{2*}*		*120*	*0.51 r^2*	
CIP	99.4	0.030	23.1	72.2	0.006	115.5	68.6	0.006	115.2	81.6	0.015	46.2	69.6	0.013	53.3
	120	*0.67 r^2*		*120*	*0.29 r^{2*}*		*120*	*0.64 r^2*		*120*	*0.97 r^2*		*120*	*0.97 r^2*	
DOX	100.0	0.032	21.7	100.0	0.030	23.1	100.0	0.041	16.9	81.9	0.013	53.3	100.0	0.059	11.8
	90	*0.85 r^2*		*120*	*0.83 r^2*		*90*	*0.83 r^2*		*120*	*0.84 r^2*		*90*	*0.96 r^2*	
FLU	82.8	0.017	40.8	81.2	0.014	49.5	70.2	0.010	69.3	67.6	0.010	69.3	82.5	0.016	43.3
	120	*0.98 r^2*		*120*	*0.97 r^2*		*120*	*0.99 r^2*		*120*	*0.98 r^2*		*120*	*0.96 r^2*	
DF	100.0	0.520	1.3	100.0	0.295	2.4	100.0	0.108	6.4	100.0	0.097	7.1	99.1	0.026	26.7
	15	*1.00 r^2*		*15*	*1.00 r^2*		*15*	*1.00 r^2*		*45*	*0.96 r^2*		*120*	*0.58 r^2*	
MET	72.3	0.011	63.0	61.7	0.008	86.6	49.6	0.005	138.6	9.6	<0.001	>693.2	64.7	0.009	77.0
	120	*0.99 r^2*		*120*	*0.98 r^2*		*120*	*0.98 r^2*		*120*	*0.11 r^{2*}*		*120*	*0.96 r^2*	

Table 3.1. *Continued*

CP	100.0	0.160	4.3	100.0	0.185	3.8	100.0	0.078	8.9	100.0	0.049	14.2	100.0	0.121	5.7
	120	*0.98 r^2*		*60*	*0.91 r^2*		*60*	*0.97 r^2*		*90*	*0.82 r^2*		*90*	*0.97 r^2*	
CB	90.5	0.019	36.5	84.4	0.019	36.5	62.3	0.008	86.6	37.9	0.004	173.3	79.4	0.014	49.5
	120	*0.99 r^2*		*120*	*0.99 r^2*		*120*	*0.98 r^2*		*120*	*0.93 r^2*		*120*	*0.97 r^2*	
TER	92.7	0.021	33.0	95.2	0.046	15.1	89.5	0.018	38.5	91.9	0.021	33.0	85.3	0.016	43.3
	120	*0.98 r^2*		*120*	*0.95 r^2*		*120*	*0.95 r^2*		*120*	*0.99 r^2*		*120*	*0.98 r^2*	
PHE	100.0	0.149	4.7	100.0	0.192	3.6	100.0	0.207	3.4	100.0	0.059	11.8	100.0	0.263	2.6
	30	*0.70 r^2*		*30*	*0.75 r^2*		*30*	*0.98 r^2*		*90*	*0.91 r^2*		*45*	*0.97 r^2*	
APAP	100.0	0.774	0.9	100.0	0.115	6.0	100.0	0.271	2.6	100.0	0.065	10.7	100.0	0.739	0.94
	15	*1.00 r^2*		*30*	*1.00 r^2*		*45*	*0.97 r^2*		*60*	*0.98 r^2*		*30*	*1.00 r^2*	
MF	17.6	0.001	693.2	42.8	0.004	179.3	0.0	-	-	29.3	0.003	231.1	72.9	0.011	63.0
	120	*0.94 r^2*		*120*	*0.74 r^2*		-	-		*120*	*0.82 r^2*		*120*	*0.71 r^2*	

[A]: First-order reaction rate equation: $-d[A]/dt$. k, the first-order rate constant, is the slope of the line.

Where **[A]** is the drug concentration and $t_{(1/2)} = \ln 2/k$.

[*]: No significant change due to moderate to low correlation coefficient in linear modelling of assumed first-order kinetics ($r^2 < 0.50$).

Comparison of the pharmaceutical degradation rate constants in Milli-Q with other matrices (**Table 3.1** and **Fig. S3** and **4** (SI **paragraph S.3.5**)), it is demonstrated that the k value decreases with increasing matrix complexity. To demonstrate the influence of co-existing substances present in these treated matrices, the overall rate constant ($\bar{k}$) was used to calculate the inhibition ratio, see **eq. 4** (Tokumura et al. 2016). A ratio higher than 1.000 suggests inhibition by constituents and organic matter in the sample matrix indicating that the aqueous composition is of major influence on plasma oxidation efficiency. The matrix complexity and interference of co-existing substances was consecutively demonstrated to be:

$$1.000_{(Milli\text{-}Q)} < 1.344_{(Synthetic\ Sewage)} < 1.893_{(Tap\ water)} < 2.119_{(Synthetic\ urine)} < 5.000_{(Urine)}.$$

$$\text{Inhibition ratio} = \frac{\bar{k}_{(Milli-Q)}}{\bar{k}_{(Matrix)}} \qquad (4)$$

It is demonstrated that the aqueous composition is of great influence on the plasma oxidation efficiency. Despite the overall inhibitory effect of co-existing substances in various tested media, synthetic sewage and tap water, compared to Milli-Q, showed improved degradation rate constants for DOX, CP, TER, PHE and MF. The relatively small improvement in degradation for these compounds is attributed to matrix conductivity. Enhanced conductivity will increase the ability of facilitating electrical current through an aqueous medium, suggesting that the pre-existence of ions in tap water and synthetic sewage accelerate the transfer of specific RONS (Brisset et al. 2011; Thirumdas et al. 2018; Hoeben et al. 2019; Shimizu et al. 2020). Increased solution conductivity also increases the current of the thermal plasma arc, promoting the chemical activity of the plasma discharge in the gas phase. A similar effect would have been expected in synthetic and diluted urine matrices, however, an inhibitory effect was observed. This effect is probably explained by the high concentration of the co-existing minerals and organic constituents present in g/L ranges compared to mg/L range in tap water and synthetic sewage water (OECD, 2001; Giannakis et al. 2018). Shih and Locke (2011) demonstrated in their study an optimal conductivity of 150 µS/cm for the production of reactive species. Further increase of conductivity (up to 500 µS/cm) resulted in a decline of radicals and molecular species formed. Due to the presence of co-existing substances there is less direct contact with water molecules to produce hydroxyl radicals (**R1**). On the other hand minerals and organic constituents may cause quenching or the production of less reactive radicals (Shih and Locke 2011; Giannakis et al. 2018; Shimizu et al. 2020). Slower and no gradual abatement kinetics was therefore also observed in urine diltued with water, showing a poor correlation of $r^2 < 0.50$ for the degradation of IOP (0.48 r^2), DIA (0.02 r^2) and MET (0.11 r^2).

3.3.2 Plasma oxidation chemistry

Many factors can influence thermal plasma degradation efficiency. In our previous study we observed that electrical power input and initial analyte concentration were important parameters (Graumans et al. 2020). Additionally, it was demonstrated that by continued activation of a relatively large volume of tap water (500 mL) and low pharmaceutical concentration (4 µg/L), a logistic oxidative degradation pattern for CP elapsed. Comparing the previously non-cooled plasma results with the current data, no logistic oxidative degradation pattern is found for CP and other treated analytes, see **Fig. S6** (SI **paragraph S.3.6).** This remarkable dissimilarity is attributed to the temperature of the plasma treated solution. Active cooling has a positive effect on the production of thermally labile species such as ozone, hydrogen peroxide and transient reactive nitrogen species, while high temperatures benefit nitric acid formation (Hoeben et al. 2019). Hydroxyl radicals (•OH) and their coupling product hydrogen peroxide (H_2O_2) are formed by plasma-water contact, either in the gas phase or at the plasma-water interface (**R1**) (Joshi and Thagard 2013). Two •OH radicals combine to form measurable hydrogen peroxide concentrations (**R2**) (Magureanu et al. 2018). On the other hand, in presence of organic molecules, such as pharmaceuticals •OH radicals will react by initiating oxidative degradation (Joshi and Thagard 2013; Magureanu et al. 2018).

$$e^- + H_2O \rightarrow HO^\bullet + H + e^- \qquad \textbf{(R1)}$$

$$HO^\bullet + HO^\bullet \rightarrow H_2O_2 \qquad \textbf{(R2)}$$

Pharmaceutical decomposition initiated by •OH radicals produced with immersed non-thermal pulsed corona plasma, was demonstrated before (Banaschik et al. 2018). Oxidative conversion levels for three identical in Milli-Q were found for DIA (40%), DF (100%) and CB (75%) within 70 min. We observed decomposition levels of 41.3%, 100% and 90.5% within 120 min for DIA, DF and CB, respectively. Although the oxidative degradation of these pharmaceuticals shows similarities, it must be noted that the plasma degradation in our study is not solely based on hydroxyl radical interaction. With plasma discharge in ambient air and striking over water, also reactive nitrogen species are transferred in the liquid matrix (Hoeben et al. 2019; Graumans et al. 2020), such as nitric oxide (NO), nitrogen dioxide (NO_2), nitrous acid (HNO_2), nitric acid (HNO_3) and peroxynitrous acid (ONOOH). In addition to oxidative degradation, these RNS can also induce nitration and nitrosation reactions (Magureanu et al. 2018; Hoeben et al. 2019). Looking at the currently tabulated conversion levels ($\bar{R}$) and corresponding half-lives ($t_{1/2}$), (**Table 3.1**), it is clear that certain molecular structures are more suspectable to plasma produced RONS than others. Aromatic ring systems, unsaturated double bonds (C = C) and functional

groups with electron donating properties have increased reactivity towards electrophilic oxidising agents (•OH or NO_2^+) (Brown, 2007; Joshi and Thagard 2013; Banaschik et al. 2018; Magureanu et al. 2018). The reactivity of aromatic ring systems is however, not self-evident since an electrophile, such as an hydroxyl radical, is needed to interact (Brown, 2007).

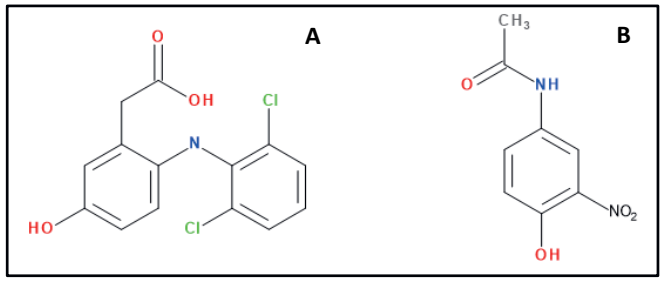

Fig. 3.3. During thermal plasma treatment distinct chemical processes will occur according to the produced RONS. Several RONS will initiate chemical processes on reactive molecular structures containing aromatic rings, unsaturated bonds or electron donating function groups.•OH radical attack is the favoured degradation pathway, reacting for example rapidly with the aromatic ring of DF by forming 4-hydroxy-DF (**A**). Additionally, nitration processes will also occur where for example NO_2• radicals can add to aromatic ring of APAP by producing 3-nitro-APAP (**B**).

Table 3.2.

Average pH values of ***n*=2** thermal plasma treated matrices

150W Plasma	**Milli-Q Water pH x̄**	**Tap Water pH x̄**	**Synthetic Urine pH x̄**	**Urine pH x̄**	**Synthetic Sewage pH x̄**
Start $_{0\ min}$	5.0	7.7	6.5	7.4	6.9
End$_{120\ min}$	1.6	1.6	2.2	2.5	1.7

A technology such as plasma-induced water activation is used to generate electrophilic compounds, demonstrating that •OH radicals readily initiate an addition reaction by binding to an aromatic ring system, **Fig 3.3A**. (Banaschik et al. 2018). A similar reaction pathway is expected during our thermal plasma treatment process, but are complemented by nitration processes (Magureanu et al. 2018; Hoeben et al. 2019; Graumans et al. 2020). With prolonged thermal plasma activation, the aqueous matrix pH is decreased by RONS (**Table 3.2**). Nitration reactions usually occur at acidic pH (<6), where a nitronium ion (NO_2^+) is substituted or added as an electrophile at the aromatic ring system (Squadrito and Pryor 1998; Brown, 2007). Chiron et al 2010, identified 3-nitro-APAP as the nitration transformation product of APAP in WWTPs (Chiron et al. 2010), see **Fig. 3.3B**. Nitration reactions in WWTP are initiated by nitrifying bacteria who produce nitric oxide (NO•). NO• is a precursor for nitrating agents such as

peroxynitrite ($ONOO^-$). In acidic samples ONOOH is very unstable and will rapidly decompose into $^{\bullet}OH$, $NO_2^{\bullet}$ and HNO_3 (Chiron et al. 2010; Jewell et al. 2014; Hoeben et al. 2019). Additionally, $ONOO^-$ can also react with CO_2 yielding $NO_2^{\bullet}$ and $CO_3^{\bullet-}$ radicals (Chiron et al. 2010). For thermal plasma activation it is expected that similar RONS are produced (**R3-6**). However, it is expected that the combined attack of hydroxyl radical and molecular oxygen is the main degradation pathway in this thermal plasma study and that nitration oxidation will complement the oxidative process under favourable circumstances (Chiron et al. 2010; Jewell et al. 2014; Thirumdas et al. 2018; Magureanu et al. 2018; Hoeben et al. 2019). Our previous study on degradation data of CP without active cooling indicated pharmaceutical dissolution after prolonged activation (Graumans et al. 2019). This suggests that minimal $^{\bullet}OH$ radicals were formed, but that molecular dissolution was catalysed by acidic pH (<6) and increasing water temperature, both acting as stimulants for the nitration reaction rate (Chiron et al. 2010).

$$e^- + N_2 \rightarrow N^{\bullet} + N^{\bullet} + e^- \quad \textbf{(R3)}$$

$$N^{\bullet} + O_2 \rightarrow NO^{\bullet} + O^{\bullet} \quad \textbf{(R4)}$$

$$NO^{\bullet} + O_2^{\bullet-} \rightarrow ONOO^- \quad \textbf{(R5)}$$

$$ONOO^- + H^+ \rightarrow NO_2^{\bullet} + HO^{\bullet} \quad \textbf{(R6)}$$

3.3.3 UV-C/H_2O_2 oxidative chemistry

UV-C/H_2O_2 advanced oxidation process is another useful technique for the degradation of micropollutants such as pharmaceuticals (Wols et al. 2013). During the application with UV-C/H_2O_2 treatment, certain molecules are sensitive for both interactions and are rapidly converted by photolysis and hydroxyl radical attack (Wols et al. 2013). Hydrogen peroxide in the gas phase is rapidly dissociated by UV photons, producing highly reactive hydroxyl radicals ($^{\bullet}OH$) that can interact with nearly all organic compounds (von Sonntag 2008; Zhao et al. 2014). $^{\bullet}OH$ radicals will bind to C = C or C = N double bonds, initiate hydrogen (H) abstraction, or trigger electron transfer reactions (von Sonntag 2008; Banaschik et al. 2018). According to the degradation results (**Fig. 3.4**), it is seen that UV-C/H_2O_2 attacks nearly all pristine molecular structures completely in Milli-Q water, **Table 3.3**. Pseudo first-order reaction kinetics ranged between 0.007 up to 0.591 min^{-1}, including corresponding half-lives ($t_{1/2}$) between 0.4 and 99.0 min. In contrast to thermal plasma treatment, the complete conversion of IOM, IOP and DIA with UV-C/H_2O_2 is most remarkable, since the molecular reactivity of these molecules is relatively low (Bourin et al. 1997). DIA is weak acidic compound, where IOM and IOP are both nonionised over a wide pH range, see **Table S5** (SI **paragraph S.3.7**).

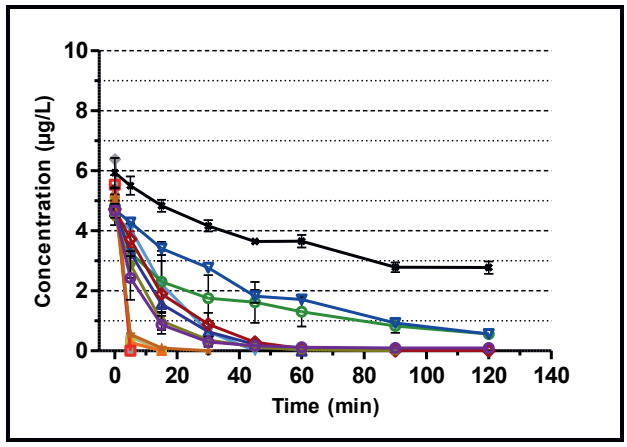

Fig. 3.4. UV-C/H_2O_2 oxidative degradation pattern in Milli-Q for the compounds **IOM** (●), **IOP** (■), **DIA** (▲), **CIP**(◆), **DOX**(▼), **FLU**(○), **DF**(□), **MET**(△), **CP**(▽), **CB**(◇), **TER**(●), **PHE**(★), **APAP**(○) and **MF**(✖).

The fully substituted aromatic ring with iodine atoms is characteristic for contrast agents, since these structures facilitate X-ray absorption during clinical diagnosis (Bourin et al. 1997; Borowska et al. 2015). That these compounds are difficult to decompose during plasma oxidation is explained by the fully substituted aromatic ring, where the iodine functional groups hinder the availability of the unsaturated C- atoms (Rosati 1994; Bourin et al. 1997; Zhao et al. 2014; Banaschik et al. 2018). Assuming that hydroxyl radical attack is the major pathway during thermal plasma degradation study, it confirms that slow molecular invasion can occur (Banaschik et al. 2018). On the other hand it is noteworthy, that the hydroxyl radical can attack on the ipso positions of the aromatic ring, as observed with e.g. DIA, IOP and IOM (Jeong et al. 2010). Despite their slow chemical reactivity towards •OH radicals, iodinated compounds are light sensitive Photolysis of these molecules causes deiodination (Eloy et al. 1991; Wols et al. 2013). Allard et al. 2016 demonstrated rapidly photolytically degraded IOP and DIA up to >90% within 2 min in deionised water by immersed UV irradiation at 254 nm (Allard et al. 2016). Although we use UV/H_2O_2 treatment, similar fast complete conversion levels were found for IOM, IOP and DIA within 15 min, demonstrating that the used UV-C source (254 nm) is the most important technique for contrast agent degradation. In accordance with the study of Wols, we found that the majority of pharmaceuticals do not photolytically degrade at 254 nm UV irradiation. Based on their data it was seen that DF, PHE and FLU can moderately decompose photolytically in Milli-Q, where MET, CP, CB, APAP and MF are scarcely sensitive to UV-C irradiation (Wols et al. 2013). The poorest conversion levels were observed for APAP, CP and MF. Although UV-C/H_2O_2 treatment is an interplay between photochemical

degradation accompanied with •OH radicals, we found that that UV-C irradiation has a large impact on the molecular degradation.

Table 3.3.

Pharmaceutical removal by UV-C/H_2O_2 treatment in different matrices

	Milli-Q Water			Tap Water			Synthetic Urine			Urine			Synthetic Sewage		
	$\bar{R}$(%)	$k_{(min^{-1})}$	$t_{1/2}$	$\bar{R}$(%)	$k_{(min^{-1})}$	$t_{1/2}$	$\bar{R}$(%)	$k_{(min^{-1})}$	$t_{1/2}$	$\bar{R}$(%)	$k_{(min^{-1})}$	$t_{1/2}$	$\bar{R}$(%)	$k_{(min^{-1})}$	$t_{1/2}$
	$C_{t(min)}$		(min)	$C_{t(min)}$		(min)	$C_{t(min)}$		(min)	$C_{t(min)}$		(min)	$C_{t(min)}$		(min)
IOM	100.0	0.477	1.6	100.0	0.464	1.5	80.7	0.014	49.0	43.7	0.005	138.6	100.0	0.124	5.6
	15	*1.00 r^2*		*15*	*1.00 r^2*		*120*	*0.97 r^2*		*120*	*0.58 r^2*		*30*	*0.99 r^2*	
IOP	100.0	0.587	1.2	100.0	0.361	1.9	85.3	0.015	46.2	53.2	0.007	99.0	100.0	0.101	6.9
	15	*1.00 r^2*		*15*	*1.00 r^2*		*120*	*0.98 r^2*		*120*	*0.84 r^2*		*30*	*0.99 r^2*	
DIA	100.0	0.591	1.2	100.0	0.848	0.8	86.3	0.018	38.5	39.8	0.005	138.6	100.0	0.126	5.5
	15	*1.00 r^2*		*15*	*1.00 r^2*		*120*	*0.97 r^2*		*120*	*0.88 r^2*		*30*	*0.98 r^2*	
CIP	100.0	n/a [A]	-	100.0	0.292	2.4	86.2	0.015	46.2	8.6	0.001	693.2	100.0	0.159	4.4
	15	-		*30*	*0.99 r^2*		*120*	*0.95 r^2*		*120*	*0.44 r^2 **		*60*	*0.99 r^2*	
DOX	100.0	0.067	10.4	n.d.	-	-	60.5	0.007	99.0	23.8	0.003	231.1	83.0	0.014	49.5
	45	*0.97 r^2*		-	-		*120*	*0.86 r^2*		*120*	*0.44 r^2 **		*120*	*0.92 r^2*	
FLU	87.9	0.016	43.3	100.0	0.109	6.4	62.5	0.008	86.6	18.5	0.002	346.6	94.8	0.027	25.7
	120	*0.95 r^2*		*60*	*0.86 r^2*		*120*	*0.99 r^2*		*120*	*0.85 r^2*		*120*	*0.84 r^2*	
DF	100.0	n/a	-	100.0	1.853	0.4	100.0	0.046	15.1	69.7	0.010	69.3	99.3	0.036	19.3
	15	-		*15*	*1.00 r^2*		*120*	*0.97 r^2*		*120*	*0.99 r^2*		*120*	*0.56 r^2*	
MET	100.0	0.068	10.2	97.3	0.043	16.1	12.1	0.001	693.2	3.7	0.002	346.6	46.1	0.005	138.6
	60	*0.99 r^2*		*120*	*0.99 r^2*		*120*	*0.85 r^2*		*120*	*0.59 r^2*		*120*	*0.90 r^2*	

Table 3.3. *Continued*

CP	87.9	0.018	38.5	53.2	0.017	40.8	4.6	n.d.	-	6.6	<0.001	>693.2	17.8	0.001	693.2
	120	*0.99 r^2*		*120*	*0.99 r^2*		*120*	-		*120*	*0.39 r^2 **		*120*	*0.54 r^2*	
CB	100.0	0.075	9.2	88.5	0.019	99.0	8.1	0.001	693.2	N.C.	-	-	27.9	0.003	231.1
	120	*0.99 r^2*		*120*	*0.99 r^2*		*120*	*0.36 r^2 **		-	-		*120*	*0.81 r^2*	
TER	100.0	0.079	8.8	100.0	n.d.	-	53.1	0.005	138.6	4.1	<0.001	>693.2	70.7	0.009	77.0
	90	*0.99 r^2*		*15*	-		*120*	*0.92 r^2*		*120*	*0.05 r^2 **		*120*	*0.98 r^2*	
PHE	100.0	0.249	2.8	100.0	0.013	1.6	78.5	0.013	53.3	35.0	0.004	173.3	100.0	0.110	63.0
	30	*0.93 r^2*		*45*	*0.99 r^2*		*120*	*0.99 r^2*		*120*	*0.92 r^2*		*120*	*0.99 r^2*	
APAP	97.8	0.031	22.4	100.0	0.127	5.5	24.1	0.002	346.6	N.C.	-	-	70.1	0.009	77.0
	120	*0.75 r^2*		*30*	*0.91 r^2*		*120*	*0.95 r^2*		-	-		*90*	*0.95 r^2*	
MF	52.9	0.007	99.0	97.4	0.028	24.8	40.7	0.003	231.1	11.3	0.001	693.2	9.6	0.002	346.6
	120	*0.92 r^2*		*120*	*0.73 r^2*		*120*	*0.52 r^2*		*120*	*0.68 r^2*		*120*	*0.47 r^2 **	

[A]: No reaction rate could be determined, by the rapid interaction of the pharmaceutical with either H_2O_2 or UV-C irradiation.

[*]: No significant change due to moderate to low correlation coefficient in linear modelling of assumed first-order kinetics ($r^2 < 0.50$).

3.3.4 Effect of complex matrices on UV-C/H_2O_2 treatment

Also during UV-C/H_2O_2 oxidative treatment the matrix complexity has a significant effect on the oxidative degradation of molecules. Using again the inhibition factor (**Eq. 4**), it has been observed that the coexisting substances in the aqueous matrix have even a greater influence on UV-C/H_2O_2 oxidation than during plasma treatment. The pharmaceutical degradation kinetics (**Table 3.3**) decrease when the matrix complexity increases:

$$1.000_{(Milli\text{-}Q)}: 0.544_{(Tap\ water)} < 3.115_{(Synthetic\ Sewage)} < 15.283_{(Synthetic\ urine)} < 54.00_{(Urine)}.$$

The rapid conversion levels in Milli-Q are presumably caused by the absence of minerals and organic impurities. Retardation of the chemical degradation kinetics in complex matrices like synthetic urine, diluted urine and synthetic sewage are attributed to minerals and the natural organic matter. Organic impurities, such as urea, meat extract and peptone will absorb UV light at the expense of a less effective photolytic process. Indirectly the production of •OH radicals is also diminished and minerals such as phosphate and chlorine will induce the production of less reactive secondary radicals (**R7-8**) (Borowska et al. 2015; Giannakis et al. 2018).

$$HO^{\bullet} + Cl^{-} \rightarrow HOCl^{\bullet -} \qquad \textbf{(R7)}$$

$$HO^{\bullet} + HPO_4^{2-} \rightarrow HPO_4^{\bullet -} + HO^{-} \qquad \textbf{(R8)}$$

On the other hand, it was observed that the MF oxidation is increased in tap water. Chemical degradation kinetics are improved in tap water matrix (0.028 min^{-1}) compared to Milli-Q (0.007 min^{-1}), showing 97.4% versus 52.9% degradation within 120 min, respectively. This effect is attributed to photoreactive NO_3^- (Lin et al. 2020), and in this study also improved degradation of MF was demonstrated in water samples with amplified environmental factors, compared to pure water. Their experimental design was based on simulating environmental photolysis by using 6h of UV-A irradiation at 40 cm distance. During this process, reactive oxygen species (ROS) are formed confirming that •OH radical attack is the favoured MF degradation pathway (Lin et al. 2020). Improved degradation results were found in the presence of high concentrations NO_3^- (0.60 – 0.62 mg/L) and to a lesser extent Cl^- (up to <4 mg/L), which both promote the photo-reactivity by producing •OH radicals (**R9-R11**) (Wang et al. 2017; Lin et al. 2020) As seen in the suggested chemical reactions, it is expected that primarily NO_2 and NO_3 will play an improved role in UV-C/H_2O_2 tap water. As demonstrated in **Table S3** (SI **paragraph S.3.3),** it is seen that both Cl_2 and NO_3^- are present in concentrations exceeded the threshold of <4.0 mg/L (Lin et al. 2020).

$$NO_3^- \xrightarrow{UV} NO_3^{-*} \qquad \textbf{(R9)}$$

$$NO_3^{-*} \rightarrow NO_2^{\bullet} + O^- \quad \textbf{(R10)}$$

$$O^- + H_2O \rightarrow HO^{\bullet} + HO^- \quad \textbf{(R11)}$$

3.3.5 Pharmaceutical extraction using solid phase extraction and liquid-liquid extraction

A versatile SPE methodology was developed in synthetic sewage water for the detection of 14 different pharmaceuticals in raw hospital and residential wastewater samples. The extraction method was developed and optimised for synthetic sewage water to achieve an optimum recovery in a sterile matrix with comparable properties as raw wastewater. Due to the wide range of physicochemical properties of our selected pharmaceuticals (n = 14), the current developed SPE and LLE methodology are a compromise to achieve the best overall extraction efficiency, see supporting information **paragraph S.3.8** for the detailed results. The currently developed SPE methodology has recovery percentages (S%) ranging from 27 up to > 100.0% for 13 pharmaceuticals in synthetic sewage water, see **Fig. 3.5**.

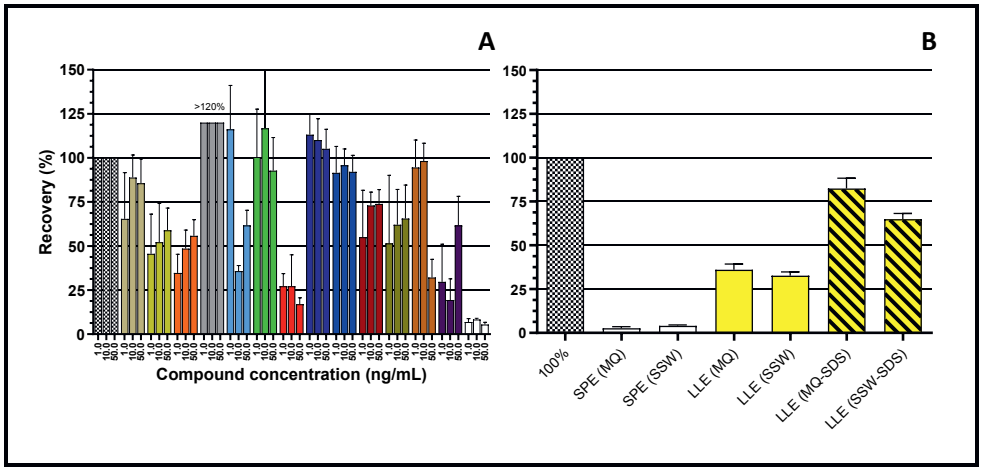

Fig. 3.5. SPE recovery percentages obtained in spiked synthetic sewage water (**A**). The extraction of known concentrations 1.0, 10.0 and 50.0 µg/L is compared to **100%(▩)** recovery for the compounds; **IOM** (■), **IOP** (■), **DIA** (■), **CIP**(■), **DOX**(■), **FLU**(■), **DF**(■), **MET**(■), **CP**(■), **CB**(■), **TER**(■), **PHE**(■), **APAP**(■) and **MF**(□). Liquid-liquid extraction compared to SPE extraction (**B**). Recovery was determined for 50 µg/L **MF**(□), without (■) and with SDS (▨).

The extraction of MF, was insufficient, since recovery percentages using Oasis HLB SPE cartridges were very low (S% >10.0). To minimise LC-MS/MS system contamination or have any recovery loss of other pharmaceuticals, an additional liquid-liquid extraction at subzero temperatures from Yoshida et al. (1999) was modified especially for MF (Yoshida and Akane 1999). SDS was added to the sample to initiate a cation-anion interaction between MF and SDS. ACN was added to extract the SDS-MF complex from the aqueous matrix. As presented in **Fig.**

3.5B, it is seen that the LLE method can extract MF now with much better recovery, ranging from 64.9 up to ~100%.

3.3.6 Pharmaceutical detection and mitigation

The optimised SPE and LLE extraction methods were used on real wastewater samples taken from a hospital and residential area (**Fig 3.6**). The concentrations (µg/L) of the 10 identified pharmaceuticals were comparable with other studies of Vieno et al. (2006); Yin et al. (2010), Petrie et al. (2016) and Ajo et al. (2018). Results reported for IOM and APAP are considered semi-quantitative because these values were extrapolated in a range beyond the highest standard concentration (100 µg/L). Even with this limitation of our analytical method, nearly all 14 selected pharmaceuticals were detected in the hospital effluent (**Table 3.4**). The presence of IOM, DIA and CP, illustrates the difference between hospital (HSW) and domestic sewage water (DSW), since contrast agents and certain anticancer drugs are hospital administered only pharmaceuticals. Absence of IOP, is clarified by the fact that IOM is the mainly used contrast agent for radiographic examinations at the Radboudumc.

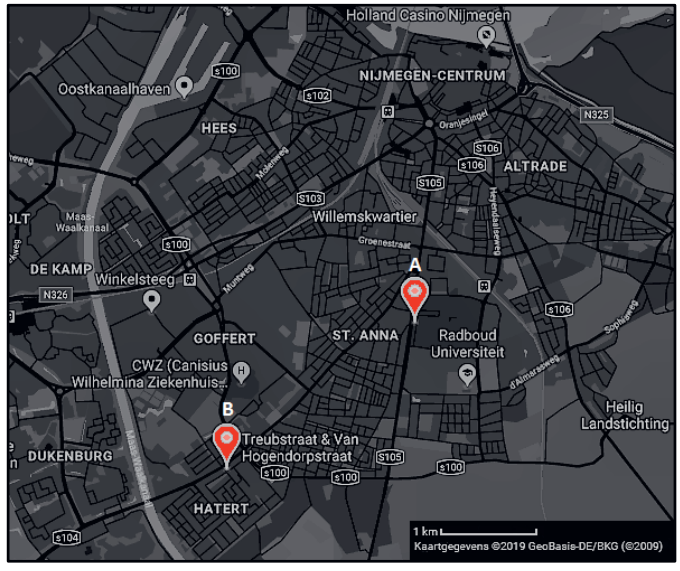

Fig. 3.6. Wastewater sampling points in the city of Nijmegen (the Netherlands). Sewage water was taken from a well at the Radboud University Medical Center **(A)** and in a residential area **(B)**. The sewer system of the end of pipe hospital effluent has no connection to the domestic sewage water well.

Table 3.4.
Pharmaceutical detection in hospital sewage water compared to domestic sewage water in the city of Nijmegen.

Hospital sewage water (A)
Thursday – Monday (12 - 16 Sep 2019, including a weekend)
x̄ Concentration (µg/L)
(±sd) *n* = 4

IOM[B]	IOP	DIA	DOX	CIP	FLU	DF	MET	CP	CB	TER	PHE	APAP	MF
2013.3 (±121.2)	n.d.	8.2 (±1.3)	n.d.	15.8 (±4.6)	0.16 (±0.05)	1.9 (±1.7)	0.97 (±0.14)	0.08 (±0.03)	0.15 (±0.09)	n.d.	n.d.	0.43[A]	30.1 (±13.6)

Hospital sewage water (A)
Monday – Thursday (16 - 19 Sep 2019, working days)
x̄ Concentration (µg/L)
(±sd) *n* = 4

IOM	IOP	DIA	DOX	CIP	FLU	DF	MET	CP	CB	TER	PHE	APAP	MF
2387.3 (±190.9)	n.d.	10.1 (±1.9)	n.d.	14.5 (±4.9)	0.15 (±0.04)	3.1 (±3.6)	1.3 (±0.3)	0.34 (±0.10)	0.08 (±0.23)	n.d.	n.d.	82.1 (±81.9)	36.8 (±14.9)

Hospital sewage water (Pooled)
x̄ Concentration (µg/L)
(±sd) *n* = 2

IOM	IOP	DIA	DOX	CIP	FLU	DF	MET	CP	CB	TER	PHE	APAP	MF
2070.5 (±99.8)	n.d.	7.8 (±0.4)	n.d.	11.6 (±1.6)	0.20 (±0.02)	0.3 (±0.05)	1.2 (±0.08)	0.22 (±0.01)	0.17 (±0.10)	n.d.	n.d.	0.07[A] (±0.16)	19.0 (±1.6)

Domestic sewage water (B)
Thursday (31 Oct 2019)
x̄ Concentration (µg/L)
(±sd) *n* = 4

IOM	IOP	DIA	DOX	CIP	FLU	DF	MET	CP	CB	TER	PHE	APAP	MF
n.d.	n.d.	n.d.	n.d.	1.1 (±0.5)	0.5 (±0.4)	5.6 (±4.7)	2.5 (±0.7)	n.d.	1.9 (±0.7)	n.d.	n.d.	482.9[B] (±286.2)	76.4 (±30.0)

[A]: It is recommended to analyse wastewater within 24h, to minimise biodegradation of APAP.
[B]: Determined concentrations exceeding the calibration range were quantified by linear extrapolation using the corresponding slope and intercept prepared in synthetic sewage water.

Despite the frequent usage of antibiotics, DOX has not been detected in HSW and DSW, due to its limited stability and affinity for charged cations Ca^{2+} and Mg^{2+} (Soeborg et al. 2004; Loftsson 2014). Tetracycline antibiotics, such as DOX, are stable under acidic conditions but undergo chemical reactions at neutral and basic pH, like epimerisation where hydroxyl and hydrogen group substituents exchange within the molecule by forming iso- or anhydrotetracyclines (Loftsson 2014). Tetracyclines predominantly absorb to sediment particles making it difficult to determine detectable amounts in wastewater samples (Thornton, 2001). That TER and PHE have not been found in the sewage water samples might be attributed to fact that other pharmaceuticals are used with the same therapeutic effect. Alternatives for TER and PHE are salbutamol and propyphenazone, molecules with very similar chemical properties and therapeutic effects (Zuehlke et al. 2007). Additionally, the route of discharge is also of importance, since concentrations of pharmaceuticals can vary per region. It is expected that the presence of TER is limited in urban sewage water samples, since the compound is mainly used as food additive in the veterinary sector to increase the amounts of lean meat of livestock (Zhou et al. 2017). The concentrations of pharmaceuticals detected in both HSW and DSW, provides qualitative information about their consumption. In the HSW it is worth mentioning the difference between the weekday and weekend sample, where the DSW sample reflects the continuous emission of prescription and over the counter medicines.

3.3.6.1 Oxidative degradation chemistry in hospital sewage water

Previous pharmaceutical oxidative degradation results were obtained in a controlled setting. To evaluate the efficiency of plasma-induced water activation and UV-C/H_2O_2 on untreated hospital effluent, pharmaceutical decomposition of the 10 identified compounds was determined, see **Fig. 3.7**. The overall conversion levels for IOM, DIA, CIP, FLU, DF, MET, CP, CB, APAP and MF are all near equivalent to the results obtained in the synthetic sewage water matrix. This is remarkable since the determined concentrations for IOM (~2400 µg/L), DIA (~10 µg/L), CIP (~13 µg/L), APAP (~300 µg/L) and MF (~35 µg/L) were all much higher in HSW than in the spiked (5 µg/L) synthetic sewage water matrix, see **Table S8** (SI **paragraph S.3.10**). According to the controlled experimental results, it has become clear, that the efficiency of pharmaceutical degradation mainly depends on pH, matrix complexity and oxidative technique used. A high pharmaceutical concentration is also of influence, but primarily slows down the rate of chemical degradation (Graumans et al. 2019). That the high concentration of IOM with UV-C/H_2O_2 treatment decreases so rapidly, is attributed to its sensitivity to UV irradiation. To demonstrate effectiveness of both oxidative treatment

techniques in hospital effluent, the total mass of the revealed pharmaceuticals was calculated according to a previously described method (Ajo et al. 2018). The overall conversion level was calculated with and without the contrast agents since the mass based occurrence of IOM and DIA was relatively high compared to the other pharmaceuticals.

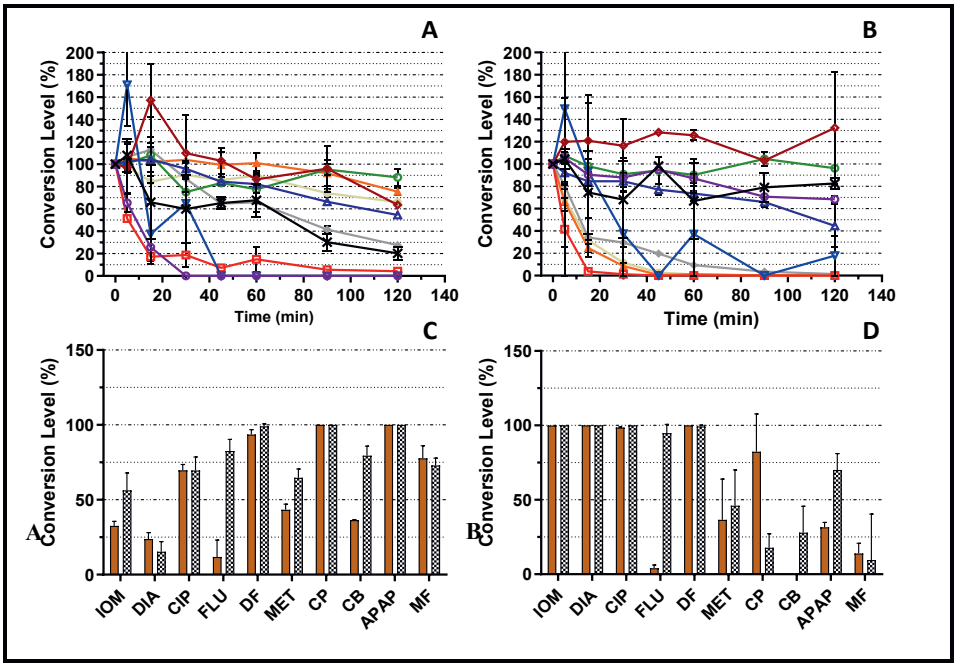

Fig. 3.7. Thermal plasma oxidation (**A**) was applied on hospital sewage water (HSW, *n* =3). 10 compounds were identified, showing the conversion levels for; **IOM** (●, 32.5%), **DIA** (▲, 23.8%), **CIP**(◆, 69.7%), **FLU**(○, 11.8%), **DF**(□, 93.6%), **MET**(△, 43.3%), **CP**(▽, 100.0%), **CB**(◇, 36.4%), **APAP**(○, 100.0%), **MF**(✖, 77.7%). UV-C/H_2O_2 oxidative degradation (**B**) demonstrated; **IOM** (●, 99.9%), **DIA** (▲, 100.0%), **CIP**(◆, 98.6%), **FLU**(○, 4.0%), **DF**(□, 100.0%), **MET**(△, 36.5%), **CP**(▽, 82.3%), **CB**(◇, N.C), **APAP**(○, 31.6%), **MF**(✖, 13.9%). For both techniques the pharmaceutical decomposition in HSW (■) was compared to the controlled degradation results in synthetic sewage water (▩). It is illustrated that both plasma oxidation (**C**) and UV-C/H_2O_2 (**D**) oxidative treatment in HSW initiate equivalent abatement as in the simulated matrix.

Table 3.5.

Total identified pharmaceutical concentration in hospital sewage water, demonstrating the effectiveness of plasma oxidation and UV/H_2O_2 treatment with and without contrast agents.

AOP	Total Conc. pharmaceuticals (µg/L)	Removal (%)	Total Conc. w/o IOM and DIA (µg/L)	Removal (%) w/o IOM and DIA
Plasma 150W$_{Start}$	2782.1	41.6	344.1	96.7
End$_{120\ min}$	1624.7		11.2	
UV-C/H_2O_2	2881.9	91.4	371.8	33.2
End$_{120\ min}$	248.5		248.3	

According to the results provided in **Table 3.5** and **S8** (SI **paragraph S.3.10**), it is suggested that thermal plasma treatment has the advantage over UV/H_2O_2 treatment, since in addition to ROS, also RNS are continuously produced in plasma activated water. With the exception of IOM and DIA, thermal plasma oxidative degradation proves its effectiveness in very complex matrices. The less gradual chemical degradation observed, during oxidative treatment in HSW is attributed to the matrix complexity. In our study only 10 compounds were detected in the HSW, but it is important to mention that many more analytes are to be expected (Ajo et al. 2018). Besides the pharmaceuticals that were not determined in this study, it is anticipated that molecules such as soaps, detergents, biotransformation products and hormones are also present in HSW. All these compounds will have an effect on the overall degradation efficiency e.g. competitive inhibition. The observed increase in sample concentration overtime for the analytes CP and CB is caused by their metabolites. During oxidative treatment, their non-detected biological metabolites are reformed into the pristine structures. This will cause an increased peak value relative to the measured initial concentration. Continuation of the oxidative treatment will cause further abatement and make it possible to degrade the compound completely (Aziz et al. 2018; Ajo et al. 2018; Graumans et al. 2020).

3.3.7 Strengths and limitations of the study

We developed an experimental set-up to provide insight into the degradation of 14 pharmaceuticals in complex matrices by use of AOP. The application of plasma treatment compared to UV-C/H_2O_2 on simulated matrices, indicates dependency of the degradation efficiency on matrix complexity and also varies with the method of oxidative treatment and the structural properties of the pharmaceuticals tested. The simulation matrices were compared with end-of-pipe hospital sewage water, sampled and processed by advanced oxidation. Due to matrix complexity and an unexpected broad concentration range in real life wastewater our analytical approach for synthetic sewage water showed some limitations for quantification of pharmaceuticals like IOM and APAP. Additionally, our lowest calibration point (0.5 µg/L) did not optimally serve quantification of FLU, DF, CP and CB, since their determined concentrations ranged between the LOD and lowest calibration point in synthetic sewage water. Nonetheless, this laboratory study represents a useful first step in the experimental validation of plasma activation technology to complement onsite wastewater treatment.

3.4 Conclusion

With this study we have extensively studied the degradation of pharmaceuticals in multiple complex matrices using thermal plasma and UV/H_2O_2 oxidative treatment. Despite the matrix

complexity has each technique its own added value towards specific pharmaceutical classes. Single dose hydrogen peroxide in stationary UV-C/H_2O_2 treatment has a temporary effect, and involved photons cannot produce RNS, whereas ongoing plasma activation can produce both ROS and RNS continuously. The continuous production of reactive species makes plasma activation an useful technique for the application in complex matrices such as hospital effluent. The pharmaceutical degradation by temperature-controlled thermal plasma treatment is complemented by nitrification under acidic conditions. Further research using cell-based assays should reveal whether the toxicity of contaminated matrices is decreased.

Acknowledgements

Financial support was made possible by the INTERREG Deutschland-Nederland program [grant number 142118]. The authors would like to thank VitalFluid who provided the PAW lab unit and UV-C source.

Supplementary data

The supporting information contains additional data on the physicochemical properties of the tested pharmaceuticals, including the irradiance calculation and all figures regarding oxidative degradation.

Literature

Ajo, P., Preis, S., Vornamo, T., Mänttäri, M., Kallioinen, M., & Louhi-Kultanen, M. (2018). Hospital wastewater treatment with pilot-scale pulsed corona discharge for removal of pharmaceutical residues. *Journal of Environmental Chemical Engineering*, *6*(2), 1569–1577. https://doi.org/10.1016/j.jece.2018.02.007

Allard, S., Criquet, J., Prunier, A., Falantin, C., Le Person, A., Yat-Man Tang, J., & Croué, J.-P. (2016). Photodecomposition of iodinated contrast media and subsequent formation of toxic iodinated moieties during final disinfection with chlorinated oxidants. *Water Research*, *103*, 453–461. https://doi.org/10.1016/j.watres.2016.07.050

Almeida, A. M., Castel-Branco, M. M., & Falcão, A. C. (2002). Linear regression for calibration lines revisited: weighting schemes for bioanalytical methods. *Journal of Chromatography B*, *774*(2), 215–222. https://doi.org/10.1016/S1570-0232(02)00244-1

Banaschik, R., Jablonowski, H., Bednarski, P. J., & Kolb, J. F. (2018). Degradation and intermediates of diclofenac as instructive example for decomposition of recalcitrant pharmaceuticals by hydroxyl radicals generated with pulsed corona plasma in water. *Journal of Hazardous Materials*, *342*, 651–660. https://doi.org/10.1016/j.jhazmat.2017.08.058

Banaschik, R., Lukes, P., Jablonowski, H., Hammer, M. U., Weltmann, K.-D., & Kolb, J. F. (2015). Potential of pulsed corona discharges generated in water for the degradation of persistent pharmaceutical residues. *Water Research*, *84*, 127–135. https://doi.org/10.1016/j.watres.2015.07.018

Beier, S., Köster, S., Veltmann, K., Schröder, H., & Pinnekamp, J. (2010). Treatment of hospital wastewater effluent by nanofiltration and reverse osmosis. *Water Science and Technology*, *61*(7), 1691–1698. https://doi.org/10.2166/wst.2010.119

Borowska, E., Felis, E., & Żabczyński, S. (2015). Degradation of Iodinated Contrast Media in Aquatic Environment by Means of UV, UV/TiO2 Process, and by Activated Sludge. *Water, Air, & Soil Pollution*, *226*(5), 151. https://doi.org/10.1007/s11270-015-2383-9

Bourin, M., Jolliet, P., & Ballereau, F. (1997). An Overview of the Clinical Pharmacokinetics of X-Ray Contrast Media. *Clinical Pharmacokinetics*, *32*(3), 180–193. https://doi.org/10.2165/00003088-199732030-00002

Brisset, J.-L., Benstaali, B., Moussa, D., Fanmoe, J., & Njoyim-Tamungang, E. (2011). Acidity control of plasma-chemical oxidation: applications to dye removal, urban waste abatement and microbial inactivation. *Plasma Sources Science and Technology*, *20*(3), 034021. https://doi.org/10.1088/0963-0252/20/3/034021

Brown, T.L., Bursten, B.E., Langford, S., Sagatys, D., Duffy (2007) Alkenes, Alkynes and Arenes Chemistry; The central science a broad perspective. Pearson Education Australia, French Forest, p 888-937

Chiron, S., Gomez, E., & Fenet, H. (2010). Nitration Processes of Acetaminophen in Nitrifying Activated Sludge. *Environmental Science & Technology*, *44*(1), 284–289. https://doi.org/10.1021/es902129c

Eloy, R., Corot, C., & Belleville, J. (1991). Contrast media for angiography: Physicochemical properties, pharmacokinetics and biocompatibility. *Clinical Materials*, *7*(2), 89–197. https://doi.org/10.1016/0267-6605(91)90045-H

Ferrando-Climent, L., Rodriguez-Mozaz, S., & Barceló, D. (2014). Incidence of anticancer drugs in an aquatic urban system: From hospital effluents through urban wastewater to natural environment. *Environmental Pollution*, *193*, 216–223. https://doi.org/10.1016/j.envpol.2014.07.002

Gerrity, D., Stanford, B. D., Trenholm, R. A., & Snyder, S. A. (2010). An evaluation of a pilot-scale nonthermal plasma advanced oxidation process for trace organic compound degradation. *Water Research*, *44*(2), 493–504. https://doi.org/10.1016/j.watres.2009.09.029

Giannakis, S., Androulaki, B., Comninellis, C., & Pulgarin, C. (2018). Wastewater and urine treatment by UVC-based advanced oxidation processes: Implications from the interactions of bacteria, viruses, and chemical contaminants. *Chemical Engineering Journal*, *343*, 270–282. https://doi.org/10.1016/j.cej.2018.03.019

Graumans, M. H. F., Hoeben, W. F. L. M., Russel, F. G. M., & Scheepers, P. T. J. (2020). Oxidative degradation of cyclophosphamide using thermal plasma activation and UV/H2O2 treatment in tap water. *Environmental Research*, *182*. https://doi.org/10.1016/j.envres.2019.109046

Gu, H., Liu, G., Wang, J., Aubry, A.-F., & Arnold, M. E. (2014). Selecting the Correct Weighting Factors for Linear and Quadratic Calibration Curves with Least-Squares Regression Algorithm in Bioanalytical LC-MS/MS Assays and Impacts of Using Incorrect Weighting Factors on Curve Stability, Data Quality, and Assay Performance. *Analytical Chemistry*, *86*(18), 8959–8966. https://doi.org/10.1021/ac5018265

Hama Aziz, K. H., Miessner, H., Mueller, S., Mahyar, A., Kalass, D., Moeller, D., Khorshid, I., & Rashid, M. A. M. (2018). Comparative study on 2,4-dichlorophenoxyacetic acid and 2,4-dichlorophenol removal from aqueous solutions via ozonation, photocatalysis and non-thermal plasma using a planar falling film reactor. *Journal of Hazardous Materials*, *343*, 107–115. https://doi.org/10.1016/j.jhazmat.2017.09.025

Hoeben, W. F. L. M., van Ooij, P. P., Schram, D. C., Huiskamp, T., Pemen, A. J. M., & Lukeš, P. (2019). On the Possibilities of Straightforward Characterization of Plasma Activated Water. *Plasma Chemistry and Plasma Processing*, *39*(3), 597–626. https://doi.org/10.1007/s11090-019-09976-7

Jeong, J., Jung, J., Cooper, W. J., & Song, W. (2010). Degradation mechanisms and kinetic studies for the treatment of X-ray contrast media compounds by advanced oxidation/reduction processes. *Water Research*, *44*(15), 4391–4398. https://doi.org/10.1016/j.watres.2010.05.054

Jewell, K. S., Wick, A., & Ternes, T. A. (2014). Comparisons between abiotic nitration and biotransformation reactions of phenolic micropollutants in activated sludge. *Water Research*, *48*, 478–489. https://doi.org/10.1016/j.watres.2013.10.010

Joshi, R. P., & Thagard, S. M. (2013). Streamer-Like Electrical Discharges in Water: Part II. Environmental Applications. *Plasma Chemistry and Plasma Processing*, *33*(1), 17–49. https://doi.org/10.1007/s11090-013-9436-x

Köhler, C., Venditti, S., Igos, E., Klepiszewski, K., Benetto, E., & Cornelissen, A. (2012). Elimination of pharmaceutical residues in biologically pre-treated hospital wastewater using advanced UV irradiation technology: A comparative assessment. *Journal of Hazardous Materials*, *239–240*, 70–77. https://doi.org/10.1016/j.jhazmat.2012.06.006

Li, Y., Niu, X., Yao, C., Yang, W., & Lu, G. (2019). Distribution, Removal, and Risk Assessment of Pharmaceuticals and Their Metabolites in Five Sewage Plants. *International Journal of Environmental Research and Public Health*, *16*(23), 4729. https://doi.org/10.3390/ijerph16234729

Lin, W., Zhang, X., Li, P., Tan, Y., & Ren, Y. (2020). Ultraviolet photolysis of metformin: mechanisms of environmental factors, identification of intermediates, and density functional theory calculations. *Environmental Science and Pollution Research*, *27*(14), 17043–17053. https://doi.org/10.1007/s11356-020-08255-9

Loftsson T (2014) Tetracyclines Drug Stability for Pharmaceutical Scientists

Magureanu, M., Bradu, C., & Parvulescu, V. I. (2018). Plasma processes for the treatment of water contaminated with harmful organic compounds. *Journal of Physics D: Applied Physics*, *51*(31), 313002. https://doi.org/10.1088/1361-6463/aacd9c

Magureanu, M., Mandache, N. B., & Parvulescu, V. I. (2015). Degradation of pharmaceutical compounds in water by non-thermal plasma treatment. *Water Research*, *81*, 124–136. https://doi.org/10.1016/j.watres.2015.05.037

Marković, M., Jović, M., Stanković, D., Kovačević, V., Roglić, G., Gojgić-Cvijović, G., & Manojlović, D. (2015). Application of non-thermal plasma reactor and Fenton reaction for degradation of ibuprofen. *Science of The Total Environment*, *505*, 1148–1155. https://doi.org/10.1016/j.scitotenv.2014.11.017

Miller, J. N., Miller, J. C. (2010). In Statistics and Chemometrics for Analytical Chemistry (pp. 110-153): Pearson.

OECD (2001) OECD GUIDELINE FOR THE TESTING OF CHEMICALS Simulation Test - Aerobic Sewage Treatment: 303 A: Activated Sludge Units - 303 B: Biofilms. https://www.oecd-ilibrary.org/

Peake, B. M., Braund, R., Tong, A. Y. C., & Tremblay, L. A. (2016). *The Life-cylce of pharmaceuticals in the environment*. Woodhead Publishin, Elsevier.

Pemen, A. J. M., van Ooij, P. P., Beckers, F. J. C. M., Hoeben, W. F. L. M., Koonen-Reemst, A. M. C. B., Huiskamp, T., & Leenders, P. H. M. (2017). Power Modulator for High-Yield Production of Plasma-Activated Water. *IEEE Transactions on Plasma Science*, *45*(10), 2725–2733. https://doi.org/10.1109/TPS.2017.2739484

Petrie, B., Youdan, J., Barden, R., & Kasprzyk-Hordern, B. (2016). Multi-residue analysis of 90 emerging contaminants in liquid and solid environmental matrices by ultra-high-performance liquid chromatography tandem mass spectrometry. *Journal of Chromatography A*, *1431*, 64–78. https://doi.org/10.1016/j.chroma.2015.12.036

Rosati, G. (1994). Clinical pharmacology of iomeprol. *European Journal of Radiology*, *18*, S51–S60. https://doi.org/10.1016/0720-048X(94)90094-9

Shih, K.-Y., & Locke, B. R. (2011). Optical and Electrical Diagnostics of the Effects of Conductivity on Liquid Phase Electrical Discharge. *IEEE Transactions on Plasma Science*, *39*(3), 883–892. https://doi.org/10.1109/TPS.2010.2098052

Shimizu, T., Kishimoto, N., & Sato, T. (2020). Effect of electrical conductivity of water on plasma-driven gas flow by needle-water discharge at atmospheric pressure. *Journal of Electrostatics*, *104*, 103422. https://doi.org/10.1016/j.elstat.2020.103422

Søeborg, T., Ingerslev, F., & Halling-Sørensen, B. (2004). Chemical stability of chlortetracycline and chlortetracycline degradation products and epimers in soil interstitial water. *Chemosphere*, *57*(10), 1515–1524. https://doi.org/10.1016/j.chemosphere.2004.09.020

Souza, F. S., & Féris, L. A. (2016). Hospital and Municipal Wastewater: Identification of Relevant Pharmaceutical Compounds. *Water Environment Research*, *88*(9), 871–877. https://doi.org/10.2175/106143016X14609975747603

Squadrito, G. L., & Pryor, W. A. (1998). Oxidative chemistry of nitric oxide: the roles of superoxide, peroxynitrite, and carbon dioxide. *Free Radical Biology and Medicine*, *25*(4–5), 392–403. https://doi.org/10.1016/S0891-5849(98)00095-1

Suarez, S., Lema, J. M., & Omil, F. (2009). Pre-treatment of hospital wastewater by coagulation–flocculation and flotation. *Bioresource Technology*, *100*(7), 2138–2146. https://doi.org/10.1016/j.biortech.2008.11.015

Thirumdas, R., Kothakota, A., Annapure, U., Siliveru, K., Blundell, R., Gatt, R., & Valdramidis, V. P. (2018). Plasma activated water (PAW): Chemistry, physico-chemical properties, applications in food and agriculture. *Trends in Food Science & Technology*, *77*, 21–31. https://doi.org/10.1016/j.tifs.2018.05.007

Thornton L, Butler, D., Docx, P., Hession, M., Makropoulos, C., McMullen, M., Nieuwenhuijsen, M., Pitman, A., Rautiu, R., Sawyer, R., Smith, S., White D. Wilderer, P., Paris, S., Marani, D., Braguglia, C., Palerm, J., (2001) Pollutants in urban waste water and sewage sludge. European Commission, Luxembourg

Vieno, N. M., Tuhkanen, T., & Kronberg, L. (2006). Analysis of neutral and basic pharmaceuticals in sewage treatment plants and in recipient rivers using solid phase extraction and liquid chromatography–tandem mass spectrometry detection. *Journal of Chromatography A*, *1134*(1–2), 101–111. https://doi.org/10.1016/j.chroma.2006.08.077

von Sonntag, C. (2008). Advanced oxidation processes: mechanistic aspects. *Water Science and Technology*, *58*(5), 1015–1021. https://doi.org/10.2166/wst.2008.467

Wang, Y., Roddick, F. A., & Fan, L. (2017). Direct and indirect photolysis of seven micropollutants in secondary effluent from a wastewater lagoon. *Chemosphere*, *185*, 297–308. https://doi.org/10.1016/j.chemosphere.2017.06.122

Wols, B. A., Hofman-Caris, C. H. M., Harmsen, D. J. H., & Beerendonk, E. F. (2013). Degradation of 40 selected pharmaceuticals by UV/H2O2. *Water Research*, *47*(15), 5876–5888. https://doi.org/10.1016/j.watres.2013.07.008

Yin, J., Yang, Y., Li, K., Zhang, J., & Shao, B. (2010). Analysis of Anticancer Drugs in Sewage Water By Selective SPE and UPLC-ESI-MS-MS. *Journal of Chromatographic Science*, *48*(10), 781–789. https://doi.org/10.1093/chromsci/48.10.781

Yoshida, M., & Akane, A. (1999). Subzero-Temperature Liquid−Liquid Extraction of Benzodiazepines for High-Performance Liquid Chromatography. *Analytical Chemistry*, *71*(9), 1918–1921. https://doi.org/10.1021/ac981276g

Zhao, C., Arroyo-Mora, L. E., DeCaprio, A. P., Sharma, V. K., Dionysiou, D. D., & O'Shea, K. E. (2014). Reductive and oxidative degradation of iopamidol, iodinated X-ray contrast media, by Fe(III)-oxalate under UV and visible light treatment. *Water Research*, *67*, 144–153. https://doi.org/10.1016/j.watres.2014.09.009

Zhou, L., Sleiman, M., Ferronato, C., Chovelon, J.-M., de Sainte-Claire, P., & Richard, C. (2017). Sulfate radical induced degradation of β2-adrenoceptor agonists salbutamol and terbutaline: Phenoxyl radical dependent mechanisms. *Water Research*, *123*, 715–723. https://doi.org/10.1016/j.watres.2017.07.025

Zuehlke, S., Duennbier, U., & Heberer, T. (2007). Investigation of the behavior and metabolism of pharmaceutical residues during purification of contaminated ground water used for drinking water supply. *Chemosphere*, *69*(11), 1673–1680. https://doi.org/10.1016/j.chemosphere.2007.06.020

Supplemental Information for Chapter 3

This additional document is equipped with information to support the main text. In **paragraph S.3.1** the UV-C irradiance is estimated using a mathematical model. Dimensions and parameters needed for the calculation are illustrated in **Fig. S1** and **Table S1.** In **paragraph S.3.2** is our predicted UV-C irradiance compared to measured data. **Paragraph S.3.3** contains **Table S3**, showing the physicochemical parameters of the used tap water. The optimised analytical LC-MS/MS methodology is given in **paragraph S.3.4**, reporting the MRM acquisition parameters, linearity and LOD in **Table S4.** To support the degradation data from the main text, **Fig. S3-5** are added in SI **paragraph S.3.5**. **Paragraph S.3.6** contains **Fig. S6**, where the difference between cooled and non-cooled plasma activation on CP degradation is illustrated. **Paragraph S7** is added to support the main text by demonstrating the pharmaceutical dissociation. For each tested pharmaceutical the acid and base dissociation is given, see **Table S5. Paragraph S.3.8** and **S.3.9** demonstrates the SPE and LLE optimisation data. **Table S6** and **S7** contains all the recovery data obtained in Milli-Q and synthetic sewage water. To supplement the degradation figures obtained in HSW, **paragraph S.3.10** is added.

S.3.1 Fluence (UV-Dose) prediction for Bench-Scale experiments

In our previous study (Graumans et al. 2020) we estimated the possible irradiance by using a mathematical model described by Kowalski. With this model the UV power output (W) is divided by the lamp surface (cm^2) and multiplied by the view factor (*F*). The view factor is derived from the cylindrical shape of the lamp including the distance between the lamp and water surface. The predicted irradiance at that time was found to be ~114 W/m^2 (11.4 mW/cm^2). However, to be more concise, the UV-dose entering the water matrix is now estimated and corrected for its double cylindrical shape, see **Fig S1**.

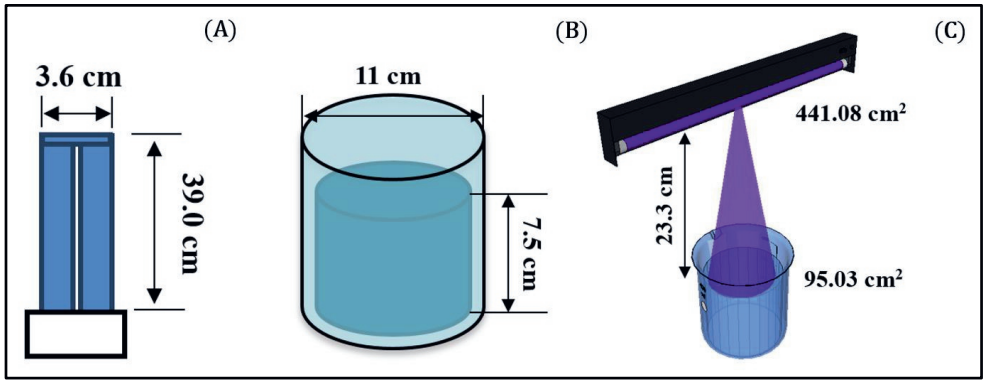

Fig. S1. Schematic representation of the lamp (**A**) used glass beaker including the water matrix (**B**) and bench-scale set up (**C**). The lamp surface is determined to be 441.08 cm^2, where the matrix surface in the glass beaker is 95.03 cm^2. During UV-C irradiation only 21.5% ((95.03/441.08)•100%) of the total lamp irradiance, *I,* will reach the matrix solution.

Irradiance equation: **(A1)**

$$I = \frac{E_{uv}}{2 \bullet \pi \bullet r \bullet l} \bullet F$$

$I = Irradiance\ (mW/cm^2)$

$E_{uv} = UV\ power\ output\ (mW)$

$F = View\ factor\ calculation$

Table S1.
Calculated irradiance levels using UV-C lamp specifications

Lamp	UV-C_{output} (mW)	Length *l* (cm)	Radius *r* (cm)	Distance *d* (cm)	Lamp Surface Irradiance (mW/cm^2)	View factor (F)	Predicted irradiance at water surface (mW/cm^2)
Current study Philips PL-L 60/4P HO	19000.0	39.0	1.8	23.3	43.1	0.13	5.70
Graumans et al. (2020) Philips PL-L 60/4P HO	19000.0	39.0	0.9	23.3	86.2	0.13	11.40
Wols et al. (2013) Philips PL-L 60	18795.0	39.0	1.8	30.0	42.6	0.10	4.26

When using 254 nm irradiation, four different correction factors are needed to estimate the UV-dose entering the water matrix. Equations **A2-5** are used according to Bolton et al. (2003) (Bolton et al. 2001; Bolton and Linden 2003).

Reflection Factor: **(A2)**

Reflection factor = (1 – *R*)

R = Average reflectance (200 – 300 nm) at the air-water interface:

Air: 1.000 (n_1)

Water: 1.372 (n_2)

Fresnel's law (no angle equation): $(\frac{n_1-n_2}{n_1+n_2})^2 = R$

Water Factor: **(A3)**

Water factor = $\frac{1-10^{-E(254nm)\cdot d}}{E(254nm)\cdot d\cdot \ln(10)}$

E(254nm): Absorption coefficient at 254 nm

d: matrix depth in cm

Divergence Factor: **(A4)**

Divergence Factor = $\frac{L}{L+d}$

L: Distance from the lamp to the matrix surface in cm

d: matrix depth in cm^2

Calculation of the expected UV-C irradiance entering the solution: **(A5)**

$$I \bullet pf \bullet (1 - R) \bullet \frac{1-10^{-E(254nm)\bullet d}}{E(254nm)\bullet d \bullet \ln(10)} \bullet \frac{L}{L+d}$$

$I =$ Irradiance (mW/cm^2)

$pf = Petri\ factor$ 0.9

$(1 - R) = 0.98$

E(254nm):

Distilled water: 0.007[3]

Tap water: 0.02[3]

$$\frac{1-10^{-0.007\bullet 7.5}}{0.007\bullet 7.5\bullet \ln(10)} = 0.94$$

d = 7.5 cm matrix depth

L = 23.3 cm

$$\frac{23.3}{(23.3+7.5)} = 0.76$$

Correction for the irradiance reaching the solution surface (21.5%):

5.70 mW/cm^2 • 0.22 = 1.23 mW/cm^2

Estimated UV-C dose entering the solution:

1.23 mW/cm^2 • 0.9 • 0.98 • 0.94 • 0.76 = 0.77 mW/cm^2

0.77 mW/cm^2 • t (s) = 0.77 mJ/cm^2

S.3.2 Comparing measured UV-dose with predictive data

In the study of Wols (Wols et al. 2013) a similar UV-C source was used, a Philips PLL60W. The measured irradiance entering the water matrix for this light source was given to be 0.63 mW/cm^2. During their bench-scale experiment a petri dish of 100 mL with a solution depth of 1.61 cm was irradiated at a distance of 30 cm. The 254 nm transmittance of the Milli-Q solution was noted to be 98.2%, which corresponds to an absorbance of 0.0078 (*2-log(98.2)*). Using once again the equations **A1-5**, it is demonstrated that our UV-dose prediction roughly corresponds to actual measured data. As it was stated that 100 mL is used with a depth of 1.6 cm, we assumed that a standard petri dish with dimensions of 10.0 cm (r: 5 cm) • 20 cm (h) was used. A similar petri dish can contain ~ 158 mL ($\pi \bullet r^2 \bullet h$), which will be sufficient for their bench-scale experiment. The surface area of the irradiated solution in this petri dish will be than ~78.5 cm^2 ($\pi \bullet r^2$). When also using the UV- lamp Philips PLL60W, 17.8% ((78.5/441.08) • 100%) of the UV irradiance will reach the water surface of the petri dish. The view factor (F) based on Kowalski (Kowalski, 2009) will be then 0.10 at 30 cm distance.

$Petri\ factor$ 0.9

$(1 - R) = 0.975$

E(254nm): 0.0078

$$\frac{1-10^{-0.0078 \cdot 1.6}}{0.0078 \cdot 1.6 \cdot \ln(10)} = 0.99$$

d = 1.6 cm matrix depth

L = 30.0 cm

$$\frac{30.0}{(30.0+1.6)} = 0.95$$

0.63 mW/cm^2/0.9/0.975/0.99/0.95 = 0.77 mW/cm^2

Correction for the irradiance reaching the solution surface (17.8%):

0.77 mW/cm^2 / 0.18 = 4.26 mW/cm^2

4.26 mW/cm^2/ $F_{(\text{view factor 30 cm})}$ 0.10 = 42.60 mW/cm^2

$I = \frac{E_{uv}}{2 \cdot \pi \cdot r \cdot l}$ = 42.6 mW/cm^2 = $\frac{E_{uv}}{441.08\text{cm}2}$

E_{uv} = (42.60 mW/cm^2 • 441.08 cm^2) = 18795.01 mW (~19W)

Table S2.

Rate constant data compared to literature references (Pereira et al. 2007; Wols et al. 2013)

Compound	***Graumans*** **Milli-Q Water** k (cm^2/mJ)	***Wols*** **Milli-Q Water** k (cm^2/mJ)	***Pereira*** **Milli-Q Water** k (cm^2/mJ)
Iomeprol (IOM)	0.0103	-	-
Iopamidol (IOP)	0.0127	-	-
Diatrizoic Acid (DIA)	0.0128	0.0053	-
Doxycycline (DOX)	0.0002	-	-
Ciprofloxacin (CIP)	n.d.	-	n.d.
Fluoxetine (FLU)	0.0003	0.0249	-
Diclofenac (DF)	n.d.	0.0281	-
Metoprolol (MET)	0.0015	0.0217	-
Cyclophosphamide (CP)	0.0004	0.0090	-
Carbamazepine (CB)	0.0016	0.0257	0.0109
Terbutaline (TER)	0.0017	-	-
Phenazone (PHE)	0.0054	0.0171	-
Acetaminophen (APAP)	0.0007	0.0194	-
Metformin (MF)	0.0001	0.0037	-

S.3.3 Physicochemical properties of the used tap water

During our oxidative degradation study, tap water from Vitens was used. Tap water delivered to the Radboud university medical center is extracted at the source Heumensoord. After drink water preparation by Vitens, they report publicly the physicochemical water properties of their product. Important parameters are adopted and presented in Table S3, showing the average numbers, including minimum and maximum values over the period Jan – Dec 2019 (n = 52 measurements).

Table S3.
Adopted parameters from water extraction point Heumensoord

Measured parameter	Unit	Average (minimum, maximum)
Turbidity	NTU[A]	0.24 (<0.1; 0.45)
Total Organic Carbon (TOC)	mg/L	< 0.5 (<0.5; 0.9)
Acidity	pH	7.73 (7.57; 7.94)
Minerals	mg/L	-
Cl_2		28 (25; 29)
PO_4		< 0.03 (<0.03; <0.03)
Si		5.80(5.80; 5.81)
SO_4		47.0(44.0; 49.0)
Nitrogen compounds	mg/L	-
NH_4		< 0.03 (<0.03; <0.03)
NO_2		< 0.01 (<0.01; <0.01)
NO_3		17.4 (14.3; 19.6)

[A]: Nephelometric Turbidity Unit

S.3.4 LC-MS/MS optimisation parameters

To detect and distinguish 14 different analytes, pharmaceutical selectivity was determined by multi reaction monitoring (MRM). For each compound a quantification and target transition was acquired by using direct MS/MS infusion, **Table S4.** To analyse all 14 selected compounds in one method, a multi-method was developed, see **Fig. S2**. A calibration curve ranging from 0.5 – 100 µg/L was prepared in Milli-Q water + 0.1% FA. Prior to testing the oxidative degradation in different aqueous media, a matching calibration curve was freshly prepared in the same matrix (n = 6; 0.5 – 100 µg/L). Limits of detection (LOD) for all pharmaceuticals were calculated according the lowest measurable calibration point multiplied by the obtained signal-to-noise ratio of the observable peak (Yin et al. 2010).

$$LOD = Conc. \bullet \frac{3}{S/N} \qquad \textbf{(B1)}$$

Table S4.
LC-MS/MS method optimisation parameters

Compound	**Transition** [M+H] (MRM)	**Correlation Coefficient** (r^2) (n = 3) Linear range (µg/L) (Milli-Q, 0.1% FA)	**Milli-Q 0.1% FA** (n = 4) LOD (µg/L)	**SPE Synthetic Sewage** (n = 3) LOD (µg/L)
Iomeprol (IOM)	(778.03 > 405.21) (778.03 > 288.10)	0.99 0.5 – 100	0.023	0.019
IOP-d8	(786 > 391)	-	-	
Iopamidol (IOP)	(777.777 > 558.797) (777.777 > 386.965)	0.99 0.5 – 100	0.052	0.005
IOP-d8	(786 > 391)	-	-	
Diatrizoic Acid (DIA)	(614.777 > 360.917) (614.777 > 233.018)	0.99 0.5 – 100	0.002	0.006
DIA-d6	(621 > 367)	-	-	
Doxycycline (DOX)	(445.16 > 410.15) (445.16 > 427.90)	0.99 1.0 – 100	0.205	0.003
Ciprofloxacin (CIP)	(332.16 > 231.08) (332.16 > 245.13)	0.98 0.5 – 100	0.002	0.001
Fluoxetine (FLU)	(310.224 > 148.035) (310.224 > 43.848)	0.99 0.5 – 100	0.003	0.001
FLU-d5	(315 > 153)	-	-	
Diclofenac (DF)	(295.904 > 214.804) (295.904 > 150.951)	0.99 0.5-100	0.087	0.025
DF-d4	(299.9 > 155)	-	-	

Table S4. *Continued*

Metoprolol (MET)	(268.266 > 116.031) (268.266 > 98.017)	0.99 0.5-100	0.003	0.001
MET-d7	(275 > 123)	-	-	
Cyclophosphamide (CP)	(260.986 > 139.929) (260.986 > 105.919)	0.99 0.5-100	0.046	0.011
CP-d4	(265 > 109.9)	-	-	
Carbamazepine (CB)	(236.968 > 178.876) (236.968 > 165.019)	0.99 0.5-100	0.001	0.011
CB-d10	(247 > 204)	-	-	
Terbutaline (TER)	(226.224 > 170.019) (226.224 > 106.999)	0.99 0.5-100	0.002	0.001
TER-d9	(235 > 153)	-	-	
Phenazone (PHE)	(189.032 > 131) (189.032 > 103.878)	0.99 0.5-100	0.131	0.102
PHE-d3	(192 > 77)	-	-	
Acetaminophen (APAP)	(151.968> 109.915) (151.968> 64.844)	0.99 0.5-100	0.241	0.152
ACE-d4	(156 > 69)	-	-	
Metformin (MF)	(129.968> 70.94) (129.968> 59.947)	0.99[A] 0.5-100	0.109	0.017
MF-d6	(136 > 77)	-	-	

[A]: Quadratic curve fitting ($y = ax^2 + bx + c$)

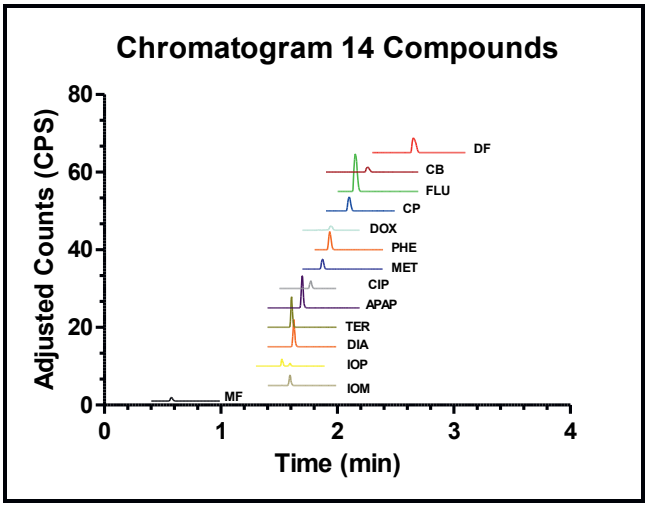

Fig. S2. This chromatogram illustrates the separation of 14 different pharmaceuticals. Rapid and selective identification is possible with this multi-method, showing retention times within 3 minutes.

S.3.5 Controlled thermal plasma and UV/H_2O_2 oxidative degradation in different aqueous matrices

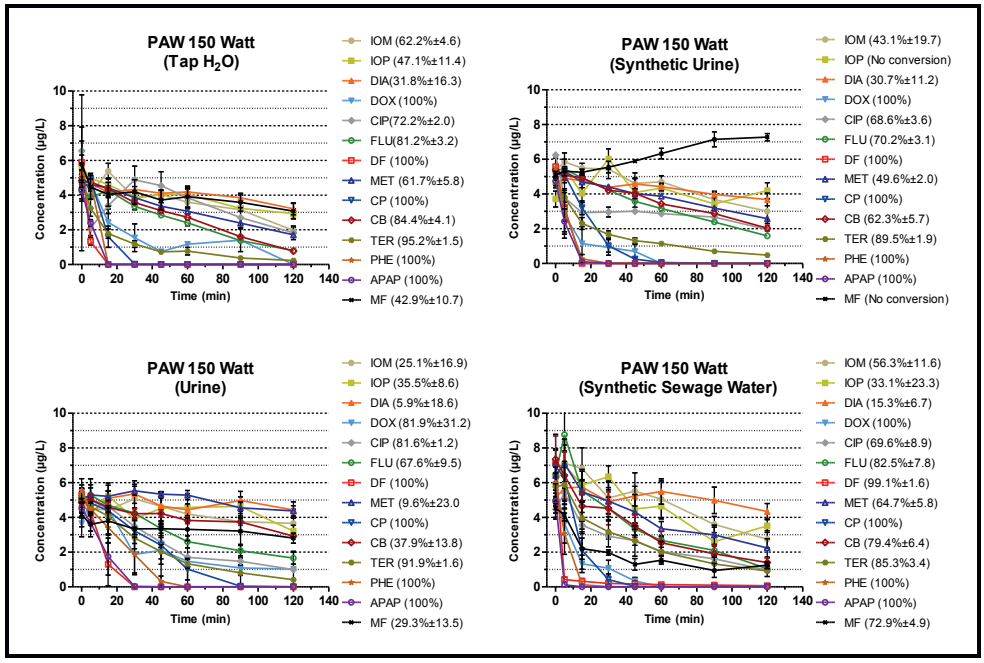

Fig. S3. Pharmaceutical oxidative degradation in the matrices, tap water, synthetic urine, human urine and synthetic sewage water. Based on the degradation curves, it is observed that the chemical degradation kinetics elapses exponential and that in the complex matrices all tested pharmaceuticals are altered or completely diminished.

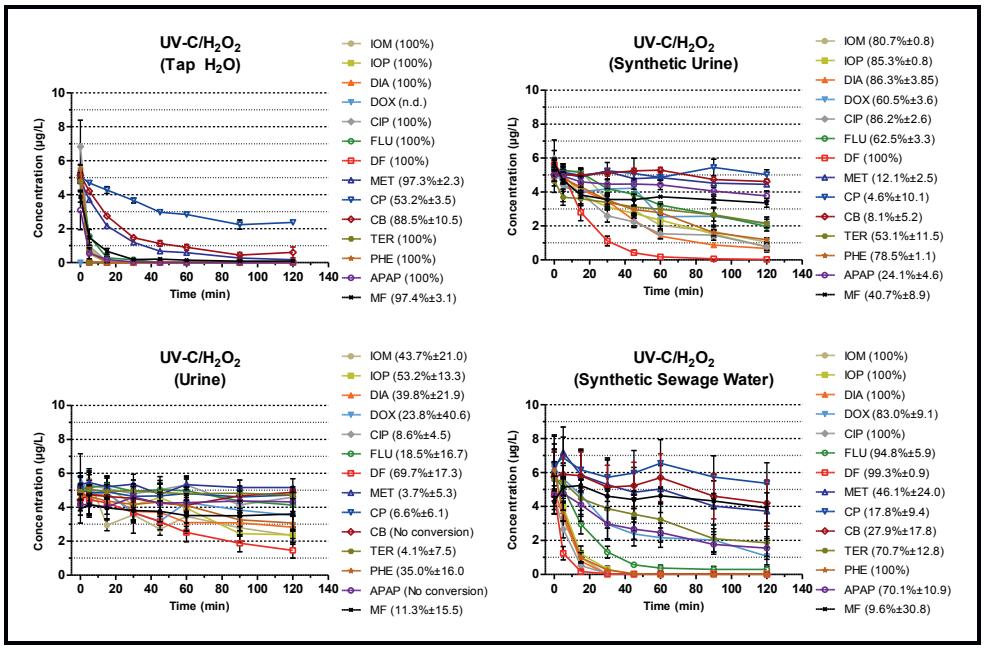

Fig. S4. Oxidative degradation results obtained with UV-C/H_2O_2 treatment. It is illustrated that the pharmaceutical degradation in complex matrices such as urine is less effective compared to Milli-Q (**Fig. 3.4** main text) where no coexisting substances are present. Despite the complexity of the aqueous medium, it is observed that the contrast agents rapid decrease in synthetic sewage water. On the other hand, compounds such as CP, CB and MF are poorly degraded.

Calculation *t-statistic* using r^2 of 0.50:

According to the oxidative degradation presented in **Fig. 3.2**, **3.4** (main text), **S3** and **S4**, all abatement curve fittings are log-normal transformed. In **Fig. S5** is the linear time-based degradation plot given for thermal plasma and UV-C/H_2O_2 treatment in Milli-Q water. The slope of these linear curves represents the first-order rate constant (k) as presentenced in **Table 3.1** and **3.3** of the main text. To confirm the linear correlation of the pseudo first-order degradation kinetics, a *two-sided t*-test was performed. As null hypothesis (H_0) "*no correlation for first-order degradation rate*" was selected with a significance level of $p = 0.05$. According to (n - 2) degrees of freedom, *t-critical* value is: 2.45 (Miller and Miller 2010). According to 8 time-based degradation points the degrees of freedom is 6.

$$t = \frac{r \bullet \sqrt{n-2}}{\sqrt{1-r^2}} \qquad \frac{0.71 \bullet \sqrt{8-2}}{\sqrt{1-0.50^2}} = 2.45 \qquad \textbf{(B2)}$$

t = *t-calculated*

According to the calculated *t-calculated*, ($r^2 > 0.50$) demonstrates significant correlation for first-order degradation kinetics.

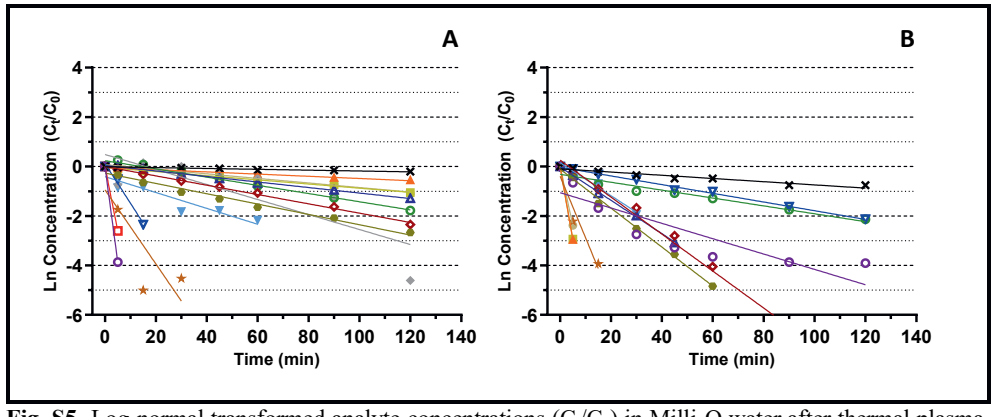

Fig. S5. Log-normal transformed analyte concentrations (C_t/C_0) in Milli-Q water after thermal plasma treatment (**A**) and UV-C/H_2O_2 oxidation (**B**). Time-dependent degradation curves of **Fig. 3.2** and **3.4** of the main text were log-normal transformed to generate a linear line, the slope represents the rate constant (k) of this first-order reaction rate plot. **IOM** (●), **IOP** (■), **DIA** (▲), **CIP**(◆), **DOX**(▼), **FLU**(○), **DF**(□), **MET**(△), **CP**(▽), **CB**(◇), **TER**(●), **PHE**(★), **APAP**(○) and **MF**(✖). Degradation curves in other matrices were also log-normal transformed, the rate constant (k) is presented in **Table 3.1.** and **3.3.** of the main text.

S.3.6 Non-cooled CP degradation compared to cooled plasma oxidative degradation

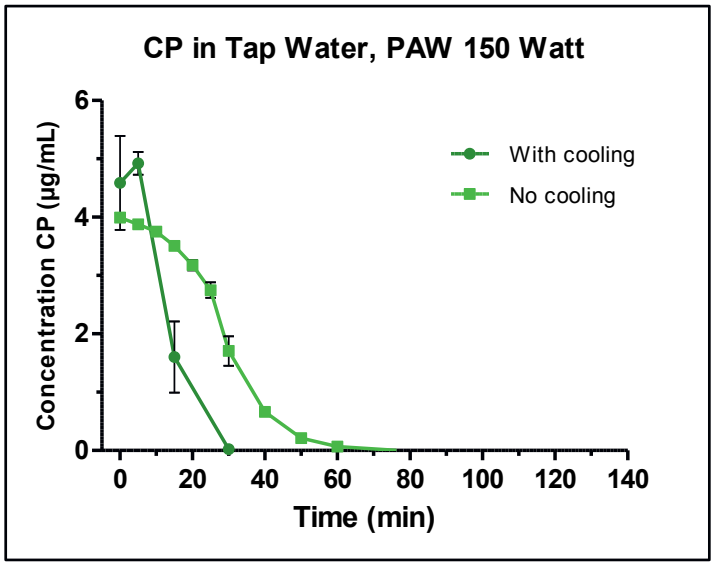

Fig. S6. Two different degradation curves of CP treated in tap water using an active cooled plasma system (●) compared to no active cooled plasma system (■). The distinctive logistic curve observed when using no cooled plasma is attributed to the ascending water temperature suppressing the formation of hydrogen peroxide. The active cooling stimulates the formation of more RONS, resulting in rapid chemical degradation kinetics (Hoeben, Graumans).

S.3.7 Molecular ionisation

Organic molecules do have ionisable centres, better known as p*K*a values. These p*K*a values do determine the ability of a molecule whether it will protonate or deprotonate at a certain pH. Protonating molecules are defined as acidic (*HA*), where basic species are proton acceptors (A^-). Using the Arrhenius definition the ionisation of an acid (*HA*) is demonstrated in water:

$$HA + H_2O \overset{K_a}{\Leftrightarrow} H_3O^+ + A^-$$

The dissociation constant, K_a, is a measure to demonstrate the acidic strength of an ionised compound:

$$K_a = \frac{[H_3O^+]\,[A^-]}{[HA]}$$

Taking the negative logarithm of K_a ($-\log_{10} K_a$) will give the p*K*a value. Ionised species will have increased water solubility caused by ionisable centres such as carboxylic acids, hydroxyl or amino groups (Bell, 2006). An example is given for FLU where it is seen that under acidic conditions the amine group will protonate, producing thus a more water soluble ion, **Table S5** (Bell, 2006; Nakamura et al. 2008). Regarding to acid-base reactions, it is stated that a base accepts a proton. However, according to the Lewis acid-base definition, a base will use nonbonding electrons to bind to a released proton or something else (Brown, 2007). From this principle it is reasoned that no proton is needed, and that nonbonding electrons of a Lewis-base ($B:^-$) can react with an electron deficient Lewis-acid (*H:A*). This principle is emphasised in the organic chemistry as a reaction where an electrophile (acid), will accept electrons from a nucleophile (base) to form a new covalent bond:

$$B:^- \rightarrow H:A \;\rightleftharpoons\; B:H + :A^-$$

For all tested pharmaceuticals the ionisation degree at a certain pH is determined using their strongest acidic and basic p*K*a values. Not all pharmaceuticals can produce ionic species, such as nonionic monomeric compounds IOM and IOP. These contrast agents are especially developed to be inert and non-toxic (Bourin et al. 1997). For all other compounds the ionisation degree is plotted against pH, including their corresponding anionic or cationic structure, **Table S5**.

Table S5.
Pharmaceutical acid and base dissociation data according to the pH range 0-14

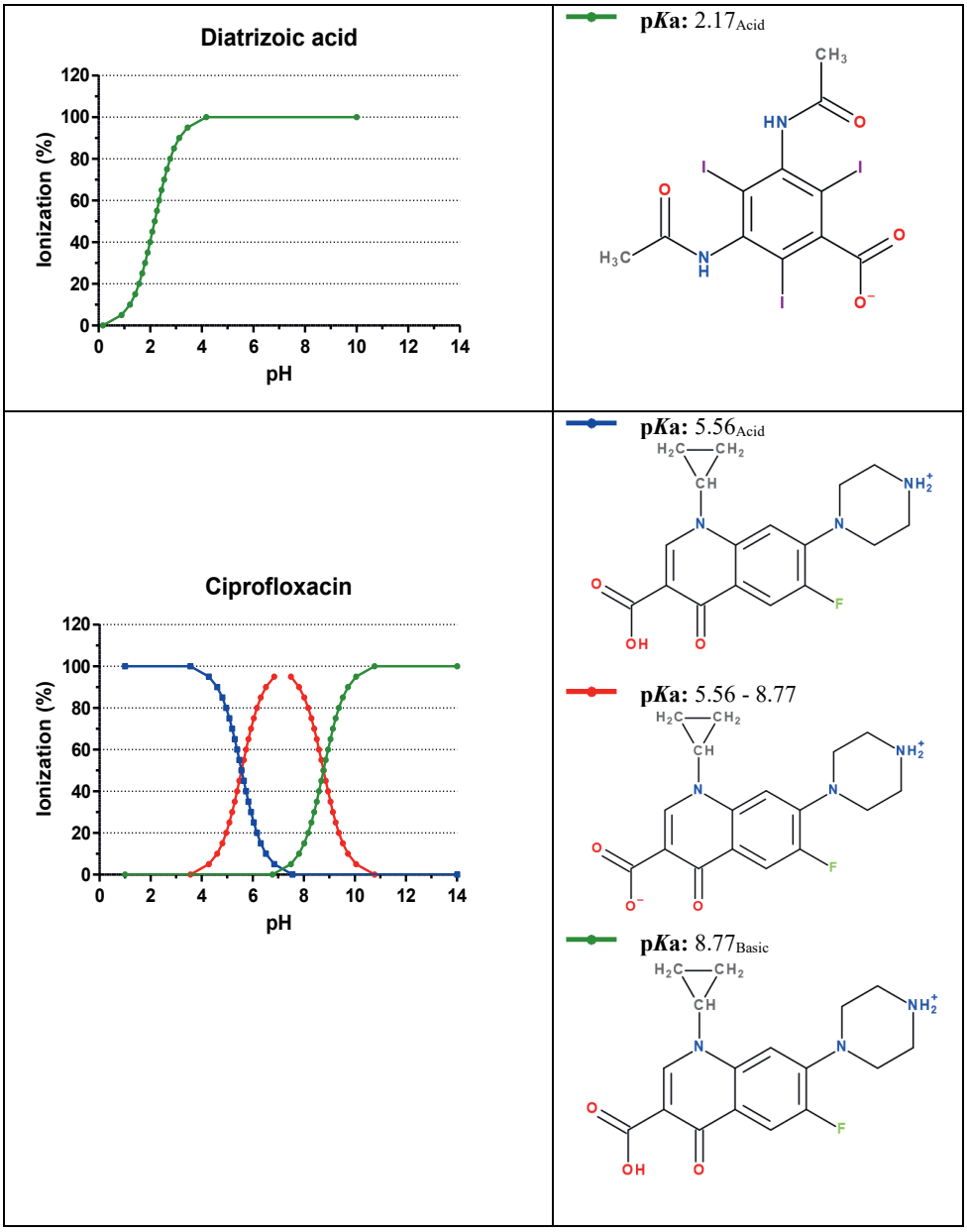

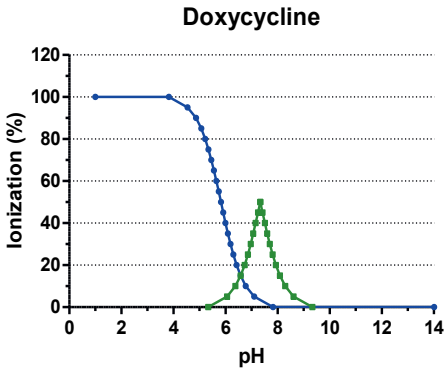
Doxycycline
Ionization (%)
pH

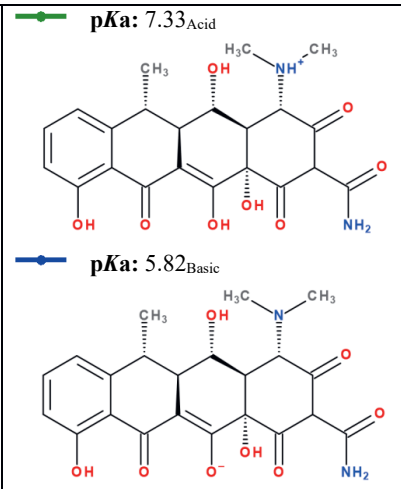
pKa: 7.33Acid
pKa: 5.82Basic

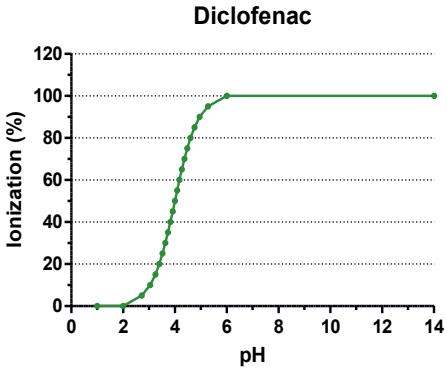
Diclofenac
Ionization (%)
pH

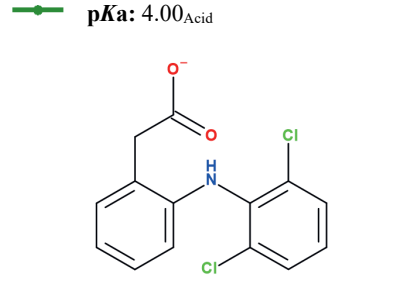
pKa: 4.00Acid

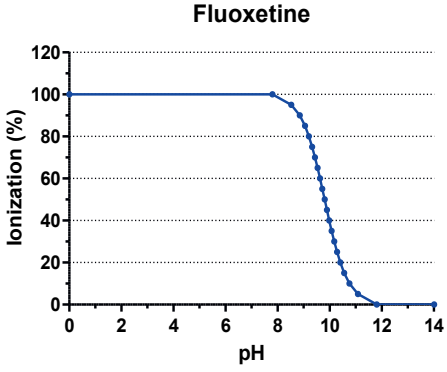
Fluoxetine
Ionization (%)
pH

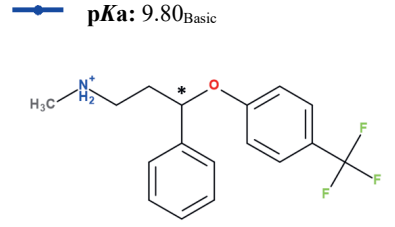
pKa: 9.80Basic

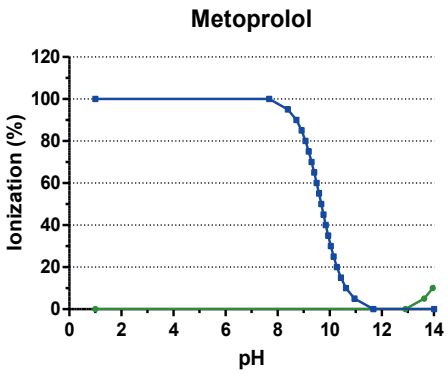

p*Ka*: 14.09$_{Acidic}$

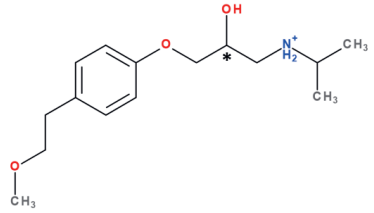

p*Ka*: 9.67$_{Basic}$

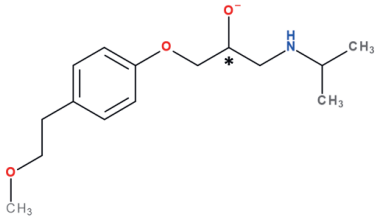

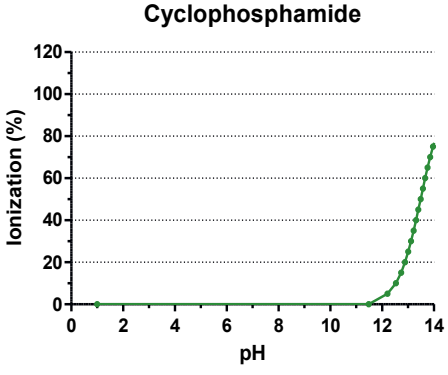

p*Ka*: 13.48$_{Acidic}$

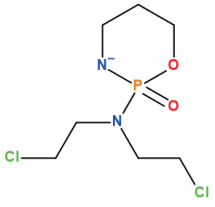

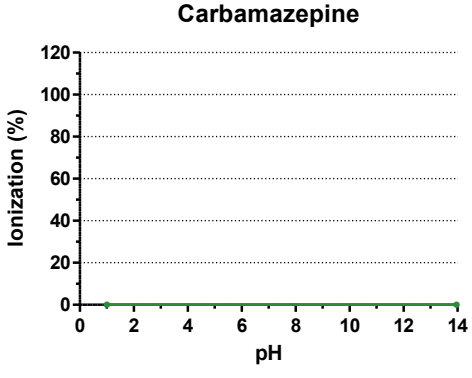

p*Ka*: 15.96$_{Acidic}$

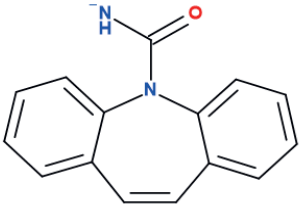

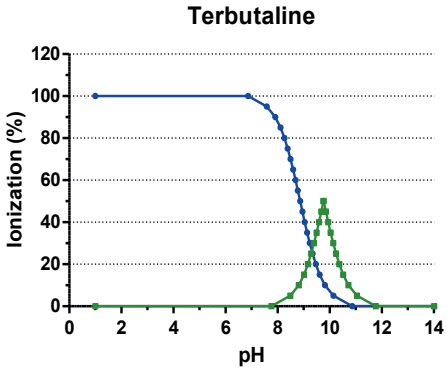

p*Ka*: 9.76$_{\text{Acidic}}$

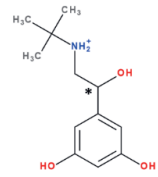

p*Ka*: 8.86$_{\text{Acidic}}$

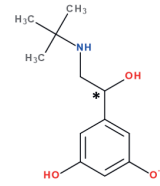

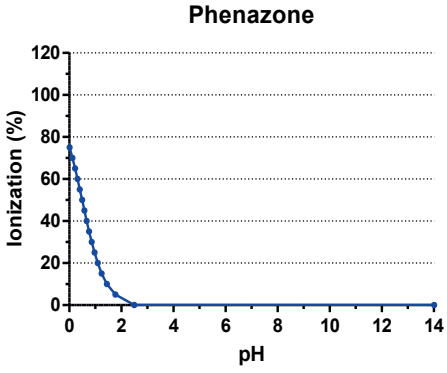

p*Ka*: 0.49$_{\text{Basic}}$

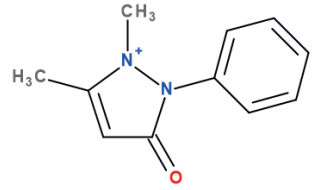

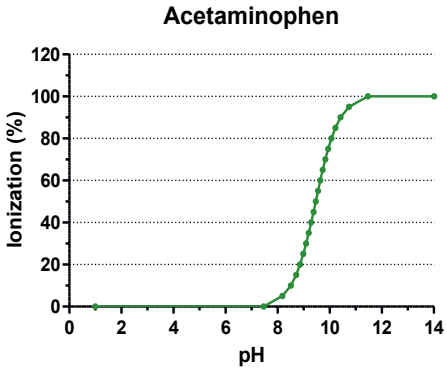

p*Ka*: 9.46$_{\text{Acidic}}$

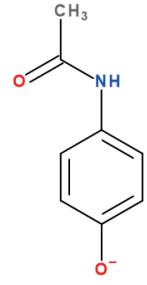

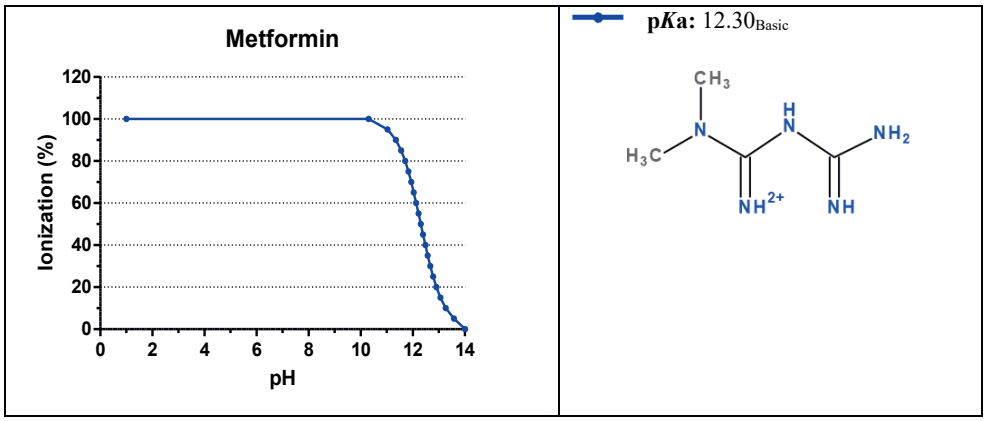

S.3.8 SPE recovery data

Oasis HLB SPE cartridges were selected based on their generic solid phase sorbent and their use in similar studies (Vieno et al. 2006; Yin et al. 2010; Echeverría et al. 2013; Ferrando-Climent et al. 2014; Ngubane et al. 2019) Oasis HLB SPE sorbent packing initiates lipophilic and hydrophilic interaction, which is generated by divinylbenzene and *N*-vineylpyrrolidone molecules (Vieno et al. 2006). Pharmaceutical recovery (*S*%) data obtained in Milli-Q and synthetic sewage water is provided in **Table S6.** To extract the pharmaceuticals from a complex aqueous matrix, the samples were first acidified to a pH of ~2.2. Acidic buffer was used to increase the extraction efficiency of the contrast agent IOP, IOM and to lower the ionised structure of compounds such as DIA DF and APAP (Echeverría et al. 2013). The neutral compounds CB, CP and PHE are known to be stable under acidic conditions. Good recovery results were achieved for the basic structures DOX, CIP, FLU, MET, and TER, demonstrating that the low pH has a minimal effect on the SPE recovery. This was also described by Vieno et al. 2006, who found that acidic pH has no pronounced effect on the recovery of the basic compounds MET and CIP when using Oasis HLB SPE cartridges. However, in contrast to other SPE studies, our extraction methodology appeared not optimal for DF. A likely explanation is that because neutralised DF has a very high affinity for the SPE sorbent (Log *P* 4.06), 5 mL of MeOH as elution solvent is not sufficient to recover all the retained DF molecules. A specific study on the SPE extraction of NSAIDs optimised their elution step by using 5 mL MeOH and 5 mL ACN (Ngubane et al. 2019). The high lipophilicity of DF could also explain its long retention on the stationary phase of our LC column, and that eluting only starts until nearly 100% ACN was used, see **Fig. S2** (SI **paragraph S.3.4**).

Table S6

SPE recovery data in Milli-Q and synthetic sewage water matrix for the concentrations 1.0, 10 and 50 ng/mL

Compound	Milli-Q Matrix $\bar{x}$ (*S*%) (±sd)	RSD (%)	Synthetic Sewage Water $\bar{x}$ (*S*%) (±sd)	RSD (%)
Iomeprol (IOM)				
1.0 ng/mL (*n* = 3)	38.0 (±24.7)	64.9	65.4 (±26.2)	40.1
10.0 ng/mL (*n* = 3)	52.5 (±16.2)	30.9	88.9 (±12.7)	14.3
50.0 ng/mL (*n* = 3)	61.8 (±17.2)	27.6	85.6 (±13.8)	16.2
Iopamidol (IOP)				
1.0 ng/mL (*n* = 6)	28.2 (±10.1)	36.0	45.6 (±22.5)	49.4
10.0 ng/mL (*n* = 6)	31.1 (±15.2)	48.9	52.2 (±22.0)	42.2
50.0 ng/mL (*n* = 6)	38.2 (±11.2)	29.5	58.9 (±12.6)	21.4
Diatrizoic Acid (DIA)				
1.0 ng/mL (*n* = 6)	49.3 (±7.1)	14.5	34.7 (±10.6)	30.7
10.0 ng/mL (*n* = 6)	49.4 (±17.4)	35.3	48.6 (±10.4)	21.4
50.0 ng/mL (*n* = 6)	56.5 (±14.9)	26.4	55.8 (±9.1)	16.4
Ciprofloxacin (CIP)				
1.0 ng/mL (*n* = 3)	40.7 (±10.6)	26.1	168.4 (±20.0)	11.9
10.0 ng/mL (*n* = 3)	36.4 (±14.3)	39.1	172.0 (±35.8)	20.8
50.0 ng/mL (*n* = 3)	50.9 (±9.0)	17.7	148.7 (±20.3)	13.6
Doxycycline (DOX)				
1.0 ng/mL (*n* = 2)	61.1 (±5.7)	9.3	116.2 (±24.9)	21.4
10.0 ng/mL (*n* = 3)	41.8 (±2.5)	6.0	13.0 (±3.1)	23.9
50.0 ng/mL (*n* = 3)	55.2 (±6.6)	12.0	61.7 (±8.6)	13.9
Fluoxetine (FLU)				
1.0 ng/mL (*n* = 6)	58.6 (±19.1)	32.6	100.5 (±11.0)	10.9
10.0 ng/mL (*n* = 6)	49.6 (±11.6)	23.4	116.8 (±46.3)	39.6
50.0 ng/mL (*n* = 6)	59.7 (±11.2)	18.7	92.8 (±18.7)	20.2
Diclofenac (DF)				
1.0 ng/mL (*n* = 4)	22.9 (±13.7)	60.0	27.2 (±7.2)	26.6
10.0 ng/mL (*n* = 6)	21.8 (±6.6)	30.2	27.2 (±17.8)	65.7
50.0 ng/mL (*n* = 6)	20.7 (±7.8)	37.5	17.0 (±3.6)	21.1
Metoprolol (MET)				
1.0 ng/mL (*n* = 6)	100.7 (±8.3)	8.3	113.2 (±11.6)	10.2
10.0 ng/mL (*n* = 6)	104.9 (±5.2)	5.0	110.1 (±12.1)	11.0
50.0 ng/mL (*n* = 6)	101.2 (±5.8)	5.7	105.2 (±11.4)	10.4
Cyclophosphamide (CP)				
1.0 ng/mL (*n* = 6)	104.8 (±12.1)	11.5	91.5 (±15.0)	16.3
10.0 ng/mL (*n* = 6)	96.2 (±2.3)	2.4	95.8 (±9.3)	9.8
50.0 ng/mL (*n* = 6)	92.2 (±2.2)	2.4	92.1 (±9.3)	10.1

Table S6 *Continued*

Carbamazepine (CB)				
1.0 ng/mL (n = 6)	84.3 (±16.7)	19.8	55.0 (±26.6)	48.4
10.0 ng/mL (n = 6)	77.8 (±4.0)	5.1	73.0 (±7.6)	10.4
50.0 ng/mL (n = 6)	77.2 (±13.1)	16.9	73.9 (±8.1)	11.0
Terbutaline (TER)				
1.0 ng/mL (n = 6)	59.0 (±17.0)	28.9	51.5 (±38.6)	75.0
10.0 ng/mL (n = 6)	64.0 (±10.5)	16.4	62.1 (±20.0)	32.2
50.0 ng/mL (n = 6)	67.1 (±8.8)	13.2	65.6 (±19.0)	28.9
Phenazone (PHE)				
1.0 ng/mL (n = 6)	93.6 (±9.9)	10.6	94.6 (±15.5)	16.4
10.0 ng/mL (n = 6)	91.2 (±4.2)	4.6	98.2 (±10.1)	10.3
50.0 ng/mL (n = 6)	89.7 (±5.1)	5.7	99.4 (±9.2)	9.2
Acetaminophen (APAP)				
1.0 ng/mL (n = 4)	94.4 (±21.9)	23.3	29.7 (±21.3)	71.6
10.0 ng/mL (n = 5)	95.9 (±4.3)	4.5	49.4 (±12.0)	24.3
50.0 ng/mL (n = 6)	99.7 (±4.3)	4.3	61.7 (±16.5)	26.8

S.3.9 Metformin liquid-liquid extraction

The extraction of MF with SPE was insufficient, since recovery percentages using Oasis HLB cartridges were very low (S% >10.0). Similar results were presented by Petrie et al. (2016), showing S% <1.0 in crude wastewater and Oertel et al. (2018), who found a S% < 10.0 at neutral (7) and basic (3) pH using also Oasis HLB cartridges. An alternative extraction approach was utilised by direct injection of crude wastewater into the LC-MS system. The crude wastewater was filtrated and diluted in MeOH (Petrie et al. 2016; Oertel et al. 2018). Oertel et al (2018), proposed to reduce the double-charged cationic MF molecule, by increasing the pH, thus allowing hydrophilic extraction of MF with a S% > 56.0 on Oasis HLB cartridges. AbuRuz et al. (2003) proposed ion pair solid phase extraction by adding sodium dodecyl sulphate (SDS) into the SPE cartridge, showing an impressive > S% 98.0 (AbuRuz et al. 2003). According to AbuRuz et al (2003), SDS was added to initiate a cation-anion interaction between MF and SDS. MF is in its cationic form at neutral and acidic pH (AbuRuz et al. 2003). The anionic group of SDS can bind to the positively charged MF molecules, see **Fig. S7.** Since SDS has hydrophilic and lipophilic chemical properties, caused by the sulphate group attached to a hydrocarbon tail, the non-polar hydrocarbon tail will have more affinity for the organic layer.

Table S7.
Metformin recovery percentages in Milli-Q and synthetic sewage water by using SPE and LLE

SPE	Milli-Q Matrix	RSD	Synthetic Sewage Water	RSD
	$\bar{x}$ (*S*%) (±sd)	(%)	$\bar{x}$ (*S*%) (±sd)	(%)
Metformin (MF)				
1.0 ng/mL (*n* = 3)	2.8 (±0.6)	21.7	6.9 (±1.9)	27.4
10.0 ng/mL (*n* = 3)	5.5 (±1.4)	25.4	8.3 (±0.7)	8.7
50.0 ng/mL (*n* = 3)	3.6 (±1.7)	46.3	5.5 (±1.2)	22.3
LLE	**Milli-Q Matrix**	**RSD**	**Synthetic Sewage Water**	**RSD**
	$\bar{x}$ (*S*%) (±sd)	(%)	$\bar{x}$ (*S*%) (±sd)	(%)
Metformin (MF)				
1.0 ng/mL (*n* = 3)	118.1 (±3.8)	3.2	110.6 (±26.3)	23.8
10.0 ng/mL (*n* = 3)	148.6 (±5.8)	3.9	135.9 (±12.7)	9.4
50.0 ng/mL (*n* = 3)	82.4 (±8.4)	10.2	64.9 (±4.7)	7.3

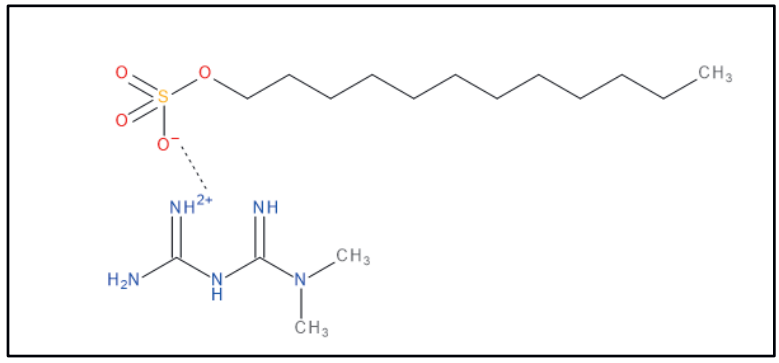

Fig. S7. The proposed chemical interaction between the anionic group of SDS with the cationic charged group of metformin. The hydrocarbon tail of SDS will have more affinity for the ACN layer during the used LLE extraction.

S.3.10 Hospital sewage water pharmaceutical concentration

Because the contrast agents IOM and DIA are ~87% of the total pharmaceutical concentration, the total removal (%) was calculated without these compounds (w/o X-ray), see **Table S8**. Based on these results it is seen that thermal plasma treatment as an advantage over UV/H_2O_2 when the concentrations of the contrast agents are not included. A similar result was seen by Ajo et al. 2018, where caffeine produced a similar masking effect.

Table S8.

Determined pharmaceutical concentrations in HSW prior thermal plasma and UV-C/H_2O_2 analysis (n = 3)

Hospital sewage water
Monday – Thursday (16 - 19 Sep 2019)
x̄ Concentration (µg/L)
(±sd) n = 3

AOP	IOM	DIA	CIP	FLU	DF	MET	CP	CB	APAP	MF	Total Conc.	Total $\bar{R}$ (%)	Total Conc. w/o X-ray	Total $\bar{R}$ (%) w/o X-ray
Plasma 150W$_{Start}$	2425.4 (±90.3)	12.6 (±1.6)	13.2 (±2.8)	0.4 (±0.03)	1.1 (±0.5)	1.9 (±0.5)	0.2 (±0.1)	0.4 (±0.1)	293.9 (±64.4)	33.0 (±4.2)	2782.1	-	344.1	
End$_{120\ min}$	1603.7 (±108.5)	9.5 (±1.3)	3.5 (±0.2)	0.3 (±0.01)	0.03 (±0.02)	1.1 (±0.3)	0.0	0.2 (±0.1)	0.0	6.4 (±1.9)	1624.7	41.6	11.2	96.7
UV-C/ H_2O_2	2497.2 (±41.1)	12.7 (±1.5)	13.5 (±2.8)	0.3 (±0.02)	1.4 (±0.6)	1.9 (±0.5)	0.2 (±0.1)	0.4 (±0.1)	323.5 (±7.9)	30.6 (±1.6)	2881.9	-	371.8	
End$_{120\ min}$	0.2 (±0.1)	0.0	0.2 (±0.1)	0.3 (±0.02)	0.0	1.0 (±0.6)	0.1 (±0.1)	0.4 (±0.1	221.1 (±5.0)	25.2 (±1.5)	248.5	91.4	248.3	33.2

Literature

AbuRuz, S., Millership, J., & McElnay, J. (2003). Determination of metformin in plasma using a new ion pair solid phase extraction technique and ion pair liquid chromatography. *Journal of Chromatography B*, *798*(2), 203–209. https://doi.org/10.1016/j.jchromb.2003.09.043

Ajo, P., Preis, S., Vornamo, T., Mänttäri, M., Kallioinen, M., & Louhi-Kultanen, M. (2018). Hospital wastewater treatment with pilot-scale pulsed corona discharge for removal of pharmaceutical residues. *Journal of Environmental Chemical Engineering*, *6*(2), 1569–1577. https://doi.org/10.1016/j.jece.2018.02.007

Bell S (2006) Forensic chemistry. Pearson Prentice Hall, New Jersey

Bolton, J. R., Bircher, K. G., Tumas, W., & Tolman, C. A. (2001). Figures-of-merit for the technical development and application of advanced oxidation technologies for both electric- and solar-driven systems (IUPAC Technical Report). *Pure and Applied Chemistry*, *73*(4), 627–637. https://doi.org/10.1351/pac200173040627

Bolton, J. R., & Linden, K. G. (2003). Standardization of Methods for Fluence (UV Dose) Determination in Bench-Scale UV Experiments. *Journal of Environmental Engineering*, *129*(3), 209–215. https://doi.org/10.1061/(ASCE)0733-9372(2003)129:3(209)

Bourin, M., Jolliet, P., & Ballereau, F. (1997). An Overview of the Clinical Pharmacokinetics of X-Ray Contrast Media. *Clinical Pharmacokinetics*, *32*(3), 180–193. https://doi.org/10.2165/00003088-199732030-00002

Brown, T.L., Bursten, B.E., Langford, S., Sagatys, D., Duffy, N.(2007) Chemistry; The central science

Echeverría, S., Herrero, P., Borrull, F., Fontanals, N., & Pocurull, E. (2013). Performance of zwitterionic hydrophilic interaction LC for the determination of iodinated X-ray contrast agents. *Journal of Separation Science*, *36*(23), 3688–3695. https://doi.org/10.1002/jssc.201300702

Graumans, M. H. F., Hoeben, W. F. L. M., Russel, F. G. M., & Scheepers, P. T. J. (2020). Oxidative degradation of cyclophosphamide using thermal plasma activation and UV/H2O2 treatment in tap water. *Environmental Research*, *182*. https://doi.org/10.1016/j.envres.2019.109046

Kowalski, W. (2009). *Ultraviolet Germicidal Irradiation Handbook*. Springer Berlin Heidelberg. https://doi.org/10.1007/978-3-642-01999-9

Miller, J. N., Miller, J. C. (2010). In Statistics and Chemometrics for Analytical Chemistry (pp. 110-153): Pearson.

Nakamura, Y., Yamamoto, H., Sekizawa, J., Kondo, T., Hirai, N., & Tatarazako, N. (2008). The effects of pH on fluoxetine in Japanese medaka (Oryzias latipes): Acute toxicity in fish larvae and bioaccumulation in juvenile fish. *Chemosphere*, *70*(5), 865–873. https://doi.org/10.1016/j.chemosphere.2007.06.089

Ngubane, N. P., Naicker, D., Ncube, S., Chimuka, L., & Madikizela, L. M. (2019). Determination of naproxen, diclofenac and ibuprofen in Umgeni estuary and seawater: A

case of northern Durban in KwaZulu–Natal Province of South Africa. *Regional Studies in Marine Science*, *29*, 100675. https://doi.org/10.1016/j.rsma.2019.100675

Oertel, R., Baldauf, J., & Rossmann, J. (2018). Development and validation of a hydrophilic interaction liquid chromatography-tandem mass spectrometry method for the quantification of the antidiabetic drug metformin and six others pharmaceuticals in wastewater. *Journal of Chromatography A*, *1556*, 73–80. https://doi.org/10.1016/j.chroma.2018.04.068

Pereira, V. J., Weinberg, H. S., Linden, K. G., & Singer, P. C. (2007). UV Degradation Kinetics and Modeling of Pharmaceutical Compounds in Laboratory Grade and Surface Water via Direct and Indirect Photolysis at 254 nm. *Environmental Science & Technology*, *41*(5), 1682–1688. https://doi.org/10.1021/es061491b

Philips PL-L 60W/4P HO product leaflet Website; https://www.assets.lighting.philips.com/is/content/PhilipsLighting/fp927909004007-pss-global

Wols, B. A., Hofman-Caris, C. H. M., Harmsen, D. J. H., & Beerendonk, E. F. (2013). Degradation of 40 selected pharmaceuticals by UV/H2O2. *Water Research*, *47*(15), 5876–5888. https://doi.org/10.1016/j.watres.2013.07.008

Yin, J., Yang, Y., Li, K., Zhang, J., & Shao, B. (2010). Analysis of Anticancer Drugs in Sewage Water By Selective SPE and UPLC-ESI-MS-MS. *Journal of Chromatographic Science*, *48*(10), 781–789. https://doi.org/10.1093/chromsci/48.10.781

Chapter 4

Cytotoxicity effects determination after pharmaceutical oxidative treatment

Martien H.F. Graumans, Hedwig van Hove, Tom Schirris,
Wilfred F.L.M. Hoeben, Maurice F.P. van Dael,
Frans G.M. Russel, Paul T.J. Scheepers

Published in:
Chemosphere 303, September 2022

Abstract

Pharmaceutical residues are released in the aquatic environment due to incomplete removal from wastewater. With the presence of multiple chemicals in sewage waters, contaminants may adversely affect the effectiveness of a wastewater treatment plant (WWTP). In certain cases, discharged metabolites are transformed back into their pristine structure and become bioactive again. Other compounds are persistent and can withstand conventional wastewater treatment. When WWTP effluents are released in surface waters, pristine and persistent chemicals can affect the aquatic environment. To complement WWTPs and circumvent incomplete removal of unwanted chemicals or pharmaceuticals, on-site wastewater treatment can contribute to their removal. Advanced oxidation processes (AOPs) are very powerful techniques for the abatement of pharmaceuticals, however, under certain circumstances reactive toxic by-products can be produced. We studied the application of on-site AOPs in a laboratory setting. It is expected that treatment at the contamination source can eliminate the worst polluters. Thermal plasma and UV/H_2O_2 oxidation were applied on simulation matrices, Milli-Q and synthetic sewage water spiked with 10 different pharmaceuticals in a range of 0.1 up to 2400 µg/L. In addition, untreated end-of-pipe hospital effluent was also subjected to oxidative treatment. The matrices were activated for 180 min and added to cultured HeLa cells. The cells were 24h and 48h exposed at 37 ºC and subsequently markers for oxidative stress and viability were measured. During the UV/H_2O_2 treatment periods no toxicity was observed. After thermal plasma activation of Milli-Q water (150 and 180 min) toxicity was observed. Direct application of thermal plasma treatment in hospital sewage water caused elimination of toxic substances. The low cytotoxicity of treated pharmaceutical residues is likely to become negligible if plasma pre-treated on-site wastewater is further diluted with other sewage water streams, before reaching the WWTP. Our study suggests that AOPs may be promising technologies to remove a substantial portion of pharmaceutical components by degradation at the source. Further studies will have to be performed to verify the feasibility of upscaling this technology from the benchtop to practice.

4.1 Introduction

Many different anthropogenic pollutants are discarded via industrial, domestic and hospital sewage water for removal in wastewater treatment plants (WWTPs). At WWTPs multiple steps are applied to reduce the content of suspended solids and overall organic carbon by 80 to 90% (Peake et al., 2016). Due to the complexity of sewage water and the presence of multiple chemicals such as personal care products, industrial compounds, pesticides, detergents and pharmaceuticals, individual pollutants or mixtures may adversely affect the WWTP removal efficiency causing inhibitory or toxic effects by affecting the bioactivity of activated sludge (Carucci et al., 2006; Henriques et al., 2007; Vasiliadou et al., 2018). This leads to incomplete WWTP removal or enzymatic conversion of metabolites into the original bioactive structure. Emissions of insufficiently treated WWTP may have adverse effects in the aquatic environment (Ajo et al., 2018; Abbas et al., 2019; Moermond et al., 2020; van Bergen et al., 2021). The occurrence of pharmaceutical residues in the environment is a known risk for aquatic ecosystems, antimicrobial resistance and drinking water quality (Isidori et al., 2016; Peake et al., 2016, Vasiliadou et al., 2018). Despite the difficulty to reveal the complete ecotoxicological effect of pharmaceuticals in water, the potential risk for water quality of various compounds is well demonstrated by bioassays or *in silico* tools (Fent et al., 2006; de Garcia et al., 2014; Abbas et al., 2019). For the removal of residual pharmaceutical compounds, different techniques could be applied either at WWTPs or at drinking water production facilities by treatment with membrane filtration, reversed osmosis, powdered activated carbon in activated sludge (PACAS) or advanced oxidation processes (AOPs) (Beier et al., 2010; Streicher et al., 2016; Banaschik et al. 2018; Ajo et al., 2018). Where certain techniques rely on the removal by transferring pollutants to another phase or an adsorbent, AOPs in contrast, are based on oxidation reactions with reactive species for the degradation of micropollutants (Magureanu et al., 2018; Ma et al., 2021). For example, with UV-C irradiation of hydrogen peroxide (H_2O_2), hydroxyl radicals ($^{\bullet}OH$) are formed which react with organic molecules. Another AOP is plasma technology, where electric energy is discharged into gas phase over a liquid containing residual pharmaceuticals. The energetic electrons effectively induce excitation, dissociation and ionisation of the gas discharge medium, yielding amongst others nitrogen and oxygen-based excited states, radical species and ions. Primarily produced reactive nitrogen (RNS) and reactive oxygen species (ROS) will react with pathogens and organic molecules by disinfecting and degrading pollutants in wastewater (Shen et al., 2016; Gerrity et al., 2010, Back et al., 2018; Thirumdas et al., 2018). It is demonstrated that AOPs including plasma oxidation are promising techniques for on-site wastewater treatment prior to conventional WWTP (Ajo et al., 2018;

Graumans et al., 2021). Despite the rapid degradation of organic molecules and disinfection properties, certain AOPs may also produce harmful oxidation by-products, which can be temporal upon reaction progress and degree of mineralisation (Parkinson et al., 2001; Heringa et al., 2011; Hofman-Caris et al., 2015; Jaeger et al., 2015 Dong et al., 2017; Du et al., 2017; Sillanpää et al., 2018; Gilca et al., 2020). Formation of toxic oxidative intermediates is especially of concern for drinking water production (Parkinson et al., 2001; Heringa et al., 2011; Hofman-Caris et al., 2015). Photocatalytic removal of natural organic matter (NOM), using techniques like UV/H_2O_2 and UV/O_3 in combination with medium pressure lamps (MP) can convert micropollutants in even more harmful components by the reaction between NOM, nitrate and photolytically produced radicals (Parkinson et al., 2001; Heringa et al., 2011; Hofman-Caris et al., 2015; Gilca et al., 2020). Next to that, in presence of bromide, the AOP ozonation (O_3) can generate bromated toxic by-products (Wu et al., 2019; Yang et al., 2021). Additional filtration steps with activated carbon are needed for the removal of these toxic intermediates formed by oxidation (Heringa et al., 2011; Back et al., 2018). To circumvent and minimise the formation of oxidative by-products, it is suggested to apply AOPs early in the wastewater chain. By reducing pharmaceutical residues and pathogens at the contamination source, conventional wastewater treatment plants are relieved and complemented. To investigate the suitability of plasma technology as a pretreatment technique for hospital sewage water, we tested oxidatively treated matrices on HeLa-cells. The cellular system was directly exposed to the oxidatively treated matrices and overall toxicity was evaluated. HeLa cells are uterus tumour cells of human origin, which can proliferate rapidly, making them a suitable cell line for cytotoxicity assays (Symons et al., 2001).

4.2 Materials and Methods

4.2.1 Chemicals and reagents

Cyclophosphamide (CP) (Endoxan®) was obtained from Baxter (Utrecht, the Netherlands) and iomeprol (IOM) (Iomeron®) was purchased from Bracco (Konstanz, Germany). Diatrizoic acid (DIA), fluoxetine (FLU), diclofenac (DF), metoprolol (MET), carbamazepine (CB), acetaminophen (APAP), ciprofloxacin (CIP) and metformin (MF), with a >98% purity were purchased from either Sigma Aldrich/Fluka Analytical (Zwijndrecht, the Netherlands) or Merck Group (Darmstadt, Germany). Stock solutions with a concentration of 1.0 mg/mL for all 10 pharmaceuticals were prepared in 50:50 (v/v) methanol water. Ultrapure water was tapped using a Milli-Q Academic A10 system with a resistivity of 18 MΩ•cm (Millipore, Amsterdam the Netherlands) and methanol (MeOH, UPLC grade) was retrieved from Boom B.V. (Meppel, the Netherlands). Compounds needed for the preparation of synthetic sewage water included NaCl, KCl, $CaCl_2 \bullet 2H_2O$, K_2HPO_4, $MgSO_4$, urea, peptone and meat extract and were purchased from Sigma Aldrich/Fluka Analytical (Zwijndrecht, the Netherlands) or Merck Group (Darmstadt, Germany). Cell medium constituents Dulbecco's Modified Eagle's medium (DMEM), foetal calve serum (FCS), oxidative stress probe CM-H_2DCFDA and viability marker crystal violet were purchased at Gibco Life Technologies, (Waltham, Massachusetts, USA), Greiner Bio One (Alphen aan den Rijn, the Netherlands), Thermo Fisher Scientific (Waltham, Massachusetts, USA) and Sigma Aldrich/Fluka Analytical (Zwijndrecht, the Netherlands) respectively.

4.2.2 Cell culture

HeLa cells (American Type Culture Collection, CCL-2) were maintained at 37 °C in a humidified atmosphere of 5% (v/v) CO_2 in DMEM medium containing 25 mM glucose, GlutaMAX, 1 mM pyruvate supplemented with 10% (v/v) FCS. Medium was renewed 2-3 times a week and cells were passed (1:10) every week after trypsinisation with 0.05% trypsin-EDTA in serum free medium when cells reached approximately 90% confluence.

4.2.3 Simulation matrices and hospital sewage water

To evaluate toxicity before and after UV-C/H_2O_2 and thermal plasma induced oxidation, Milli-Q water and synthetic sewage water matrices were spiked with a mixture of 10 pharmaceuticals IOM, DIA, CIP, FLU, DF, MET, CP, CB, APAP and MF, see **Table S2**. Pharmaceuticals were individually spiked from freshly prepared 1 mg/mL stock solution. From the 1 mg/mL stock solution consecutive concentrations of 24000, 100, 150, 20, 40, 20, 40, 20, 850, 370 µg/L were prepared in 500 mL Milli-Q or SSW. The prepared amounts in the simulation matrices were a

tenfold higher than measured in raw hospital sewage water, this to simulate the detected concentration (1.0 – 2400 µg/L) in the cell system (Graumans et al., 2021).

4.2.3.1 Synthetic sewage

Synthetic sewage water (SSW) was freshly prepared prior to each experiment. The composition of SSW was prepared according a standardised protocol from the Organization for Economic Co-operation and Development (OECD). 100 mL of freshly tapped Milli-Q was used to prepare all analytes separately. The final composition of SSW consists of the salts: 28.0 mg K_2HPO_4, 7.0 mg NaCl, 3.0 mg $CaCl_2 \bullet 2H_2O$ and 0.5 mg $MgSO_4$ including organic constituents 160.0 mg Peptone, 110.0 mg Meat Extract, 30.0 mg Urea dissolved in 1000 mL Milli-Q water (OECD, 2001).

4.2.3.2 Hospital sewage water

End-of-pipe hospital sewage water (HSW) was used during plasma and UV-C/H_2O_2 treatment. HSW was derived from a composite sample, which was periodically sampled between Monday – Thursday 16–19 September, 2019 (Graumans et al., 2021). The collected HSW was directly filtered upon arrival in the laboratory using vacuum filtration with a Whatman Filter grade 1 (Maidstone, United Kingdom). Different aliquots were prepared and stored in the freezer (-20 °C) till analysis. Prior to oxidative treatment, 500 mL frozen HSW samples were thawed and subsequently poured in a glass beaker.

4.2.4 Oxidative treatment and cellular exposure

500 mL of simulation matrices were activated in triplicate (n = 3) and exposed to HeLa cells after treatment using plasma and UV-C/H_2O_2 treatment. Both AOPs, were also used for the duplicate (n = 2) treatment of 500 mL of HSW samples, prior to cellular incubation. Cells were seeded in 96-wells plates (BD Falcon 96 well imaging plate black/clear, Fisher Scientific) (24h) prior to exposure. During HeLa cell exposure the untreated and treated matrices were added in triplicate (n = 3 wells), dissolved in a 1:10 concentration ratio (20 µL sample: 180 µL medium (v/v)) serum-free DMEM medium. For each experiment three controls were taken in the form of a medium control, vehicle control and a cytotoxic positive control using 500 µM H_2O_2. The cell plates were incubated for 24h and 48h at 37 °C in a humidified atmosphere of 5% (v/v) CO_2.

4.2.4.1 Thermal plasma treatment

A laboratory-scale plasma activation unit from VitalFluid (Eindhoven, the Netherlands) was used for plasma discharge in the matrices. The plasma unit comprises a 150 Watt (W), 1 MHz dual resonant power modulator (Pemen et al. 2017; Hoeben et al. 2019). The test samples were placed in a 800 mL glass beaker and thermal plasma discharges were applied with maximum

power output of 150 Watt (W) in ambient air over water. During this process electrical discharges with typically 8 kV peak-to-peak voltage were generated. To maintain the temperature of the treated solution below 35 °C during 180 min plasma activation, a Peltier cooling was applied.

4.2.4.2 UV-C/H_2O_2

For the UV-C irradiation a modified Aetaire UV air disinfection unit was used. UV-C irradiation is 180 min stationary applied through an opening of 28 cm x 7 cm. UV-C is irradiated at 253.7 nm (Philips PL-L 60W/4P HO UV-C lamp, Eindhoven, the Netherlands) with a distance of 20 cm between the lamp and aqueous matrix surface. At the start of the experiment 0.22 mM (~ 10 mg/L) hydrogen peroxide (H_2O_2) from J.T. Baker, Avantor Performance Materials (Deventer, the Netherlands) is added to the matrix. Minimising reflection and UV scattering, a container with an aperture (12 cm, wide) was placed over the 800 mL glass beaker.

4.2.5 Oxidative stress and viability assay

4.2.5.1 Oxidative stress probe CM-H_2DCFDA

After 24h and 48h incubation cells were washed with 200 µL PBS. Next, cells were stained with 5µM CM-H_2DCFDA probe diluted in serum-free DMEM. Cells were incubated for 30 minutes at 37 °C before the access medium containing the probe was aspirated and were washed with PBS. To induce fluorescent signal, 100 µL of 500 µM H_2O_2 was added to the culture medium. Cells were incubated for 5 min at 37 °C and the fluorescence was measured at 488/520 nm using a microplate spectrophotometer from Molecular Devices, Multimode Microplate Reader Spectramax iD5 (San Jose, USA).

4.2.5.2 Cell viability marker Crystal Violet

After cellular exposure, medium was removed and washed with PBS. Subsequently, 50 µL 0.5% (v/v) crystal violet solution was added to the cells and placed for 20 min at room temperature. The crystal violet marker will stain both proteins and nuclei, but, when cells undergo apoptosis, a lower amount of crystal violet staining will occur since death cells are detached and thus not visualised (Feoktistova et al., 2016). After incubation at room temperature, the staining solution is removed and cells were washed thoroughly 5 times with PBS. Plates were air-dried for 4 hours before the addition of 100 µL methanol, which will dissolve the crystal violet marker. Crystal violet absorbance is measured at 570 nm using a microplate spectrophotometer from Molecular Devices, Multimode Microplate Reader Spectramax iD5 (San Jose, USA).

4.2.6 Data analysis

Fluorescence and viability levels were plotted according to **eq. 1** by using GraphPad Prism 5.03 and 9 statistical software (GraphPad Inc., CA, USA). The amount of fluorescence produced compared to the medium control, was used as a measure for oxidative stress. Fluorescence levels above >100.0% do indicate oxidative stress levels deviating from to the medium control. **Eq. 1** is also applicable to calculate cell viability levels. Apparent cell viability (%) were determined by taking the crystal violet absorbance of a sample divided by the absorbance of the medium control multiplied by 100%. Cell viability levels lower than <50% were classified as severe cytotoxic.

$$Oxidative\ stress\ (\%) = \frac{Fluorescence_{(sample)}}{Fluorescence_{(Medium\ control)}} \bullet 100\% \qquad (\mathbf{1})$$

For each untreated (0 min) or oxidatively treated sample (5-180 min), three independent wells were 24h and 48h exposed to the HeLa cells. The mean ($\bar{x}$) value was calculated for each treatment period, including the standard deviation (σ) and the standard error of the mean (SEM). To confirm a significant difference in cell viability levels after an oxidation experiment, one-way analysis of variance (ANOVA) was applied. For the determination of statistically significant effects per treated time-period compared to the 100% medium control, the T-statistic was calculated, using Bonferroni's Multiple comparison test in GraphPad Prism 5.03 and 9.3.1 statistical software. Statistically significant effects are labelled with an asterisk (*): *; $p < 0.05$, **; $p < 0.01$ and ***; $p < 0.001$ (Miller and Miller 2010).

4.3 Results and Discussion

4.3.1 Assay optimisation

The effectiveness and sensitivity of the HeLa cytotoxicity assay was determined by using a fixed volume of 20 µL hydrogen peroxide (H_2O_2) at different concentrations. H_2O_2 is a known cytotoxic compound, since it is a source of hydroxyl radicals (•OH) when exposed to UV irradiation. •OH radicals in a cell system will initiate lipid peroxidation and DNA hydroxylation (Day and Suzuki, 2005; Ayuso et al., 2020). The inactivation applicability of aqueous H_2O_2 was demonstrated *in vitro* on human and murine tumour cell lines. To observe cytotoxic effects after 24h H_2O_2 exposure, CM-H_2DCFDA fluorescent probe and crystal violet were used as markers for oxidative stress and cell viability, respectively. Ascending H_2O_2 concentrations cause oxidative stress and reduce viability levels significantly, see **Fig. 4.1**. and **Table S1.** As demonstrated in this figure H_2O_2 concentrations higher than >100 µM do cause a decline in viability. Elevated fluorescence signal, compared to apparent viability of control, is a measure for cellular oxidative stress.

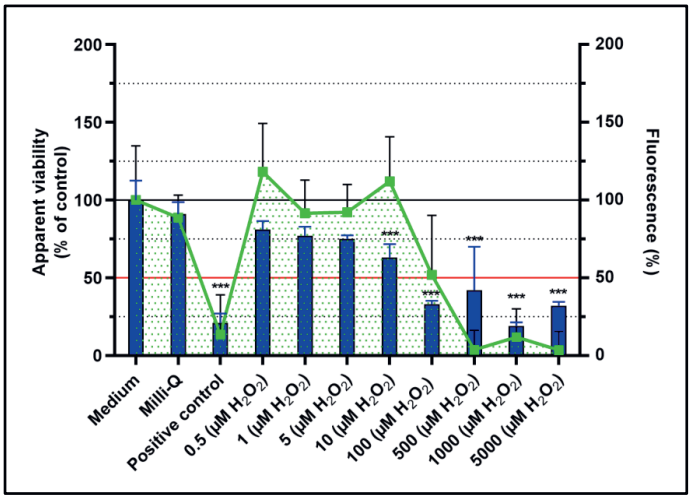

Fig. 4.1. Different concentrations of 20 µL H_2O_2 were added to cultivated HeLa cells, compared to a medium control and positive control (500 µM H_2O_2). CM-H_2DCFDA fluorescence probe was used to indicate oxidative stress (■). Crystal violet staining was used to confirm cell viability levels (■) ***; $p < 0.001$ (t-test with Bonferroni correction).

Increased fluorescence levels relative to the medium control, taken as 100%, indicate cellular oxidative stress (expressed as % relative to the medium control). When CM-H_2DCFDA probe is oxidised by intracellular reactive oxygen species (ROS), a fluorescent adduct is produced within the living cell (**Fig S1**). In case of apoptosis the probe will leak out and is washed away during the colouring process. Crystal violet staining is a useful marker for the verification of

viability (Sliwka et al., 2016; Feoktistova et al., 2016). Compared to enzymatic colourants the crystal violet indicator tags proteins and the external surface of the DNA double helix. By measuring the absorbance of the coloured product, viable adherent cells are quantified. With a plotted dose-response curve, the half maximal effect concentration (EC_{50}) was calculated for the different H_2O_2 concentrations **Fig S4.2**. EC_{50} values of 99 µM and 16 µM were found with CM-H_2DCFDA and crystal violet indicators, respectively. The difference between the EC_{50} values is explained by the different cellular targets of both markers (Feoktistova et al., 2016; Ayuso et al., 2020). The observed fluorescence signal, even in a case of cellular decline, might overestimate the viability when CM-H_2DCFDA probe is used alone. It was demonstrated in intestinal (IPEC-J2) cells that cellular efflux of the CM-H_2DCFDA probe can occur. Other interfering factors were attributed to the washing buffer, polystyrene well plate or from non-oxidised probe (Ayuso et al., 2020). To minimise autofluorescence we also measured empty polystyrene wells. Despite differences between the EC_{50} values for CM-H_2DCFDA and crystal violet, 500 µM H_2O_2 can be used as a positive control for confirmation of detected cell death. With 500 µM H_2O_2 viability levels less than <25% for both CM-H_2DCFDA (14 ± 25%) and crystal violet (21 ± 6%) markers were found.

4.3.2 Cytotoxicity of thermal plasma degradation

4.3.2.1 Plasma treatment of spiked Milli-Q water

Xenobiotics such as pharmaceuticals can generate reactive oxygen species (ROS) in living organisms during metabolism (Lutterbeck et al., 2017). Insufficient inactivation of ROS can cause damage to cellular macromolecules and too high concentrations of endogenously produced ROS (H_2O_2 and O_2^-) might initiate apoptosis (Ayuso et al., 2020). To simulate a contaminated water matrix, 10 different pharmaceuticals were spiked in Milli-Q water (see supplemental information paragraph **S2)**. Milli-Q water is a clean matrix that can be used to show the possible effects of produced oxidative degradation intermediates as a reference without the influence of other constituents (Banashik et al., 2018; Graumans et al., 2021). During a previous degradation study we spiked Milli-Q with an initial concentration of 5 µg/L for the tested pharmaceuticals. After 120 min plasma activation, different conversion levels were found for the parent compounds, having abatement levels for IOM (67%), DIA (41%), CIP (99%), FLU (83%), DF (100%), MET (72%), CP (100%), CB (91%), APAP (100%) and MF (18%) (Graumans et al., 2021). Milli-Q used as vehicle control did not show any significant abnormalities compared to the medium control, see **Fig. 4.2A**. No decline in viability was observed for the untreated Milli-Q sample containing 10 pharmaceuticals after 24h exposure. Expected is that the initial concentrations are too low to cause acute toxicity or cell death. Only

moderately cellular oxidative stress is observed, mainly for the plasma activated periods 5 and 90-180 min. In contrast, after 48h exposure, a clear elevation in fluorescence signal was detected for the treatment periods 5 and 15 min in combination with a severe decrease in viability levels for treatment duration 90, 120 and 180 min (significantly different $p < 0.05$ from the medium control). Here also the untreated matrix (0 min) resulted to some extent in increased fluorescence (~156%), indicating that prolonged exposure to a pharmaceutical mixture influences cellular homeostasis, see **Fig. 4.2B**.

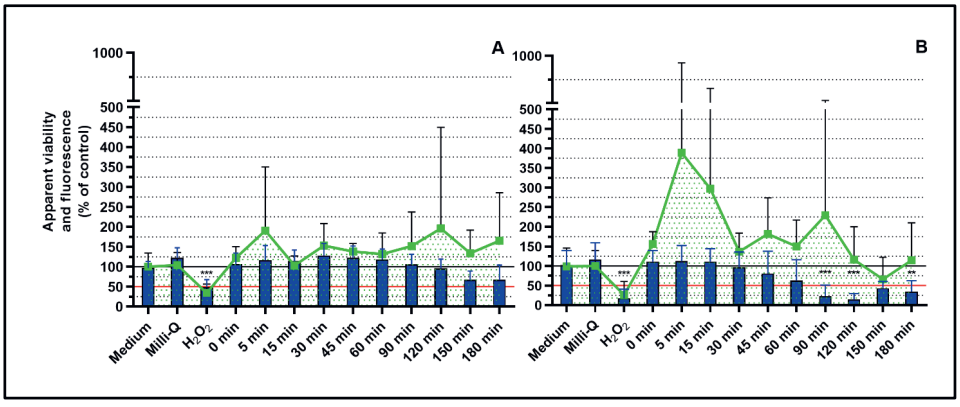

Fig. 4.2. Milli-Q water matrix spiked with pharmaceutical residues was 0-180 min plasma treated and subsequently added to cultured HeLa cells for 24 hours (**A**) and 48 hours (**B**). CM-H_2DCFDA (■) fluorescent tag is used to demonstrate oxidative stress, the crystal violet colourant (■) is applied for the viability confirmation. The black line (—) is used as reference to indicate the unaffected HeLa cell condition (100%, medium control). The red line (—) demonstrates 50% cell viability. **; $p < 0.01$ and ***; $p < 0.001$ (t-test with Bonferroni correction).

During thermal plasma treatment, reactive nitrogen (RNS) and oxygen species (ROS) are produced. These reactive species cause pharmaceutical degradation. In our previous study, we have demonstrated in Milli-Q water that 100% degradation for DF and APAP occurs within 15 min and complete CP elimination in 30 min (Graumans et al., 2021). The elevated fluorescence levels observed for plasma treatment periods of 5 and 15 min indicated that rapidly produced degradation intermediates may cause cellular oxidative stress. According to other oxidation studies it is well explained that during oxidative treatment multiple transformation intermediates are formed (Lutterbeck et al. 2017, Banaschik et al., 2018, Graumans et al., 2020). Lutterbeck demonstrated for the CP alone 5 different intermediates after UV/H_2O_2 and UV/TiO_2 treatment. In a similar study with non-thermal plasma treatment a four-step degradation pathway was anticipated for DF with the possibility for the formation of 21 different intermediates (Banaschik et al., 2018). During a qualitative pharmaceutical degradation study we have also demonstrated multiple reaction intermediates for the

compounds CB, DF and APAP (see supplemental information paragraph **S4.3)**. Identification of these degradation intermediates could have provided more information regarding their toxicity. However, based on the high levels of oxidative stress, seen in the cell system after 48h incubation, it is most likely that intermediates generated in Milli-Q water cause this unwanted cellular effect. Next to increased oxidative stress levels, a decrease in cell viability was seen. Statistically significant differences among the medium control for treatment periods 90, 120 and 180 min were observed (one-way ANOVA, $p < 0.05$), see supplemental information **Table S5**. Substantial decrease in viability levels were primarily demonstrated for the prolonged plasma treatment periods longer than 90 min. A decrease in viability may not be solely attributed to the formed degradation intermediates, but could have also been caused by the reactivity of plasma activated water itself (Hoeben et al, 2019; Graumans et al., 2021). Prolonged plasma activation results in an acidic environment (**Table S17**). Under less neutral circumstances (pH <6) nitration reactions may complement the hydroxyl radical interaction during plasma oxidation (Magureanu et al., 2018; Hoeben et al., 2019; Graumans et al., 2020 Graumans 2021). Although RNS are useful for chemical degradation, incorporation of nitrogen containing compounds into aromatic structures can result in mutagenic by-products (Hofman-Caris et al., 2015). On the other hand, reactive species cannot react exhaustively in Milli-Q water, due to the absence of larger organic molecules or buffering minerals (Giannakis et al. 2018). The methanol fraction (0.64 mM) derived from all diluted stock standards was 1.3% (v/v) in 500 mL test matrix. It is expected that the methanol content is also rapidly broken down by oxidation products. This effect was demonstrated by Popov et al. (2010), who showed a gradual decline of 43 mM CH_3OH using UV/H_2O_2 oxidation. As reported by Hoeben et al., 2019, prolonged plasma activation will increase the concentration of reactive species such as H_2O_2, HNO_2, HNO_3 and transient reactive nitrogen species. They used a similar thermal plasma generator to produce 4900 µM (NO_2^-), 1800 µM (NO_3^-) and 370 µM (H_2O_2) in deionised water during 120 Watt plasma activation for 25 min (Hoeben et al., 2019). Compared to our EC_{50} values it was found that <100 µM H_2O_2 is already a sufficient concentration to induce cytotoxicity resulting in substantial viability loss. Because of the continuous addition of multiple reactive oxygen and nitrogen species, it is explicable why HeLa cell viability decreases after 48h exposure.

4.3.2.2 Plasma treatment synthetic sewage water

Synthetic sewage water (SSW) is a suitable surrogate matrix for studying pharmaceutical degradation in actual wastewater (OECD 2001; Ajo et al. 2018). In our previous study, 5 µg/L was selected as initial pharmaceutical concentration in SSW. The conversion levels by thermal

plasma activation were; IOM (56%), DIA (15%), CIP (70%), FLU (83%), DF (99%), MET (65%), CP (100%), CB (79%), APAP (100%) and MF (73%) (Graumans et al., 2021). To detect possible cytotoxicity after thermal plasma activation in a more realistic environment than Milli-Q water, a surrogate synthetic for sewage water was prepared. Comparing synthetic sewage water cytotoxicity results with plasma-treated Milli-Q water, a direct difference in oxidative stress and viability was detected, see **Fig 4.3**. Measured elevated levels in viability >120% indicate that cell growth occurred. Increased viability levels were also seen for the vehicle control samples, representing that SSW matrix might have contributed beneficially to cell medium quality. Certain constituents from SSW matrix, such as mineral salts, can maintain osmotic balance and organic residues, such as meat extract and peptone, act as building blocks (Arora et al., 2013). Regarding the oxidative stress levels, a less pronounced increase in fluorescence was seen after 24h and 48h cellular incubation. Lower variance between the datapoints may be explained by a less hostile reactive environment in synthetic sewage matrix compared to Milli-Q water. It is expected that with the presence of minerals and organic constituents, plasma-produced reactive species are inhibited or transformed into less reactive radicals (Giannakis et al. 2018; Graumans et al., 2021). Using the viability confirmation assay by staining of biomass, it is seen that the majority of the exposed cells do not die or detach in the cell system, see **Fig. 4.3A**. For the 5 to 120 min plasma-treatment periods no statistically significant differences ($p < 0.05$) were observed, only a significant reduction in viability was found. The gradual decline in viability was 35, 46% and 34 and 42% for prolonged treatment periods of 150 and 180 min, respectively, following 24h and 48h of cellular exposure (see **Table S8** and **S9** in the supplemental information). For the treatment periods of 5 to 120 min, it is expected that minerals and organic constituents in SSW do have sufficient buffer capacity to inhibit RNS and ROS. On the other hand, in AOP systems where $^{\bullet}OH$ radicals are continuously generated, organic matter can act as an additional source for oxidative species by forming transient organic matter radical species ($DOM^{\bullet}$) (Westerhoff et al., 2007; Dong et al., 2012; Peake et al., 2016).

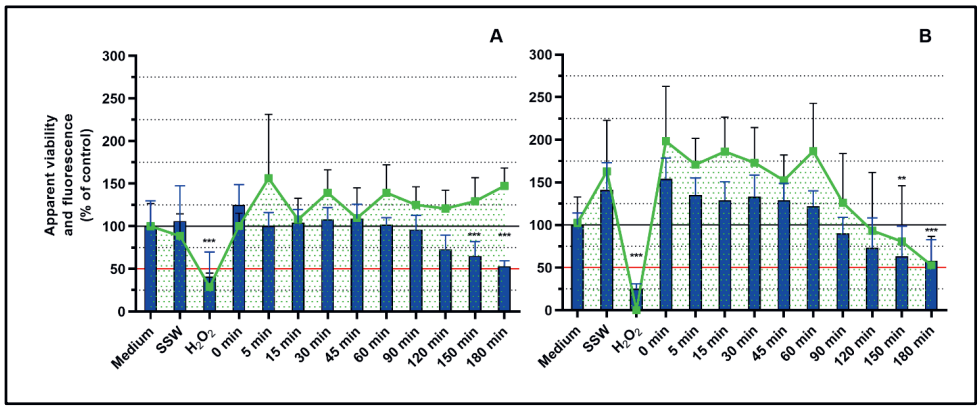

Fig. 4.3. Synthetic sewage water matrix containing 10 pharmaceutical residues was plasma treated and subsequently incubated for 24 hours (**A**) and 48 hours (**B**). CM-H_2DCFDA (■) fluorescent tag is used to demonstrate oxidative stress and the crystal violet colourant (■) is applied for confirming viability. Unaffected HeLa cell condition (100%, medium control) is represented by (—). The red line (—) demonstrates the 50%, viability. **; $p < 0.01$ and ***; $p < 0.001$ (t-test with Bonferroni correction).

Therefore, after plasma degradation it is expected that in the absence of high concentrations of pharmaceutical residues, organic matter will be an additional source for reactive species. As for Milli-Q water, the gradual decrease in viability after prolonged plasma activation is attributed to additionally produced reactive species, affecting the ambient HeLa cell environment (Hoeben et al., 2019; Trebinska-Stryjewska et al., 2020). The very minimal cytotoxicity observed in our laboratory set-up is likely to become negligible when plasma pre-treated on-site wastewater is further diluted with other sewage water streams before reaching conventional sewage treatment. By using AOPs in healthcare facilities, the pharmaceutical residues can be degraded when concentrations are still high, eliminating a substantial portion of components by degradation at the source.

4.3.2.3 Toxicity of hospital sewage water

To understand how thermal plasma oxidation performs in a real sewage water sample, untreated and oxidatively treated hospital wastewater (HSW) was exposed to cultured HeLa cells for 24h and 48h. In our a previous degradation study 10 pharmaceuticals were detected in a concentration range of 0.1-2400 µg/L. Direct application of 120 min plasma activation resulted in the abatement for IOM (33%), DIA (24%), CIP (70%), FLU (12%), DF (94%), MET (43%), CP (100%), CB (36%), APAP (100%) and MF (78%) (Graumans et al., 2021). The HSW is a much more complex matrix than spiked Milli-Q and synthetic sewage water. This may explain the viability drop of ~65% after 24h incubation (see **Fig. 4.4A**). By application of 150 Watt thermal plasma, this effect is, however, rapidly intervened after 30 min treatment, since similar viability levels were produced for the medium control. A completely different response was

observed after 48h of cellular exposure, in which no decline was found in viability for untreated HSW. The observed crystal violet signal (111% ±47) in combination with low fluorescence levels indicated that organic contaminants reacted with crystal violet.

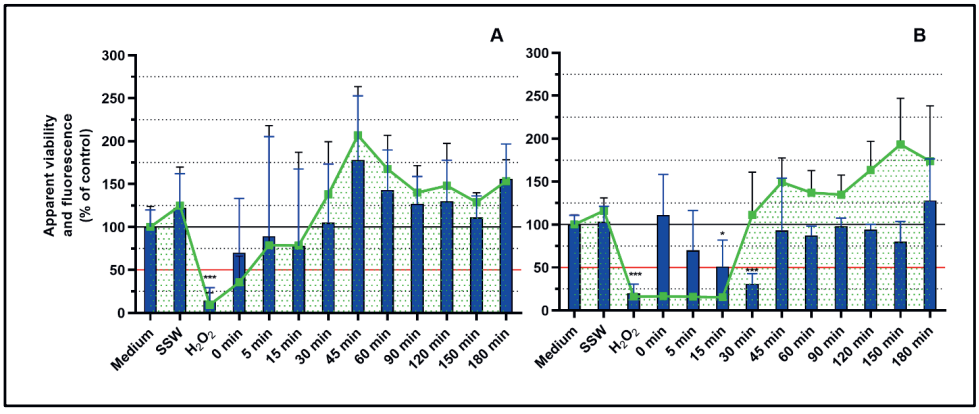

Fig. 4.4. HSW treated with 150W thermal plasma. HeLa cells were 24h (**A**) and 48h (**B**) incubated. Fluorescent tag CM-H_2DCFDA (■) was added to observe oxidative stress and crystal violet colourant (■) was used to confirm cell viability. The black line (—) is used as reference to indicate the unaffected HeLa cell condition, the red line (—) demonstrates 50% viability. *; $p < 0.05$, and ***; $p < 0.001$ (t-test with Bonferroni correction).

That the viability level of the untreated HSW sample increased from 35% (24h) to 111.0% (48h) after prolonged cellular incubation, indicates the growth of bacteria. From other studies it is known that many different strains of bacteria co-exist in sewage water (Chahal et al., 2016). Based on the very low CM-H_2DCFDA fluorescence signal at 0 min (17% ±3), which is almost equal to that of the H_2O_2 control (16% ±4), it is suggested that crystal violet colourant visualised bacterial biomass. Crystal violet is a known colourant for Gram-positive bacteria (Davies et al.; 1983). According to the cellular interaction of CM-H_2DCFDA probe, it is further endorsed that primarily Gram-positive bacteria are visualised in untreated HSW, since certain prokaryotic cells do not produce glutathione (Smirnova et al., 2005; Fahey et al., 2013). CM-H_2DCFDA probe binds to the thiol-group of glutathione, in case of oxidative stress reactive oxygen species do produce a fluorescent adduct. Abatement of viability levels for timepoints 5, 15 and 30 min further endorse the suggestion that bacteria are degraded by disinfectant properties of plasma oxidation (Thrimudas et al. 2018). Comparison of the HSW data with the simulation matrices, makes it difficult to determine the exact contaminants that cause direct toxicity of the untreated HSW samples. It is expected that the cocktail of untreated HSW contains pharmaceutical residues, metabolites, detergents, hormones, pathogens and bacteria who all might contribute to viability reduction (Ajo et al., 2018; Abbas et al., 2019). That cell viability levels decrease

after the addition of untreated wastewater is in line with other studies (Zegura et al. (2009); Jaeger et al., 2015). During our experimental set up we added 20 µL matrix in 180 µL medium (10% (v/v)) untreated and oxidatively treated matrix to HeLa cells. In the study of Zegura et al. (2009), human liver cells (HepG2) were exposed for 20h to different volumes of 0, 5, 10, 20, 30 and 40% industrial effluent, hospital effluent, WWTP effluent and river water. In their study cell viability reduction levels of 30% were considered as cytotoxic. Different volumes of industrial effluent and river water showed a dose-dependent decrease in cell viability. For the same 10% volume, only river water indicated a significant reduction of viable HepG2 cells. The direct toxicity we found for 10% v/v untreated HSW might be explained by the water composition and that the concentration of pharmaceutical residues is highest at the contamination source. In the study of Zegura et al., 2009, no direct cytotoxicity of HepG2 cells exposed to 40% v/v for 20h incubation was seen, but 2 out of their 5 HSW samples were found to be genotoxic. Incubation of untreated HSW for 20h did not immediately result in a major decrease of HepG2 cells, probably because of filtration through a 0.22 µm filter, prior to cellular exposure (Zegura et al., 2009).

In our preliminary HSW experiment, we also applied a filtration step using Costar® Spin-X® centrifuge filtration tubes (0.22 µm). During this exploratory experiment only oxidative stress levels of ~177% ± 46 for filtered HSW were determined compared to 11% ± 7 for unfiltered HSW, see supplementary paragraph **S.4.6**. Based on this result we suggest that filtration removes bacterial toxins. To demonstrate the most realistic effect of plasma treatment on HSW, we decided to not use a filtration step prior to cellular incubation. To determine potential toxicity of real wastewater samples it must be noted that too much sample preparation can lead to miss interpretation (Abbas et al., 2019). Despite that the HSW matrix can cause difficulty in visualising the viability levels of HeLa cells using crystal violet, it is clear from the overall results that plasma treatment will have an overall beneficial effect on wastewater quality. Plasma oxidative treatment of 45 min will result in a better cellular environment, since HeLa cell viability loss is reversed.

4.3.3 Cytotoxicity measurements before and after UV-C/H_2O_2 treatment

The use of UV-C/H_2O_2 is also an effective technology for the degradation of pharmaceutical residues. Photolysis of a hydrogen peroxide solution will produce reactive hydroxyl radicals (•OH), which interact with nearly all organic compounds. To investigate whether UV-C/H_2O_2 treatment might generate harmful oxidative degradation products, cytotoxicity of HeLa cells was measured for untreated and treated Milli-Q, SSW and HSW, respectively (**Fig. 4.5A-F**). During an earlier oxidative degradation study, pharmaceuticals (5 µg/L) were spiked in Milli-Q and SSW. It was found that the parent compounds were rapidly converted between 9.6 and 100% using 120 min UV-C/H_2O_2 treatment. The detected pharmaceutical concentrations in HSW showed conversion levels of 4 up to 100% (Graumans et al. 2021). No direct decrease in viability levels (>50%) was observed compared to the 500 µM H_2O_2 positive control condition. More specifically, for the oxidative treatment of spiked Milli-Q water, minimal effect on the HeLa cells was found after 24h exposure. Elevated fluorescence levels were only seen after 48h cellular incubation, indicating that during prolonged UV-C/H_2O_2 oxidative treatment intermediates are formed which initiate oxidative stress levels. Since Milli-Q is a clean matrix, it is plausible that degradation intermediates were derived from the initial spiked pharmaceuticals (paragraph **S.4.3**). As compared to plasma oxidation, UV-C/H_2O_2 treatment resulted in a less hostile cellular environment. A minimal decrease in cell viability levels were found after UV-C/H_2O_2 oxidation, which might be caused by the addition of 10 mg/L (220 µM) H_2O_2 at the start of the treatment period. In contrast to the continuously generated RNS and ROS species with plasma oxidation, we expect that the photolysis reaction between UV-C and H_2O_2 is more exhaustive in nature. With UV-C irradiation the highest emitted energy photons (254 nm, 4.9 eV) cannot photochemically split atmospheric oxygen, nor water, thus ozone and direct hydroxyl radical formation do not occur. Next to that, no RNS such as HNO_2, HNO_3 and ONOOH are introduced in the matrix during UV-C/H_2O_2 treatment, leading to a less acidic and reactive water environment (**Table S19**). On the other hand, photolysis of the residual pharmaceuticals by UV-C photons is likely, including the rapid chemical degradation by •OH radicals derived from the single added 10 mg/L (220 µM) H_2O_2 solution (Graumans 2021). Important to mention is that in SSW and HSW, UV-C irradiation is absorbed by organic constituents, and that the formed •OH radicals are likely to be quenched or inhibited by minerals such as phosphate or chlorine (Giannakis et al. 2018; Graumans et al., 2021). Despite the inhibitory effects of organic constituents during oxidative degradation, other studies found that application of UV irradiation in drinking water with high natural organic matter (NOM) content

can generate mutagenic degradation by-products (Parkinson et al., 2001; Heringa et al., 2011; Hofman-Caris et al., 2015).

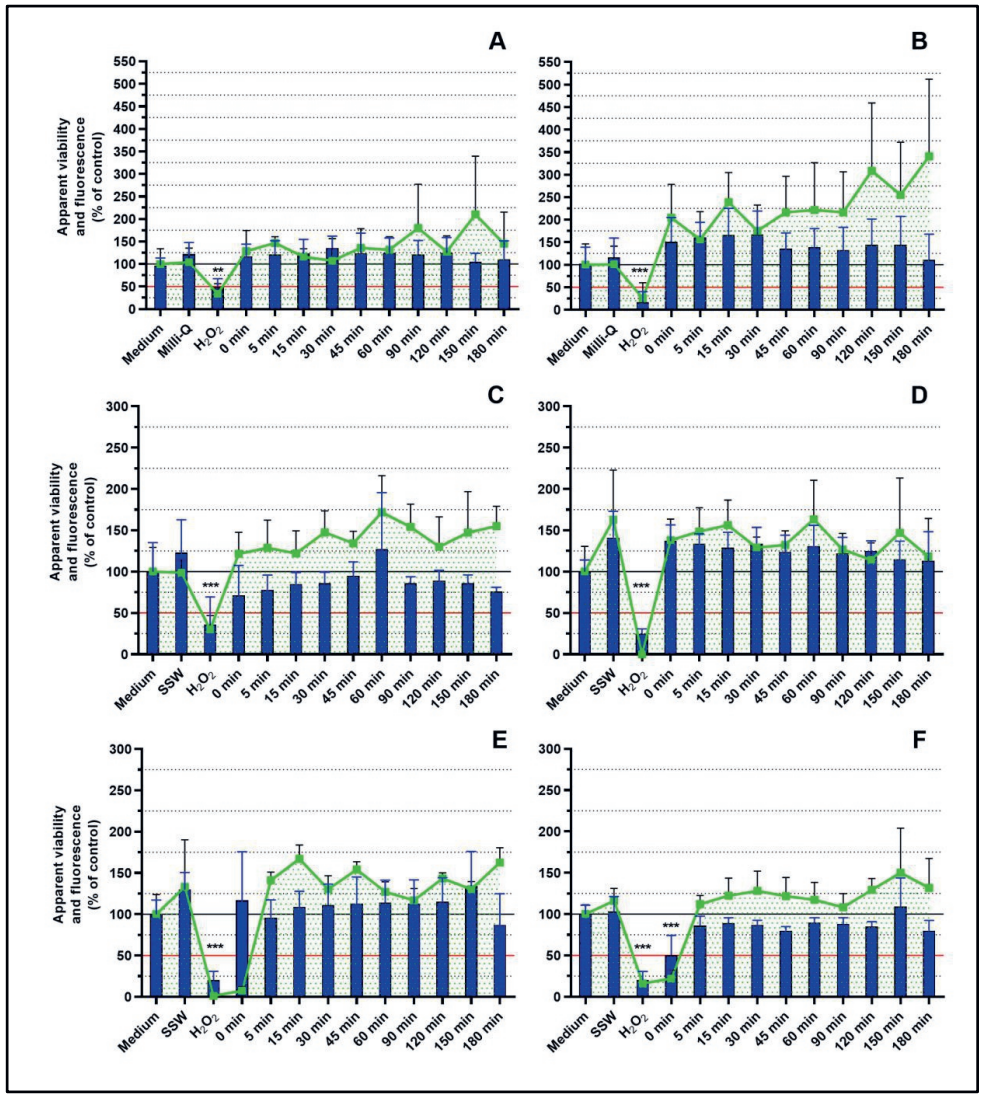

Fig. 4.5. UV-C/H_2O_2 oxidative treatment applied to different spiked matrices. Oxidative stress was measured with CM-H_2DCFDA (■) and cell viability is confirmed with crystal violet colourant (■). The black line (—) is the 100% reference and the red line (—) demonstrates 50% viability. The oxidative treatment effects of Milli-Q water were measured for 24h (**A**) and 48h (**B**) on HeLa cells. These effects were also examined after treatment of synthetic sewage 24h (**C**) and 48h (**D**) and 24h (**E**) and 48h (**F**) incubated hospital sewage water. ***; $p < 0.001$ (t-test with Bonferroni correction).

With the application of AOPs at the wastewater source, a different NOM content is expected compared to surface or ground water used for drinking water preparation. From our oxidatively treated SSW and HSW samples, minimal direct cytotoxic effects were found, since a decrease in viability levels was not detected, see **Fig. 4.5C-F**. This can be partly explained by the use of a low-pressure UV lamp at 254 nm in contrast to a medium pressure UV lamp, which was applied in the studies of Heringa et al. (2011) and Hofman-Caris et al. (2015). Medium pressure lamps emit multiple UV wavelengths between 200 and 300 nm, causing changes in the molecular NOM structure (Heringa et al., 2011). In the presence of NO_3, MP UV irradiation can produce mutagenic by-products, between photolytic nitrate products and NOM (Hofman-Caris., 2015). Furthermore, by alteration of the NOM structure, bound heavy metals could be released, increasing the toxicity (Parkinson et al., 2001). Next to the UV-C source, also the concentration and composition of NOM is of importance since this mixture of constituents will affect the chemical degradation efficiency greatly. Westerhoff and co-workers (2007) found that their reference NOM from Suwannee River fulvic acid water (US) had much higher UV 254 nm absorbance than their WWTP reference sample. Based on this observation, it is expected that during our UV-C/H_2O_2 experiment lower photolysis of NOM in HSW occurred. This supports our observations of the rapid degradation of UV-C absorbing x-ray contrast agents IOM and DIA (Graumans et al., 2021). NOM material with unsaturated double bonds (C = C) are prone to absorb UV within the range of 250 to 280 nm. It is expected for our oxidatively treated matrices SSW and HSW that the NOM content had a different composition, which is less prone to direct change in molecular structure after 254 nm irradiation. The minimal cytotoxic effects in HeLa cells exposed to UV-C/H_2O_2-treated SSW and HSW suggests that this could be a useful on-site sewage water treatment technique.

4.3.4 Strengths and limitations of the cytotoxicity experimentation

One of the strengths of this experimental study is that the cytotoxicity levels were measured for multiple oxidatively treated wastewater matrices and hospital sewage water, see **Fig. 4.6**. Cytotoxicity was determined before and after thermal plasma and UV-C/H_2O_2 treatment, demonstrating the usefulness of advanced oxidation at a contamination source. Our laboratory-scale setup may serve as an indicator for further experimental design for the application of advanced oxidation technology. On the other hand, it is important to mention that a limitation of our work is that we have obtained cytotoxicity results based on a mixture of pharmaceuticals in a wide concentration range. It is therefore difficult to establish whether an individual compound or a mixture effect has caused the harmful cellular effects. On top of that, with the

application of thermal plasma activation and UV-C/H_2O_2 treatment, distinct chemical degradation kinetics occur, producing different reactive species. For translation of the cytotoxic results, an additional mutagenic or more specific ecotoxicity assay could elucidate or underpin specific observations. The usage of crystal violet for assessing cell viability is not the most appropriate control for our complex HSW matrix, but, in combination with the CM-H_2DCFDA probe informative results on oxidative stress and viability were obtained. With the current experimental setup we have demonstrated the possibilities of advanced oxidation of end-of-pipe contaminated water matrices, the performance of which could have been explained even better with the oxidative degradation of multiple source oriented sewage water compositions. This laboratory-scale experiment is therefore the preferred step to develop a pilot-testing system for the treatment of specialised hospital wastewater streams.

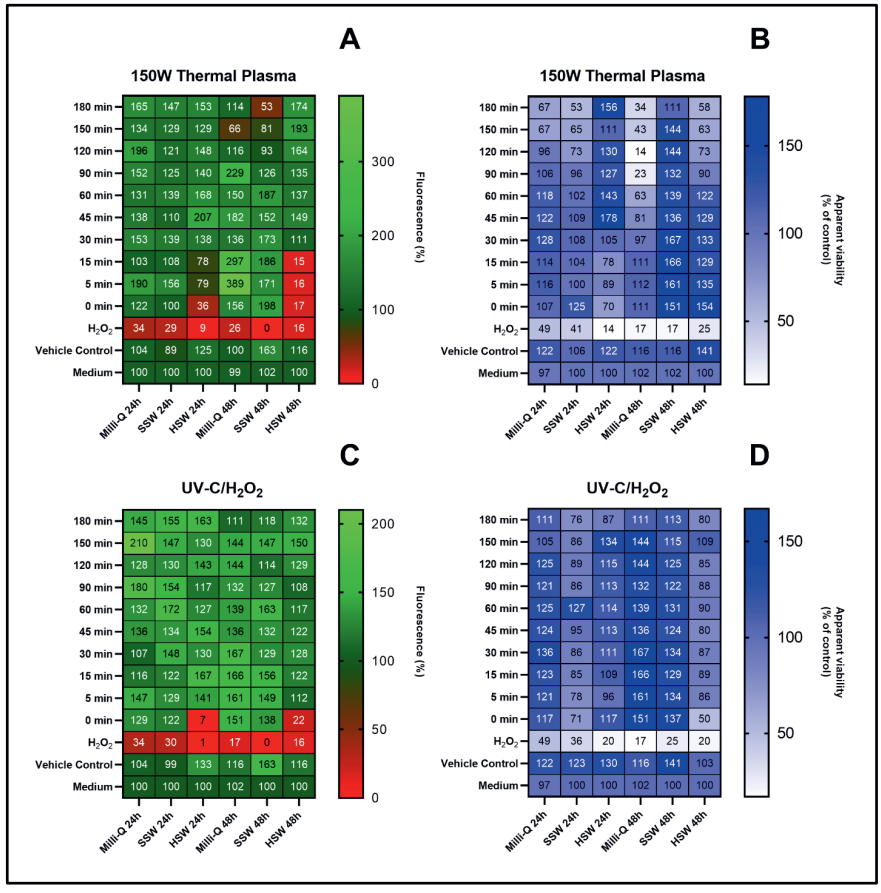

Fig. 4.6. Combined cytotoxicity results obtained in different oxidatively treated matrices Milli-Q, SSW, HSW. A heatmap visualisation is used to compare the oxidative stress results (**A** and **C**) and viability levels (**B** and **D**).

4.4. Conclusion

From the results it is clear that the initial concentration of pharmaceuticals, the composition of the matrix, oxidative treatment duration, the amount of formed oxidative species and the ability of the cellular system to recover, are all determinants of residual toxicity. Our experimental setup showed that both thermal plasma and UV-C/H_2O_2 are capable of substantially degrading pharmaceuticals in hospital sewage water. Our results may therefore contribute to the adoption of both oxidative technologies for the pre-treatment of wastewater with a high load of pharmaceuticals at the source. Plasma activation provides a continuous production of ROS and RNS, which may directly affect cell viability in Milli-Q water if not diluted or inhibited. Further studies are required, including bioassays, which inform the potential impact on the aqueous ecosystem. Direct application of AOPs at the contamination source is considered a promising technology to reduce pharmaceuticals in sewage water at the source.

Declaration of competing interest

None

Acknowledgement

The MEDUWA project and this work were supported by the INTERREG Deutschland-Nederland program [Grant number 142118]. We would like thank VitalFluid for their help in providing the thermal plasma unit and UV-C source. The authors also would like to thank Charlotte Hoogstraten and Tim Somers for their technical advice and help with a control experiment at the laboratory.

Supplemental information

The supporting information contains additional data for the clarification of the presented cytotoxicity data.

Literature

Abbas, A., Schneider, I., Bollmann, A., Funke, J., Oehlmann, J., Prasse, C., Schulte-Oehlmann, U., Seitz, W., Ternes, T., Weber, M., Wesely, H., & Wagner, M. (2019). What you extract is what you see: Optimising the preparation of water and wastewater samples for in vitro bioassays. *Water Research*, *152*, 47–60. https://doi.org/10.1016/j.watres.2018.12.049

Ajo, P., Preis, S., Vornamo, T., Mänttäri, M., Kallioinen, M., & Louhi-Kultanen, M. (2018). Hospital wastewater treatment with pilot-scale pulsed corona discharge for removal of pharmaceutical residues. *Journal of Environmental Chemical Engineering*, *6*(2), 1569–1577. https://doi.org/10.1016/j.jece.2018.02.007

Ayuso, M., Van Cruchten, S., & Van Ginneken, C. (2020). A Medium-Throughput System for In Vitro Oxidative Stress Assessment in IPEC-J2 Cells. *International Journal of Molecular Sciences*, *21*(19), 7263. https://doi.org/10.3390/ijms21197263

Back, J. O., Obholzer, T., Winkler, K., Jabornig, S., & Rupprich, M. (2018). Combining ultrafiltration and non-thermal plasma for low energy degradation of pharmaceuticals from conventionally treated wastewater. *Journal of Environmental Chemical Engineering*, *6*(6), 7377–7385. https://doi.org/10.1016/j.jece.2018.07.047

Banaschik, R., Jablonowski, H., Bednarski, P. J., & Kolb, J. F. (2018). Degradation and intermediates of diclofenac as instructive example for decomposition of recalcitrant pharmaceuticals by hydroxyl radicals generated with pulsed corona plasma in water. *Journal of Hazardous Materials*, *342*, 651–660. https://doi.org/10.1016/j.jhazmat.2017.08.058

Beier, S., Köster, S., Veltmann, K., Schröder, H., & Pinnekamp, J. (2010). Treatment of hospital wastewater effluent by nanofiltration and reverse osmosis. *Water Science and Technology*, *61*(7), 1691–1698. https://doi.org/10.2166/wst.2010.119

Carucci, A., Cappai, G., & Piredda, M. (2006). Biodegradability and Toxicity of Pharmaceuticals in Biological Wastewater Treatment Plants. *Journal of Environmental Science and Health, Part A*, *41*(9), 1831–1842. https://doi.org/10.1080/10934520600779000

Chahal, C., van den Akker, B., Young, F., Franco, C., Blackbeard, J., & Monis, P. (2016). *Pathogen and Particle Associations in Wastewater* (pp. 63–119). https://doi.org/10.1016/bs.aambs.2016.08.001

Davies, J. A., Anderson, G. K., Beveridge, T. J., & Clark, H. C. (1983). Chemical mechanism of the Gram stain and synthesis of a new electron-opaque marker for electron microscopy which replaces the iodine mordant of the stain. *Journal of Bacteriology*, *156*(2), 837–845. https://doi.org/10.1128/jb.156.2.837-845.1983

Day, R. M., & Suzuki, Y. J. (2005). Cell Proliferation, Reactive Oxygen and Cellular Glutathione. *Dose-Response*, *3*(3), dose-response.0. https://doi.org/10.2203/dose-response.003.03.010

Dong, M. M., & Rosario-Ortiz, F. L. (2012). Photochemical Formation of Hydroxyl Radical from Effluent Organic Matter. *Environmental Science & Technology*, *46*(7), 3788–3794. https://doi.org/10.1021/es2043454

Dong, S., Nguyen, T. H., & Plewa, M. J. (2017). Comparative mammalian cell cytotoxicity of wastewater with elevated bromide and iodide after chlorination, chloramination, or ozonation. *Journal of Environmental Sciences*, *58*, 296–301. https://doi.org/10.1016/j.jes.2017.03.030

Du, Y., Wu, Q.-Y., Lu, Y., Hu, H.-Y., Yang, Y., Liu, R., & Liu, F. (2017). Increase of cytotoxicity during wastewater chlorination: Impact factors and surrogates. *Journal of Hazardous Materials*, *324*, 681–690. https://doi.org/10.1016/j.jhazmat.2016.11.042

Fahey, R. C. (2013). Glutathione analogs in prokaryotes. *Biochimica et Biophysica Acta (BBA) - General Subjects*, *1830*(5), 3182–3198. https://doi.org/10.1016/j.bbagen.2012.10.006

Fent, K., Weston, A., & Caminada, D. (2006). Ecotoxicology of human pharmaceuticals. *Aquatic Toxicology*, *76*(2), 122–159. https://doi.org/10.1016/j.aquatox.2005.09.009

Feoktistova, M., Geserick, P., & Leverkus, M. (2016). Crystal Violet Assay for Determining Viability of Cultured Cells. *Cold Spring Harbor Protocols*, *2016*(4), pdb.prot087379. https://doi.org/10.1101/pdb.prot087379

Gerrity, D., Stanford, B. D., Trenholm, R. A., & Snyder, S. A. (2010). An evaluation of a pilot-scale nonthermal plasma advanced oxidation process for trace organic compound degradation. *Water Research*, *44*(2), 493–504. https://doi.org/10.1016/j.watres.2009.09.029

Giannakis, S., Androulaki, B., Comninellis, C., & Pulgarin, C. (2018). Wastewater and urine treatment by UVC-based advanced oxidation processes: Implications from the interactions of bacteria, viruses, and chemical contaminants. *Chemical Engineering Journal*, *343*, 270–282. https://doi.org/10.1016/j.cej.2018.03.019

Gilca, A. F., Teodosiu, C., Fiore, S., & Musteret, C. P. (2020). Emerging disinfection byproducts: A review on their occurrence and control in drinking water treatment processes. *Chemosphere*, *259*, 127476. https://doi.org/10.1016/j.chemosphere.2020.127476

Graumans, M. H. F., Hoeben, W. F. L. M., Russel, F. G. M., & Scheepers, P. T. J. (2020). Oxidative degradation of cyclophosphamide using thermal plasma activation and UV/H2O2 treatment in tap water. *Environmental Research*, *182*. https://doi.org/10.1016/j.envres.2019.109046

Graumans, M. H. F., Hoeben, W. F. L. M., van Dael, M. F. P., Anzion, R. B. M., Russel, F. G. M., & Scheepers, P. T. J. (2021). Thermal plasma activation and UV/H2O2 oxidative degradation of pharmaceutical residues. *Environmental Research*, *195*. https://doi.org/10.1016/j.envres.2021.110884

Henriques, I. D. S., Kelly, R. T., Dauphinais, J. L., & Love, N. G. (2007). Activated Sludge Inhibition by Chemical Stressors—A Comprehensive Study. *Water Environment Research*, *79*(9), 940–951. https://doi.org/10.2175/106143007X156709

Heringa, M. B., Harmsen, D. J. H., Beerendonk, E. F., Reus, A. A., Krul, C. A. M., Metz, D. H., & IJpelaar, G. F. (2011). Formation and removal of genotoxic activity during UV/H2O2–GAC treatment of drinking water. *Water Research*, *45*(1), 366–374. https://doi.org/10.1016/j.watres.2010.08.008

Hoeben, W. F. L. M., van Ooij, P. P., Schram, D. C., Huiskamp, T., Pemen, A. J. M., & Lukeš, P. (2019). On the Possibilities of Straightforward Characterization of Plasma Activated Water. *Plasma Chemistry and Plasma Processing*, *39*(3), 597–626. https://doi.org/10.1007/s11090-019-09976-7

Hofman-Caris, C. H. M., Harmsen, D. J. H., Wols, B. A., Beerendonk, E. F., & Keltjens, L. L. M. (2015). Determination of Reaction Rate Constants in a Collimated Beam Setup: The Effect of Water Quality and Water Depth. *Ozone: Science & Engineering*, *37*(2), 134–142. https://doi.org/10.1080/01919512.2014.939740

Hofman-Caris, R., ter Laak, T., Huiting, H., Tolkamp, H., de Man, A., van Diepenbeek, P., & Hofman, J. (2019). Origin, Fate and Control of Pharmaceuticals in the Urban Water Cycle: A Case Study. *Water*, *11*(5), 1034. https://doi.org/10.3390/w11051034

Isidori, M., Lavorgna, M., Russo, C., Kundi, M., Žegura, B., Novak, M., Filipič, M., Mišík, M., Knasmueller, S., de Alda, M. L., Barceló, D., Žonja, B., Česen, M., Ščančar, J., Kosjek, T., & Heath, E. (2016). Chemical and toxicological characterisation of anticancer drugs in hospital and municipal wastewaters from Slovenia and Spain. *Environmental Pollution*, *219*, 275–287. https://doi.org/10.1016/j.envpol.2016.10.039

Jaeger, N., Moraes, J. P., Klauck, C. R., Gehlen, G., Rodrigues, M. A. S., & Ziulkoski, A. L. (2015). Cytotoxicity assays to evaluate tannery effluents treated by photoelectrooxidation. *Brazilian Journal of Biology*, *75*(4 suppl 2), 53–61. https://doi.org/10.1590/1519-6984.01713suppl

Lutterbeck, C. A., Machado, Ê. L., & Kümmerer, K. (2015). Photodegradation of the antineoplastic cyclophosphamide: A comparative study of the efficiencies of UV/H2O2, UV/Fe2+/H2O2 and UV/TiO2 processes. *Chemosphere*, *120*, 538–546. https://doi.org/10.1016/j.chemosphere.2014.08.076

Ma, D., Wei, J., Zhang, H., Zhou, Y., Shen, J., Wang, L., & Zhang, P. (2019). Acute toxicity evolution during ozonation of mono-chlorophenols and initial identification of highly toxic intermediates. *Environmental Science: Processes & Impacts*, *21*(9), 1509–1518. https://doi.org/10.1039/C9EM00225A

Magureanu, M., Bradu, C., & Parvulescu, V. I. (2018). Plasma processes for the treatment of water contaminated with harmful organic compounds. *Journal of Physics D: Applied Physics*, *51*(31), 313002. https://doi.org/10.1088/1361-6463/aacd9c

Magureanu, M., Mandache, N. B., & Parvulescu, V. I. (2015). Degradation of pharmaceutical compounds in water by non-thermal plasma treatment. *Water Research*, *81*, 124–136. https://doi.org/10.1016/j.watres.2015.05.037

Miller, J. N., Miller, J. C. (2010). In Statistics and Chemometrics for Analytical Chemistry (pp. 110-153): Pearson.

OECD (2001) OECD Guideline for the testing of chemicals Simulation Test - Aerobic Sewage Treatment: 303 A: Activated Sludge Units - 303 B: Biofilms. https://www.oecd-ilibrary.org/

Moermond C.T.A., Montforts, M.H.M.M., Roex, E.W.M., Venhuis B.J. (2020). *Pharmaceutical residues and water quality: an update*.

Ortiz de García, S. A., Pinto Pinto, G., García-Encina, P. A., & Irusta-Mata, R. (2014). Ecotoxicity and environmental risk assessment of pharmaceuticals and personal care products in aquatic environments and wastewater treatment plants. *Ecotoxicology*, *23*(8), 1517–1533. https://doi.org/10.1007/s10646-014-1293-8

Parkinson, A. (2001). Preliminary toxicity assessment of water after treatment with uv-irradiation and UVC/H2O2. *Water Research*, *35*(15), 3656–3664. https://doi.org/10.1016/S0043-1354(01)00096-3

Peake, B. M., Braund, R., Tong, A. Y. C., & Tremblay, L. A. (2016). The Life-cylce of pharmaceuticals in the environment. Woodhead Publishin, Elsevier.

Pemen, A. J. M., van Ooij, P. P., Beckers, F. J. C. M., Hoeben, W. F. L. M., Koonen-Reemst, A. M. C. B., Huiskamp, T., & Leenders, P. H. M. (2017). Power Modulator for High-Yield Production of Plasma-Activated Water. *IEEE Transactions on Plasma Science*, *45*(10), 2725–2733. https://doi.org/10.1109/TPS.2017.2739484

Popov, E., Mametkuliyev, M., Santoro, D., Liberti, L., & Eloranta, J. (2010). Kinetics of UV−H_2O_2 Advanced Oxidation in the Presence of Alcohols: The Role of Carbon Centered Radicals. *Environmental Science & Technology*, *44*(20), 7827–7832. https://doi.org/10.1021/es101959y

Rantanen, P.-L., Keinänen-Toivola, M. M., Ahonen, M., González-Martínez, A., Mellin, I., & Vahala, R. (2020). Decreased natural organic matter in water distribution decreases nitrite formation in non-disinfected conditions, via enhanced nitrite oxidation. *Water Research X*, *9*, 100069. https://doi.org/10.1016/j.wroa.2020.100069

Shen, J., Tian, Y., Li, Y., Ma, R., Zhang, Q., Zhang, J., & Fang, J. (2016). Bactericidal Effects against S. aureus and Physicochemical Properties of Plasma Activated Water stored at different temperatures. *Scientific Reports*, *6*(1), 28505. https://doi.org/10.1038/srep28505

Sillanpää, M., Ncibi, M. C., & Matilainen, A. (2018). Advanced oxidation processes for the removal of natural organic matter from drinking water sources: A comprehensive review. *Journal of Environmental Management*, *208*, 56–76. https://doi.org/10.1016/j.jenvman.2017.12.009

Śliwka, L., Wiktorska, K., Suchocki, P., Milczarek, M., Mielczarek, S., Lubelska, K., Cierpiał, T., Łyżwa, P., Kiełbasiński, P., Jaromin, A., Flis, A., & Chilmonczyk, Z. (2016). The Comparison of MTT and CVS Assays for the Assessment of Anticancer Agent Interactions. *PLOS ONE*, *11*(5), e0155772. https://doi.org/10.1371/journal.pone.0155772

Smirnova, G. V., & Oktyabrsky, O. N. (2005). Glutathione in Bacteria. Biochemistry (Moscow), 70(11), 1199–1211. https://doi.org/10.1007/s10541-005-0248-3

Streicher, J., Ruhl, A. S., Gnirß, R., & Jekel, M. (2016). Where to dose powdered activated carbon in a wastewater treatment plant for organic micro-pollutant removal. *Chemosphere*, *156*, 88–94. https://doi.org/10.1016/j.chemosphere.2016.04.123

Symons, M. C. R., Rusakiewicz, S., Rees, R. C., & Ahmad, S. I. (2001). Hydrogen peroxide: a potent cytotoxic agent effective in causing cellular damage and used in the possible treatment for certain tumours. *Medical Hypotheses*, *57*(1), 56–58. https://doi.org/10.1054/mehy.2000.1406

Thirumdas, R., Kothakota, A., Annapure, U., Siliveru, K., Blundell, R., Gatt, R., & Valdramidis, V. P. (2018). Plasma activated water (PAW): Chemistry, physico-chemical properties, applications in food and agriculture. *Trends in Food Science & Technology*, *77*, 21–31. https://doi.org/10.1016/j.tifs.2018.05.007

Trebinska-Stryjewska, A., Swiech, O., Opuchlik, L. J., Grzybowska, E. A., & Bilewicz, R. (2020). Impact of Medium pH on DOX Toxicity toward HeLa and A498 Cell Lines. *ACS Omega*, *5*(14), 7979–7986. https://doi.org/10.1021/acsomega.9b04479

van Bergen, T. J. H. M., Rios-Miguel, A. B., Nolte, T. M., Ragas, A. M. J., van Zelm, R., Graumans, M., Scheepers, P. T. J., Jetten, M. S. M., Hendriks, A. J., & Welte, C. U. (2021). Do initial concentration and activated sludge seasonality affect pharmaceutical biotransformation rate constants? *Applied Microbiology and Biotechnology*, *105*(16–17). https://doi.org/10.1007/s00253-021-11475-9

Vasiliadou, I. A., Molina, R., Martinez, F., Melero, J. A., Stathopoulou, P. M., & Tsiamis, G. (2018). Toxicity assessment of pharmaceutical compounds on mixed culture from activated sludge using respirometric technique: The role of microbial community structure. *Science of The Total Environment*, *630*, 809–819. https://doi.org/10.1016/j.scitotenv.2018.02.095

Westerhoff, P., Mezyk, S. P., Cooper, W. J., & Minakata, D. (2007). Electron Pulse Radiolysis Determination of Hydroxyl Radical Rate Constants with Suwannee River Fulvic Acid and Other Dissolved Organic Matter Isolates. *Environmental Science & Technology*, *41*(13), 4640–4646. https://doi.org/10.1021/es062529n

Wu, Q.-Y., Zhou, Y.-T., Li, W., Zhang, X., Du, Y., & Hu, H.-Y. (2019). Underestimated risk from ozonation of wastewater containing bromide: Both organic byproducts and bromate contributed to the toxicity increase. *Water Research*, *162*, 43–52. https://doi.org/10.1016/j.watres.2019.06.054

Yang, J., Dong, Z., Jiang, C., Wang, C., & Liu, H. (2019). An overview of bromate formation in chemical oxidation processes: Occurrence, mechanism, influencing factors, risk assessment, and control strategies. *Chemosphere*, *237*, 124521. https://doi.org/10.1016/j.chemosphere.2019.124521

Žegura, B., Heath, E., Černoša, A., & Filipič, M. (2009). Combination of in vitro bioassays for the determination of cytotoxic and genotoxic potential of wastewater, surface water and drinking water samples. *Chemosphere*, *75*(11), 1453–1460. https://doi.org/10.1016/j.chemosphere.2009.02.041

Supplemental Information for Chapter 4

This supplemental data document provides additional information to support the main text. In **paragraph S.4.1** the assay optimization is given, showing the intracellular interaction of CM-H_2DCFDA and the dose-response relationship compared to crystal violet. In **paragraph S.4.2** a table with pharmaceutical structures is provided. Our qualitative study on the detection of degradation intermediates is presented in **paragraph S.4.3**. Intermediates were detected for the compounds carbamazepine (**CB**), diclofenac (**DF**) and acetaminophen (**APAP**). **Paragraph S.4.4** contains the statistical data interpretation regarding one-way analysis of variance (ANOVA) including the Bonferroni's Multiple comparison test output per oxidative treatment technique. Experimental data regarding pH effect on the HeLa cell system is placed in **paragraph S.4.5** and filtration data prior to cellular exposure is found in **paragraph S.4.6**.

S.4.1 CM-H_2DCFDA assay optimisation

During the staining process 5-(and 6-)chloromethyl-2′,7′-dichlorodihydrofluorescein diacetate, acetyl ester (CM-H_2DCFDA) is passively incorporated into living cells. By the intracellular reaction of the enzyme esterase the acetate groups of CM-H_2DCFDA are cleaved, see **Fig. S1**. Intracellular glutathione will bind with the chloromethyl group. Glutathione is an antioxidant, protecting the cell against reactive oxygen species. Due to the binding of CM-H_2DCFDA at the thiol-group, reactive oxygen species produce a fluorescent adduct. In case of apoptosis the fluorescent adduct is washed away, but in case of oxidative stress elevated amounts of fluorescence are measured (Johnson (2010) Chapter 15 and 18; Invitrogen manual 2006; Ayuso et al., 2020).

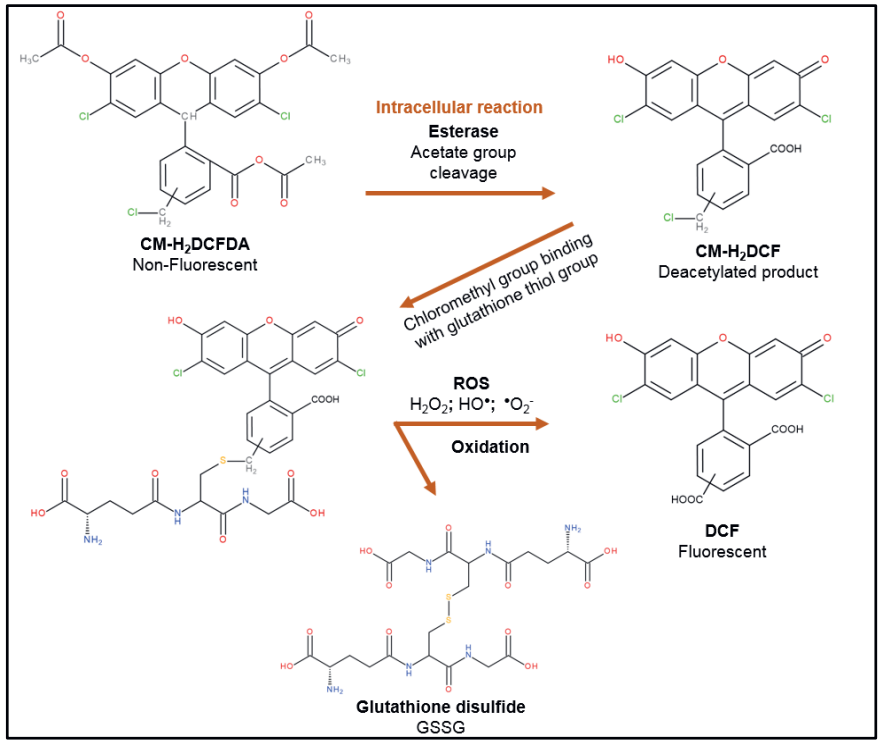

Fig. S1. Simplification of the intracellular reaction of CM-H_2DCFDA. A deacetylated oxidised product dichlorodihydrofluorescein (DCF) is formed by ROS species. The amount of fluorescent product is an indication for the severity of oxidative stress.

Usually in healthy aerobic cells the amount of reactive oxygen species (ROS) is well controlled. In case of oxidative stress, the ROS levels are increased causing disruption or alteration in crucial biological events (Symons et al. 2001). To measure oxidative stress and cell death with CM-H_2DCFDA, different concentrations of hydrogen peroxide (H_2O_2) were used, see **Fig S2**.

Crystal violet staining was used to measure cell viability, see Fig **S2** and Table **S1**. EC_{50} values of 99 µM and 16 µM were found for CM-H_2DCFDA and crystal violet indicators, respectively. The EC_{50} values were determined by using the logarithmic concentration EC_{50} shift plot function in GraphPad. Log EC_{50} values 1.9 and 1.2 were transformed to calculate the H_2O_2 concentrations. To achieve cell death, 500 µM H_2O_2 was selected as respectable positive control concentration. Hydrogen peroxide is cytotoxic depending on the amount added to the cells (Symons et al., 2001; Day and Suzuki, 2005; Ayuso et al., 2020). The cytotoxic reaction of H_2O_2 is attributed to the presence of the 0.1 mg/L Ferric Nitrate ($Fe(NO_3)_3$ in the medium. In the presence of iron, it is expected that a Fenton reaction is initiated producing reactive hydroxyl radicals (•OH) (**R1**).

$$Fe^{3+} + H_2O_2 \rightarrow Fe^{2+} + HOO^{\bullet} + H^{+} \qquad \textbf{R1}$$

$$Fe^{2+} + H_2O_2 \rightarrow {}^{\bullet}OH + HO^{-} \qquad \textbf{R2}$$

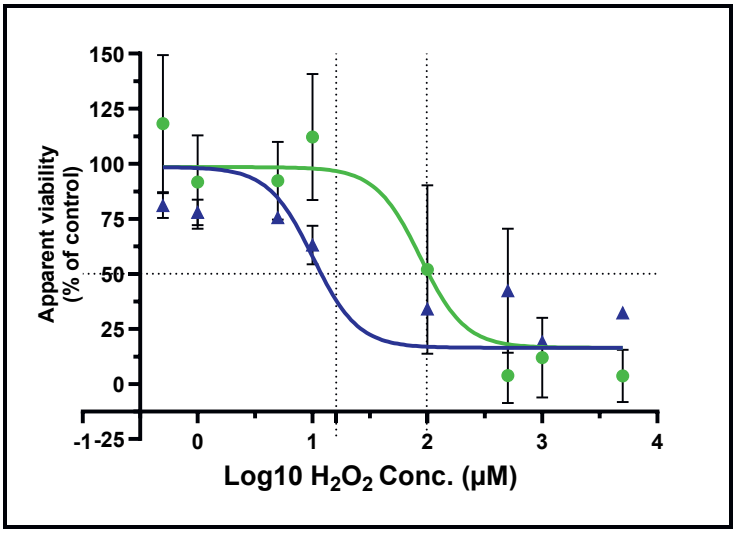

Fig. S2. A dose-response curve for the H_2O_2 dilution series. To visualise the apparent cell viability the fluorescent tag CM-H_2DCFDA (●) and Crystal Violet colourant (▲) were used. Noticeable difference is seen between the assays, having a log EC_{50} of 1.9 and 1.2 µM H_2O_2, respectively.

In addition to the reaction of Fe^{3+} with H_2O_2, aerobic cells do need oxygen (O_2) for energy consumption. When O_2 accepts an extra electron, the superoxide radical (•O_2^-) is formed, which reduces Fe^{3+} into Fe^{2+}. Fe^{2+} is the main initiator of the Fenton process, causing rapid formation of •OH (**R2**). Excess of ROS species such as H_2O_2, •OH and •O_2^-, will cause cellular damage on components such as proteins, lipids and DNA. Irreversible damage leads to cell apoptosis.

Table S1.

Concentration experiment using hydrogen peroxide on HeLa cells

Positive control H_2O_2 concentrations 24h exposed to HeLa cells (Crystal Violet)											
Viability (%)	Medium	MQ	500 µM H_2O_2	0.5 µM H_2O_2	1.0 µM H_2O_2	5.0 µM H_2O_2	10.0 µM H_2O_2	100.0 µM H_2O_2	500.0 µM H_2O_2	1000.0 µM H_2O_2	5000.0 µM H_2O_2
x̄	100	92	21	81	78	76	63	34	42	19	32
±SE	±4	±3	±2	±4	±4	±3	±6	±2	±20	±2	±2
Wells (n)	*8*	*8*	*8*	*3*	*3*	*3*	*3*	*3*	*3*	*3*	*3*
T_{stat}	-	*1.4*	*14.0*	*2.5*	*2.9*	*3.2*	*4.8*	*8.7*	*7.6*	*10.6*	*8.9*
T_{crit}	-	*2.9*	*2.9*	*4.5*	*4.5*	*4.5*	*4.5*	*4.5*	*4.5*	*4.5*	*4.5*
Significant	-	*No*	***	*No*	*No*	*No*	***	***	***	***	***

Statistically significant effects are denoted as ***; $p < 0.001$

S.4.2 Pharmaceutical structure

Table S2.

Pharmaceutical classification and physicochemical properties of the 10 selected compounds.

Structure	**Classification and physicochemical properties**
Iomeprol (IOM) 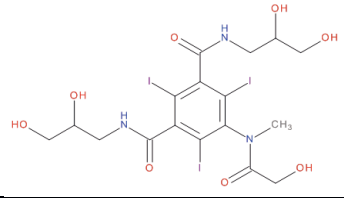	*Contrast agent* Cas: **78649-41-9** $C_{17}H_{22}I_3N_3O_8$ ***M.W.:*** *777.085* **Log *P*:** -3.08
Diatrizoic acid (DIA) 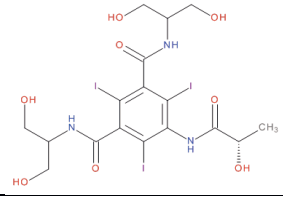	*Contrast agent* Cas: **117-96-4** $C_{11}H_9I_3N_2O_4$ ***M.W.:*** *613.914* **Log *P*:** 2.89
Ciprofloxacin (CIP) 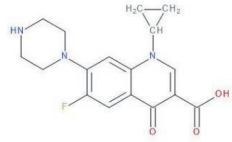	*Antibiotic* Cas: **85721-33-1** $C_{17}H_{18}FN_3O_3$ ***M.W.:*** *331.341* **Log *P*:** 0.65
Fluoxetine (FLU) 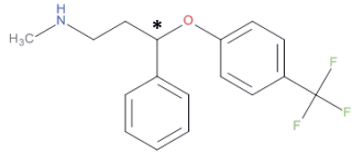	*Antidepressant* Cas: **54910-89-3** $C_{17}H_{18}F_3NO$ ***M.W.:*** *309.326* **Log *P*:** 4.09

Diclofenac (DF) 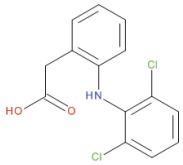	*Nonsteroidal anti-inflammatory drug (NSAID)* Cas: **15307-86-5** $C_{14}H_{11}Cl_2NO_2$ ***M.W.:*** *296.149* **Log *P*:** 4.06
Metoprolol (MET) 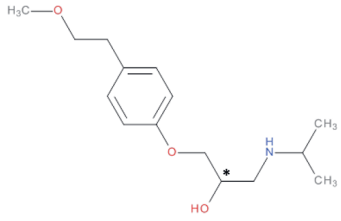	*Beta blocker* Cas: **37350-58-6** $C_{15}H_{25}NO_3$ ***M.W.:*** *267.364* **Log *P*:** 1.79
Cyclophosphamide (CP) 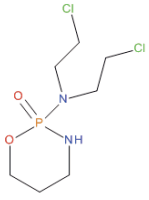	*Anticancer agent* Cas: **50-18-0** $C_7H_{15}Cl_2N_2O_2P$ ***M.W.:*** *261.086* **Log *P*:** 0.23
Carbamazepine (CB) 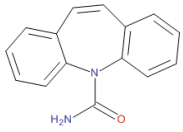	*Anti-epileptic* Cas: **298-46-4** $C_{15}H_{12}N_2O$ ***M.W.:*** *236.269* **Log *P*:** 2.67
Acetaminophen (APAP) 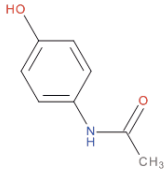	*Analgesic* Cas: **103-90-2** $C_8H_9NO_2$ ***M.W.:*** *151.163* **Log *P*:** 0.34
Metformin (MF) 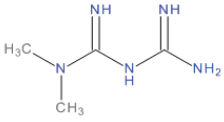	*Antidiabetic* Cas: **657-24-9** $C_4H_{11}N_5$ ***M.W.:*** *129.164* **Log *P*:** -2.31

S.4.3 Oxidative degradation products

A qualitative advanced oxidation experiment was applied to observe the formation of possible degradation intermediates. These degradation intermediates were detected using HLPC-UV analysis. The relative HPLC-UV detector response provides qualitative information on the initial pharmaceutical degradation and the formation of intermediates. For this experiment a sufficient detectable amount of either carbamazepine (**CB**), diclofenac (**DF**) or acetaminophen (**APAP**) has been added to 500 mL of Milli-Q water. Subsequently, 150 Watt plasma activation was applied to the **CB** sample. For the degradation of **DF** and **APAP** both plasma activation and UV-C/H_2O treatment were used. For different oxidative treated timepoints a sample was taken and analysed using HPLC-UV detection. The rapid qualitative screening method is applied by using reversed phase separation with an Agilent, Eclipse XDB-$C_{18,}$ 5 µM, 4.6 x 150 mm column. The column temperature was set on 40 ºC with a gradient program as given in **Table S3** applying a flow of 1ml/min. The detector wavelength was set on 254 nm.

Table S3.
Gradient program Agilent HPLC 1200 series

Time (min)	% Mobile phase A Milli-Q; 0.1% Formic Acid (v/v)	% Mobile phase B Acetonitrile
0	90	10
1	90	10
10	40	60
12	0	100
14	0	100
16	90	10
20	90	10

During the HPLC-UV analysis, a control injection with Milli-Q and H_2O_2 was used. 10 mg/mL concentration of H_2O_2 is injected to determine whether this compound is produced during thermal plasma activation. Comparing the Milli-Q blank injecting with the H_2O_2 sample) a measurable peak was found at Rt (1.44 min), see **Fig S3B**. Plasma oxidation of **CB** is demonstrated in **Fig S4** and **DF** in **Fig S5**. Multiple degradation intermediates were produced during the degradation studies of both compounds. Based on the blank controls, it is expected that the peak that appears at R_t (1.33 min) (**Fig S4B, C** and **Fig S5B, C**) might indicate the formation of H_2O_2. This is in line with the observations in the study of Hoeben et al. (2019), where it was found that during 120 Watt plasma activation, 370 µM (H_2O_2) was formed. However, it must be mentioned that there is a deviation in the retention time compared to the control, which might be caused by the acidity of the plasma activated water itself. Changes in the pH during chromatography influences the elution of certain compounds.

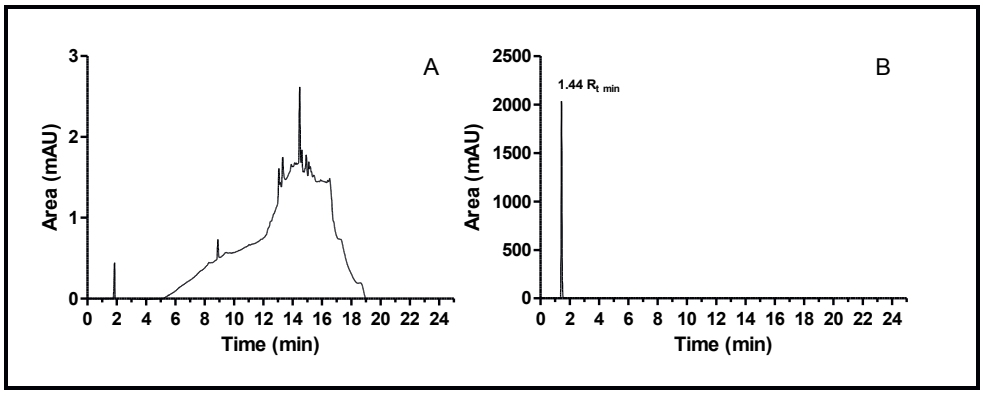

Fig. S3. Qualitative chromatograms of the control samples Milli-Q (**A**) and H_2O_2 (**B**), observing a measurable peak at retention time 1.44 ($R_{t\,min}$).

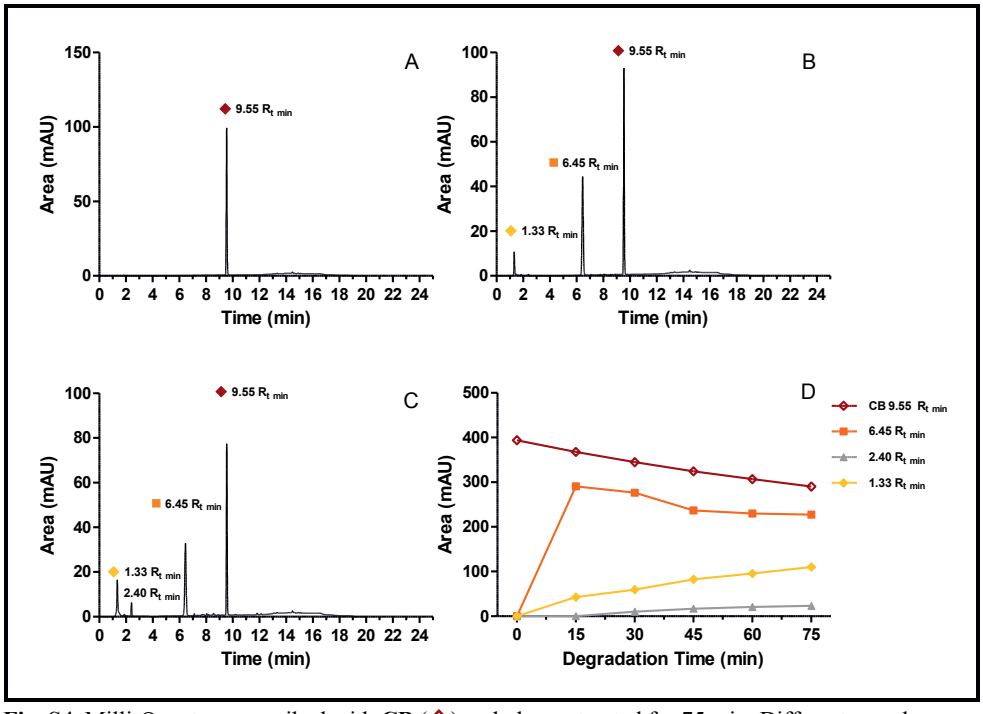

Fig. S4. Milli-Q water was spiked with **CB** (◇) and plasma treated for 75 min. Different samples were taken to observe the formation of degradation intermediates. (**A**) represented an initial CB sample 9.55 $R_{t\,min}$, 15 min (**B**) and 60 min (**C**) are thermal plasma treatment times. With HPLC-UV analysis a relative detector response demonstrated the abatement kinetics of CB. In addition to the degradation kinetics of the parent molecule, multiple reaction intermediates were detected (**D**); 6.45 $R_{t\,min}$ (■), 2.40 $R_{t\,min}$ (▲) and ; 1.33 $R_{t\,min}$ (◆).

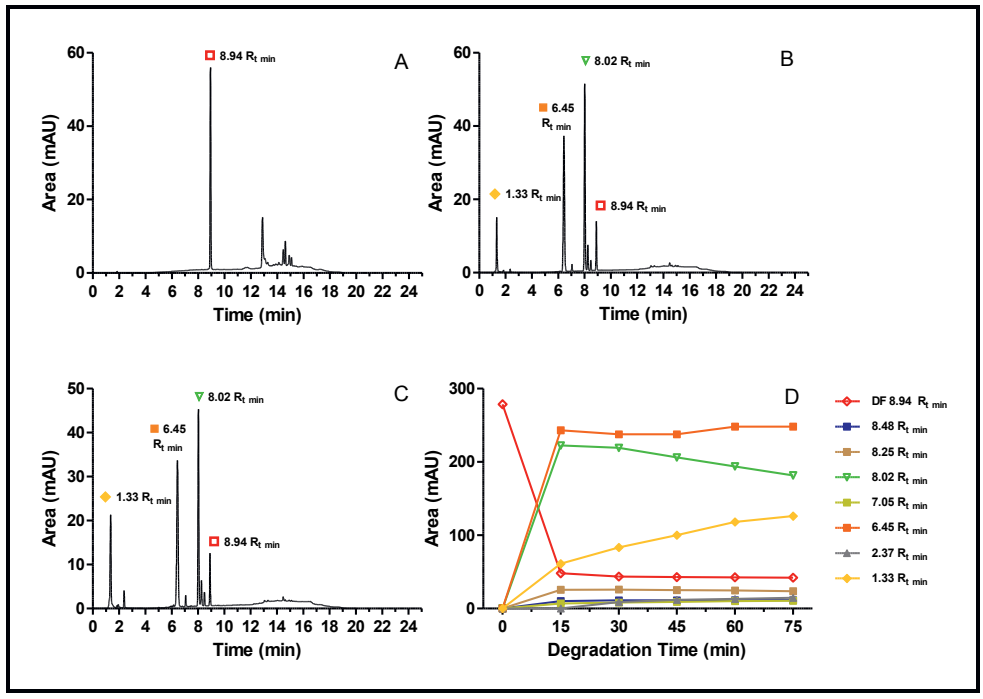

Fig. S5 Milli-Q water was spiked with **DF** (□) and plasma treated for 75 min. Different samples were taken to observe the formation of degradation intermediates. 0 min (**A**) represented an untreated DF sample 8.94 ($R_{t\ min}$), 15 min (**B**) and 60 min (**C**) are thermal plasma treatment times. With HPLC-UV analysis qualitatively the abatement kinetics of DF is demonstrated. In addition to the degradation kinetics of the parent pharmaceutical, multiple reaction intermediates were detected (**D**); 8.48 $R_{t\ min}$ (■), 8.25 $R_{t\ min}$ (■), 8.02 $R_{t\ min}$ (▽), 7.05 $R_{t\ min}$ (■), 6.45 $R_{t\ min}$ (■), 2.40 $R_{t\ min}$ (▲) and 1.33 $R_{t\ min}$

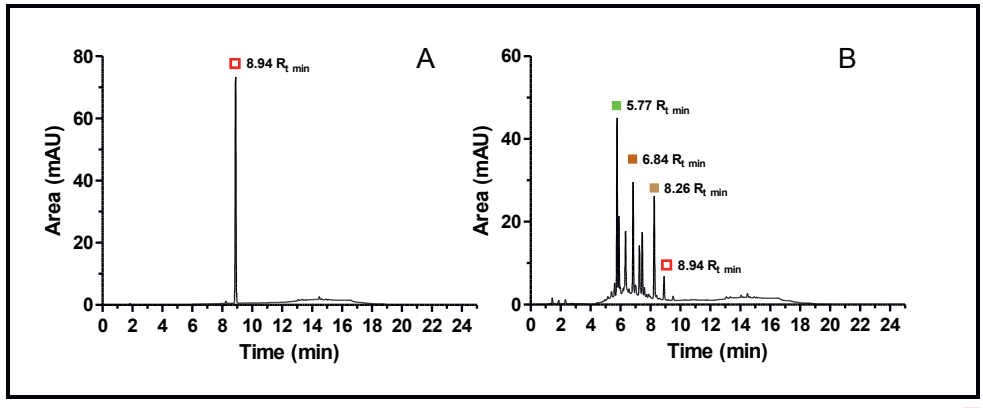

Fig. S6. Milli-Q water was spiked with **DF** (**A**) and 15 min treated with UV-C/H_2O_2. The initial DF □ (8.94 $R_{t\ min}$) is very rapidly degraded, producing multiple intermediates (**B**). Distinct degradation intermediates were determined compared to **DF** plasma treatment. Major HPLC peaks for oxidative degradation intermediates were seen at 8.26 $R_{t\ min}$ (■),6.84 $R_{t\ min}$ (■) and 5.77 $R_{t\ min}$ (■).

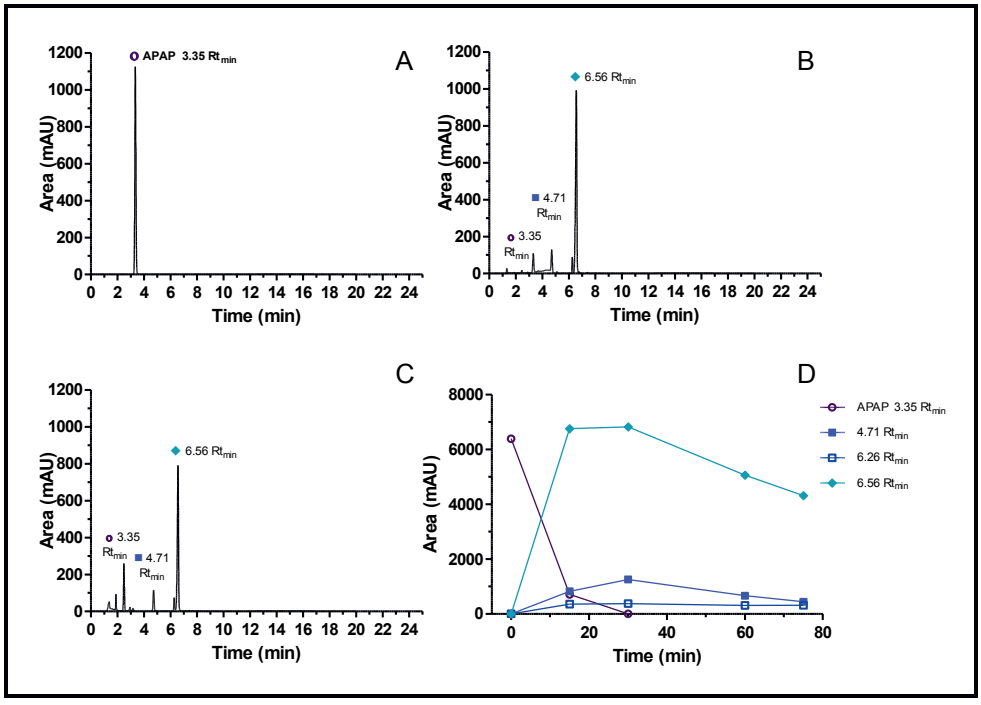

Fig. S7. Milli-Q water was spiked with **APAP** (**A**) and 75 min treated using thermal plasma activation. The initial **APAP** ○ concentration was determined at 3.35 $R_{t\ min.}$ and showed to be rapidly degraded in Milli-Q. During this plasma oxidation reaction multiple intermediates were formed after 15 min (**B**). These formed reaction intermediates are derived from APAP showing peaks at 4.71 $R_{t\ min}$ (■), 6.26 $R_{t\ min}$ (□) and 6.56 $R_{t\ min}$ (◆). Prolonged plasma activation will also degrade these intermediates (**C** and **D**).

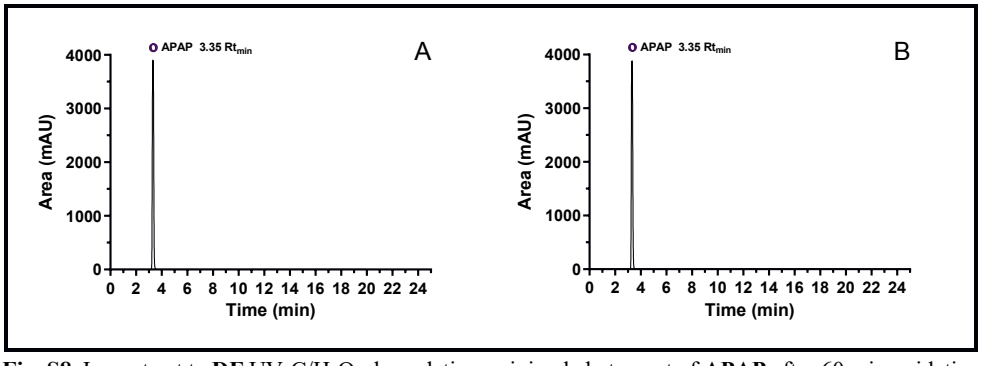

Fig. S8. In contrast to **DF** UV-C/H_2O_2 degradation, minimal abatement of **APAP** after 60 min oxidative treatment (**B**) has been observed. A similar observation for this result was already demonstrated in SSW and HSW, where it was found that interfering minerals and organic matter inhibit the oxidation reaction (Graumans et al 2021).

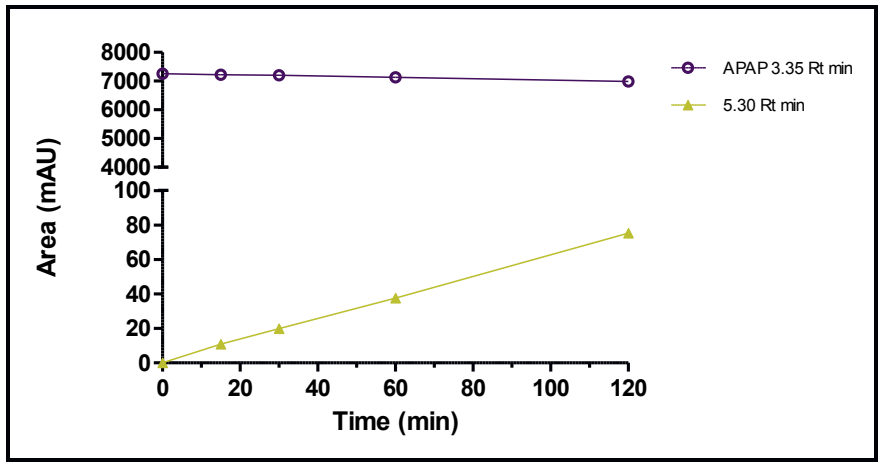

Fig. S9. In addition to the slower chemical degradation kinetics using UV-C/H_2O_2 treatment, it is expected that the high concentration added in Milli-Q also causes slower abatement. Looking to the qualitative degradation results it was found that also a reaction intermediate is formed (▲5.30 $R_{t\ min}$).

S.4.4 Statistical data interpretation, cell viability levels stained with crystal violet

With one-way analysis of variance (ANOVA) it was found that the means are significantly different for 150 W plasma activation in Milli-Q after incubating to HeLa cells for 24h (F_{stat}: 5.30 > F_{crit}: 1.88; P = <0.01) and 48h (F_{stat}: 11.67 > F_{crit}: 1.83; P = 0.01), see table **S4** and **S5**. With a Bonferroni's Multiple Comparison Test, the medium control (~100%) was compared to the mean values ($\bar{x}$) of the exposed samples. Statistically significant effects are labelled as *; $p < 0.05$, **; $p < 0.01$ and ***; $p < 0.001$.

Table S4.

Plasma-treated MQ matrix with 10 spiked pharmaceuticals, 24h exposed.

24h 150 Watt PAW – Crystal Violet													
Viability (%)	Medium	MQ	500 µM H_2O_2	0 min	5 min	15 min	30 min	45 min	60 min	90 min	120 min	150 min	180 min
x̄	98	123	50	107	117	114	128	122	119	107	96	67	67
±SE	4	±10	±7	±12	±17	±12	±14	±13	±12	±11	±10	±10	±17
Wells (n)	*16*	*8*	*8*	*6*	*6*	*6*	*6*	*6*	*6*	*6*	*6*	*6*	*6*
T_{stat}	-	*2.1*	*3.9*	*0.7*	*1.4*	*1.2*	*2.3*	*1.8*	*1.6*	*0.7*	*0.1*	*2.3*	*2.3*
T_{crit}	-	*2.9*	*2.9*	*3.1*	*3.1*	*3.1*	*3.1*	*3.1*	*3.1*	*3.1*	*3.1*	*3.1*	*3.1*
Significant	-	*No*	***	*No*	*No*	*No*	*No*	*No*	*No*	*No*	*No*	*No*	*No*

Table S5.

Plasma treated MQ matrix with 10 spiked pharmaceuticals, 48h exposed.

48h 150 Watt PAW – Crystal Violet													
Viability (%)	Medium	MQ	500 µM H_2O_2	0 min	5 min	15 min	30 min	45 min	60 min	90 min	120 min	150 min	180 min
x̄	102	117	18	112	112	112	98	81	63	24	15	44	35
±SE	±8	±11	±6	±11	±14	±12	±14	±20	±19	±10	±6	±10	±13
Wells (n)	*24*	*16*	*16*	*8*	*9*	*9*	*9*	*9*	*9*	*9*	*9*	*4*	*6*
T_{stat}	-	*1.14*	*6.8*	*0.6*	*0.7*	*0.6*	*0.3*	*1.4*	*2.6*	*5.2*	*5.7*	*2.8*	*3.8*
T_{crit}	-	*2.6*	*2.6*	*2.9*	*2.8*	*2.8*	*2.8*	*2.8*	*2.8*	*2.8*	*2.8*	*3.7*	*3.1*
Significant	-	*No*	***	*No*	*No*	*No*	*No*	*No*	*No*	***	***	*No*	**

UV-C/H_2O_2 activation in Milli-Q caused significant differences between samples after 24h (F_{stat}: 9.4 > F_{crit}: 1.83; P = <0.001) and 48h cellular incubation (F_{stat}: 3.87 > F_{crit}: 1.88; P = <0.001). This significance difference was only found for the positive control 500 µM H_2O_2, see table **S6** and **S7**.

Table S6.

UV-C/H_2O_2-treated MQ matrix with 10 spiked pharmaceuticals, 24h exposed.

24h UV-C/H_2O_2 – Crystal Violet													
Viability (%)	Medium	MQ	500 µM H_2O_2	0 min	5 min	15 min	30 min	45 min	60 min	90 min	120 min	150 min	180 min
x̄	98	123	49	118	122	124	137	124	125	122	126	106	112
±SE	±4	±10	±7	±12	±14	±14	±12	±20	±15	±14	±15	±8	±18
Wells (n)	*16*	*8*	*8*	*6*	*6*	*6*	*6*	*6*	*6*	*6*	*6*	*6*	*6*
T_{stat}	-	*1.9*	*3.6*	*1.3*	*1.6*	*1.7*	*2.6*	*1.8*	*1.9*	*1.6*	*1.9*	*0.6*	*1.0*
T_{crit}	-	*2.9*	*2.9*	*3.1*	*3.1*	*3.1*	*3.1*	*3.1*	*3.1*	*3.1*	*3.1*	*3.1*	*3.1*
Significant	-	*No*	**	*No*	*No*	*No*	*No*	*No*	*No*	*No*	*No*	*No*	*No*

Table S7.

UV-C/H_2O_2 treated MQ matrix with 10 spiked pharmaceuticals, 48h exposed.

48h UV-C/H_2O_2 – Crystal Violet													
Viability (%)	Medium	MQ	500 µM H_2O_2	0 min	5 min	15 min	30 min	45 min	60 min	90 min	120 min	150 min	180 min
x̄	102	117	18	152	161	166	167	137	140	133	145	144	112
±SE	±8	±11	±6	±19	±12	±21	±19	±12	±15	±18	±20	±28	±26
Wells (n)	*24*	*16*	*16*	*9*	*9*	*9*	*9*	*9*	*9*	*9*	*9*	*6*	*6*
T_{stat}	-	*0.9*	*5.5*	*2.7*	*3.2*	*3.4*	*3.5*	*1.9*	*2.0*	*1.6*	*2.3*	*1.9*	*0.4*
T_{crit}	-	*2.6*	*2.6*	*2.8*	*1.8*[A]	*2.8*[A]	*2.8*[A]	*2.8*	*2.8*	*2.8*	*2.8*	*2.8*	*2.8*
Significant	-	*No*	***	*No*	*	**	**	*No*	*No*	*No*	*No*	*No*	*No*

[A]: The significant difference observed in these samples are attributed to cell proliferation caused by increased levels >100% compared to the medium control.

Using ANOVA there were significant differences in fluorescent signal in exposed HeLa cells after 24h (F_{stat}: 10.4 > F_{crit}: 1.83; P = <0.001) and 48h (F_{stat}: 25.9 > F_{crit}: 1.83; P = <0.001) after the addition of plasma treatment in SSW, see table **S8** and **S9**.

Table S8.

Plasma-treated SSW matrix with 10 spiked pharmaceuticals, 24h exposed.

24h 150 Watt PAW – Crystal Violet													
Viability (%)	Medium	SSW	500 µM H_2O_2	0 min	5 min	15 min	30 min	45 min	60 min	90 min	120 min	150 min	180 min
x̄	100	106	42	126	101	105	109	110	103	97	73	66	54
±SE	±6	±13	±9	±9	±6	±6	±5	±6	±3	±6	±6	±6	±2
Wells (n)	*24*	*12*	*12*	*8*	*9*	*9*	*9*	*9*	*9*	*9*	*9*	*9*	*9*
T_{stat}	-	*0.7*	*6.8*	*2.6*	*0.1*	*0.5*	*0.9*	*1.0*	*0.3*	*0.3*	*2.8*	*3.6*	*4.8*
T_{crit}	-	*2.7*	*2.7*	*2.9*	*2.8*	*2.8*	*2.8*	*2.8*	*2.8*	*2.8*	*2.8*	*2.8*	*2.8*
Significant	-	*No*	***	*No*	*No*	*No*	*No*	*No*	*No*	*No*	*No*	***	***

Table S9.

Plasma-treated SSW matrix with 10 spiked pharmaceuticals, 48h exposed.

48h 150 Watt PAW – Crystal Violet													
Viability (%)	Medium	SSW	500 µM H_2O_2	0 min	5 min	15 min	30 min	45 min	60 min	90 min	120 min	150 min	180 min
x̄	100	141	26	155	136	133	123	130	123	91	73	64	59
±SE	±3	±10	±2	±9	±7	±9	±7	±7	±6	±7	±13	±13	±9
Wells (n)	*22*	*12*	*12*	*9*	*9*	*9*	*9*	*9*	*9*	*9*	*9*	*9*	*9*
T_{stat}	-	*4.7*	*8.4*	*5.6*	*3.7*	*2.9*	*3.4*	*3.0*	*2.3*	*1.0*	*2.7*	*3.7*	*4.3*
T_{crit}	-	*2.7*	*2.7*	*2.8*	*2.8*	*2.8*	*2.8*	*2.8*	*2.8*	*2.8*	*2.8*	*2.8*	*2.8*
Significant	-	***[A]	***	***[A]	**[A]	*No*	*[A]	*No*	*No*	*No*	*No*	**	***

[A]: Increased viability level derived from SSW cause statistical significance. It is suggested that SSW act as nutrient in the cellular matrix, stimulating cell proliferation. Significant decrease in viability compared to the medium control is a reference for cytotoxicity.

Significant differences in the results were observed after 24h (F_{stat}: 3.6 > F_{crit}: 1.88; P = <0.001) and 48h (F_{stat}: 22.4 > F_{crit}: 1.83; P = <0.001) cellular incubation. HeLa cells were exposed to UV-C/H_2O_2 treated SSW spiked with 10 pharmaceuticals, see table **S10** and **S11**.

Table S10.

UV-C/H_2O_2-treated SSW matrix with 10 spiked pharmaceuticals, 24h exposed

24h UV-C/H_2O_2 – Crystal Violet													
Viability (%)	Medium	SSW	500 µM H_2O_2	0 min	5 min	15 min	30 min	45 min	60 min	90 min	120 min	150 min	180 min
x̄	100	124	36	72	79	86	87	96	128	86	89	87	76
±SE	±9	±15	±13	±16	±8	±16	±6	±8	±31	±4	±6	±5	±2
Wells (n)	*16*	*8*	*8*	*6*	*6*	*6*	*6*	*6*	*6*	*6*	*6*	*6*	*6*
T_{stat}	-	*1.7*	*4.5*	*1.8*	*1.3*	*0.9*	*0.9*	*0.3*	*1.8*	*0.9*	*0.7*	*0.8*	*1.5*
T_{crit}	-	*2.9*	*2.9*	*3.1*	*3.1*	*3.1*	*3.1*	*3.1*	*3.1*	*3.1*	*3.1*	*3.1*	*3.1*
Significant	-	*No*	***	*No*	*No*	*No*	*No*	*No*	*No*	*No*	*No*	*No*	*No*

Table S11.

UV-C/H_2O_2-treated SSW matrix with 10 spiked pharmaceuticals, 48h exposed

48h UV-C/H_2O_2 – Crystal Violet													
Viability (%)	Medium	SSW	500 µM H_2O_2	0 min	5 min	15 min	30 min	45 min	60 min	90 min	120 min	150 min	180 min
x̄	100	141	26	138	135	130	134	124	131	123	126	116	114
±SE	±3	±10	±2	±7	±4	±7	±7	±7	±9	±7	±4	±8	±13
Wells (n)	*22*	*12*	*12*	*9*	*9*	*9*	*9*	*9*	*9*	*9*	*9*	*9*	*9*
T_{stat}	-	*5.3*	*9.5*	*4.4*	*4.0*	*3.5*	*4.0*	*2.8*	*3.6*	*2.6*	*2.9*	*1.8*	*1.6*
T_{crit}	-	*2.7*	*2.7*	*2.8*	*2.8*	*2.8*	*2.8*	*2.8*	*2.8*	*2.8*	*2.8*	*2.8*	*2.8*
Significant	-	***[A]	***	***[A]	**[A]	*[A]	*[A]	*No*	**[A]	*No*	*No*	*No*	*No*

[A]: Increased viability level derived from SSW cause statistical significance. It is suggested that SSW act as nutrient in the cellular matrix, stimulating cell proliferation. Significant decrease in viability compared to the medium control is a reference for cytotoxicity.

For the untreated and plasma-treated HSW samples significant differences in the results were detected after 24h (F_{stat}: 6.1 > F_{crit}: 1.83; P = <0.001) and 48h (F_{stat}: 6.8 > F_{crit}: 1.87; P = <0.001), see table **S12** and **S13**.

Table S12.

Plasma-treated HSW matrix, 24h exposed

24h 150 Watt PAW – Crystal Violet													
Viability (%)	Medium	SSW	500 µM H_2O_2	0 min	5 min	15 min	30 min	45 min	60 min	90 min	120 min	150 min	180 min
x̄	100	123	14	71	90	79	105	179	144	128	130	111	157
±SE	±5	±10	±4	±22	±41	±32	±24	±27	±17	±11	±17	±11.	±18
Wells (n)	*20*	*16*	*16*	*9*	*9*	*9*	*9*	*9*	*9*	*9*	*9*	*9*	*9*
T_{stat}	-	*1.2*	*4.3*	*1.3*	*0.4*	*0.9*	*0.2*	*3.3*	*1.8*	*1.2*	*1.3*	*0.4*	*2.1*
T_{crit}	-	*2.6*	*2.6*	*2.8*	*2.8*	*2.8*	*2.8*	*2.8*	*2.8*	*2.8*	*2.8*	*2.8*	*2.8*
Significant	-	*No*	***	*No*	*No*	*No*	*No*	*	*No*	*No*	*No*	*No*	*No*

Table S13.

Plasma-treated HSW matrix, 48h exposed

48h 150 Watt PAW – Crystal Violet													
Viability (%)	Medium	SSW	500 µM H_2O_2	0 min	5 min	15 min	30 min	45 min	60 min	90 min	120 min	150 min	180 min
x̄	100	103	20	112	71	52	32	94	88	99	95	81	129
±SE	±3	±7	±4	±21	±21	±14	±5	±27	±5	±4	±3	±11	±22
Wells (n)	*16*	*8*	*8*	*6*	*6*	*6*	*6*	*6*	*6*	*6*	*6*	*6*	*6*
T_{stat}	-	*0.2*	*5.8*	*0.8*	*1.9*	*3.2*	*4.5*	*0.4*	*0.8*	*0.1*	*0.3*	*1.6*	*1.9*
T_{crit}	-	*2.9*	*2.9*	*3.1*	*3.1*	*3.1*	*3.1*	*3.1*	*3.1*	*3.1*	*3.1*	*3.1*	*3.1*
Significant	-	*No*	***	*No*	*No*	*	***	*No*	*No*	*No*	*No*	*No*	*No*

For the untreated and UV-C/H_2O_2-treated HSW samples significant differences in the results were detected after 24h (F_{stat}: 6.2 > F_{crit}: 1.88; P = <0.001) and 48h (F_{stat}: 17.2 > F_{crit}: 1.88; P = <0.001), see table **S14** and **S15**.

Table S14.

UV-C/H_2O_2-treated HSW matrix, 24h exposed

24h UV-C/H_2O_2 – Crystal Violet													
Viability (%)	Medium	SSW	500 µM H_2O_2	0 min	5 min	15 min	30 min	45 min	60 min	90 min	120 min	150 min	180 min
x̄	100	131	20	118	97	109	111	114	115	114	116	135	87
±SE	±4	±8	±4	±26	±10	±9	±12	±14	±12	±13	±13	±19	±17
Wells (n)	*16*	*8*	*8*	*6*	*6*	*6*	*6*	*6*	*6*	*6*	*6*	*6*	*6*
T_{stat}	-	*2.3*	*5.9*	*1.2*	*0.2*	*0.6*	*0.7*	*0.9*	*1.0*	*0.9*	*1.0*	*2.3*	*0.9*
T_{crit}	-	*2.9*	*2.9*	*3.1*	*3.1*	*3.1*	*3.1*	*3.1*	*3.1*	*3.1*	*3.1*	*3.1*	*3.1*
Significant	-	*No*	***	*No*	*No*	*No*	*No*	*No*	*No*	*No*	*No*	*No*	*No*

Table S15.

UV-C/H_2O_2-treated HSW matrix, 48h exposed

48h UV-C/H_2O_2 – Crystal Violet													
Viability (%)	Medium	SSW	500 µM H_2O_2	0 min	5 min	15 min	30 min	45 min	60 min	90 min	120 min	150 min	180 min
x̄	100	103	20	51	87	89	87	80	90	89	86	110	81
±SE	±3	±7	±4	±11	±5	±3	±3	±2	±3	±3	±3	±16	±6
Wells (n)	*16*	*8*	*8*	*6*	*6*	*6*	*6*	*6*	*6*	*6*	*6*	*6*	*6*
T_{stat}	-	*0.5*	*11.7*	6.5	1.7	1.5	1.7	2.7	1.3	1.5	1.9	1.3	2.5
T_{crit}	-	*2.9*	*2.9*	*3.1*	*3.1*	*3.1*	*3.1*	*3.1*	*3.1*	*3.1*	*3.1*	*3.1*	*3.1*
Significant	-	*No*	***	***	*No*	*No*	*No*	*No*	*No*	*No*	*No*	*No*	*No*

S.4.5 pH effect on ambient cell conditions

During plasma discharge multiple ROS and RNS are produced and dissolved in the treated matrix. Introduction of RNS in a treated water environment will make the matrix acidic. This effect mainly occurs in a matrix with minimal buffer capacity or by long plasma activation (Graumans et al., 2021). When exposing HeLa cells to xenobiotics or an acidic environment, biological functions can be altered. If the optimal cellular conditions are affected, cells experience oxidative stress or viability levels are decreased. In the study of Trebinska-Stryjewska (2020) it was found that cell viability levels decrease with 50% when incubating cells for 24h in a medium with a pH of 6.3. The viability declines even with 70% when incubating the cells for 48h. To see whether our HeLa cells are sensitive to pH, a working solution (n = 5) of acidic acid (CH_3COOH) in MQ and SSW was prepared. The concentration ranged from 10.000 to 0.5 µM and cells were exposed for 24h and 48h in a ratio of 1:10. To determine the pH of the CH_3COOH samples, three dilution series of 1000, 50, 1, 0.5 µM were prepared in Dulbecco's Modified Eagle's medium. Next to that, the pH of unspiked simulation matrices MQ and SSW were tested in duplicate (n = 2). The pH for these matrices was measured and in in a similar 1:10 ratio dissolved in medium. To have feasible quantities for pH measurement, a tenfold volume was taken by dissolving 200 µL sample in 1800 µL medium. Measured pH values were taken over an oxidative treatment period of 120 min, results are given in **Table S16-20**.

Table S16.
pH values CH_3COOH dilution series in medium

200 µL in 1800 µL medium (v/v)		
µM	**CH_3COOH-MQ**	**CH_3COOH-SSW**
1000	3.1	3.1 ± 0.1
50	4.4 ± 0.1	4.1 ± 0.2
1	6.8 ± 0.8	5.1 ± 0.2
0.5	7.7 ± 0.5	7.1 ± 0.5
Blank matrix	7.8 ± 0.4	7.8 ± 0.3

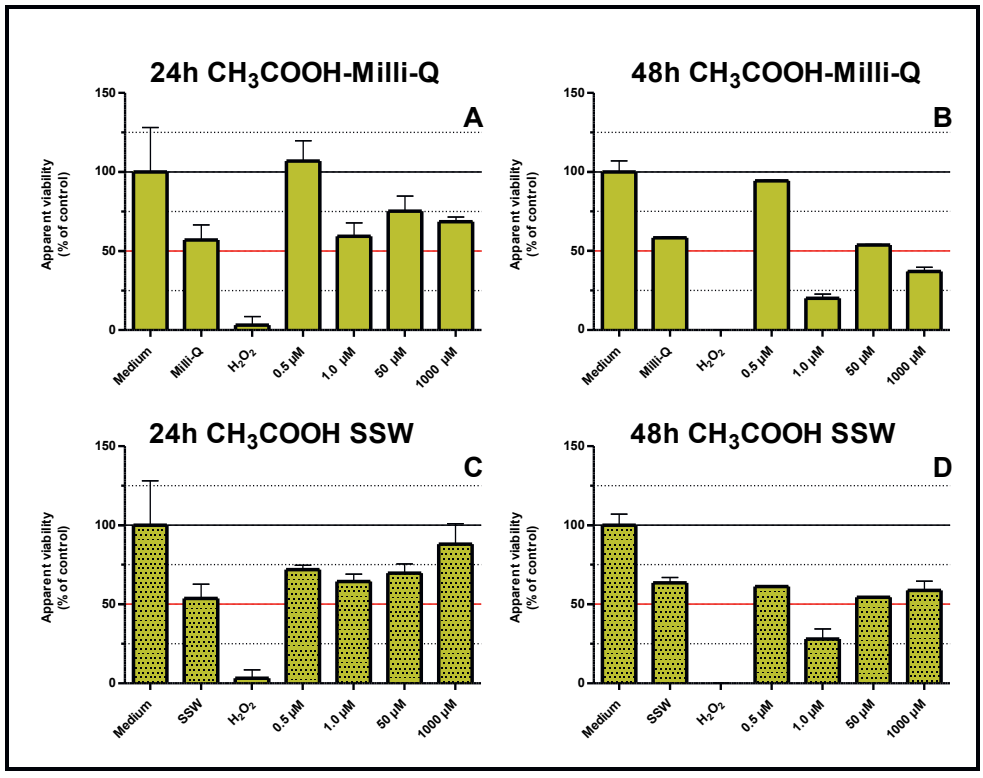

Fig. S10. HeLa cell viability levels are stained with crystal violet. The black line (—) represent the unexposed medium control and the red line (—) shows 50% viability level. 24h exposure to acidic acid samples indicate some lowered viability but no severe levels compared to the H_2O_2 control. Most declined levels are seen for CH_3COOH in Milli-Q indicating levels <50% viability for 1.0 and 1000 µM.

Table S17.

pH values for 500 mL oxidative treated Milli-Q

500 mL Milli-Q		
Treatment time (min)	**150 W Plasma**	**UV-C/H_2O_2**
Start 0	4.9	5.2 ± 0.3
End 120	1.7	7.6 ± 0.3

Table S18.

pH values for 500 mL oxidative treated Milli-Q diluted in medium

200 µL Milli-Q water in 1800 µL medium (v/v)		
Treatment time (min)	**150 W Plasma**	**UV-C/H_2O_2**
0	7.4 ± 0.2	7.4 ± 0.1
15	7.4 ± 0.1	7.5
45	7.2 ± 0.2	7.4 ± 0.1
60	7.1	7.5 ± 0.2
120	7.3	7.5 ± 0.1

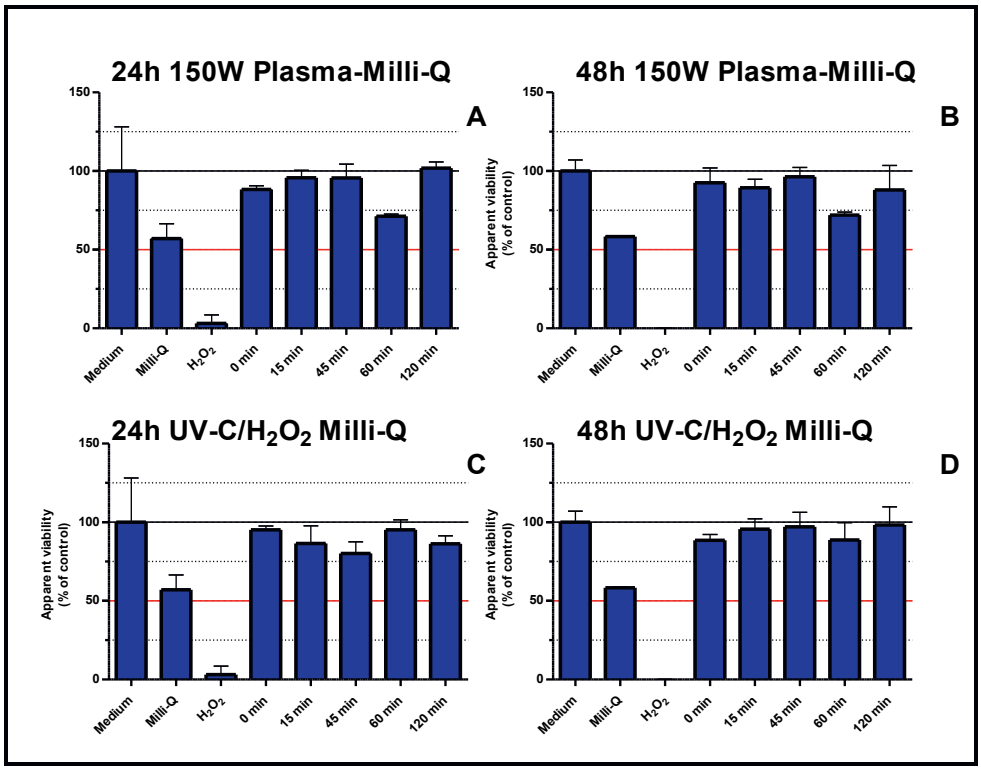

Fig. S11. HeLa cell viability levels exposed to 150 W plasma and UV-C/ H_2O_2 oxidative treated Milli-Q. HeLa cells are with crystal violet. The black line (—) represents the unexposed medium control and the red line (—) shows 50% viability level. No severe decline in viability levels was measured. Just as observed with the pH values in **Table S4**, the medium environment is minimally affected.

Table S19.
pH values for 500 mL oxidative treated SSW

500 mL SSW		
Treatment time (min)	**150 W Plasma**	**UV-C/H_2O_2**
Start 0	6.5	6.5 ± 0.1
End 120	1.9	6.8 ± 0.7

Table S20.
pH values for 500 mL oxidative treated Milli-Q diluted in medium

200 µL SSW in 1800 µL medium (v/v)		
Treatment time (min)	**150 W Plasma**	**UV-C/H_2O_2**
0	7.4 ± 0.1	7.4 ± 0.1
15	7.4 ± 0.1	7.5 ± 0.2
45	7.3	7.4 ± 0.1
60	7.3	7.4
120	7.3 ± 0.2	7.4 ± 0.3

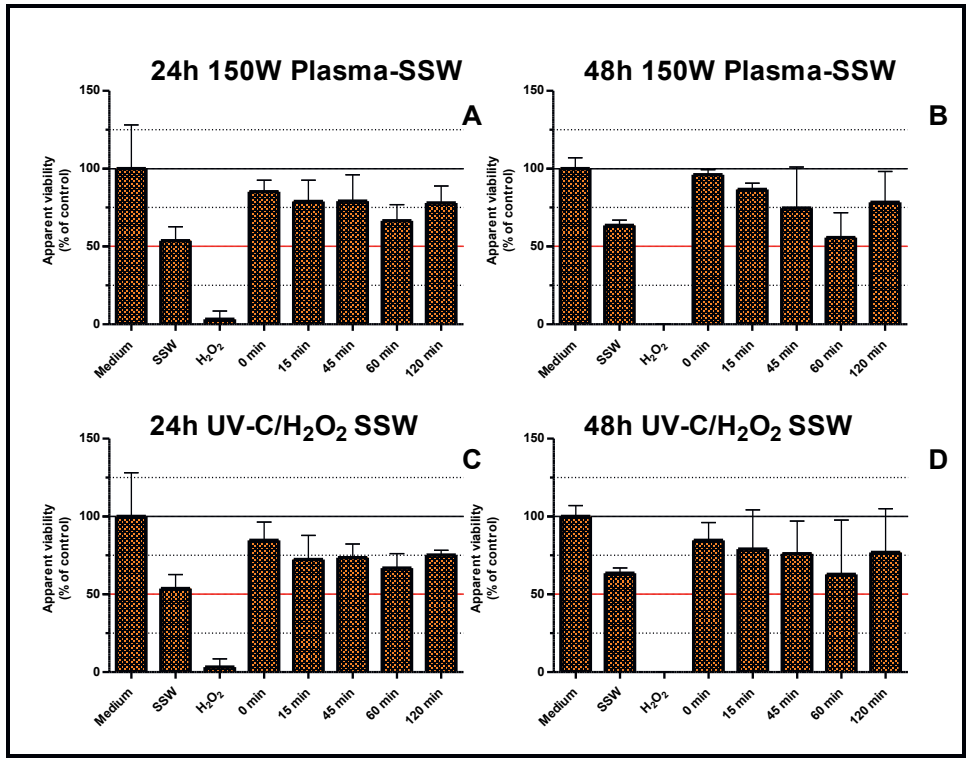

Fig. S12. HeLa cell viability levels exposed to 150 W plasma and UV-C/ H_2O_2 treated SSW. Similar as for Milli-Q water, minimal decline in cell viability is seen. HeLa cells are stained with crystal violet. The black line (—) represent the unexposed medium control and the red line (—) shows 50% viability level.

S.4.6 Filtered hospital sewage water oxidative treatment

Spin-X centrifugal tubes from Costar (Salt Lake City, USA) were used. Spin-X tubes were equipped with a 0.22 µm cellulose acetate filter placed on top of a 2.0 mL tube. To filter a HSW sample, an Eppendorf MiniSpin (Nijmegen, the Netherlands) centrifuge was used for 5 min at maximum speed (134000 rpm). After spinning, a less suspended wastewater sample was transferred to the cultivated HeLa cells. The unfiltered HSW was also used to expose HeLa cells. From the unfiltered sample it is clear that HeLa cells did not tolerate 24h exposure to sewage water. Comparing the filtered results with the unfiltered results, see **Fig. 4.4** (main text), the crystal violet marker indicated viability levels for untreated HSW samples after 24h and 48h incubation. In contrast, no fluorescence signal was detected, indicating the presence of many different bacteria in HSW. From this result it is expected that mainly gram-positive bacteria are stained with crystal violet. Despite the detection of only gram-positive bacteria in unfiltered samples, it must be mentioned that also gram-negative bacteria will be present in HSW. For example, *Escherichia coli*, an intestine gram-negative bacterium, is usually present in HSW (Chahal et al., 2016). To see whether bacterial toxins have an influence on cell viability, different lipopolysaccharide (LPS) concentrations were added to HeLa cells, see **Fig S14**. LPS is present on the outer membrane of gram-negative bacteria, and is therefore a suitable endotoxin to analyse whether it could affect ambient cell conditions. Despite the elevated fluorescence levels (~177% at 0 min) after filtration, it is expected that bacteria are easily eliminated. For example, *Escherichia coli* has a radius of 0.5 µm and 1.0 – 2.0 µm, so it is most likely removed after filtration **(**Riley et al., 1999**)**.

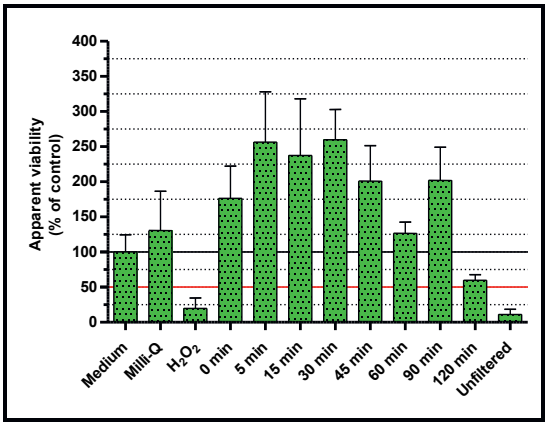

Fig. S13. Contribution of bacterial toxins to the cytotoxicity of untreated HSW. Samples were first filtered using a Costar® Spin-X® centrifuge tube filter with a pore size of 0.22 µm. Comparing the unfiltered sample with 0 min (filtered HSW) sample, it is seen that filtration has an effect on the cellular viability.

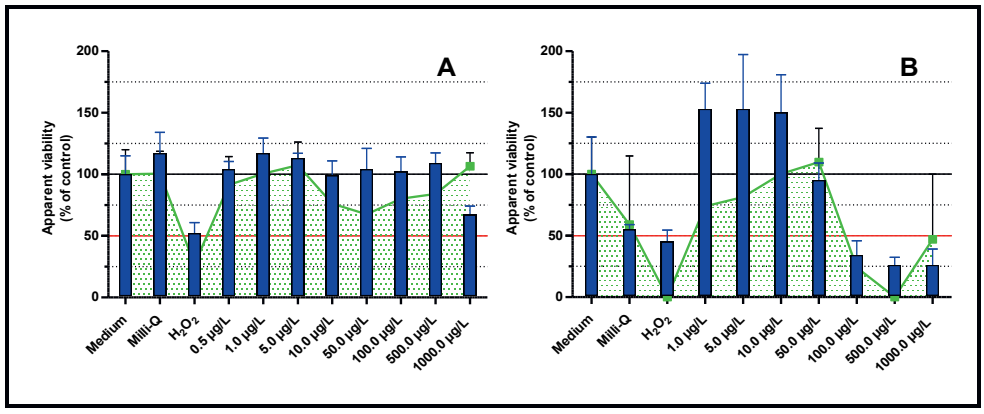

Fig. S14 Increasing lipopolysaccharide (LPS) concentrations were added to HeLa cells to observe possible toxicity from this compound. The black line (—) indicates unaffected HeLa cells and the red line (—) demonstrates 50% viability. 24h exposure to LPS minimally affects the HeLa cells (**A**), showing also minimal oxidative stress caused by this xenobiotic. Prolonged exposure to LPS for 48h (**B**) demonstrates a severe decline in cell viability for the concentrations 100, 500 and 1000 µg/L LPS.

Literature

Ayuso, M., Van Cruchten, S., & Van Ginneken, C. (2020). A Medium-Throughput System for In Vitro Oxidative Stress Assessment in IPEC-J2 Cells. *International Journal of Molecular Sciences*, *21*(19), 7263. https://doi.org/10.3390/ijms21197263

Chahal, C., van den Akker, B., Young, F., Franco, C., Blackbeard, J., & Monis, P. (2016). *Pathogen and Particle Associations in Wastewater* (pp. 63–119). https://doi.org/10.1016/bs.aambs.2016.08.001

Invitrogen Reactive Oxygen Species (ROS) Detection Reagents.

Johnson, I. D. (2010). The Molecular Probes® Handbook: A Guide to Fluorescent Probes and Labeling Technologies. Chapter 15: Assays for Cell Viability, Proliferation and Function.

Johnson, I. D. (2010). The Molecular Probes® Handbook: A Guide to Fluorescent Probes and Labeling Technologies. Chapter 18: Probes for Reactive Oxygen Species, Including Nitric Oxide.

Graumans, M. H. F., Hoeben, W. F. L. M., van Dael, M. F. P., Anzion, R. B. M., Russel, F. G. M., & Scheepers, P. T. J. (2021). Thermal plasma activation and UV/H2O2 oxidative degradation of pharmaceutical residues. *Environmental Research*, *195*. https://doi.org/10.1016/j.envres.2021.110884

Hoeben, W. F. L. M., van Ooij, P. P., Schram, D. C., Huiskamp, T., Pemen, A. J. M., & Lukeš, P. (2019). On the Possibilities of Straightforward Characterization of Plasma Activated Water. *Plasma Chemistry and Plasma Processing*, *39*(3), 597–626. https://doi.org/10.1007/s11090-019-09976-7

Riley, M. (1999). Size limits of very small microorganisms: proceedings of a workshop. Washington (DC), National Academy of Sciences.

Symons, M. C. R., Rusakiewicz, S., Rees, R. C., & Ahmad, S. I. (2001). Hydrogen peroxide: a potent cytotoxic agent effective in causing cellular damage and used in the possible treatment for certain tumours. *Medical Hypotheses*, *57*(1), 56–58. https://doi.org/10.1054/mehy.2000.1406

Trebinska-Stryjewska, A., Swiech, O., Opuchlik, L. J., Grzybowska, E. A., & Bilewicz, R. (2020). Impact of Medium pH on DOX Toxicity toward HeLa and A498 Cell Lines. *ACS Omega*, *5*(14), 7979–7986. https://doi.org/10.1021/acsomega.9b04479

Chapter 5

In silico ecotoxicity assessment of residual pharmaceuticals in wastewater following oxidative treatment

Martien H.F. Graumans, Ad J.M. Ragas, Wilfred F.L.M. Hoeben,
Frans G.M. Russel, Paul T.J. Scheepers

Environmental Research 243, February 2024

Abstract

Advanced oxidation processes such as thermal plasma activation and UV-C/H_2O_2 treatment are considered as complementary applications for the degradation of pharmaceutical residues in wastewater prior to convention wastewater treatment. It is supposed that direct oxidative treatment can lower the toxicity of hospital sewage water (HSW).

The aim of this study was to predict the ecotoxicity for three aquatic species before and after oxidative treatment of 10 quantified pharmaceuticals in hospital sewage water. With the application of oxidative chemistry, pharmaceuticals are degraded into transformation products before reaching complete mineralisation. To estimate the potential ecotoxicity for fish, Daphnia and green algae ECOSAR quantitative structure-activity relationship software was used. Structure information from pristine pharmaceuticals and their oxidative transformation products were calculated separately and in a mixture computed to determine the risk quotient (RQ).

Calculated mixture toxicities for 10 compounds found in untreated HSW resulted in moderate-high RQ predictions for all three aquatic species. Compared to untreated HSW, 30-min treatment with thermal plasma activation or UV-C/H_2O_2 resulted in lowered RQs. For the expected transformation products originating from fluoxetine, cyclophosphamide and acetaminophen increased RQs were predicted. Prolongation of thermal plasma oxidation up to 120 min predicted low-moderate toxicity in all target species. It is anticipated that further degradation of oxidative transformation products will end in less toxic aliphatic and carboxylic acid products. Predicted RQs after UV-C/H_2O_2 treatment turned out to be still moderate-high.

In conclusion, *in silico* extrapolation of experimental findings can provide useful predicted estimates of mixture toxicity. However due to the complex composition of wastewater this *in silico* approach is a first step to screen for ecotoxicity. It is recommendable to confirm these predictions with ecotoxic bioassays.

5.1 Introduction

Good water quality is of key importance for humans, animals and the environment. Pharmaceuticals released in the hydrosphere can severely affect surface water and drinking water sources depending on their concentration and composition (Peake, 2016). For example, British waters were described as a chemical cocktail of sewage, agriculture and plastic polluting waste (House of Commons Environmental Audit Committee, 2022b). In the Netherlands, water pollution is also primarily determined by high levels of nutrients, plant protection product residues, industrial waste, pharmaceuticals and veterinary medicines (Driezum et al., 2020; Moermond et al., 2020). Water pollution is common, differs per region and is often source-specific regarding the type of pollutant (Peake, 2016). In the European Union, monitoring programs are used to detect and manage emerging pollutants (Moermond et al., 2020; 2000/60/EG, 2000).

In addition to other pollutants are pharmaceuticals widespread in the aquatic environment. Due to their physicochemical properties and bioactivity too high concentrations can cause ecotoxicological effects (Moermond et al., 2020; Peake, 2016). Introduction of pharmaceuticals is originating from wastewater treatment plants (WWTP), surface runoff, illegal dumping sites and landfills. WWTP are not designed for the removal of pharmaceuticals, however biodegradation occurs for certain residues. Toxic chemicals can also affect the biofilm inhibiting the treatment systems (Vasiliadou et al., 2018). Also, the continuous introduction of pollutants complicates the complete removal of contaminants (Ortiz de García et al., 2014). Other problems for conventional WWTPs are chemical persistence, or the biotransformation of pharmaceutical metabolites into their original structure (Ajo et al., 2018). In the case of old sewer systems it is even possible that untreated sewage water is released from overflow points directly into surface waters (Egli et al., 2023). Annually up to >39 million tonnes of untreated wastewater end-up in the river Thames, London UK, via sewage overflow points (Egli et al., 2023).

To complement conventional wastewater treatment, additional technologies, such as advanced oxidation processes (AOPs) are available. The basic principle of AOPs are based on the production of reactive oxygen (ROS) and nitrogen species (RNS) for the degradation of substances in wastewater (Ajo et al., 2018; Banaschik et al., 2018; Wang & Wang, 2021). ROS and RNS could be generated by either Fenton reaction, UV, photolytic, ozonation or (non-) thermal gas discharge reactions wastewater (Ajo et al., 2018; Banaschik et al., 2018; Wang & Wang, 2021). However, too short treatment times will result in incomplete mineralisation and

can cause the formation of potentially toxic intermediates such as epoxides, hydroperoxides, quinones, and hydroxy-, nitro- or nitroso functionality (**Table S1**; Graumans et al., 2020; Rayaroth et al., 2022; Sharma et al., 2018; Shi et al., 2023; Vogna et al., 2002; Wang & Wang, 2021). The introduction of AOPs for wastewater treatment at the source is expected to be a highly effective approach to reduce unwanted medicines in their concentrated presence. With the deployment of AOPs at the WWTP it is expected that more input energy is needed to degrade pharmaceuticals diluted by multiple wastewater streams (Ajo et al., 2018; Back et al., 2018).

In vitro toxicity testing is considered suitable to evaluate efficacy by comparing the cytotoxicity of wastewater before and after treatment with plasma oxidation (Graumans et al., 2022). In our previous studies, we used thermal plasma activation for the oxidative degradation of pharmaceutical residues (Graumans et al., 2020, 2021). We used reconstituted (simulated) wastewater and real-life hospital sewage water. Pharmaceutical residues were rapidly degraded using UV/H_2O_2 and plasma-activated treatment. Additionally, a cytotoxicity assay was applied to determine the harmfulness of hospital sewage water before and after oxidative treatment in a human cell culture. This resulted in minimal toxicity after direct thermal plasma treatment (Graumans et al., 2022). Due to the complexity of wastewater it can be difficult to attribute an observed effect to original products or its corresponding transformation product formed during human metabolism, microbial biotransformation or oxidative conversion (Drzymała & Kalka, 2020). More specific ecotoxicity tests are needed to translate the results from lab-based cytotoxicity testing results to environmental relevant conditions. Multiple bioassays are available to determine whether individual pharmaceutical residues and their mixtures in complex matrices contribute to unwanted ecotoxic effects (Abbas et al., 2019; De Baat et al., 2020; Wang & Wang, 2021). However, the deployment of bioassays can be time-consuming and expensive, and some are laborious regarding sample preparation and involvement of test organisms (Abbas et al., 2019; Kar et al., 2020; Wang & Wang, 2021; Žegura et al., 2009). Therefore, extensive experimental (eco)toxicological data on individual substances present in a mixture is often of limited availability (Orias & Perrodin, 2013; Sanderson, 2003; Khan et al., 2019; Reuschenbach et al., 2008; Wang & Wang, 2021). To complement toxicity assay results, computational predictions can be used as a first-tier approach to explore potential ecotoxicity. Quantitative structure-activity relationship (QSAR) tools can serve as an early warning system by predicting possible acute or long-term effects (Drzymała & Kalka, 2020; Khan et al., 2019; Tay & Madehi, 2015; Wang & Wang, 2021). With the input of substance specific parameters,

such as a characterised chemical structure, a toxicity estimate is calculated based on a mathematical relationship between predicted and measured physicochemical properties of compounds present in a training set (Walker, 2012). Regarding aquatic ecotoxicity, the ecological structure-activity relationship (ECOSAR) tool from the United States Environmental Protection Agency (US EPA) is proposed to predict acute and chronic effects in fish, Daphnia and green algae (Mayo-Bean, 2012). The ECOSAR tool provides a toxicity estimate derived from a linear relationship between predicted log $P_{\text{octanol/water}}$ and corresponding measured toxicity values. Based on functional groups of the inserted molecular structure the median effect or lethal concentration is computerised. Despite its usability and rapidity in providing information, (Q)SAR software is in general just a screening method. Output data is therefore primarily an indicative measure, providing effect concentrations with a substantial degree of uncertainty. However, for a rapid screening of the magnitude of the toxic effect, *in silico* risk assessment is a useful approach e.g. to inform further selection of dedicated bioassays.

The aim of this study is to estimate whether *in silico* tools can be used to calculate ecotoxicity indicators from untreated and oxidatively treated wastewater. Additionally, the calculated risk levels for each individual compound and a hypothetical pharmaceutical mixture were used to predict whether advanced oxidation processes could be beneficial prior to conventional wastewater treatment.

5.2 Methodology

Molecular structures needed for the *in silico* predictions were retrieved from our optimisation experiment Graumans et al. (2020), degradation study Graumans et al. (2021) and cytotoxicity analysis Graumans et al. (2022). For this *in silico* study, a versatile set of 10 pharmaceuticals formerly detected in hospital sewage water were used as model compounds. The 10 quantified compounds were selected as model compounds due to their distinct physicochemical properties and hospital wastewater relevance. Actual measured pharmaceutical concentrations and abatement kinetics were used in combination with (Q)SAR software. Estimated effect concentrations were used to calculate the PNEC values. Risk quotients for fish, Daphnia and green algae were calculated by using measured environmental concentration (MEC) and estimated PNEC values. We compared our computed predictions with experimental findings from studies in the field of oxidative treatment (Banaschik et al., 2018; Hoeben et al., 2000; Nowak et al., 2020), risk assessments (Backhaus & Faust, 2012; Kar et al., 2020; Khan et al., 2019; Ortiz de García et al., 2014) and (eco)toxicity (Osawa et al., 2019; Česen, et al., 2016a; Česen, et al., 2016b; Drzymała & Kalka, 2020; Grzesiuk et al., 2018; Sousa & Nunes, 2021; Xie et al., 2022).

5.2.1 Measured environmental concentration (MEC)

For the MEC determination end-of-pipe hospital sewage water (HSW) was analysed. HSW was a composite sample taken at the Radboud University Medical Center (Graumans et al., 2021). The composite sample was pooled from different days; Monday - Thursday 16-19 September 2019. Upon arrival in the laboratory HSW was filtered by vacuum filtration, placed in aliquots and stored until analysis and subsequent oxidative treatment. Ten pharmaceuticals were quantified in HSW using solid phase extraction (SPE) combined with liquid chromatography mass spectrometry (LC-MS/MS). Detected pharmaceuticals were the X-ray contrast agents iomeprol (IOM), and diatrizoic acid (DIA), the antibiotic cipfrofloxacin (CIP), the antidepressant fluoxetine (FLU), the NSAID diclofenac (DF), the beta-blocker metoprolol (MET), the cytostatic cyclophosphamide (CP), the anti-epileptic carbamazepine (CB), the analgesic acetaminophen (APAP), and the antidiabetic metformin (MF). In HSW the detected residue concentrations were: 2387.3 µg/L IOM, 10.1 µg/L DIA, 14.5 µg/L CIP, 0.15 µg/L FLU, 3.1 µg/L DF, 1.3 µg/L MET, 0.34 µg/L CP, 0.1 µg/L CB, 82.1 µg/L APAP and 36.8 µg/L MF.

5.2.2 Oxidative degradation

Kinetics of thermal plasma and UV-C/H_2O_2 oxidation in complex matrices were earlier determined for pharmaceuticals as a function of time. To evaluate whether these treated

pharmaceutical residues represent a risk for the aquatic environment we used our previous determined concentrations of our 10 model pharmaceuticals as our reference values (**Table S2-4**) (Graumans et al., 2021).

5.2.2.1 Thermal plasma treatment

Filtered HSW sample, 500 mL was treated in a laboratory-scale plasma activation unit (VitalFluid, Eindhoven, the Netherlands). As previously described, plasma discharges were applied directly in actively stirred HSW matrix using the maximum available power output of 150 W for a duration of 120 min. Plasma discharge was performed at ambient air, and the water temperature was maintained between 20 – 35 °C. At multiple time-periods, samples were taken to measure the oxidative degradation kinetics, expressed as the conversion level ($\bar{R}$ %) (Graumans et al., 2021).

5.2.2.2 UV-C/H_2O_2 oxidative treatment

During UV-C/H_2O_2 treatment, UV-C irradiation was applied using a modified Aetaire UV air disinfection unit. The UV-C source (Philips PL-L 60W/4P HO; Eindhoven, the Netherlands) was placed 20 cm above the 500 mL HSW sample. To initiate oxidative treatment, 0.22 mM (~10 mg/L) hydrogen peroxide solution (Avantor Performance Materials; Deventer, the Netherlands) was added at the start of the experiment. UV-C/H_2O_2 was also applied for a duration of 120 min, actively vortexed and water temperature remained at ambient temperature during treatment (5.7 mW/cm^2 at the water surface Graumans et al. 2021).

5.2.3 Oxidative transformation product selection

With the application of advanced oxidation processes (AOPs), original pharmaceutical structures were rapidly degraded. Depending on the treatment time, original structures are completely or partially converted into oxidative degradation intermediates. To investigate whether these degradation products contribute to toxicity, we used our previously measured conversion levels ($\bar{R}$ %:) after 30 min oxidative treatment. According to literature references that also applied AOPs, we selected for each pharmaceutical one possible TP (**Table S8**), which was characterised after hydroxyl radical oxidation (•OH). It is expected for thermal plasma and UV-C/H_2O_2 oxidation that •OH reactions are prevalent (Graumans et al., 2021), initiating pharmaceutical decomposition by hydroxylation reactions. Characterised TPs were found in literature studies (Banaschik et al., 2018; Drzewicz et al., 2019; Hollman et al., 2020; Humayun et al., 2021; Jaén-Gil et al., 2019; Nowak et al., 2020; Straub et al., 2019; Tisler & Zwiener, 2019; Vogna et al., 2002; X. Wang et al., 2019). It was found with prolonged oxidative degradation up to 120 min using plasma or UV-C/H_2O_2 treatment that further degradation of

TPs occurred (Graumans et al., 2020). Using determined abatement kinetics ($\bar{R}$ %: $C_{t\ 15\ min,\ 30\ min,\ 60\ min}$) (Graumans et al. 2021) for the selected TPs, the potential formation of single carboxylic acids or aliphatic structures was hypothesised. Carboxylic acids or aliphatic structures were also selected according to identified products found in oxidative treatment studies (**Table S8**), (Banaschik et al., 2018; Bocos et al., 2016; HU et al., 2019; Isarain-Chávez et al., 2011; Li et al., 2021; Markiewicz et al., 2017; Ou et al., 2016; Qutob et al., 2022; Tisler et al., 2019; Yang et al., 2018). References were retrieved from either Science Direct, Web of Science or PubMed using keywords matching the pristine substance name combined with an oxidative treatment technique (**Table S8**).

5.2.4 Predictive ecotoxicity

5.2.4.1 Predicted no-effect concentration (PNEC) using ECOSAR software

For modelling we used ECOSAR v2.2 as developed by the United States Environmental protection agency (US EPA). ECOSAR software is especially designed for the prediction of short-term and long-term ecotoxic effects determined for specific chemical substances. The ECOSAR output data is computed as effect concentration (EC_{50}), mortality concentration (LC_{50}) and a chronic toxicity value for group model-organisms: fish, Daphnia and green algae. The median effect concentrations (EC_{50} and LC_{50}) for a specific chemical substance is computed by ECOSAR software from a linear relationship between the chemical partition coefficient (Log $P_{o/w}$) and toxicity values from a training set (Backhaus & Faust, 2012; Kar et al., 2020; Mayo-Bean, 2012, Walker, 2012). Chronic effect estimate values (ChV) are expressed as the geometric mean of the lowest observed effect concentration (LOEC) and no observed effect concentration (NOEC). Chronic estimates are computed by ECOSAR according to the mathematical equation $10^{(\log (LOEC \cdot NOEC)/2)}$ (Mayo-Bean, 2012). Data used in the ECOSAR training set is obtained from experimentally determined acute and inhibitory parameters according to ecotoxic testing conditions (Reuschenbach et al., 2008b). Experimental ecotoxicity data for fish, Daphnia and green algae are often obtained according to national or international guidelines such as the organisation for economic cooperation and development (OECD) (*Test No. 201: Alga, Growth Inhibition Test*, 2006; *Test No. 202: Daphnia Sp. Acute Immobilisation Test*, 2004; *Test No. 203: Fish, Acute Toxicity Test*, 2019). As suggested by the OECD, fish should be juveniles and Daphnia should be less than 24h old. For green algae specific strains *Pseudokirchneriella subcapitata* and *Scenedesmus subspicatus* are recommended.

For our $PNEC_{acute}$ estimates we used the median acute effect concentrations computed by ECOSAR. Depending on the entered molecular structure, output data is predicted for multiple QSAR classes. For our study we selected the most appropriate substructure matching with the actual input molecule.

In case of limited toxicity information towards the most reactive functional group it is implied to select the most conservative prediction to obtain an accurate estimate. (ECOSAR 6.6.4). Uptake in fish, Daphnia and green algae will predominately occur via water. According to ECHA guidance when calculating an acute PNEC an assessment factor is used to address the difference between bioassay data, laboratory data and real-life conditions. To derive a $PNEC_{acute}$ value for an aqueous compartment using short-term ecotoxicity data, we applied the suggested assessment factor of 1000 (Backhaus & Faust, 2012; Kar et al., 2020; Mayo-Bean, 2012; Walker, 2012). This factor is assumed to account for all relevant uncertainties and variability, biological variance, intra- and interlaboratory variation.

5.2.4.2 Risk quotient (RQ) levels

Ecotoxicity was expressed as a risk quotient (RQ; **Eq. 1**). To assess the risk of the pharmaceutical mixture in HSW, t measured environmental concentration (MEC) and ECOSAR predicted no-effect concentration ($PNEC_{actue}$) were calculated according to **Eq. 1**:

$$RQ = \frac{MEC}{PNEC} \quad \textbf{Eq. 1}$$

RQ = Risk quotient

MEC = Measured environmental concentration (mg/L)

$PNEC_{acute}$ = Predicted no-effect concentration (lowest EC_{50} or LC_{50}/1000)

In this study the ratio between exposure and potential (eco)toxic effects characterise the ecotoxicological risk (Escher et al., 2011). Ecotoxicity levels were determined for fish, Daphnia, and green algae. The calculated risk quotient was expressed in four classification values: < 0.1 (■ Insignificant); 0.1 – 1.0 (■ Low); 1.0 – 10 (■ Moderate) and > 10 (■ High) (Peake et al., 2016; Wennmalm & Gunnarsson, 2009).

5.2.4.3 Prediction of mixture toxicity

Next to the individually obtained risk quotient results, also mixture toxicity of the untreated and treated HSW matrix was predicted. Mixture toxicity is calculated for the quantified pharmaceuticals in wastewater. Providing solely RQ values of single components might underestimate the actual mixture toxicity. A mathematical model was used for determining the mixture toxicity based on additivity (Backhaus & Faust, 2012; Loewe & Muischnek, 1926). Additivity is not limited to low concentration ranges but can be expected as default for all

mixtures. To estimate the environmental risk of a mixture, a simplified scenario is predicted by the concentration addition concept (Altenburger et al., 2000; Backhaus & Faust, 2012; Escher et al., 2020). With this conservative assumption it is anticipated that for each pharmaceutical component in a mixture its present fraction contributes to a similar pharmacological response in an organism (Backhaus & Faust, 2012; Česen et al., 2016b; Drzymała & Kalka, 2020; Escher et al., 2020; Peake, 2016, Roos et al., 2012). For a mixture matrix with *n* compounds, **Eq. 2** is used. For each individual compound, the EC_{50} or LC_{50} value was selected as provided by ECOSAR software.

$$EC_{mix} = 1/\sum_{c=1}^{n} \frac{p_c}{EC_{50\,C}} \quad \textbf{Eq. 2}$$

$$\Sigma\, P/EC_{50} = [\left(\frac{P_{c1}}{EC_{50\,c1}}\right) + \left(\frac{P_{c2}}{EC_{50\,c2}}\right) + \left(\frac{P_{c3}}{EC_{50\,c3}}\right) + \left(\frac{P_{cn}}{EC_{50\,cn}}\right)]$$

EC_{mix} = Calculated effect concentration of the mixture (mg/L)

P_c = Fraction of a single compound

$\Sigma P_c = 1$ = Sum of the total fraction

$EC_{50\,c\,n}$ = Median effect concentration of single compound (mg/L)

5.2.5 Data analysis

Molecular structures were drawn using version 22.1 from BIOVIA Draw 2022 software, Dassault Systèmes (Vélizy-Villacoublay, France) and simplified molecular-input line-entry system (SMILES) notations were generated. To estimate the effect concentration (EC_{50}) or mortality concentration (LC_{50}), the SMILES notations used as input for the ECOSAR run. Acute ecotoxicity was calculated by selecting the most conservative effect concentration (**Table S2-9**). To calculate and visualise the RQ, statistical software from GraphPad Prism 9.3.1 (GraphPad Inc., CA, USA) was used.

5.3 Results and Discussion

5.3.1 Predicted aquatic ecotoxicity of untreated HSW

$PNEC_{acute}$ values for fish and Daphnia were retrieved for 96h and 48h mortality concentrations (LC_{50}) and a 96h median effect concentrations (EC_{50}) was used for green algae (**Table S2-S4**). The calculated risk quotient per compound is visualised categorically, showing the potential ecotoxicity per species, see **Fig. 5.1**. RQ values for calculated each pharmaceutical separately, indicate an insignificant to moderate risk for fish. A high risk was predicted for acetaminophen (APAP) towards Daphnia and green algae species. Moderate toxicity was also expected for untreated FLU in green algae. The average species vulnerability for the 10 characterised compounds was assessed as *Daphnia* > *green algae* > *fish.*

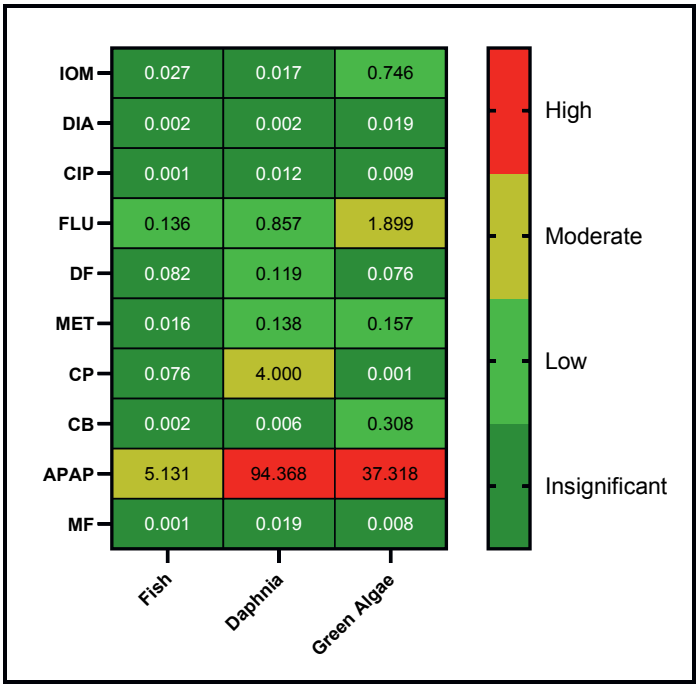

Fig. 5.1. RQ values for ten pharmaceuticals iomeprol (IOM), and diatrizoic acid (DIA), cipfrofloxacin (CIP), fluoxetine (FLU), diclofenac (DF), metoprolol (MET), cyclophosphamide (CP), carbamazepine (CB), acetaminophen (APAP), and metformin (MF) were presented in the following risk categories; insignificant ■ <0.1; low ■ 0.1-1.0; moderate ■ 1.0 - 10.0; high ■ >10.0.

5.3.2 Comparison of reported aquatic ecotoxicity data with ECOSAR computerised results

The high-risk levels we identified for APAP were compared with the data from an actual ecotoxicity study performed on Daphnia species (Sousa & Nunes, 2021). In their study, Daphnia species showed to be vulnerable to environmentally APAP concentrations in surface

water. Acute immobilisation was an evaluated end-point, with EC_{50} values of 3.18 and 30.5 mg/L observed for *Daphnia magna* and *Daphnia longispina*, respectively. Also, the effect on glutathione S-transferases (GSTs) levels was analysed, but no inhibitory of GTSs enzyme activity was found in *Daphnia longispina*, whereas in *Daphnia magna* 0.04 mg/L APAP inhibited GST activity. Comparing measured bioassay values with our calculated *in silico* LC_{50} value of 0.87 µg/L (**Table S3**), showed that the ECOSAR acute toxicity prediction is conservative specified (Sousa & Nunes, 2021). Establishing an RQ value for the bioassay measured effect concentrations (EC_{50} values 3.18 and 30.5 mg/L) indicated that untreated APAP (0.0821 mg/L) pose a high (RQ 25.5) to moderate (RQ 2.7) environmental risk for *Daphnia magna* and *Daphnia longispina*, respectively. Comparing these RQ values with the risk quotients we calculated for Daphnia (RQ 94.4), shows that the ECOSAR prediction of: 0.87 mg/L $PNEC_{acute}$ (Phenol amide; Daphnia LC_{50} 48h) results in similar risk classification. Even with the conservative assessment factor (1000) application, a consistently lower $PNEC_{acute}$ 0.87 µg/L is calculated, but for the RQ determination it is seen that the estimated risk is still in the same order of magnitude, as the RQ (25.5) for *Daphnia magna*.

A moderate risk level (RQ 4) was estimated for Daphnia when exposed to untreated CP ($3.4 \cdot 10^{-4}$ mg/L) which is not surprising, since experimental ecotoxicity studies demonstrated similar risk levels in aquatic organisms (Osawa et al., 2019; Česen, et al., 2016a; Česen et al., 2016b; Grzesiuk et al., 2018). In the bioassay study of Grzesiuk et al., (2018), 5-day old *Daphnia magna* clones were exposed to environmentally relevant CP concentration ($1.0 \cdot 10^{-5}$ mg/L). Disturbance of the proteome in *Daphnia magna* clones were detected, including a lower growth rate in CP-exposed groups compared to controls. No acute toxicity was measured in crustaceans *Cerio daphnia dubia* or *Thamnocephalus platyurus*, and also no toxicity was observed in green algae *Pseudokirchneriella subcapitata* exposed to aqueous relevant CP concentrations Česen et al., (2016a),. That acute toxicity was not observed in green algae is in line with our calculated insignificant ecotoxicity level (RQ < 0.1) (**Fig. 5.1**). It is to be expected that acute ecotoxicity from CP mainly occurs after metabolic activation. CP is a prodrug and needs biotransformation to produce genotoxic intermediates (Osawa et al., 2019). This effect is demonstrated in a bioassay when the supernatant of liver homogenates is used (S9 metabolism) leading to a positive finding in the Ames test that is attributed to carboxy-CP as the genotoxic intermediate (Česen et al., 2016b).

The moderate toxicity (RQ < 2) classification we found for FLU in green algae, is most likely explained by the low concentration ($1.5 \cdot 10^{-4}$ mg/L) found in HSW, since high ecotoxicity

effects are detectable in microalgae *Chlorella pyrenoidosa* after exposure to five FLU levels (0.1 up to 1 mg/L) in an experiment that was linked to an ECOSAR assessment (Xie et al., 2022). Comparison of experimental bioassay data with our *in silico* ecotoxicity predictions demonstrate comparable results for FLU, CP and APAP. Although a predictive tool is more conceptual in nature than actual bioassays, the ecotoxicity determination will depend on multiple factors. Influences that cause potential ecotoxicity of an organism are the concentration, exposure duration, molecular structure, metabolic bioactivation and species vulnerability.

5.3.3 Mixture toxicity prediction of untreated HSW

Based on the currently presented data, it should be noted that pharmaceuticals are not discharged into sewage water as individual substances but as complex mixtures with the presence of many other constituents such as detergents, disinfectants, metabolites, hormones and heavy metals (Emmanuel et al., 2005; Laquaz et al., 2018; Orias & Perrodin, 2013). Certain combinations of pharmaceuticals can cause potentiated effects (Osawa et al., 2019). It is therefore anticipated that ecotoxicity in a realistic scenario cannot solely derive from a single substance. Despite the incomplete information about the composition of HSW, we estimated the concentration addition toxicity for the 10 identified substances. The total MEC for 10 quantified pharmaceuticals (2.54 mg/L), is divided by the calculated effect concentration of the mixture (EC_{mix}) per species, 0.46 mg/L (fish), 0.025 mg/L (Daphnia) and 0.063 mg/L (green algae) (**Eq. 2**), see supplementary information **Table S5-7**. These EC_{mix} concentrations for untreated HSW indicate consecutively toxic RQ values; 5.5, 100.8 and 40.5 for fish, Daphnia, and green algae, respectively (**Fig. 5.2**).

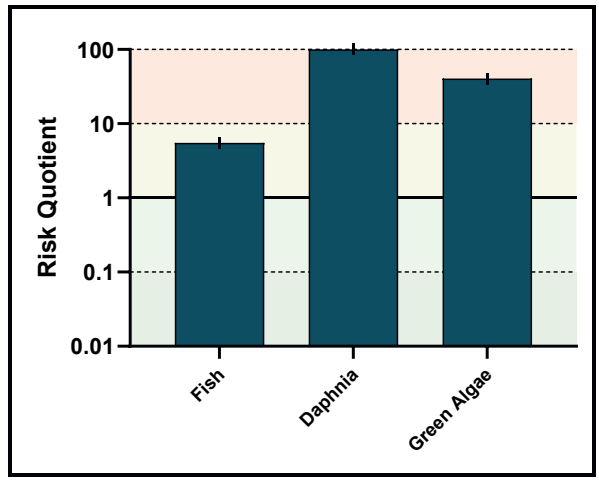

Fig. 5.2. Theoretically determined mixture toxicity of untreated HSW. RQs are calculated for fish, Daphnia and green algae species. The ecotoxicological risk is categorically visualised as: insignificant ■ <0.1; low ■ 0.1-1.0; moderate ■ 1.0 - 10.0; high ■ >10.0 (colours are translucent).

According to the determined RQs, the untreated pharmaceutical cocktail appears to pose a moderate environmental risk for fish and high ecotoxicity is anticipated for Daphnia and green algae (RQ > 10). Comparing these acute mixture effect concentrations (EC_{mix}) with the European Chemicals Bureau classifications, in support of EU-directive 93/67/EEC; 72h > toxicity EC_{50} levels are given as; *not classified* (>100 mg/L); *harmful* (10-100 mg/L); *toxic* (1-10 mg/L) and *very toxic* (<1 mg/L), it is seen that the calculated EC_{mix} values could be considered very toxic for all species. (Regulation (EC) No 1907/2006, 2006; 93/67/EEC, 1993; Xie et al., 2022).

Comparison of our calculated EC_{mix} values with actually measured ecotoxicity assays, demonstrate that moderate to high toxic classifications are a respectable prediction for Daphnia and green algae (Emmanuel et al., 2005; Laquaz et al., 2018; Orias & Perrodin, 2013). In the review study of Orias & Perrodin (2013), ecotoxicity was identified for mixture HSW effluents with strong PNEC values close to individual tested substance levels of 10^{-8} µg/L. It was noted from their 10 evaluated ecotoxicity studies that HSW effluent can produce notable variation in toxicity results between hospitals, exposed organisms (*Daphnia magna, Vibrio fisheri or Pseudokirchneriella subcapitata*), filtered or unfiltered effluent and wastewater taken during day or night periods demonstrating that the mortality EC_{50} (%)values range from 0.7 up to 90% (Orias & Perrodin, 2013). In the short term ecotoxicity study of Emmanuel et al. (2005), the algae growth and Daphnia mobility were tested after exposure to unfiltered HSW. It was found that there was acute toxicity for *Daphnia magna* species since the French threshold of 2 Toxic

units (TU) was exceeded with 43 and 58 TU respectively for 24h and 48h exposure data. It is however assumed in their study that high ammonium (NH_4^+) levels might cause the observed toxicity (Emmanuel et al., 2005). Nevertheless, similar results were found in the study of Laquaz et al. 2018, demonstrating elevated ecotoxicity levels in *Daphnia magna* and *Pseudokirchneriella subcapitata* exposed to untreated HSW compared to the exposure scenarios of urban wastewater, mixed hospital and urban wastewater and WWTP treated water (Laquaz et al., 2018). In this study the observed HSW ecotoxicity results were attributed to the complex composition having high concentrations of specific determined pharmaceuticals (acetaminophen, ketoprofen, ciprofloxacin, sulfamethoxazole and vancomycin), adsorbable organic halides (AOX), ammonium and non-ionic detergents (Laquaz et al., 2018).

That our computed mixture toxicity indicates a higher acute ecotoxic risk classification than the individual calculated RQ values is further explained by the assumption of additivity. Due to the small fractions of potential toxic pharmaceuticals present in HSW, the effects derived for FLU, CP and APAP are added up in combination with the other low and insignificant ecotoxic pharmaceutical fractions. Compared to the previously assessed separate RQ values, it is seen that with our *in silico* mixture prediction Daphnia is also determined as the most vulnerable species, *Daphnia* > *green algae* > *fish*. With the concentration (2.54 mg/L) the assumption of additivity for the 10 pharmaceuticals (IOM, DIA, CIP, FLU, DF, MET, CP, CB, APAP and MF) in Daphnia cause the highest risk. This is comparable with the overall susceptibility order obtained for 2986 pharmaceuticals by Sanderson et al. (2004), where the susceptibility was ranked as *Daphnia* > *fish* > *green algae* (Kar et al., 2020; Sanderson et al., 2004). In their study, using ECOSAR, it was found that the most prominent predicted pharmaceutical classes are anti-anxiety medication, antipsychotics, cardiovascular, corticosteroids, gastrointestinal, hypnotics, sedatives and thyroid pharmaceuticals (Kar et al., 2020; Sanderson et al., 2004). Next to the differences between individual and mixture toxicity, the mode-of-action of a specific pharmaceutical in fish will be different from Daphnia or green algae (Kar et al., 2020; Sangion & Gramatica, 2016). Although fish is at a higher trophic level, Daphnids are predicted to be the most vulnerable species to aquatic pollutants. Within the hydrosphere ecosystem, Daphnids form an important link between microbials, algae and higher trophic levels, making this species a valuable bioindicator in toxicity testing (Tiwari et al., 2021). A similar observation was done in a quantitative activity-activity relationship study, where the interspecies correlation between *Daphnia Magna* and fish *Pimephales promelas* and *Oncorhynchus mykiss* was demonstrated, indicating that Daphnia toxicity could serve as proxy for fish toxicity (Kar et al., 2020; Sangion

& Gramatica, 2016). When using the concentration addition assumption, the exact mode of action for each compound is not taken into account, resulting in a selection bias with respect to toxicophoric structures that might inhibit or stimulate the organisms bioactivation.

5.3.4 Predicted ecotoxicity of oxidative treated HSW

5.3.4.1 Thermal plasma treatment

In the case of real-life sewage water samples, such as HSW, multiple other unidentified contaminants may be present next to the detected pharmaceuticals. Compounds in the matrix that contribute to overall wastewater toxicity are, hormones, metabolites, endotoxins from bacteria, disinfectants, non-ionic detergents, adsorbable organic halides (AOX) and ammonium (Ajo et al., 2018; Escher et al., 2011; Laquaz et al., 2018; Orias & Perrodin, 2013). An example of a bacterium endotoxin contributing to the wastewater toxicity might be lipopolysaccharide (LPS). In our previous study it was found that LPS affects the HeLa cell viability (>50%) when present at high concentrations (10 – 1000 µg/L) (Graumans et al., 2022). Immediate cell death in HeLa-cells was found when exposed to untreated HSW, this effect could be reversed by thermal plasma and UV-C/H_2O_2 oxidation treatment for prolonged treatment times (Graumans et al., 2022). In this *in silico* approximation, potentially formed intermediates were selected for each of our 10 reference pharmaceuticals. The amount of formed TP was extrapolated based on individual conversion levels measured ($\bar{R}$ %) after 30 min of plasma treatment in HSW (**Fig. S2**). Without the exact information on degradation pathways and which TPs are formed, we simplified this *in silico* approach by selecting only a single TP. With oxidative treatment up to 120 min it is expected that the formed TPs will be further degraded into smaller aliphatic compounds (Banaschik et al., 2018; Hoeben et al., 2000; Isarain-Chávez et al., 2011; Qutob et al., 2022; Tisler et al., 2019; Yang et al., 2018). The continuous introduction of reactive species, such as hydroxyl radicals can result in cleavage and ring opening reactions producing small aliphatic, aldehyde and carboxylic acid structures (Banaschik et al., 2018; Hoeben et al., 2000; Vogna et al., 2002), see supplementary data **Table S8**. With this QSAR approach, individual and mixture RQs were calculated for 20 and 30 substances after 30 and 120 min oxidative treatment, respectively (**Fig. 5.3**).

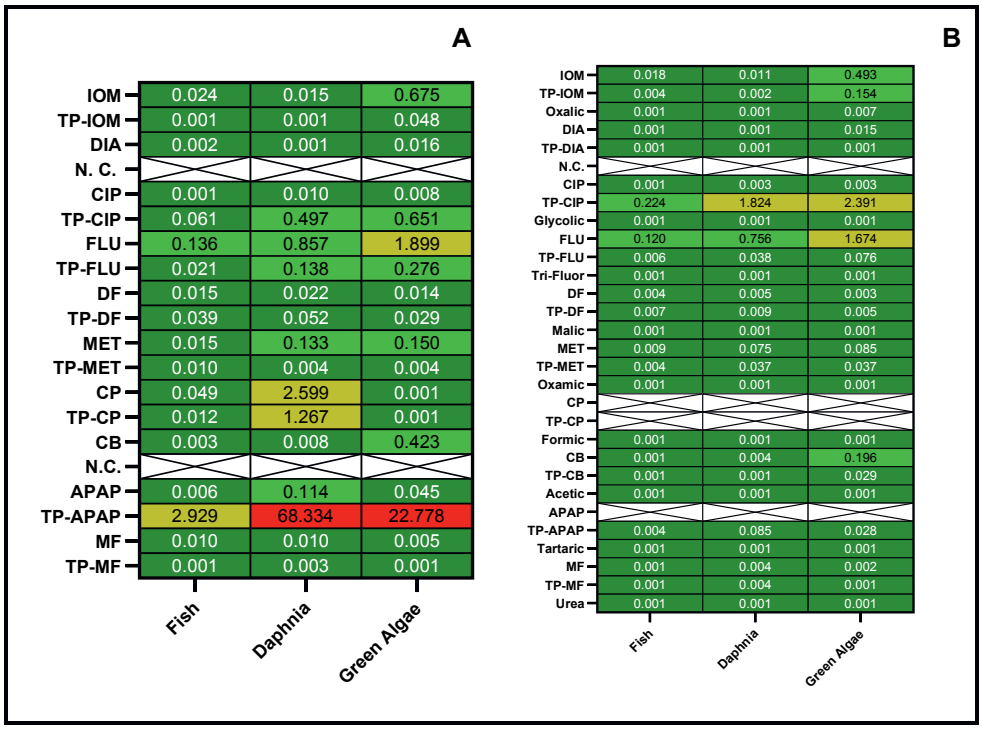

Fig. 5.3. RQ values for pharmaceuticals and their potentially formed transformation products (TP) classified in four categories: insignificant ■ <0.1; low ■ 0.1-1.0; moderate ■ 1.0 - 10.0; high ■ >10.0. Complete and no conversion (N.C.) levels are depicted as; ☒. Thermal plasma treatment was applied in HSW for 30 min (**A**) and 120 min (**B**). Remaining parental concentrations and produced TP fractions were used to calculate the RQs.

Compared to untreated HSW, the majority of the individual RQ values for each pristine pharmaceutical is decreased following thermal plasma treatment. Reduced RQ values represent lower acute ecotoxicity levels, which is in line with our previous HeLa-cell cytotoxicity assay result (Graumans et al., 2022). With the application of 30 min plasma oxidative treatment DF, CP, APAP and MF were rapidly degraded. The most prominent result is seen for APAP, showing that the high predicted risk (RQ: 94) was reduced to a low risk (RQ: 0.11), for Daphnia (**Fig. 5.3A**). Prolonged plasma activation (120 min) led to in the oxidation of all initial pharmaceutical components, resulting in at least one TP and an aliphatic structure that contributed to the cocktail of compounds used for modelling (**Fig. 5.3B**). With plasma oxidation, APAP is rapidly degraded within 30 min (**Fig. S2**). However, when APAP's potential 3-hydroxyacetaminophen oxidative TP is formed, a high ecotoxicological risk (RQ >10) is predicted. The anticipated APAP-TP is a catechol class compound (synonym 4-Acetylaminocatechol), formed during hydroxyl (•OH) oxidation of the aromatic structure (Vogna et al., 2002; Zhang et al., 2017). The anticipated risk of this intermediate is derived

from its chemical reactivity and also oxygen depleting property in aqueous environments (**Fig. S1**; Hoeben et al., 2000; Schweigert et al., 2001).

With prolonged plasma treatment, it is assumed that formed TPs will further degrade into smaller components. Oxidative pharmaceutical abatement kinetics is a complex process that follows multiple degradation pathways (Banaschik et al., 2018; Nowak et al., 2020; Zhang et al., 2017). Primarily electron donating substitutions (lone pairs of electrons on an atom bonded to a ring), unsaturated double bonds and aromatic ring systems are sensitive to electrophilic oxidising agents ($^{\bullet}OH$). With the continuous introduction of reactive species, degradation of intermediates such as catechols and quinones will eventually lead to aldehyde and carboxylic acid degradation products (Hoeben et al., 2000; Vogna et al., 2002). Regarding plasma discharge in air-over-water, it is important to mention that also nitrogen species are involved in the degradation process. Despite that for thermal plasma oxidation the major pharmaceutical degradation pathway will elapse via hydroxyl radical attack, reactive nitrogen species (RNS) might initiate nitration and nitrosation reactions under specific (pH < 6) conditions (Rayaroth et al., 2022). With the incorporation of the electrophilic nitronium ion (NO_2^+), nitro-TPs can be formed. Similar chemical reactions occur during biodegradation where nitrifying bacteria produce nitrated TPs, such as 3-nitro-APAP or DF-nitro-derivate. Microbial nitration of an aromatic ring produces nitro-derivates, see **Fig. 5.4** (Pérez & Barceló, 2008; Vieno & Sillanpää, 2014). It is expected that with the introduction of RNS similar chemical reactions occur under nitrogen favourable conditions. In a review paper of Rayaroth et al. (2022), it was stated that distinct AOPs produce RNS; $NO_3^{\bullet}$, $NO_2^{\bullet}$, $NO^{\bullet}$ and $ONOO^-$. These similar oxidative activation products are formed during thermal plasma treatment, generating nitric oxide (NO), nitrogen dioxide (NO_2), nitrous acid (HNO_2), nitric acid (HNO_3) and transient reactive oxygen and nitrogen species ($H_aN_bO_c$) in plasma activated water (Hoeben et al., 2019). Next to the formation of RNS by a plasma discharge in the atmosphere, secondary radical reactions, or degradation of constituents present in the treated matrix can result in the production of nitrogen containing compounds (Rayaroth et al., 2022). RNS are identified as species that could generate toxic nitro-containing TPs. With our ECOSAR prediction (**Table S9**) nitro-DF showed minimal acute environmental risk (RQ <1 for fish, Daphnia and Green algae), but contrary the RQ of 3-nitro-APAP is higher for fish and Daphnia species compared to 3-hydroxyacetaminophen (RQs of 3.7 for fish, 240.2 for Daphnia and 4.1 for green algae).

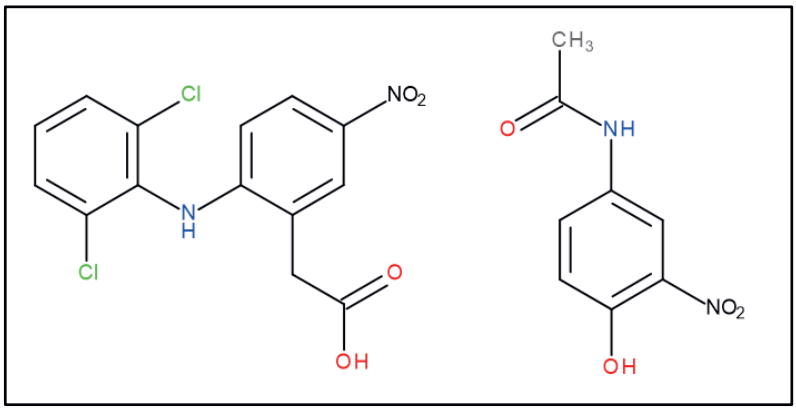

Fig. 5.4. Possible nitration reactions for DF and APAP, showing a $NO_2^{\bullet}$ attack on the aromatic ring.

5.3.4.2 UV-C/H_2O_2 treatment

According to the calculated UV-C/H_2O_2 risk levels compared to plasma treatment, the resulting mixture toxicity is more scattered, between the declined pharmaceutical concentration and the selected TPs (**Fig. 5.5)**. To calculate the RQ values for the TPs formed upon HSW treatment with UV-C/H_2O_2, the same intermediates as for plasma treatment were selected. IOM and DIA were both completely degraded within 60 min, TPs arose directly after abatement of the original structure. Despite that these compounds were present in high concentrations (2387.3 and 10.1 µg/L), minimal ecotoxicity levels were predicted for our selected IOM-TP and DIA-TP intermediates (**Table S8**). Minimal toxicity for these intermediates were predicted due to the hydrophilic structures, making the TPs less effective in penetrating cell membranes. The parental contrast agents diatrizoic acid and iopamidol, iohexol and iopromide are considered as non-toxic, however certain oxidative produced TPs are described as ambiguous after *in silico* model predictions (Nowak et al., 2020). The rapid decline of the original IOM and DIA structure with UV-C/H_2O_2 treatment may be explained by iodine substituted groups lost due to UV irradiation. Due to the high reactivity of $^{\bullet}OH$ radicals to the aromatic structure, the iodine substitutes are replaced by hydroxyl groups. These selected IOM and DIA intermediates were previously reported oxidation (Nowak et al., 2020). However, incomplete oxidative degradation and biodegradation can lead to mutagenic DIA intermediates by loss of the aliphatic side chain (Nowak et al., 2020). For substances such as CP, CB, APAP and MF, minimal abatement occurred within 30 min oxidative treatment. Prolonged UV-C/H_2O_2 oxidation resulted in degradation of these substances, but in contrast to thermal plasma treatment the abatement kinetics elapse slower. This resulted in lower concentrations of TPs, and subsequently also lower formation of aliphatic structures. The incomplete APAP removal results in minimal decrease of toxicity. Less efficient degradation with UV-C/H_2O_2 treatment is attributed to

unknown organic constituents present in the HSW matrix, inhibiting the transfer of UV irradiation and interacting with •OH radicals, by formation of secondary radicals. The slower oxidative degradation rate influences the computerised mixture ecotoxicity levels. Although not all pharmaceuticals are completely degraded, the individual acute ecotoxicity levels have declined.

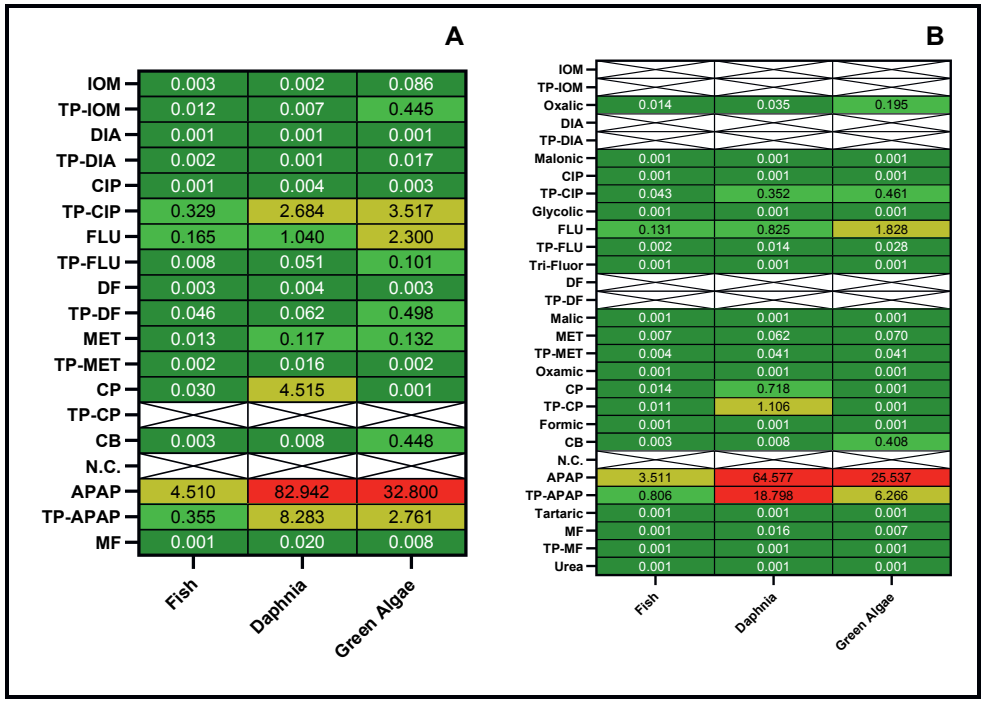

Fig. 5.5. RQ values for ten pharmaceuticals in HSW, presented in four categories; insignificant ■ <0.1; low ■ 0.1-1.0; moderate ■ 1.0 - 10.0; high ■ >10.0. UV-C/H_2O_2 treatment for 30 min **(A)** and 120 min **(B).** Complete and no conversion (N.C.) levels are depicted as; ☒. MEC values were determined based on concentrations before and after the treatment. PNEC values were based on ECOSAR predictions.

Table 5.1. Determined mixture ecotoxicity values after oxidative treatment

Species	**Untreated HSW** (RQ)	**Thermal plasma** 30 min (RQ)	**Thermal plasma** 120 min (RQ)	**UV-C/H_2O_2** 30 min (RQ)	**UV-C/H_2O_2** 120 min (RQ)
Fish	5.5	3.3	0.4	5.5	4.6
Daphnia	100.8	74.1	2.9	99.8	86.6
Green algae	40.5	27.4	5.2	43.1	34.8

For plasma application, it is expected that the potentially formed intermediates were not the end products. Further TP degradation is expected with extended treatment times due the continuous introduction of new RONS. In contrast, without additional H_2O_2, the UV-C/H_2O_2 application is

presumably exhaustive due to shortage of •OH radicals. Lower availability of •OH radicals during pharmaceutical oxidation will cause degradation pathways to be terminated. When harmful TPs are formed, next to partially degraded original pharmaceuticals it is predicted that ecotoxic effects can cause potentiated effects. This effect is calculated with the EC_{mix}, showing minimally decreased RQ values after 30 min and 120 min UV-C/H_2O_2 application (**Table 5.1**).

In a binary mixture analysis for diclofenac combined with sulfamethoxazole, it was found that the concentration addition approach underestimates the experimental toxicity on *Daphnia magna* and *Lemna minor* (aquatic freshwater plant) (Drzymała & Kalka, 2020). Both compounds have a distinct mode of action, where sulfamethoxazole (antibiotic) showed minimal toxic effects and diclofenac (NSAID) average toxicity. The binary mixture posed a synergistic effect, indicating that the combination of other toxophores could initiate, inhibit, or potentiate similar effects. Here a mixture of 10 pharmaceuticals and its 10 potentially formed intermediates were used to estimate the environmental risk. In a realistic scenario it is assumed that microbial degradation, sorption and photolysis will take place at a WWTP (Drzymała & Kalka, 2020). Aquatic species in a realistic setting are primarily exposed to substances released from WWTPs, land-runoff or accidental spill. In the case of old sewer systems, it can occur that wastewater is directly discharged into surface waters (House of Commons Environmental Audit Committee, 2022b). The aquatic concentration and composition of substances will therefore deviate continuously due to environmental emission, sorption processes with TOC, potential photolysis, flow and tidal effects (Sanderson et al., 2004).

5.3.5 Strengths and limitations of the study

A major strength of this study is the use of measured concentration data to predict the potential environmental risk supported by QSAR modelling. *In silico* effect concentrations were predictions of using ECOSAR software, demonstrating that the acute risk could be indicatively determined for 10 quantified pharmaceuticals in untreated HSW. The predictions were comparable with published results from bioassays for APAP and CP. To assess the effect of oxidatively treated HSW, degradation intermediates were selected according to literature studies who applied either UV-C/H_2O_2, non-thermal plasma degradation or another AOP using (hydroxyl) radical oxidation.

An important limitation of this study is the incomplete identification of the mixture of pharmaceutical residues in HSW. It is undisputable that also other components contribute to this complex mixture. In addition, there is a great uncertainty regarding the infinite complexity of oxidative transformation products. Although we have selected degradation intermediates

formed by similar advanced oxidation processes for our modelling, it is important to mention that the chemical abatement kinetics differ between studies according to matrix composition, initial pharmaceutical concentrations and AOP conditions applied. Without more precise knowledge of the pharmaceutical oxidative degradation pathways, it is difficult to obtain more accurate RQs. With the *in silico* additivity assumption for our mixture composition, it is expected that only a crude approximation of the risk can be presented. Nonetheless, this study demonstrates the synergies of modelling and experimental data in toxicity testing. The interaction of actual measured data as reliable input parameter and the rapidly computed estimate could serve as an early-warning system by simulations of wastewater toxicity.

5.4 Conclusion

This study demonstrates that *in silico* environmental risk assessment is a rapid method to obtain indicative (eco)toxicity predictions of pharmaceutical residuals in wastewater that, depending on the purpose, may need confirmation from experimental testing. The usage of predictive tools, such as ECOSAR combined with measured data, provides estimated effect concentrations for three distinct trophic levels, fish, Daphnia and green algae. The usage of measured data provides complementary toxicity information, showing that untreated HSW contains environmentally unwanted pharmaceutical levels. The prediction and extrapolation of oxidative treated matrices without identification and quantification of actually produced transformation products introduces substantial uncertainty. Despite this high degree of uncertainty, the estimated data are consistent with previous published findings from applications of advanced oxidation processes. Based on the extrapolated oxidation results it is expected that with the application of oxidative treatment techniques, such as thermal plasma and UV-C/H_2O_2 application, the (eco)toxicity classifications of the original products can be reduced. Having sufficiently measured parameters, *in silico* ecotoxicity estimation could serve as a valuable screening tool in risk assessment. ECOSAR software and other predictive modelling applications could complement toxicity assays in the further development of AOP technologies.

Declaration of competing interest

None.

Acknowledgement

This work was funded by the INTERREG Deutschland-Nederland program [grant number 142118]. The authors would like to thank Vitalfluid for providing their PAW lab unit and UV-C source. We also would like to thank R. Anzion, M. van Dael and H. van Hove for their valuable technical input, help and advice during the laboratory experiments.

Literature

Abbas, A., Schneider, I., Bollmann, A., Funke, J., Oehlmann, J., Prasse, C., Schulte-Oehlmann, U., Seitz, W., Ternes, T., Weber, M., Wesely, H., & Wagner, M. (2019). What you extract is what you see: Optimising the preparation of water and wastewater samples for in vitro bioassays. *Water Research*, *152*, 47–60. https://doi.org/10.1016/j.watres.2018.12.049

Ajo, P., Preis, S., Vornamo, T., Mänttäri, M., Kallioinen, M., & Louhi-Kultanen, M. (2018). Hospital wastewater treatment with pilot-scale pulsed corona discharge for removal of pharmaceutical residues. *Journal of Environmental Chemical Engineering*, *6*(2), 1569–1577. https://doi.org/10.1016/j.jece.2018.02.007

Back, J. O., Obholzer, T., Winkler, K., Jabornig, S., & Rupprich, M. (2018). Combining ultrafiltration and non-thermal plasma for low energy degradation of pharmaceuticals from conventionally treated wastewater. *Journal of Environmental Chemical Engineering*, *6*(6), 7377–7385. https://doi.org/10.1016/j.jece.2018.07.047

Backhaus, T., & Faust, M. (2012). Predictive Environmental Risk Assessment of Chemical Mixtures: A Conceptual Framework. *Environmental Science & Technology*, *46*(5), 2564–2573. https://doi.org/10.1021/es2034125

Banaschik, R., Jablonowski, H., Bednarski, P. J., & Kolb, J. F. (2018). Degradation and intermediates of diclofenac as instructive example for decomposition of recalcitrant pharmaceuticals by hydroxyl radicals generated with pulsed corona plasma in water. *Journal of Hazardous Materials*, *342*, 651–660. https://doi.org/10.1016/j.jhazmat.2017.08.058

Česen, M., Eleršek, T., Novak, M., Žegura, B., Kosjek, T., Filipič, M., & Heath, E. (2016a). Ecotoxicity and genotoxicity of cyclophosphamide, ifosfamide, their metabolites/transformation products and their mixtures. *Environmental Pollution*, *210*, 192–201. https://doi.org/10.1016/j.envpol.2015.12.017

Česen, M., Kosjek, T., Busetti, F., Kompare, B., & Heath, E. (2016b). Human metabolites and transformation products of cyclophosphamide and ifosfamide: analysis, occurrence and formation during abiotic treatments. *Environmental Science and Pollution Research*, *23*(11), 11209–11223. https://doi.org/10.1007/s11356-016-6321-1

De Baat, M. L., Van der Oost, R., Van der Lee, G. H., Wieringa, N., Hamers, T., Verdonschot, P. F. M., De Voogt, P., & Kraak, M. H. S. (2020). Advancements in effect-based surface water quality assessment. *Water Research*, *183*, 116017. https://doi.org/10.1016/j.watres.2020.116017

Driezum, van I.H., Beekman J., Loon, van A., Leerdam, van R.C., Wuijts S., Rutgers M., Boekhold S., Zijp M.C. (2020). *Staat drinkwaterbronnen*.

Drzewicz, P., Drobniewska, A., Sikorska, K., & Nałęcz-Jawecki, G. (2019). Analytical and ecotoxicological studies on degradation of fluoxetine and fluvoxamine by potassium ferrate. *Environmental Technology*, *40*(25), 3265–3275. https://doi.org/10.1080/09593330.2018.1468488

Drzymała, J., & Kalka, J. (2020). Ecotoxic interactions between pharmaceuticals in mixtures: Diclofenac and sulfamethoxazole. *Chemosphere*, *259*, 127407. https://doi.org/10.1016/j.chemosphere.2020.127407

Egli, M., Rapp-Wright, H., Oloyede, O., Francis, W., Preston-Allen, R., Friedman, S., Woodward, G., Piel, F. B., & Barron, L. P. (2023). A One-Health environmental risk assessment of contaminants of emerging concern in London's waterways throughout the SARS-CoV-2 pandemic. *Environment International*, *180*, 108210. https://doi.org/10.1016/j.envint.2023.108210

Emmanuel, E., Perrodin, Y., Keck, G., Blanchard, J.-M., & Vermande, P. (2005). Ecotoxicological risk assessment of hospital wastewater: a proposed framework for raw effluents discharging into urban sewer network. *Journal of Hazardous Materials*, *117*(1), 1–11. https://doi.org/10.1016/j.jhazmat.2004.08.032

Escher, B. I., Baumgartner, R., Koller, M., Treyer, K., Lienert, J., & McArdell, C. S. (2011). Environmental toxicology and risk assessment of pharmaceuticals from hospital wastewater. *Water Research*, *45*(1), 75–92. https://doi.org/10.1016/j.watres.2010.08.019

Escher, B. I., Stapleton, H. M., & Schymanski, E. L. (2020). Tracking complex mixtures of chemicals in our changing environment. *Science*, *367*(6476), 388–392. https://doi.org/10.1126/science.aay6636

Graumans, M. H. F., Hoeben, W. F. L. M., Russel, F. G. M., & Scheepers, P. T. J. (2020). Oxidative degradation of cyclophosphamide using thermal plasma activation and UV-H_2O_2 treatment in tap water. *Environmental Research*, *182*. https://doi.org/10.1016/j.envres.2019.109046

Graumans, M. H. F., Hoeben, W. F. L. M., van Dael, M. F. P., Anzion, R. B. M., Russel, F. G. M., & Scheepers, P. T. J. (2021). Thermal plasma activation and UV-H_2O_2 oxidative degradation of pharmaceutical residues. *Environmental Research*, *195*. https://doi.org/10.1016/j.envres.2021.110884

Graumans, M. H. F., van Hove, H., Schirris, T., Hoeben, W. F. L. M., van Dael, M. F. P., Anzion, R. B. M., Russel, F. G. M., & Scheepers, P. T. J. (2022). Determination of cytotoxicity following oxidative treatment of pharmaceutical residues in wastewater. *Chemosphere*, *303*. https://doi.org/10.1016/j.chemosphere.2022.135022

Grzesiuk, M., Mielecki, D., Pilżys, T., Garbicz, D., Marcinkowski, M., & Grzesiuk, E. (2018). How cyclophosphamide at environmentally relevant concentration influences Daphnia magna life history and its proteome. *PLOS ONE*, *13*(4), e0195366. https://doi.org/10.1371/journal.pone.0195366

Hoeben, W. F. L. M., van Ooij, P. P., Schram, D. C., Huiskamp, T., Pemen, A. J. M., & Lukeš, P. (2019). On the Possibilities of Straightforward Characterization of Plasma Activated Water. *Plasma Chemistry and Plasma Processing*, *39*(3), 597–626. https://doi.org/10.1007/s11090-019-09976-7

Hoeben, W. F. L. M., Veldhuizen, E. M. van, Rutgers, W. R., Cramers, C. A. M. G., & Kroesen, G. M. W. (2000). The degradation of aqueous phenol solutions by pulsed positive corona discharges. *Plasma Sources Science and Technology*, *9*(3), 361–369. https://doi.org/10.1088/0963-0252/9/3/315

Hollman, J., Dominic, J. A., & Achari, G. (2020). Degradation of pharmaceutical mixtures in aqueous solutions using UV/peracetic acid process: Kinetics, degradation pathways and comparison with UV/H2O2. *Chemosphere*, *248*, 125911. https://doi.org/10.1016/j.chemosphere.2020.125911

House of Commons Environmental Audit Committee. (2022). *Water quality in rivers*.

Humayun, S., Hayyan, M., Alias, Y., & Hayyan, A. (2021). Oxidative degradation of acetaminophen using superoxide ion generated in ionic liquid/aprotic solvent binary system. *Separation and Purification Technology*, *270*, 118730. https://doi.org/10.1016/j.seppur.2021.118730

Isarain-Chávez, E., Rodríguez, R. M., Cabot, P. L., Centellas, F., Arias, C., Garrido, J. A., & Brillas, E. (2011). Degradation of pharmaceutical beta-blockers by electrochemical advanced oxidation processes using a flow plant with a solar compound parabolic collector. *Water Research*, *45*(14), 4119–4130. https://doi.org/10.1016/j.watres.2011.05.026

Jaén-Gil, A., Buttiglieri, G., Benito, A., Gonzalez-Olmos, R., Barceló, D., & Rodríguez-Mozaz, S. (2019). Metoprolol and metoprolol acid degradation in UV/H2O2 treated wastewaters: An integrated screening approach for the identification of hazardous transformation products. *Journal of Hazardous Materials*, *380*, 120851. https://doi.org/10.1016/j.jhazmat.2019.120851

Kar, S., Sanderson, H., Roy, K., Benfenati, E., & Leszczynski, J. (2020). Ecotoxicological assessment of pharmaceuticals and personal care products using predictive toxicology approaches. *Green Chemistry*, *22*(5), 1458–1516. https://doi.org/10.1039/C9GC03265G

Khan, K., Baderna, D., Cappelli, C., Toma, C., Lombardo, A., Roy, K., & Benfenati, E. (2019). Ecotoxicological QSAR modeling of organic compounds against fish: Application of fragment based descriptors in feature analysis. *Aquatic Toxicology*, *212*, 162–174. https://doi.org/10.1016/j.aquatox.2019.05.011

Laquaz, M., Dagot, C., Bazin, C., Bastide, T., Gaschet, M., Ploy, M.-C., & Perrodin, Y. (2018). Ecotoxicity and antibiotic resistance of a mixture of hospital and urban sewage in a wastewater treatment plant. *Environmental Science and Pollution Research*, *25*(10), 9243–9253. https://doi.org/10.1007/s11356-017-9957-6

Loewe, S., & Muischnek, H. (1926). Über Kombinationswirkungen. *Archiv Für Experimentelle Pathologie Und Pharmakologie*, *114*(5–6), 313–326. https://doi.org/10.1007/BF01952257

Mayo-Bean, K., Moran-Bruce, K., Nabholz, J.V., Meylan, W.M., Howard, P.H. (2012). *OPERATION MANUAL for the ECOlogical Structure-Activity Relationship Model (ECOSAR)*.

Moermond, C.T.A., Montforts, M.H.M.M., Roex E.W.M., Venhuis BJ (2020). *Pharmaceutical residues and water quality: an update*.

Nowak, A., Pacek, G., & Mrozik, A. (2020). Transformation and ecotoxicological effects of iodinated X-ray contrast media. *Reviews in Environmental Science and Bio/Technology*, *19*(2), 337–354. https://doi.org/10.1007/s11157-020-09534-0

Orias, F., & Perrodin, Y. (2013). Characterisation of the ecotoxicity of hospital effluents: A review. *Science of The Total Environment*, *454–455*, 250–276. https://doi.org/10.1016/j.scitotenv.2013.02.064

Ortiz de García, S. A., Pinto Pinto, G., García-Encina, P. A., & Irusta-Mata, R. (2014). Ecotoxicity and environmental risk assessment of pharmaceuticals and personal care products in aquatic environments and wastewater treatment plants. *Ecotoxicology*, *23*(8), 1517–1533. https://doi.org/10.1007/s10646-014-1293-8

Osawa, A, R., T. Barrocas, B., C. Monteiro, O., Oliveira, M. C., & Florêncio, M. H. (2019). Photocatalytic degradation of cyclophosphamide and ifosfamide: Effects of wastewater matrix, transformation products and in silico toxicity prediction. *Science of The Total Environment*, *692*, 503–510. https://doi.org/10.1016/j.scitotenv.2019.07.247

Peak, B. M., Braund, R., Tong, A. Y. C., & Tremblay, L. A. (2016). *The Life-cylce of pharmaceuticals in the environment*. Woodhead Publishin, Elsevier.

Pérez, S., & Barceló, D. (2008). First Evidence for Occurrence of Hydroxylated Human Metabolites of Diclofenac and Aceclofenac in Wastewater Using QqLIT-MS and QqTOF-MS. *Analytical Chemistry*, *80*(21), 8135–8145. https://doi.org/10.1021/ac801167w

Qutob, M., Hussein, M. A., Alamry, K. A., & Rafatullah, M. (2022). A review on the degradation of acetaminophen by advanced oxidation process: pathway, by-products, biotoxicity, and density functional theory calculation. *RSC Advances*, *12*(29), 18373–18396. https://doi.org/10.1039/D2RA02469A

Rayaroth, M. P., Aravindakumar, C. T., Shah, N. S., & Boczkaj, G. (2022). Advanced oxidation processes (AOPs) based wastewater treatment - unexpected nitration side reactions - a serious environmental issue: A review. *Chemical Engineering Journal*, *430*, 133002. https://doi.org/10.1016/j.cej.2021.133002

Reuschenbach, P., Silvani, M., Dammann, M., Warnecke, D., & Knacker, T. (2008). ECOSAR model performance with a large test set of industrial chemicals. *Chemosphere*, *71*(10), 1986–1995. https://doi.org/10.1016/j.chemosphere.2007.12.006

Sanderson, H. (2003). Probabilistic hazard assessment of environmentally occurring pharmaceuticals toxicity to fish, daphnids and algae by ECOSAR screening. *Toxicology Letters*, *144*(3), 383–395. https://doi.org/10.1016/S0378-4274(03)00257-1

Sanderson, H., Johnson, D. J., Reitsma, T., Brain, R. A., Wilson, C. J., & Solomon, K. R. (2004). Ranking and prioritization of environmental risks of pharmaceuticals in surface waters. *Regulatory Toxicology and Pharmacology*, *39*(2), 158–183. https://doi.org/10.1016/j.yrtph.2003.12.006

Sangion, A., & Gramatica, P. (2016). Hazard of pharmaceuticals for aquatic environment: Prioritization by structural approaches and prediction of ecotoxicity. *Environment International*, *95*, 131–143. https://doi.org/10.1016/j.envint.2016.08.008

Schweigert, N., Zehnder, A. J. B., & Eggen, R. I. L. (2001). Chemical properties of catechols and their molecular modes of toxic action in cells, from microorganisms to mammals. Minireview. *Environmental Microbiology*, *3*(2), 81–91. https://doi.org/10.1046/j.1462-2920.2001.00176.x

Sharma, A., Ahmad, J., & Flora, S. J. S. (2018). Application of advanced oxidation processes and toxicity assessment of transformation products. *Environmental Research*, *167*, 223–233. https://doi.org/10.1016/j.envres.2018.07.010

Shi, J., Jiang, J., Chen, Q., Wang, L., Nian, K., & Long, T. (2023). Production of higher toxic intermediates of organic pollutants during chemical oxidation processes: A review. *Arabian Journal of Chemistry*, *16*(7), 104856. https://doi.org/10.1016/j.arabjc.2023.104856

Sousa, A. P., & Nunes, B. (2021). Dangerous connections: biochemical and behavioral traits in Daphnia magna and Daphnia longispina exposed to ecologically relevant amounts of paracetamol. *Environmental Science and Pollution Research*, *28*(29), 38792–38808. https://doi.org/10.1007/s11356-021-13200-5

Straub, J. O., Caldwell, D. J., Davidson, T., D'Aco, V., Kappler, K., Robinson, P. F., Simon-Hettich, B., & Tell, J. (2019). Environmental risk assessment of metformin and its transformation product guanylurea. I. Environmental fate. *Chemosphere*, *216*, 844–854. https://doi.org/10.1016/j.chemosphere.2018.10.036

Tay, K. S., & Madehi, N. (2015). Ozonation of ofloxacin in water: By-products, degradation pathway and ecotoxicity assessment. *Science of The Total Environment*, *520*, 23–31. https://doi.org/10.1016/j.scitotenv.2015.03.033

Test No. 201: Alga, Growth Inhibition Test. (2006). OECD Publishing. https://doi.org/10.1787/9789264069923-en

Test No. 202: Daphnia sp. Acute Immobilisation Test. (2004). OECD. https://doi.org/10.1787/9789264069947-en

Test No. 203: Fish, Acute Toxicity Test. (2019). OECD. https://doi.org/10.1787/9789264069961-en

Regulation (EC) No 1907/2006, Pub. L. No. 1907/2006 (2006).

93/67/EEC, Pub. L. No. 93/67/EEC, Commission Directive 93/67/EEC (1993).

2000/60/EG, DIRECTIVE 2000/60/EC (2000).

Tisler, S., Zindler, F., Freeling, F., Nödler, K., Toelgyesi, L., Braunbeck, T., & Zwiener, C. (2019). Transformation Products of Fluoxetine Formed by Photodegradation in Water and Biodegradation in Zebrafish Embryos (*Danio rerio*). *Environmental Science & Technology*, *53*(13), 7400–7409. https://doi.org/10.1021/acs.est.9b00789

Tisler, S., & Zwiener, C. (2019). Aerobic and anaerobic formation and biodegradation of guanyl urea and other transformation products of metformin. *Water Research*, *149*, 130–135. https://doi.org/10.1016/j.watres.2018.11.001

Tiwari, A., Dhanker, R., Saxena, A., Goyal, S., Melchor-Martínez, E. M., Iqbal, H. M. N., & Parra-Saldívar, R. (2021). Toxicity evaluation of personal care and household products as silent killers on the survival of Daphnia magna. *Case Studies in Chemical and Environmental Engineering*, *4*, 100124. https://doi.org/10.1016/j.cscee.2021.100124

Vasiliadou, I. A., Molina, R., Martinez, F., Melero, J. A., Stathopoulou, P. M., & Tsiamis, G. (2018). Toxicity assessment of pharmaceutical compounds on mixed culture from activated sludge using respirometric technique: The role of microbial community structure. *Science of The Total Environment*, *630*, 809–819. https://doi.org/10.1016/j.scitotenv.2018.02.095

Vieno, N., & Sillanpää, M. (2014). Fate of diclofenac in municipal wastewater treatment plant — A review. *Environment International*, *69*, 28–39. https://doi.org/10.1016/j.envint.2014.03.021

Vogna, D., Marotta, R., Napolitano, A., & d'Ischia, M. (2002). Advanced Oxidation Chemistry of Paracetamol. UV/H $_2$ O $_2$ -Induced Hydroxylation/Degradation Pathways and ^{15} N-Aided Inventory of Nitrogenous Breakdown Products. *The Journal of Organic Chemistry*, *67*(17), 6143–6151. https://doi.org/10.1021/jo025604v

Walker, C.H., Sibly, R.M., Hopkin, S.P., Peakall, D.B. (2012). *Principles of Ecotoxicology* (4th ed.). CRC Press.

Wang, J., & Wang, S. (2021). Toxicity changes of wastewater during various advanced oxidation processes treatment: An overview. *Journal of Cleaner Production*, *315*, 128202. https://doi.org/10.1016/j.jclepro.2021.128202

Wang, X., Wang, Z., Tang, Y., Xiao, D., Zhang, D., Huang, Y., Guo, Y., & Liu, J. (2019). Oxidative degradation of iodinated X-ray contrast media (iomeprol and iohexol) with sulfate radical: An experimental and theoretical study. *Chemical Engineering Journal*, *368*, 999–1012. https://doi.org/10.1016/j.cej.2019.02.194

Wennmalm, Å., & Gunnarsson, B. (2009). Pharmaceutical management through environmental product labeling in Sweden. *Environment International*, *35*(5), 775–777. https://doi.org/10.1016/j.envint.2008.12.008

Xie, Z., Wang, X., Gan, Y., Cheng, H., Fan, S., Li, X., & Tang, J. (2022). Ecotoxicological effects of the antidepressant fluoxetine and its removal by the typical freshwater microalgae Chlorella pyrenoidosa. *Ecotoxicology and Environmental Safety*, *244*, 114045. https://doi.org/10.1016/j.ecoenv.2022.114045

Yang, B., Wei, T., Xiao, K., Deng, J., Yu, G., Deng, S., Li, J., Zhu, C., Duan, H., & Zhuo, Q. (2018). Effective mineralization of anti-epilepsy drug carbamazepine in aqueous solution by simultaneously electro-generated H2O2/O3 process. *Electrochimica Acta*, *290*, 203–210. https://doi.org/10.1016/j.electacta.2018.09.067

Žegura, B., Heath, E., Černoša, A., & Filipič, M. (2009). Combination of in vitro bioassays for the determination of cytotoxic and genotoxic potential of wastewater, surface water and drinking water samples. *Chemosphere*, *75*(11), 1453–1460. https://doi.org/10.1016/j.chemosphere.2009.02.041

Zhang, G., Sun, Y., Zhang, C., & Yu, Z. (2017). Decomposition of acetaminophen in water by a gas phase dielectric barrier discharge plasma combined with TiO2-rGO nanocomposite: Mechanism and degradation pathway. *Journal of Hazardous Materials*, *323*, 719–729. https://doi.org/10.1016/j.jhazmat.2016.10.008

Supplemental Information for Chapter 5

This supplemental information section supports the data presented in the main text. Each paragraph consists of tables or figures explaining the *in silico* calculations. **Paragraph S.5.1** contains **Fig. S1** and **Table S1**, showing possible substitutes of potentially formed oxidative degradation intermediates. **Paragraph S.5.2**, provide table **S2 – S4**, where the risk quotient calculation for three different trophic levels is given, exposed to untreated HSW. The concentration addition mixture toxicity calculation is given in **Table S5 – S7** presented in **paragraph S.5.3**. In **paragraph S.5.4**, **Fig. S2** and **S3** illustrate the pharmaceutical removal and assume the production of transformation products after thermal plasma oxidation and UV-C/H_2O_2 treatment. **Paragraph S.5.5** presents **Table S8** and **S9**, providing the molecular structure of potential degradation intermediates, including their ECOSAR determined EC_{50} and LD_{50} values. In **paragraph S.5.6** is **Fig. S4** depicted visualising the mixture toxicology of untreated and treated hospital sewage water.

S.5.1 Advanced oxidation transformation product formation

After hydroxylation of an aromatic ring structure, further hydroxyl radical attack can result in the formation of a catechol. Subsequent autooxidation of a catechol, in the presence of oxygen (+ O_2 → -$2H^+$), a quinone is produced including a super oxide radical ($^{\bullet}O_2^-$), which interacts in an aqueous solution with 2 H^+ to produce hydrogen peroxide (H_2O_2) (Schweigert et al., 2001).

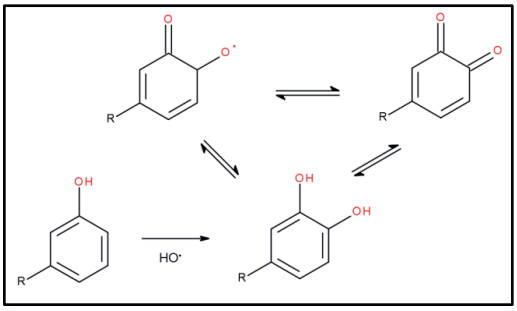

Fig S1. The formation of catechol and oxidation with available oxygen results subsequently in a more stable quinone.

Table S1.

Oxidative transformation product substitutes

Chemical intermediate name	Molecular structure
Epoxide	
Hydroperoxide	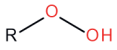
Hydroxy	
Nitroso-intermediate	
Nitro-intermediate	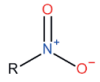
Hydroxybenzenes (Quinonic) A) Hydroquinone B) Resorcinol C) Catechol D) Benzoquinone	**A)** 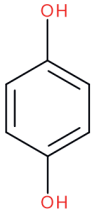 **B)** 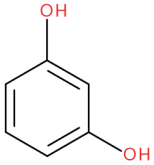 **C)** 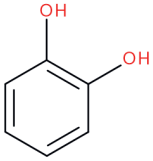 **D)** 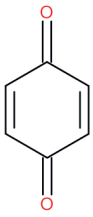

S.5.2 Calculated risk quotients untreated Hospital sewage water (HSW)

Table S2

Predicted environmental risk for Fish

Compound	HSW Conc. MEC (mg/L)[A]	ECOSAR class definition	ECOSAR Fish PNEC (mg/L)[B]	Risk quotient (RQ)	Risk level
Iomeprol Cas: **78649-41-9** $C_{17}H_{22}I_3N_3O_8$ ***M.W.:*** *777.085* **Log *P*:** -3.08	2.387	Amides	89.3	0.03	Insignificant <0.1
Diatrizoic acid Cas: **117-96-4** $C_{11}H_9I_3N_2O_4$ ***M.W.:*** *613.914* **Log *P*:** 2.89	0.0101	Amides	5.36	0.001	Insignificant <0.1
Ciprofloxacin Cas: **85721-33-1** $C_{17}H_{18}FN_3O_3$ ***M.W.:*** *331.341* **Log *P*:** 0.65	0.0145	Aliphatic amines	13.1	0.001	Insignificant <0.1
Fluoxetine Cas: **54910-89-3** $C_{17}H_{18}F_3NO$ ***M.W.:*** *309.326* **Log *P*:** 4.09	$1.5 \cdot 10^{-4}$	Aliphatic amines	0.00108	0.14	Low 0.1-1.0
Diclofenac Cas: **15307-86-5** $C_{14}H_{11}Cl_2NO_2$ ***M.W.:*** *296.149* **Log *P*:** 4.06	0.0031	Neutral organics	0.038	0.08	Insignificant <0.1
Metoprolol Cas: **37350-58-6** $C_{15}H_{25}NO_3$ ***M.W.:*** *267.364* **Log *P*:** 1.79	0.0013	Aliphatic amines	0.082	0.02	Insignificant <0.1
Cyclophosphamide Cas: **50-18-0** $C_7H_{15}Cl_2N_2O_2P$ ***M.W.:*** 261.086 **Log *P*:** 0.23	$3.4 \cdot 10^{-4}$	Esters, phosphates	0.0045	0.08	Insignificant <0.1
Carbamazepine Cas: **298-46-4** $C_{15}H_{12}N_2O$ ***M.W.:*** *236.269* **Log *P*:** 2.67	$8.0 \cdot 10^{-5}$	Substituted ureas	0.0409	0.002	Insignificant <0.1
Acetaminophen Cas: **103-90-2** $C_8H_9NO_2$ ***M.W.:*** *151.163* **Log *P*:** 0.34	0.0821	Phenol amines	0.016	5.13	Moderate 1.0-10
Metformin Cas: **657-24-9** $C_4H_{11}N_5$ ***M.W.:*** *129.164* **Log *P*:** -2.31	0.0368	Aliphatic amines	27.7	0.001	Insignificant <0.1

[A]: Pharmaceutical concentrations during working days (Mo-Thu) as analysed by Graumans et al 2021
[B]: EC_{50} value for 96 h, divided by the ECHA assessment factor of 1000

Table S3

Predicted environmental risk for Daphnia

Compound **Cas no.:**	**HSW Conc. MEC** (mg/L)[A]	**ECOSAR class definition**	**ECOSAR Daphnia PNEC** (mg/L)[B]	**Risk quotient** (RQ)	**Risk level**
Iomeprol Cas: **78649-41-9** $C_{17}H_{22}I_3N_3O_8$ ***M.W.:*** *777.085* **Log *P*:** -3.08	2.387	Amides	144.0	0.02	Insignificant <0.1
Diatrizoic acid Cas: **117-96-4** $C_{11}H_9I_3N_2O_4$ ***M.W.:*** *613.914* **Log *P*:** 2.89	0.0101	Amides	5.74	0.002	Insignificant <0.1
Ciprofloxacin Cas: **85721-33-1** $C_{17}H_{18}FN_3O_3$ ***M.W.:*** *331.341* **Log *P*:** 0.65	0.0145	Aliphatic amines	1.24	0.01	Insignificant <0.1
Fluoxetine Cas: **54910-89-3** $C_{17}H_{18}F_3NO$ ***M.W.:*** *309.326* **Log *P*:** 4.09	$1.5 \cdot 10^{-4}$	Aliphatic amines	$1.75 \cdot 10^{-4}$	0.85	Low 0.1-1.0
Diclofenac Cas: **15307-86-5** $C_{14}H_{11}Cl_2NO_2$ ***M.W.:*** *296.149* **Log *P*:** 4.06	0.0031	Neutral organics	0.0258	0.12	Low 0.1-1.0
Metoprolol Cas: **37350-58-6** $C_{15}H_{25}NO_3$ ***M.W.:*** *267.364* **Log *P*:** 1.79	0.0013	Aliphatic amines	0.0094	0.13	Low 0.1-1.0
Cyclophosphamide Cas: **50-18-0** $C_7H_{15}Cl_2N_2O_2P$ ***M.W.:*** 261.086 **Log *P*:** 0.23	$3.4 \cdot 10^{-4}$	Esters, phosphates	$8.50 \cdot 10^{-5}$	4.00	Moderate 1.0-10
Carbamazepine Cas: **298-46-4** $C_{15}H_{12}N_2O$ ***M.W.:*** *236.269* **Log *P*:** 2.67	$8.0 \cdot 10^{-5}$	Substituted ureas	0.0141	0.006	Insignificant <0.1
Acetaminophen Cas: **103-90-2** $C_8H_9NO_2$ ***M.W.:*** *151.163* **Log *P*:** 0.34	0.0821	Phenol amines	$8.74 \cdot 10^{-4}$	93.9	High >10
Metformin Cas: **657-24-9** $C_4H_{11}N_5$ ***M.W.:*** *129.164* **Log *P*:** -2.31	0.0368	Aliphatic amines	1.93	0.02	Insignificant <0.1

[A]: Pharmaceutical concentrations during working days (Mo-Thu) as analysed by Graumans et al 2021

[B]: EC_{50} value for 96 h, divided by the ECHA assessment factor of 1000

Table S4
Predicted environmental risk for Green Algae

Compound **Cas no.:**	**HSW Conc.** **MEC** (mg/L)[A]	**ECOSAR class definition**	**ECOSAR Green Algae** **PNEC** (mg/L)[B]	**Risk quotient** (RQ)	**Risk level**
Iomeprol Cas: **78649-41-9** $C_{17}H_{22}I_3N_3O_8$ ***M.W.:*** *777.085* **Log *P*:** -3.08	2.387	Amides	3.20	0.75	Low 0.1-1.0
Diatrizoic acid Cas: **117-96-4** $C_{11}H_9I_3N_2O_4$ ***M.W.:*** *613.914* **Log *P*:** 2.89	0.0101	Amides	0.52	0.02	Insignificant <0.1
Ciprofloxacin Cas: **85721-33-1** $C_{17}H_{18}FN_3O_3$ ***M.W.:*** *331.341* **Log *P*:** 0.65	0.0145	Aliphatic amines	1.62	0.009	Insignificant <0.1
Fluoxetine Cas: **54910-89-3** $C_{17}H_{18}F_3NO$ ***M.W.:*** *309.326* **Log *P*:** 4.09	$1.5 \cdot 10^{-4}$	Aliphatic amines	$7.9 \cdot 10^{-5}$	1.89	Moderate 1.0-10
Diclofenac Cas: **15307-86-5** $C_{14}H_{11}Cl_2NO_2$ ***M.W.:*** *296.149* **Log *P*:** 4.06	0.0031	Neutral organics	0.0414	0.07	Insignificant <0.1
Metoprolol Cas: **37350-58-6** $C_{15}H_{25}NO_3$ ***M.W.:*** *267.364* **Log *P*:** 1.79	0.0013	Aliphatic amines	0.00831	0.15	Low 0.1-1.0
Cyclophosphamide Cas: **50-18-0** $C_7H_{15}Cl_2N_2O_2P$ ***M.W.:*** 261.086 **Log *P*:** 0.23	$3.4 \cdot 10^{-4}$	Esters, phosphates	0.71	$4.8 \cdot 10^{-4}$	Insignificant <0.1
Carbamazepine Cas: **298-46-4** $C_{15}H_{12}N_2O$ ***M.W.:*** *236.269* **Log *P*:** 2.67	$8.0 \cdot 10^{-5}$	Substituted ureas	$2.6 \cdot 10^{-4}$	0.3	Low 0.1-1.0
Acetaminophen Cas: **103-90-2** $C_8H_9NO_2$ ***M.W.:*** *151.163* **Log *P*:** 0.34	0.0821	Phenol amines	0.0022	37.0	High >10
Metformin Cas: **657-24-9** $C_4H_{11}N_5$ ***M.W.:*** *129.164* **Log *P*:** -2.31	0.0368	Aliphatic amines	4.62	0.008	Insignificant <0.1

[A]: Pharmaceutical concentrations during working days (Mo-Thu) as analysed by Graumans et al 2021
[B]: EC_{50} value for 96 h, divided by the ECHA assessment factor of 1000

S.5.3 Calculated mixture toxicity using the concentration addition concept

Table S5

Calculated effect concentration of the mixture in Fish

Compound (*c*)	**HSW Conc. MEC (mg/L)[a]**	**Fraction (*P*)**	**LC_{50}** 96 h (mg/L)	***P/LC*$_{50}$**
Iomeprol	2.387	0.9414	89.3	0.011
Diatrizoic acid	0.0101	0.0040	5.36	0.001
Ciprofloxacin	0.0145	0.0057	13.1	0.000
Fluoxetine	$1.5 \cdot 10^{-4}$	0.0001	0.00108	0.055
Diclofenac	0.0031	0.0012	0.038	0.032
Metoprolol	0.0013	0.0005	0.082	0.006
Cyclophosphamide	$3.4 \cdot 10^{-4}$	0.0001	0.0045	0.03
Carbamazepine	$8.0 \cdot 10^{-5}$	0.0000	0.0409	0.001
Acetaminophen	0.0821	0.0324	0.016	2.024
Metformin	0.0368	0.0145	27.7	0.001
Total	2.54	1.00	***P/LC*$_{50}$**	2.16
$1/\sum_{c=1}^{n} \frac{p_c}{EC_{50\,C}} =$	***EC*$_{mix}$ *(mg/L)***			0.46
***Conc.*$_{mix}$/*EC*$_{mix}$**	2.54/0.46		**RQ_{mix}**	5.52

Table S6
Calculated effect concentration of the mixture in Daphnia

Compound (*c*)	**HSW Conc. MEC (mg/L)[a]**	**Fraction (*P*)**	**LC_{50}** 48 h (mg/L)	***P/LC*$_{50}$**
Iomeprol	2.387	0.9414	144	0.007
Diatrizoic acid	0.0101	0.0040	5.74	0.001
Ciprofloxacin	0.0145	0.0057	1.24	0.005
Fluoxetine	$1.5 \cdot 10^{-4}$	0.0001	0.000175	0.338
Diclofenac	0.0031	0.0012	0.0258	0.047
Metoprolol	0.0013	0.0005	0.00094	0.545
Cyclophosphamide	$3.4 \cdot 10^{-4}$	0.0001	$8.50 \cdot 10^{-5}$	1.58
Carbamazepine	$8.0 \cdot 10^{-5}$	0.0000	0.0141	0.002
Acetaminophen	0.0821	0.0324	0.00087	37.22
Metformin	0.0368	0.0145	1.93	0.008
Total	2.54	1.00	***P/LC*$_{50}$**	39.74
$1/\sum_{c=1}^{n} \frac{p_c}{EC_{50\,C}} =$	***EC*$_{mix}$ *(mg/L)***			0.025
***Conc.*$_{mix}$*/EC*$_{mix}$**	2.54/0.025		**RQ_{mix}**	101.6

Table S7
Calculated effect concentration of the mixture in Green algae

Compound (*c*)	**HSW Conc. MEC (mg/L)[a]**	**Fraction (*P*)**	**EC_{50}** 96 h (mg/L)	***P/EC*$_{50}$**
Iomeprol	2.387	0.9414	3.20	0.294
Diatrizoic acid	0.0101	0.0040	0.52	0.008
Ciprofloxacin	0.0145	0.0057	1.62	0.004
Fluoxetine	$1.5 \cdot 10^{-4}$	0.0001	0.000079	0.749
Diclofenac	0.0031	0.0012	0.0414	0.030
Metoprolol	0.0013	0.0005	0.00831	0.062
Cyclophosphamide	$3.4 \cdot 10^{-4}$	0.0001	0.71	0.001
Carbamazepine	$8.0 \cdot 10^{-5}$	0.0000	0.00026	0.121
Acetaminophen	0.0821	0.0324	0.0022	14.72
Metformin	0.0368	0.0145	4.62	0.003
Total	2.54	1.00	***P/EC*$_{50}$**	15.99
$1/\sum_{c=1}^{n} \frac{p_c}{EC_{50\,C}} =$	***EC*$_{mix}$ *(mg/L)***			0.063
***Conc.*$_{mix}$*/EC*$_{mix}$**	2.54/0.063		**RQ_{mix}**	40.3

S.5.4 Formation of transformation products

During oxidative degradation, original molecular structures were converted into transformation products. The removal efficiency obtained during thermal plasma and UV-C/H_2O_2 oxidation in HSW, were extrapolated as conversion levels to demonstrate the potentially formed amount of TPs. Based on results demonstrated in **Table S8**, it is expected that prolonged oxidative treatment will result in near mineralisation. For DIA and CB, chemical abatement kinetics during plasma oxidation were not immediately efficient. Also levels above 100%, were illustrated (**Fig. S2** and **S3**). Higher levels of original pharmaceutical structure produced during oxidation, indicate that metabolites present in the HSW matrix were first converted into their pristine structure, before degrading into oxidative TPs (Graumans et al., 2021).

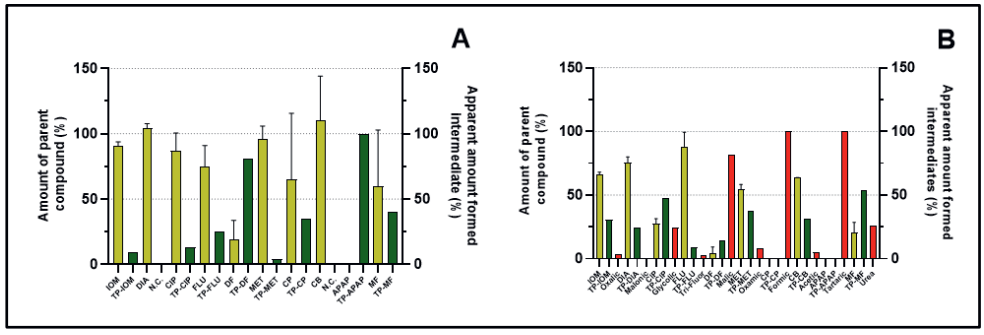

Fig. S2. To estimate the concentration of produced degradation intermediates conversion levels after 30 min (**A**) and 120 min (**B**) plasma treatment were used. Initial pharmaceutical concentrations (■) were expected to convert into degradation intermediates (■), prolonged oxidative treatment will ultimately result in aliphatic structures (■).

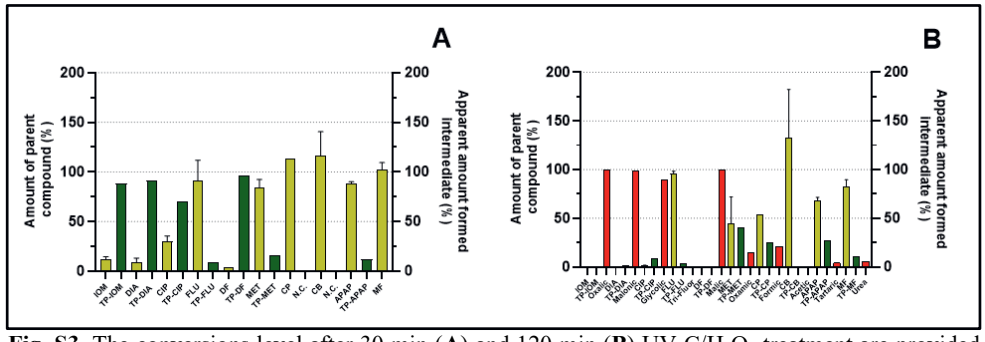

Fig. S3. The conversions level after 30 min (**A**) and 120 min (**B**) UV-C/H_2O_2 treatment are provided. The parent pharmaceutical (■) is converted into TPs (■) and subsequently into aliphatic compounds (■).

S.5.5 *In silico* determined effect concentrations for degradation intermediates

Table S8

Expected transformation products during •OH radical attack

Pharmaceutical **Molecule structure** *SMILES*	**AOP** **(min)** **Conversion (% ; *mg/L*)**	**ECOSAR PNEC** mg/L[C]		
		Fish LC_{50}	**Daphnia** LC_{50}	**Green Algae** EC_{50}
Iomeprol (IOM) **Log *P*** (-1.45)[A] CN(C1=C(C(=C(C(=C1I)C(=O)NCC(CO)O)I)C(=O)NCC(CO)O)I)C(=O)CO 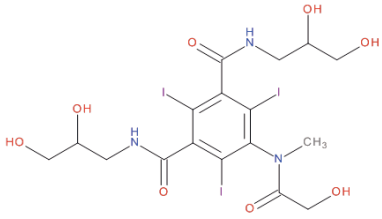	**Initial (Conc.)** *2.39 mg/L*	89.3	144.0	3.2
	PubChem: Benzenedicarboxamide 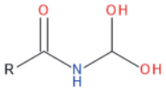 R denotes aromatic ring	*ECOSAR class definition:* Amides 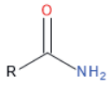		
Hypothetical formed intermediate *Smiles*	**Potentially formed TP** *mg/L*	**Fish** LC_{50}	**Daphnia** LC_{50}	**Green Algae** EC_{50}
Formed by •OH oxidation **Log *P*** (-2.01)[B] CN(C(=O)CO)c1c(O)c(C(=O)NCC(O)CO)c(O)c(C(=O)NCC(=O)CO)c1O 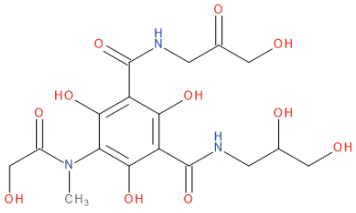	**TP-IOM**	169	303	4.75
	$PAW_{30\ min}$ 9.5% ; *0.23 mg/L* **$PAW_{120\ min}$** 30.5% ; *0.73mg/L*	**RQ** <0.1 <0.1	**RQ** <0.1 <0.1	**RQ** <0.1 0.15
	UV-C/H_2O_2 30 min 88.5%; *2.11 mg/L* **UV-C/H_2O_2 120 min** 0%; *0 mg/L*	**RQ** <0.1 -	**RQ** <0.1 -	**RQ** 0.44 -
	References TP: (Nowak et al., 2020; Wang et al., 2019)	*ECOSAR class definition:* Amides		
Hypothetical formed Carboxylic acid *Smiles*	**Conc. Oxalic acid** *mg/L*	**Fish** LC_{50}	**Daphnia** LC_{50}	**Green Algae** EC_{50}
Oxalic acid **Log *P*** (-0.26)[A] OC(=O)C(=O)O 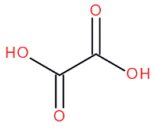	***Hypothesized according to DIA degradation reference:*** (Bocos et al., 2016)	168	67.5	12.1
	Expected degradation TP-IOM with $PAW_{60\ min}$ 3.5% ; *0.08 mg/L*	**RQ** <0.1	**RQ** <0.1	**RQ** <0.1
	Expected degradation TP-IOM with UV-C/H_2O_2 60 min 99% ; *2.39 mg/L*	**RQ** <0.1	**RQ** <0.1	**RQ** 0.2

Pharmaceutical **Molecule structure** *SMILES*	**AOP** **(min)** **Conversion (% ; *mg/L*)**	**ECOSAR PNEC** mg/L[C] **Fish** LC_{50}	**Daphnia** LC_{50}	**Green Algae** EC_{50}
Diatrizoic acid (DIA) **Log *P*** (2.89)[A] CC(=O)Nc1c(I)c(NC(=O)(C))c(I)c(C(=O)(O))c1I 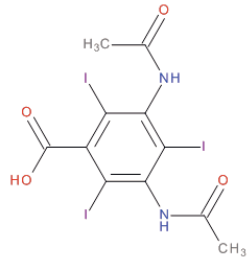	**Initial (Conc.)** *0.0101 mg/L*	5.36	5.74	0.52
	PubChem: Iodinated organic	*ECOSAR class definition:* Amides 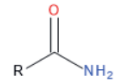		
Hypothetical formed intermediate *SMILES*	**Potentially formed TP** *mg/L*	**Fish** LC_{50}	**Daphnia** LC_{50}	**Green Algae** EC_{50}
Formed by •OH oxidation **Log *P*** (-0.50)[B] CC(=O)Nc1c(O)c(NC(=O)C)c(O)c(C(=O)O)c1O 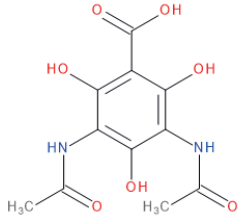	**TP-DIA**	71.2	101	3.47
	$PAW_{30\ min}$ N.C. ; *0.0* **$PAW_{120\ min}$** 24.5% ; *0.002 mg/L*	**RQ** n/a <0.1	**RQ** n/a <0.1	**RQ** n/a <0.1
	UV-C/H_2O_2 30 min 91.5%; *0.009 mg/L* **UV-C/H_2O_2 120 min** 1.3%; *$1 \cdot 10^{-4}$ mg/L*	**RQ** <0.1 <0.1	**RQ** <0.1 <0.1	**RQ** <0.1 <0.1
	References TP: (Nowak et al., 2020; Wang et al., 2019)	*ECOSAR class definition:* Amides		
Hypothetical formed Carboxylic acid *Smiles*	**Conc. Malonic acid** *mg/L*	**Fish** LC_{50}	**Daphnia** LC_{50}	**Green Algae** EC_{50}
Malonic acid **Log *P*** (-0.33)[A] OC(=O)CC(=O)O 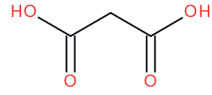	***Characterized in reference:*** (Bocos et al., 2016)	702	296	63.8
	Expected degradation TP-DIA with $PAW_{60\ min}$ N.C.	**RQ** -	**RQ** -	**RQ** -
	Expected degradation TP-DIA with UV-C/H_2O_2 60 min 98.7% ; *0.010 mg/L*	**RQ** <0.1	**RQ** <0.1	**RQ** <0.1

Pharmaceutical **Molecule structure** *SMILES*	**AOP** **(min)** **Conversion (% ; *mg/L*)**	**ECOSAR PNEC** mg/L[C]		
		Fish LC_{50}	**Daphnia** LC_{50}	**Green Algae** EC_{50}
Ciprofloxacin (CIP) **Log *P*** (-0.77)[A] C1CNCCN1c2cc3N(C4CC4)C=C(C(=O)O)C(=O)c3cc2F 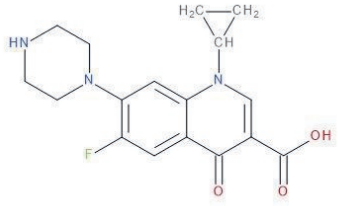	**Initial (Conc.)** *0.145 mg/L*	13.1	1.24	1.62
	PubChem: Fluoroquinolone 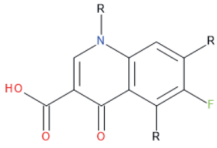	*ECOSAR class definition:* Aliphatic amines 		
Hypothetical formed intermediate *SMILES*	**Potentially formed TP** *mg/L*	**Fish** LC_{50}	**Daphnia** LC_{50}	**Green Algae** EC_{50}
Formed by •OH oxidation (UV/H_2O_2 and non-thermal plasma) **Log *P*** (2.39)[B] Fc1cc2C(=O)C=CN(C3CC3)c2cc1N4CCNCC4 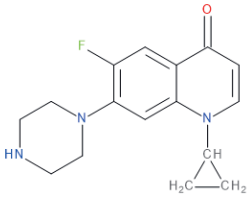	**TP-CIP**	0.031	0.0038	0.0029
	$PAW_{30\ min}$ 13.0%; *0.002 mg/L* **$PAW_{120\ min}$** 47.6% ; *0.007 mg/L*	**RQ** <0.1 <0.1	**RQ** 0.53 <0.1	**RQ** 0.69 <0.1
	UV-C/$H_2O_{2\ 30\ min}$ 70.3%; *0.010 mg/L* **UV-C/$H_2O_{2\ 120\ min}$** 8.9%; *0.001 mg/L*	**RQ** 0.32 <0.1	**RQ** 2.63 0.4	**RQ** 3.45 0.5
	References TP: (Banaschik et al., 2018a; HU et al., 2019; Ou et al., 2016)	*ECOSAR class definition:* Aliphatic amines		
Hypothetical formed Carboxylic acid *Smiles*	**Conc. Glycolic acid** *mg/L*	**Fish** LC_{50}	**Daphnia** LC_{50}	**Green Algae** EC_{50}
Glycolic acid **Log *P*** (-1.04)[A] OCC(=O)O 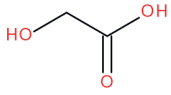	***Hypothesized according to degradation studies references:*** (Banaschik et al., 2018; HU et al., 2019; Ou et al., 2016)	355	152	35.1
	Expected degradation TP-CIP with $PAW_{60\ min}$ 24.7% ; *0.004 mg/L*	**RQ** <0.1	**RQ** <0.1	**RQ** <0.1
	Expected degradation TP-CIP with UV-C/$H_2O_{2\ 60\ min}$ 89.4% ; *0.013 mg/L*	**RQ** <0.1	**RQ** <0.1	**RQ** <0.1

Pharmaceutical **Molecule structure** *SMILES*	**AOP** **(min)** **Conversion (% ; *mg/L*)**	**ECOSAR PNEC** mg/L[C]		
		Fish LC_{50}	**Daphnia** LC_{50}	**Green Algae** EC_{50}
Fluoxetine (FLU) **Log *P*** (4.17)[A] CNCCC(c2ccccc2)Oc1ccc(cc1)C(F)(F)F 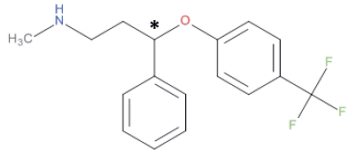	**Initial (Conc.)** *2•10^{-4} mg/L*	0.0011	1.75 •10^{-4}	7.9 •10^{-5}
	PubChem: Diphenhydramine derivate 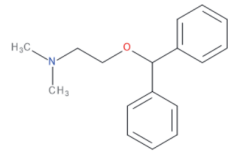	*ECOSAR class definition:* Aliphatic amines 		
Hypothetical formed intermediate *SMILES*	**Potentially formed TP** *mg/L*	**Fish** LC_{50}	**Daphnia** LC_{50}	**Green Algae** EC_{50}
Formed by •OH oxidation (UV/H_2O_2 and UV/peracetic acid) **Log *P*** (4.17)[B] CNCCC(Oc1ccc(cc1)C(F)(F)F)c2cccc(O)c2 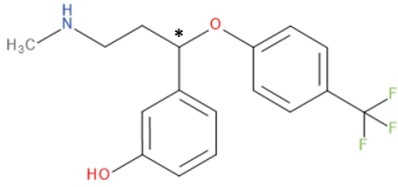	**TP-FLU**	0.0024	3.61 •10^{-4}	1.81 •10^{-4}
	$PAW_{30\ min}$ 24.9%; *5.0 • 10^{-5} mg/L* **$PAW_{120\ min}$** 9.2% ; 1.4 • *10^{-5} mg/L*	**RQ** <0.1 <0.1	**RQ** 0.13 <0.1	**RQ** 0.27 0.1
	UV-C/H_2O_2 30 min 9.2%; *1.83 • 10^{-5} mg/L* **UV-C/H_2O_2 120 min** 3.4%; *5.1 • 10^{-6} mg/L*	**RQ** <0.1 <0.1	**RQ** <0.1 <0.1	**RQ** 0.1 <0.1
	References TP: (Drzewicz et al., 2019; Hollman et al., 2020)	*ECOSAR class definition:* Aliphatic amines		
Hypothetical formed Carboxylic acid *Smiles*	**Conc. Trifluoroacetic acid** *mg/L*	**Fish** LC_{50}	**Daphnia** LC_{50}	**Green Algae** EC_{50}
Trifluoroacetic acid **Log *P*** (0.91)[A] OC(=O)C(F)(F)F 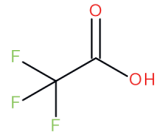	***Characterized in reference:*** (Tisler et al., 2019)	20.7	10.2	43.1
	Expected degradation TP-FLU with $PAW_{60\ min}$ 2.6% ; 3.9• *10^{-6} mg/L*	**RQ** <0.1	**RQ** <0.1	**RQ** <0.1
	Expected degradation TP-FLU with UV-C/H_2O_2 60 min 0.4% ; 5.5• *10^{-7} mg/L*	**RQ** <0.1	**RQ** <0.1	**RQ** <0.1

Pharmaceutical **Molecule structure** *SMILES*	**AOP** **(min)** **Conversion (% ; *mg/L*)**	**ECOSAR PNEC** mg/L[C]		
		Fish LC_{50}	**Daphnia** LC_{50}	**Green Algae** EC_{50}
Diclofenac (DF) **Log *P*** (4.26)[A] OC(=O)Cc1ccccc1Nc2c(Cl)cccc2Cl 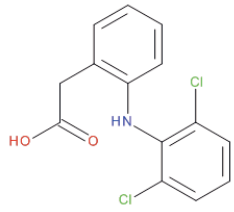	**Initial (Conc.)** *0.0031 mg/L*	0.038	0.026	0.041
	PubChem: Benzeneacetic acid 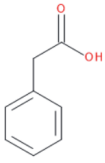	*ECOSAR class definition:* Neutral organic (Hydrocarbon structures, aromatic compounds, ketones, amides, aldehydes etc.)		
Hypothetical formed intermediate *SMILES*	**Potentially formed TP** *mg/L*	**Fish** LC_{50}	**Daphnia** LC_{50}	**Green Algae** EC_{50}
Formed by •OH oxidation (Non-thermal plasma oxidation) **Log *P*** (3.18)[B] OC(=O)Cc1ccccc1Nc2c(Cl)cc(O)cc2Cl 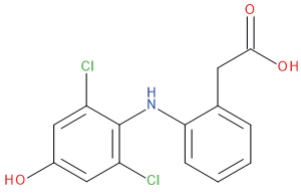	**TP-DF**	0.065	0.048	0.086
	$PAW_{30\ min}$ 81.2%; *0.0025 mg/L* **$PAW_{120\ min}$** 14.2% ; *$4 \cdot 10^{-4}$ mg/L*	**RQ** <0.1 <0.1	**RQ** <0.1 <0.1	**RQ** <0.1 <0.1
	UV-C/H_2O_2 30 min 96.4%; *0.0030 mg/L* **UV-C/H_2O_2 120 min** 0%; *0 mg/L*	**RQ** <0.1 -	**RQ** <0.1 -	**RQ** 0.1 -
	Reference TP: (Banaschik et al., 2018)	*ECOSAR class definition:* Phenol 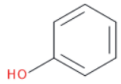		
Hypothetical formed Carboxylic acid *Smiles*	**Conc. Malic acid** *mg/L*	**Fish** LC_{50}	**Daphnia** LC_{50}	**Green Algae** EC_{50}
Malic acid **Log *P*** (-1.11)[A] OC(CC(=O)O)C(=O)O 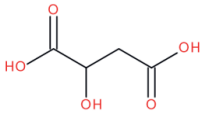	***Characterized in reference:*** (Banaschik et al., 2018)	2230	901	165
	Expected degradation TP-DF with $PAW_{60\ min}$ 81.4% ; *0.003 mg/L*	**RQ** <0.1	**RQ** <0.1	**RQ** <0.1
	Expected degradation TP-DF with UV-C/H_2O_2 60 min 100%; *0.031 mg/L*	**RQ** <0.1	**RQ** <0.1	**RQ** <0.1

Pharmaceutical **Molecule structure** *SMILES*	**AOP** **(min)** **Conversion (% ; *mg/L*)**	**ECOSAR PNEC** mg/L[C]		
		Fish LC_{50}	**Daphnia** LC_{50}	**Green Algae** EC_{50}
Metoprolol (MET) **Log *P*** (-1.76)[A] COCCc1ccc(OCC(O)CNC(C)C)cc1 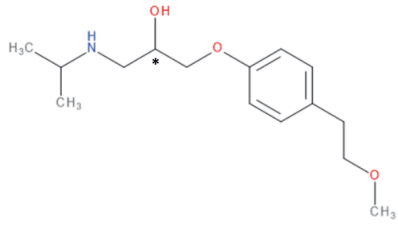	**Initial (Conc.)** *0.0012 mg/L*	0.082	0.0094	0.0083
	PubChem: Propanolamine 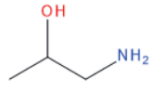	*ECOSAR class definition:* Aliphatic amines 		
Hypothetical formed intermediate *SMILES*	**Potentially formed TP** *mg/L*	**Fish** LC_{50}	**Daphnia** LC_{50}	**Green Algae** EC_{50}
Formed by •OH oxidation (UV/H_2O_2) **Log *P*** (1.40)[B] CC(C)NCC(O)COc1ccc(CCO)cc1 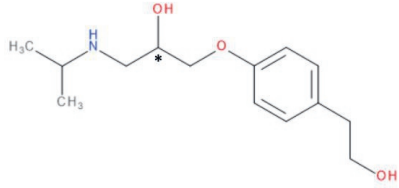	**TP-MET**	0.12	0.013	0.013
	$PAW_{30\ min}$ 4.1%; *5.36 • 10^{-5} mg/L* **$PAW_{120\ min}$** 37.3% ; *0.0005 mg/L*	**RQ** <0.1 <0.1	**RQ** <0.1 <0.1	**RQ** <0.1 <0.1
	$UV\text{-}C/H_2O_2$ 30 min 15.5%; *0.0002 mg/L* **$UV\text{-}C/H_2O_2$ 120 min** 40.8%; *0.0005 mg/L*	**RQ** <0.1 <0.1	**RQ** <0.1 <0.1	**RQ** 0.1 <0.1
	Reference TP: (Jaén-Gil et al., 2019)	*ECOSAR class definition:* Aliphatic amines		
Hypothetical formed Carboxylic acid *Smiles*	**Conc. Oxamic acid** *mg/L*	**Fish** LC_{50}	**Daphnia** LC_{50}	**Green Algae** EC_{50}
Oxamic acid **Log *P*** (-1.07)[A] NC(=O)C(=O)O 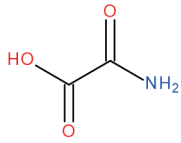	***Characterized in reference:*** (Isarain-Chávez et al., 2011)	653	247	34.3
	Expected degradation TP-MET with $PAW_{60\ min}$ 8.1% ; *1• 10^{-4} mg/L*	**RQ** <0.1	**RQ** <0.1	**RQ** <0.1
	Expected degradation TP-MET with $UV\text{-}C/H_2O_2$ 60 min 14.6% ; *0.0002 mg/L*	**RQ** <0.1	**RQ** <0.1	**RQ** <0.1

Pharmaceutical **Molecule structure** *SMILES*	**AOP** **(min)** **Conversion (% ; *mg/L*)**	**ECOSAR PNEC** mg/L[C]		
		Fish LC_{50}	**Daphnia** LC_{50}	**Green Algae** EC_{50}
Cyclophosphamide (CP) **Log *P*** (0.10)[A] C1CCNP(=O)(N(CCCl)CCCl)O1 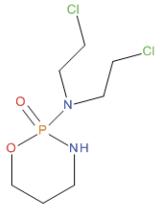	**Initial (Conc.)** *3.4 •10^{-4} mg/L*	0.0045	8.5•10^{-5}	0.71
	PubChem: n/a	*ECOSAR class definition:* Esters and phosphates 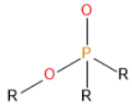		
Hypothetical formed intermediate *SMILES*	**Potentially formed TP** *mg/L*	**Fish** LC_{50}	**Daphnia** LC_{50}	**Green Algae** EC_{50}
Formed by •OH oxidation (Thermal plasma oxidation and UV/H_2O_2) **Log *P*** (-0.04)[B] ClCCN(CCCl)P1(=O)NC(=O)CCO1 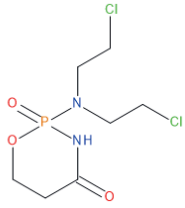	**TP-CP**	0.0096	9.4•10^{-5}	5.1
	PAW$_{30\ min}$ 35.0%; *0.00012 mg/L* **PAW$_{120\ min}$** 0% ; *0 mg/L*	**RQ** <0.1 -	**RQ** 1.28 -	**RQ** <0.1 -
	UV-C/H_2O_2 $_{30\ min}$ N.C. **UV-C/H_2O_2 $_{120\ min}$** 24.9%; *0.0001 mg/L*	**RQ** - 0.11	**RQ** - 1.1	**RQ** - <0.1
	Reference TP: (Graumans et al., 2020)	*ECOSAR class definition:* Aliphatic amines		
Hypothetical formed Carboxylic acid *Smiles*	**Conc. Formic acid** *mg/L*	**Fish** LC_{50}	**Daphnia** LC_{50}	**Green Algae** EC_{50}
Formic Acid **Log *P*** (-0.27)[A] OC=O 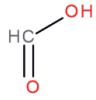	***Hypothesized according to degradation studies references:*** (Banaschik et al., 2018; Lutterbeck et al., 2015; Qutob et al., 2022)	6.13	2.77	0.81
	Expected degradation TP-CP with PAW$_{60\ min}$ 100% ; *0.00034 mg/L*	**RQ** <0.1	**RQ** <0.1	**RQ** <0.1
	Expected degradation TP-CP with UV-C/H_2O_2 $_{60\ min}$ 21.3%; 7.2 • *10^{-4} mg/L*	**RQ** <0.1	**RQ** <0.1	**RQ** <0.1

Pharmaceutical **Molecule structure** *SMILES*	**AOP** **(min)** **Conversion (% ; *mg/L*)**	**ECOSAR PNEC** mg/L[C]		
		Fish LC_{50}	**Daphnia** LC_{50}	**Green Algae** EC_{50}
Carbamazepine (CB) **Log *P*** (2.77)[A] NC(=O)N2c1ccccc1C=Cc3ccccc23 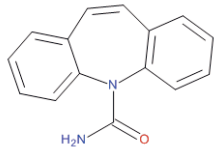	**Initial (Conc.)** *1.0 •10^{-4} mg/L*	0.041	0.014	2.6 •10^{-4}
	PubChem: Tricyclic compound 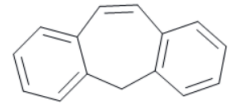	*ECOSAR class definition:* Substituted Ureas 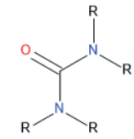		
Hypothetical formed intermediate *SMILES*	**Potentially formed TP** *mg/L*	**Fish** LC_{50}	**Daphnia** LC_{50}	**Green Algae** EC_{50}
Formed by •OH oxidation (UV/persulfate, SO4•- + •OH) **Log *P*** (0.95)[B] C1=CC=C2C(=C1)C3C(O3)C4=CC=CC=C4N2C(=O)N 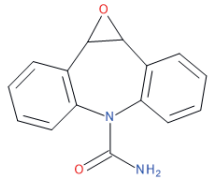	**TP-CB**	0.51	0.30	8.7 •10^{-4}
	$PAW_{30\ min}$ N.C. **$PAW_{120\ min}$** 31.5% ; *2.52 •10^{-5} mg/L*	**RQ** - <0.1	**RQ** - <0.1	**RQ** - 0.19
	UV-C/H_2O_2 30 min N.C. **UV-C/H_2O_2 120 min** N.C.	**RQ** - -	**RQ** - -	**RQ** - -
	Reference TP: (Li et al., 2021)	*ECOSAR class definition:* Substituted Ureas		
Hypothetical formed Carboxylic acid *Smiles*	**Conc. Acetic acid** *mg/L*	**Fish** LC_{50}	**Daphnia** LC_{50}	**Green Algae** EC_{50}
Acetic acid **Log *P*** (-0.22)[A] CC(=O)O 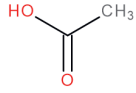	***Characterized in reference:*** (Li et al., 2021; Yang et al., 2018)	25.8	12.3	4.4
	Expected degradation TP-CB with $PAW_{60\ min}$ 4.9% ; *3.9 • 10^{-6} mg/L*	**RQ** <0.1	**RQ** <0.1	**RQ** <0.1
	Expected degradation TP-CB with UV-C/H_2O_2 60 min N.C.	**RQ** -	**RQ** -	**RQ** -

Pharmaceutical **Molecule structure** *SMILES*	**AOP** **(min)** **Conversion (% ; *mg/L*)**	**ECOSAR PNEC** mg/L[C]		
		Fish LC_{50}	**Daphnia** LC_{50}	**Green Algae** EC_{50}
Acetaminophen (APAP) **Log *P*** (0.91)[A] O=C(Nc(ccc(O)c1)c1)C 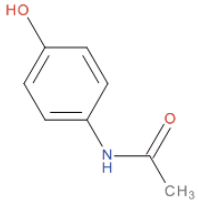	**Initial (Conc.)** *0.82 mg/L*	0.016	$8.7 \cdot 10^{-4}$	0.0022
	PubChem: P-Aminophenol 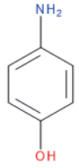	*ECOSAR class definition:* Phenol amine 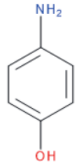		
Hypothetical formed intermediate *SMILES*	**Potentially formed TP** *mg/L*	**Fish** LC_{50}	**Daphnia** LC_{50}	**Green Algae** EC_{50}
Formed by •OH oxidation (UV/H_2O_2) **Log *P*** (0.27)[B] CC(=O)Nc1ccc(O)c(O)c1 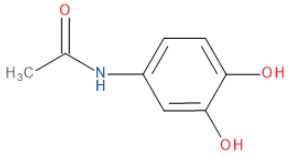	**TP-APAP**	0.03	0.0012	0.004
	$PAW_{30\ min}$ 99.9% ; *0.82 mg/L* **$PAW_{120\ min}$** 0.1% ; *$1 \cdot 10^{-4}$ mg/L*	**RQ** 27.3 <0.1	**RQ** 68.3 0.1	**RQ** 226.5 <0.1
	$UV\text{-}C/H_2O_{2\ 30\ min}$ 12.1% ; *0.01 mg/L* **$UV\text{-}C/H_2O_{2\ 120\ min}$** 27.4% ; *0.023 mg/L*	**RQ** 0.33 0.8	**RQ** 8.3 18.8	**RQ** 2.5 6.3
	References TP: (Humayun et al., 2021; Vogna et al., 2002; Zhang et al., 2017)	*ECOSAR class definition:* Phenol amine		
Hypothetical formed Carboxylic acid *Smiles*	**Conc. Tartaric acid** *mg/L*	**Fish** LC_{50}	**Daphnia** LC_{50}	**Green Algae** EC_{50}
Tartaric acid **Log *P*** (-1.83)[A] OC(C(O)C(=O)O)C(=O)O 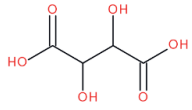	***Characterized in reference:*** (Qutob et al., 2022)	612	263	62.4
	Expected degradation TP-APAP with $PAW_{60\ min}$ 99.9% ; *0.080 mg/L*	**RQ** <0.1	**RQ** <0.1	**RQ** <0.1
	Expected degradation TP-APAP with $UV\text{-}C/H_2O_{2\ 60\ min}$ 4.1% ; *0.034 mg/L*	**RQ** <0.1	**RQ** <0.1	**RQ** <0.1

Pharmaceutical **Molecule structure** *SMILES*	**AOP** **(min)** **Conversion (% ; *mg/L*)**	**ECOSAR PNEC** mg/L[C] **Fish** LC_{50}	**Daphnia** LC_{50}	**Green Algae** EC_{50}
Metformin (MF) **Log *P*** (-0.92)[A] N=C(N)NC(=N)N(C)C 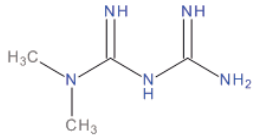	**Initial (Conc.)** *0.037 mg/L*	27.7	1.93	4.62
	PubChem: Biguanide 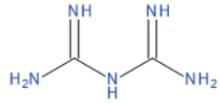	*ECOSAR class definition:* Aliphatic amines 		
Hypothetical formed intermediate *SMILES*	**Potentially formed TP** *mg/L*	**Fish** LC_{50}	**Daphnia** LC_{50}	**Green Algae** EC_{50}
Formed by aerobic bio-degradation, photo-degradation **Log *P*** (-3.57)[B] NC(=NC(=O)N)N 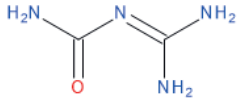	**TP-MF**	89.2	5.57	16.5
	$PAW_{30\ min}$ 40.1%; *0.015 mg/L* **$PAW_{120\ min}$** 54.0% ; *0.020 mg/L*	**RQ** <0.1 <0.1	**RQ** <0.1 <0.1	**RQ** <0.1 <0.1
	UV-C/H_2O_2 30 min N.C. **UV-C/H_2O_2 120 min** 10.9% ; *0.004 mg/L*	**RQ** - <0.1	**RQ** - <0.1	**RQ** - <0.1
	References TP: (Lin et al., 2020; Straub et al., 2019; Tisler & Zwiener, 2019)	*ECOSAR class definition:* Aliphatic amines		
Hypothetical formed Aliphatic compound *Smiles*	**Aliphatic structure** *mg/L*	**Fish** LC_{50}	**Daphnia** LC_{50}	**Green Algae** EC_{50}
Urea **Log *P*** (-1.36)[A] NC(=O)N 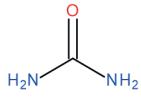	***Characterized in reference:*** (Markiewicz et al., 2017)	76.9	31.5	6.03
	Expected degradation TP-MF with $PAW_{60\ min}$ 25.7% ; *0.009 mg/L*	**RQ** <0.1	**RQ** <0.1	**RQ** <0.1
	Expected degradation TP-MF with UV-C/H_2O_2 60 min 5.8% ; *0.0021 mg/L*	**RQ** <0.1	**RQ** <0.1	**RQ** <0.1

[A]: Theoretical Log $P_{octanol/water}$ coefficient obtained via Chemicalize

[B]: Theoretical Log $P_{octanol/water}$ coefficient obtained via ECOSAR

[C]: LC_{50}/LD_{50} value for 48 or 96 h, divided by the ECHA assessment factor of 1000

Table S9

Expected transformation products after nitration, 3-nitro-APAP and nitro-DF

Hypothetical formed intermediate *SMILES*	**Potentially formed TP** *mg/L*	**Fish** LC_{50}	**Daphnia** LC_{50}	**Green Algae** EC_{50}
Potentially formed with PAW **Log *P*** (-2.11)[A] CC(=O)Nc1ccc(O)c(c1)[N](=O)O 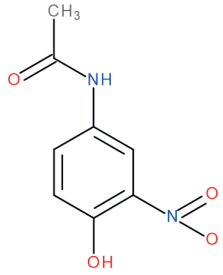	**TP-3-nitro-APAP**	0.22	0.0034	0.02
	$PAW_{30\ min}$ 99.9% ; *0.82 mg/L* **$PAW_{120\ min}$** 100% ; *0.82 mg/L*	**RQ** 3.73 3.73	**RQ** 240.18 240.18	**RQ** 4.1 4.1
	UV-C/H_2O_2 30 min 12.1% ; *0.01 mg/L* **UV-C/H_2O_2 120 min** 32.0% ; *0.03 mg/L*	**RQ** 0.05 0.14	**RQ** 2.94 8.82	**RQ** 0.5 1.5
		ECOSAR class definition: Phenol amine		

Hypothetical formed intermediate *SMILES*	**Potentially formed TP** *mg/L*	**Fish** LC_{50}	**Daphnia** LC_{50}	**Green Algae** EC_{50}
Potentially formed with PAW **Log *P*** (-2.11)[A] OC(=O)Cc1cc(ccc1Nc2c(Cl)cccc2Cl)[N](=O)O 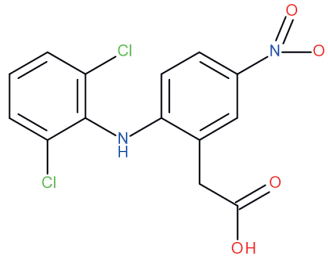	**TP-3-nitro-DF**	6.00	3.30	2.13
	$PAW_{30\ min}$ 81.2%; *0.0025 mg/L* **$PAW_{120\ min}$** 82.8% ; *0.0026 mg/L*	**RQ** <0.1 <0.1	**RQ** <0.1 <0.1	**RQ** <0.1 <0.1
	UV-C/H_2O_2 30 min 96.4%; *0.0030 mg/L* **UV-C/H_2O_2 120 min** 100%; *0.0031 mg/L*	**RQ** <0.1 <0.1	**RQ** <0.1 <0.1	**RQ** 0.1 <0.1
		ECOSAR class definition: Neutral organics (Hydrocarbon structures, aromatic compounds, ketones, amides, aldehydes etc.)		

[A]: Theoretical Log $P_{octanol/water}$ coefficient obtained via ECOSAR

S.5.6 Mixture toxicity of the oxidative treated HSW

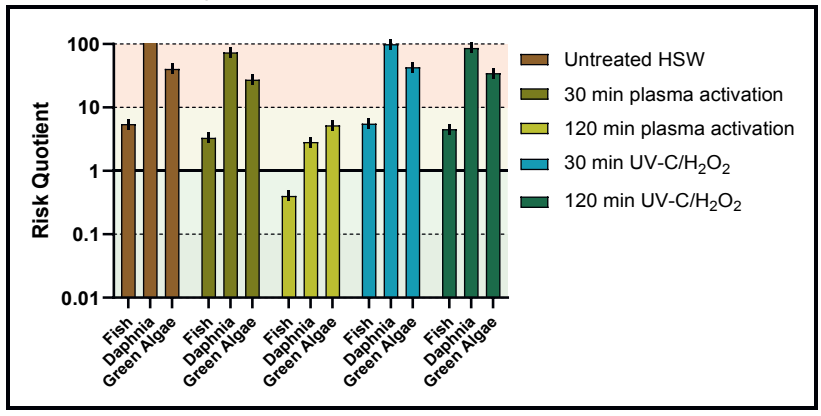

Fig. S4. Calculated concentration addition mixture toxicity. Untreated HSW is compared with the potential mixture toxicity of oxidative treated HSW. The ecotoxicological risk is categorically visualised as; insignificant ■ <0.1; low ■ 0.1-1.0; moderate ■ 1.0 - 10.0; high ■ >10.0 (colours are translucent).

Literature

Banaschik, R., Jablonowski, H., Bednarski, P. J., & Kolb, J. F. (2018). Degradation and intermediates of diclofenac as instructive example for decomposition of recalcitrant pharmaceuticals by hydroxyl radicals generated with pulsed corona plasma in water. *Journal of Hazardous Materials*, *342*, 651–660. https://doi.org/10.1016/j.jhazmat.2017.08.058

Bocos, E., Oturan, N., Sanromán, M. Á., & Oturan, M. A. (2016). Elimination of radiocontrast agent Diatrizoic acid from water by electrochemical advanced oxidation: Kinetics study, mechanism and mineralization pathway. *Journal of Electroanalytical Chemistry*, *772*, 1–8. https://doi.org/10.1016/j.jelechem.2016.04.011

Drzewicz, P., Drobniewska, A., Sikorska, K., & Nałęcz-Jawecki, G. (2019). Analytical and ecotoxicological studies on degradation of fluoxetine and fluvoxamine by potassium ferrate. *Environmental Technology*, *40*(25), 3265–3275. https://doi.org/10.1080/09593330.2018.1468488

Graumans, M. H. F., Hoeben, W. F. L. M., Russel, F. G. M., & Scheepers, P. T. J. (2020). Oxidative degradation of cyclophosphamide using thermal plasma activation and UV-H_2O_2 treatment in tap water. *Environmental Research*, *182*. https://doi.org/10.1016/j.envres.2019.109046

Graumans, M. H. F., Hoeben, W. F. L. M., van Dael, M. F. P., Anzion, R. B. M., Russel, F. G. M., & Scheepers, P. T. J. (2021). Thermal plasma activation and UV-H_2O_2 oxidative degradation of pharmaceutical residues. *Environmental Research*, *195*. https://doi.org/10.1016/j.envres.2021.110884

Hollman, J., Dominic, J. A., & Achari, G. (2020). Degradation of pharmaceutical mixtures in aqueous solutions using UV/peracetic acid process: Kinetics, degradation pathways and comparison with UV/H2O2. *Chemosphere*, *248*, 125911. https://doi.org/10.1016/j.chemosphere.2020.125911

HU, S., LIU, X., XU, Z., WANG, J., LI, Y., SHEN, J., LAN, Y., & CHENG, C. (2019). Degradation and mineralization of ciprofloxacin by gas–liquid discharge non-thermal plasma. *Plasma Science and Technology*, *21*(1), 015501. https://doi.org/10.1088/2058-6272/aade82

Humayun, S., Hayyan, M., Alias, Y., & Hayyan, A. (2021). Oxidative degradation of acetaminophen using superoxide ion generated in ionic liquid/aprotic solvent binary system. *Separation and Purification Technology*, *270*, 118730. https://doi.org/10.1016/j.seppur.2021.118730

Isarain-Chávez, E., Rodríguez, R. M., Cabot, P. L., Centellas, F., Arias, C., Garrido, J. A., & Brillas, E. (2011). Degradation of pharmaceutical beta-blockers by electrochemical advanced oxidation processes using a flow plant with a solar compound parabolic collector. *Water Research*, *45*(14), 4119–4130. https://doi.org/10.1016/j.watres.2011.05.026

Jaén-Gil, A., Buttiglieri, G., Benito, A., Gonzalez-Olmos, R., Barceló, D., & Rodríguez-Mozaz, S. (2019). Metoprolol and metoprolol acid degradation in UV/H2O2 treated wastewaters:

An integrated screening approach for the identification of hazardous transformation products. *Journal of Hazardous Materials*, *380*, 120851. https://doi.org/10.1016/j.jhazmat.2019.120851

Li, Y., Yang, Y., Lei, J., Liu, W., Tong, M., & Liang, J. (2021). The degradation pathways of carbamazepine in advanced oxidation process: A mini review coupled with DFT calculation. *Science of The Total Environment*, *779*, 146498. https://doi.org/10.1016/j.scitotenv.2021.146498

Lin, W., Zhang, X., Li, P., Tan, Y., & Ren, Y. (2020). Ultraviolet photolysis of metformin: mechanisms of environmental factors, identification of intermediates, and density functional theory calculations. *Environmental Science and Pollution Research*, *27*(14), 17043–17053. https://doi.org/10.1007/s11356-020-08255-9

Lutterbeck, C. A., Machado, Ê. L., & Kümmerer, K. (2015). Photodegradation of the antineoplastic cyclophosphamide: A comparative study of the efficiencies of UV/H2O2, UV/Fe2+/H2O2 and UV/TiO2 processes. *Chemosphere*, *120*, 538–546. https://doi.org/10.1016/j.chemosphere.2014.08.076

Markiewicz, M., Jungnickel, C., Stolte, S., Białk-Bielińska, A., Kumirska, J., & Mrozik, W. (2017). Primary degradation of antidiabetic drugs. *Journal of Hazardous Materials*, *324*, 428–435. https://doi.org/10.1016/j.jhazmat.2016.11.008

Nowak, A., Pacek, G., & Mrozik, A. (2020). Transformation and ecotoxicological effects of iodinated X-ray contrast media. *Reviews in Environmental Science and Bio/Technology*, *19*(2), 337–354. https://doi.org/10.1007/s11157-020-09534-0

Ou, H., Ye, J., Ma, S., Wei, C., Gao, N., & He, J. (2016). Degradation of ciprofloxacin by UV and UV/H 2 O 2 via multiple-wavelength ultraviolet light-emitting diodes: Effectiveness, intermediates and antibacterial activity. *Chemical Engineering Journal*, *289*, 391–401. https://doi.org/10.1016/j.cej.2016.01.006

Qutob, M., Hussein, M. A., Alamry, K. A., & Rafatullah, M. (2022). A review on the degradation of acetaminophen by advanced oxidation process: pathway, by-products, biotoxicity, and density functional theory calculation. *RSC Advances*, *12*(29), 18373–18396. https://doi.org/10.1039/D2RA02469A

Schweigert, N., Zehnder, A. J. B., & Eggen, R. I. L. (2001). Chemical properties of catechols and their molecular modes of toxic action in cells, from microorganisms to mammals. Minireview. *Environmental Microbiology*, *3*(2), 81–91. https://doi.org/10.1046/j.1462-2920.2001.00176.x

Straub, J. O., Caldwell, D. J., Davidson, T., D'Aco, V., Kappler, K., Robinson, P. F., Simon-Hettich, B., & Tell, J. (2019). Environmental risk assessment of metformin and its transformation product guanylurea. I. Environmental fate. *Chemosphere*, *216*, 844–854. https://doi.org/10.1016/j.chemosphere.2018.10.036

Tisler, S., Zindler, F., Freeling, F., Nödler, K., Toelgyesi, L., Braunbeck, T., & Zwiener, C. (2019). Transformation Products of Fluoxetine Formed by Photodegradation in Water and Biodegradation in Zebrafish Embryos (*Danio rerio*). *Environmental Science & Technology*, *53*(13), 7400–7409. https://doi.org/10.1021/acs.est.9b00789

Tisler, S., & Zwiener, C. (2019). Aerobic and anaerobic formation and biodegradation of guanyl urea and other transformation products of metformin. *Water Research*, *149*, 130–135. https://doi.org/10.1016/j.watres.2018.11.001

Vogna, D., Marotta, R., Napolitano, A., & d'Ischia, M. (2002). Advanced Oxidation Chemistry of Paracetamol. UV/H_2O_2 -Induced Hydroxylation/Degradation Pathways and ^{15} N-Aided Inventory of Nitrogenous Breakdown Products. *The Journal of Organic Chemistry*, *67*(17), 6143–6151. https://doi.org/10.1021/jo025604v

Wang, X., Wang, Z., Tang, Y., Xiao, D., Zhang, D., Huang, Y., Guo, Y., & Liu, J. (2019). Oxidative degradation of iodinated X-ray contrast media (iomeprol and iohexol) with sulfate radical: An experimental and theoretical study. *Chemical Engineering Journal*, *368*, 999–1012. https://doi.org/10.1016/j.cej.2019.02.194

Yang, B., Wei, T., Xiao, K., Deng, J., Yu, G., Deng, S., Li, J., Zhu, C., Duan, H., & Zhuo, Q. (2018). Effective mineralization of anti-epilepsy drug carbamazepine in aqueous solution by simultaneously electro-generated H_2O_2/O_3 process. *Electrochimica Acta*, *290*, 203–210. https://doi.org/10.1016/j.electacta.2018.09.067

Zhang, G., Sun, Y., Zhang, C., & Yu, Z. (2017). Decomposition of acetaminophen in water by a gas phase dielectric barrier discharge plasma combined with TiO2-rGO nanocomposite: Mechanism and degradation pathway. *Journal of Hazardous Materials*, *323*, 719–729. https://doi.org/10.1016/j.jhazmat.2016.10.008

Chapter 6

A quantum chemical approach to localise pharmaceutical oxidative reactive positions

Martien H.F. Graumans, Wilfred F.L.M. Hoeben,
Frans G.M. Russel, Paul T.J. Scheepers

Manuscript in preparation

Abstract

Pharmaceuticals are widely used for the prevention and treatment of disease or pain in humans and animals. Depending on the required therapy, many different active pharmaceutical ingredients are available. The functional groups that are especially designed for the interaction in an organism are represented by the pharmacophore, which defines the pharmacological activity of a molecule and the molecular interaction with its cellular target. Eventually pharmaceuticals are removed from the body by phase I and II metabolism, where the biotransformation reactions occurs at the most reactive structural sites of a molecule.

Via direct and indirect elimination routes medicinal residues end up in the aquatic environment. To alleviate pharmaceutical discharge in the wastewater stream, it is proposed that advanced oxidative treatment prior to conventional wastewater treatment could be useful. Following the biotransformation reactions, it is expected that the chemical abatement kinetics of oxidative treatment proceeds similarly.

The aim of this study was to use computational chemistry to perform quantum chemical calculations for the localisation of the most reactive molecular moieties. With the frontier molecular orbital calculations the nucleophilic sites of the 14 tested pharmaceuticals were determined. Comparing the determined nucleophilic sites with the measured pseudo-first order degradation kinetics from thermal plasma and UV/H_2O_2 oxidation substantiates the interaction with UV-C irradiance, ROS or RNS. Based on the localisation of the HOMO orbitals for the 14 pharmaceuticals, it is proposed that this approach could also be useful for other micropollutants.

6.1 Introduction

Active pharmaceutical ingredients (APIs) are especially designed to have similar chemical interactions as endogenous ligands. The structure that will replace a ligand and will bind to the target protein is defined as the pharmacophore. A pharmacophore represents the interaction capacities of multiple functional groups of a pharmaceutical that interacts in an organism (Kar et al., 2020). Other theoretically structural API components are vectors, carriers and vulnerable groups (Pandit, 2012). Chemical features that are commonly represented by the pharmacophore are positive and negative charge, positive and negative protonation, hydrophobicity (aliphatic and aromatic), ring aromaticity and hydrogen bond donor or acceptor (Kar et al., 2020). To eliminate the exogenous API from the body by biotransformation, Phase I metabolism occurs primarily at the API metabolic sensitive structural sites (Pandit, 2012; Z. Zhang & Tang, 2018). These so-called vulnerable groups are rapidly oxidised by cytochrome (CYP) P450 enzymes. CYP enzymes are catalytic proteins found in the endoplasmic reticulum of cells whereof the highest density is found in liver cells. These CYP enzymes are involved in the biotransformation and detoxification of endo- and exogenous substances. Depending on the molecular structure of the compound that needs to be metabolised, multiple oxygenation reactions are possible via the CYP P450 monooxygenase system, see **Table 6.1**. During Phase I metabolism, endo- or exogenous compounds are represented as a molecular-substrate (M-H). To activate the CYP P450 monooxygenase system, oxygen and nicotinamide adenine dinucleotide phosphate hydrogen (NADPH) is needed (Klaassen, 2013). The simple representation of the oxygenation of a molecular substrate is represented in (**R1**).

$$M\text{-}H + O_2 + NADPH + H^+ \rightarrow M\text{-}OH + H_2O + NADP^+ \qquad (\mathbf{R1})$$

The CYP P450 monooxygenase produced electrophilic oxo-species initiate multiple chemical oxygenation reactions at pharmaceutical vulnerable positions, (**Table 6.1**). During these chemical reactions incorporation of an oxygen atom (alkyl or side-chain hydroxylation), rearrangement reactions (causing N-, O- and S-dealkylation, N-oxidation) or sulfoxide- or epoxide formation occurs. Other Phase I initiated reactions are reduction and hydrolysis. In addition to CYP enzyme-initiated oxygenation reactions, also oxidation occurs by other enzymes (Klaassen, 2013; Pandit, 2012; Z. Zhang & Tang, 2018). The produced metabolites undergo further biotransformation via phase II reactions where a glucuronide functional group is attached. Glucuronide containing metabolites are produced to be excreted from the body via urine and faeces.

Table 6.1.
Possible CYP P450 oxidative biotransformation reactions
(Klaassen, 2013; Pandit, 2012; Z. Zhang & Tang, 2018).

Sensitive structural sites **CYP450 Phase I metabolism**	**Oxidised structural sites**
Aromatic hydroxylation and Alkyl (ethyl-group)/ Side chain hydroxylation	Hydroxylated metabolites
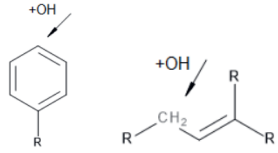	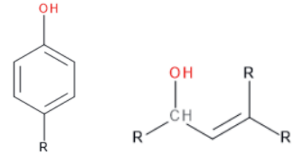
Epoxide formation	Epoxidation
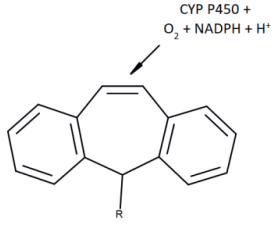	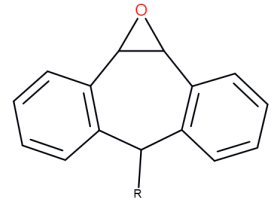
N or S- oxygenation (oxidation)	N-oxide or Sulphone formation
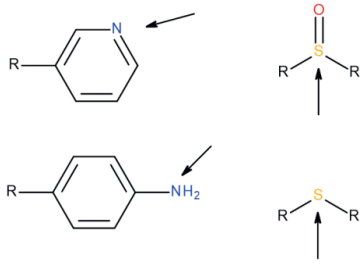	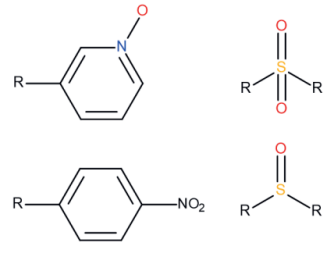
Deamination or desulphuration	Oxidative group transfer products
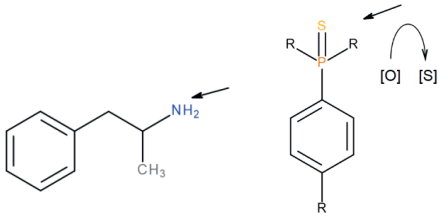	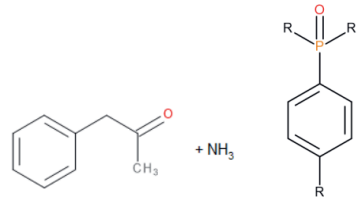

Table 6.1. *Continued*

Dealkylation of N-, O-, S- substitutes	Catalysed heteroatom products
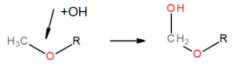	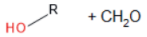
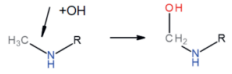	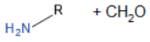
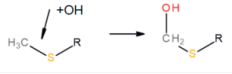	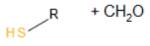

Phase I oxygenation reactions demonstrate similarities with chemical oxidative abatement kinetics initiated during advanced oxidation processes (Klaassen, 2013; Pandit, 2012; Z. Zhang & Tang, 2018, Graumans et al. 2024). Reactive oxygen species formed with AOPs can produce similar hydroxylation, dealkylation, deamination, epoxidation, dehalogenation and general oxidation degradation intermediates (Graumans et al. 2024). Similar to biotransformation, it is clear that not all pharmaceuticals are rapidly degraded by reactive oxygen species. A molecule's stability and reactivity are important properties to demonstrate its potential toxicity but also its ability to (bio)degrade (Kar et al., 2020; Kostal et al., 2015; Nolte et al., 2020; Voutchkova-Kostal et al., 2012). According to quantitative structure-toxicity relationship (QSTR) studies the (eco)toxicity of molecules are predicted according to physicochemical properties. In the QSTR study of Khan et al. (2018) strong hydrophobic properties were correlated with toxicity (Kar et al., 2020; Khan et al., 2019; Voutchkova-Kostal et al., 2012). Functional groups such as aliphatic ethers (R-O-R'), esters (RCOOR') and increased O atom content, improve the capability of forming hydrogen bonds. This increased hydrophilicity reduces toxicity (Kar et al., 2020; Khan et al., 2019). As previously discussed, it is seen that the pharmacophore represents the most important physicochemical properties of an API (Kar et al., 2020; Khan et al., 2019). These physicochemical properties of a molecule can be derived from quantum chemical analysis (Fukui et al., 1961; Kar et al., 2020; Kostal et al., 2015; Voutchkova-Kostal et al., 2012). Regarding a molecule, its reactivity frontier molecular orbitals (FMO) play an important role in chemical reaction and bonding (Engel, 2006; Murrel, 1985; Royal Society of Chemistry, 2006). These outermost orbitals can be distinguished between highest occupied molecular orbitals (HOMO) and lowest unoccupied molecular orbitals (LUMO). The highest occupied molecular orbital energy (E_{HOMO}) (eV) is used to demonstrate nucleophilicity (Asghar et al., 2019; Nolte et al., 2020). It is expected that nucleophilic molecules with high E_{HOMO}

energy are more prone to electrophilic attack since they can donate their electrons to an electrophilic specie, such as, $^{\bullet}OH$, $HO_2^{\bullet}$, $^1O_2$, O_3, $SO_4^{\bullet-}$, H_2O_2, or NO_2^+ (Asghar et al., 2019; Kar et al., 2020; Nolte & Peijnenburg, 2017; Önlü & Saçan, 2017). Oxidising agents $^{\bullet}OH$ and NO_2^+ are expected to be produced with thermal plasma and indicate to react as electrophilic species. In **Table 6.2** we demonstrate for each tested pharmaceutical its calculated E_{HOMO} energy. Furthermore, in addition to nucleophilicity, also the gap energy HOMO-LUMO (ΔE) is determined. The energy separation between HOMO-LUMO energy levels is described as a simple quantum chemical measure to indicate kinetic stability and the possibility to form covalent bonds (Fukui et al., 1952, 1961; Kar et al., 2020; Voutchkova-Kostal et al., 2012). A large energy difference between the HOMO and LUMO implies lower chemical reactivity and thus molecular stability (Karelson et al., 1996). Furthermore, the HOMO-LUMO gap demonstrates also the excitation energy, which is a useful approximation to determine a molecule's absorption wavelength (Karelson et al., 1996). During wavelength absorption with energy similar to that of ΔE, an electron from the HOMO (ground state) is moved into the LUMO (excited state). Quantum chemical properties were computed using open-source chemical software packages. **Paragraph 6.2.2**, describes the computational methodology applied to determine the molecular descriptors for our tested pharmaceuticals.

6.2 Methodology

6.2.1 Pharmaceutical selection and chemical abatement kinetics

A versatile set of 14 different pharmaceuticals was selected as previously tested in the studies Graumans et al. (2020, 2021, 2022 and 2024). The compounds used for the quantum chemical calculations were; iomeprol (IOM), iopamidol (IOP), diatrizoic acid (DIA), doxycycline (DOX), ciprofloxacin (CIP), fluoxetine (FLU), diclofenac (DF), metoprolol (MET), cyclophosphamide (CP), carbamazepine (CB), terbutaline (TER), phenazone (PHE), acetaminophen (APAP) and metformin (MF). For the comparison of quantum chemical parameters with chemical abatement kinetics, the previously determined thermal plasma and UV-C/H_2O_2 oxidation results from the studies Graumans et al. (2021) and Graumans et al. (2022) were consulted.

6.2.2 Quantum chemical property calculation

For each tested pharmaceutical, multiple software packages were used to calculate the quantum chemical parameters. At start, the PubChem database (PUBCHEM) was searched to retrieve the 3D molecular structure coordinates for each pharmaceutical in SDF format. These 3D molecular coordinates were subsequently imported in Avogadro molecule editor and visualiser

software, Version 1.1.1 (SourceForge, San Diego, USA). Molecular orbital package, MOPAC2016 software (Stewart Computational Chemistry, Paddington Circle, USA) was used to calculate quantum chemical descriptors for each molecule. Calculations were done according to parameterisation method 6 (PM6), which is a semi-empirical quantum calculation to determine the electronic structure and heat formation based on the molecular geometry. With this chemical computation the molecular orbitals were located and their quantum chemical parameters E_{HOMO} and E_{LUMO} energy (eV) were defined. To visualise the generated MOPAC output file, Jmol open-source software (SourceForge, San Diego, USA) was used. The computed energy values E_{HOMO} (eV), E_{LUMO} (eV) and HOMO-LUMO energy gap (ΔE), **Eq. 1**, were used to estimate the stability and reactivity of pharmaceuticals.

$$\text{Energy gap } \Delta E \text{ (eV)} = E_{LUMO}\,(eV) - E_{HOMO}\,(eV) \qquad (\mathbf{1})$$

6.3. Results and Discussion

6.3.1 Oxidative degradation chemistry

Application of thermal plasma treatment compared to UV/H_2O_2 in a controlled environment revealed the first-order abatement kinetics for 14 pharmaceuticals (Graumans et al., 2021). Spiked Milli-Q water elucidates the genuine chemical abatement of the pharmaceuticals since no other constituents or minerals inhibit or catalyse degradation efficiency. A maximum plasma discharge of 150 W was selected based on previously presented optimisation results (Graumans et al., 2020). With thermal plasma treatment hydrogen peroxide (H_2O_2), hydroxyl radicals ($^{\bullet}OH$), nitric oxide (NO), nitrogen dioxide (NO_2), nitrous acid (HNO_2), nitric acid (HNO_3) and other transient reactive oxygen and nitrogen species ($H_aN_bO_c$) are generated. The concentration of NO_2^- (4.9 mM), NO_3^- (1.8 mM) and H_2O_2 (0.37 mM) were measured after 120 Watt thermal plasma discharge using the same technology as in the current research project (Hoeben et al., 2019). It is likely that with 150 Watt plasma discharge a higher amount of ROS and RNS is formed. With UV-C/H_2O_2 treatment 0.22 mM H_2O_2 is only added once and with UV-C irradiance no RNS species are formed. During photocatalysis the 0.22 mM H_2O_2 is converted into $^{\bullet}OH$ radicals. Noteworthy is that the concentration of H_2O_2 used during UV-C irradiance is lower than the plasma-produced H_2O_2 concentration. To indicate a correlation between the quantum chemically calculated E_{HOMO} energy and pseudo-first order (k min^{-1}) degradation kinetics, HOMO (eV) energy and abatement kinetics were placed in descending order from high to low for each pharmaceutical, **Table 6.2**.

Table 6.2.
Pharmaceutical E_{HOMO} energy compared with the chemical abatement kinetics in Milli-Q

Molecule	E_{HOMO} (eV)	Thermal plasma Milli-Q k (min^{-1})	UV-C/H_2O_2 Milli-Q k (min^{-1})
Acetaminophen	-8.491	0.774	0.031
Diclofenac	-8.508	0.520	1.000
Phenazone	-8.637	0.149	0.249
Carbamazepine	-8.712	0.019	0.075
Metoprolol	-8.764	0.011	0.068
Metformin	-8.824	0.001	0.007
Ciprofloxacin	-8.920	0.030	1.000
Terbutaline	-8.976	0.021	0.079
Fluoxetine	-9.206	0.017	0.016
Doxycycline	-9.320	0.032	0.067
Diatrizoic acid	-9.323	0.004	0.591
Cyclophosphamide	-9.744	0.160	0.018
Iopamidol	-9.933	0.008	0.587
Iomeprol	-10.264	0.009	0.477

High ***Low***

Table colours represent the descending order from the highest to lowest E_{HOMO} energy and pseudo-first order kinetics.

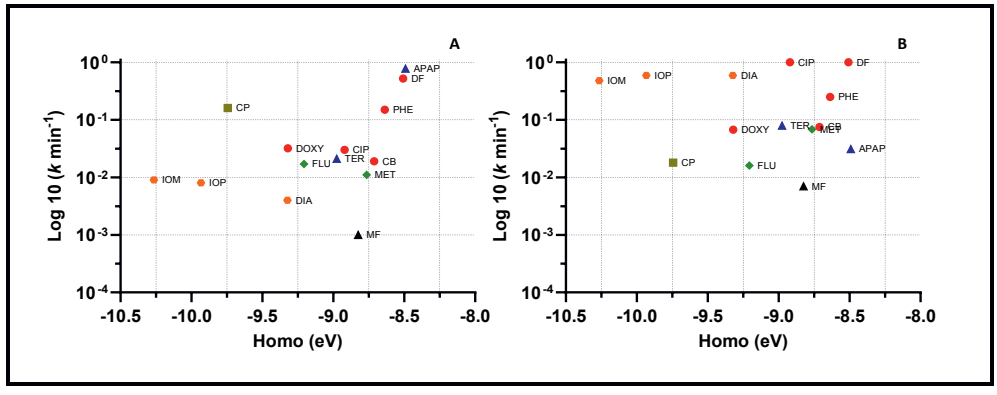

Fig. 6.1. E_{HOMO} energy (eV) plotted against logarithm transformed degradation kinetics (k min^{-1}) observed after thermal plasma (**A**) and UV-C/H_2O_2 (**B**) oxidative treatment in Milli-Q water. Pharmaceutical compounds were subdivided into phenol derivatives (▲), benzene derivatives (●), benzene amide derivatives (●), mono-and di-oxybenzene (◆), aliphatic heteromonocyclic (▲) and aliphatic acyclic (■) structures. The pharmaceutical compound classification was adapted following the study of Lee et al. (2015).

The quantum chemical parameter E_{HOMO} (eV) for the 14 pharmaceuticals indicate a possible relationship between nucleophilicity and our previously found oxidative pseudo-first order degradation kinetics (**Table 6.2**). However, due to the limited number of tested pharmaceuticals (**Fig. 6.1**) no statistical correlation could be determined between the oxidative degradation kinetics and the calculated quantum chemical E_{HOMO} energy (eV). In a more extensive study on second-order rate constant kinetics retrieved from micropollutant (n = 216) ozonation were compared to quantum chemical E_{HOMO} (M. Lee et al., 2015). The aromatic micropollutants (n = 112) were subdivided in multiple chemical classes demonstrating correlation between localised HOMO and second-order rate constants. Correlation coefficients (R^2) listed in ascending order were; 0.82, 0.85, 0.87, 0.94 and 0.95 for benzene derivatives, anilines, mono- and di-oxybenzenes, phenols and trimethoxybenzenes, respectively (Lee et al., 2015). For benzene derivatives the HOMO is primarily positioned at ring structures, where those for aliphatic amines and alkenes can be localised at nitrogen lone-pair electrons, spread over C=C double bonds or substituents (Lee et al., 2015). The degradation results found for the tested pharmaceuticals APAP, DF and PHE treated with thermal plasma oxidation present a strong relationship, indicating that specific moieties of these molecules behave as electron donors. As previously stated, it is found that the $^{\bullet}OH$ plays a predominant role in both thermal plasma and UV-C/H_2O_2 oxidation (Graumans et al., 2020, 2021 and 2024). This is not solely based on the generated number of reactive species but also linked to the oxidation potentials of involved RONS (Bartberger et al., 2002; Cuerda-Correa et al., 2019; Hoeben, 2000; Rumble, 2023):

$^{\bullet}OH$ *(2.73 eV)* > **O_3** *(2.08 eV)* > **H_2O_2** *(1.78 eV)* > **$HO_2^{\bullet}$** *(1.65 eV)* > ONOOH *(1.60 eV)* > **NO_2** *(1.04 eV)* > **NO_3^-** *(0.96 eV)*

Table 6.3.
Oxidatively produced RONS half reactions including their reduction potential

Half reactions	E^0 (V)
$OH + H^+ + e^- \rightleftharpoons H_2O$	2.73
$O_3 + 2\ H^+ + 2\ e^- \rightleftharpoons O_2 + H_2O$	2.08
$H_2O_2 + 2\ H^+ + 2\ e^- \rightleftharpoons 2\ H_2O$	1.78
$HO_2 + 3\ H^+ + 3\ e^- \rightleftharpoons 2\ H_2O$	1.65
$ONOOH + H^+ + e^- \rightleftharpoons NO_2 + H_2O$	1.60
$NO_2 + H_2O \rightleftharpoons ONOOH + H^+$	1.04
$NO_3^- + 3\ H^+ + 2\ e\text{-} \rightleftharpoons HNO_2 + H_2O$	0.96

As a result, the visualised HOMO locations indicate structural moieties where $^{\bullet}OH$ radicals can react (**Table 6.4**). The three main chemical reactions initiated by $^{\bullet}OH$ radicals are:

1) Hydrogen (H) atom abstraction from aliphatic saturated (C-C) compounds at C-H positions;
2) Hydroxylation at unsaturated (C=C) alkene and aromatic compounds;
3) Hydroxyl radical interactions with S-, N- or P containing molecules (Minakata et al., 2009, 2015).

Table 6.4.
Pharmaceutical structures, physicochemical and quantum chemical properties

2D Pharmaceutical structures	Physico-chemical properties	3D Pharmaceutical structures with highest occupied molecular orbital (HOMO)			Expected oxidative degradation intermediates according to located HOMO position
		E_{HOMO} (eV)	E_{LUMO} (eV)	Energy gap ΔE (eV)	
Acetaminophen 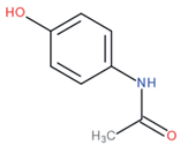	**g/mol** 151.16 **Log $P_{o/w}$** 0.91 **Pk_a** 9.46	-8.491	-0.059	8.432 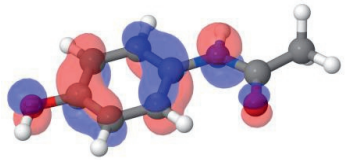	Acetaminophen → Hydroxylation 4-Acetylaminocatechol/ 3-Hydroxyacetaminophen 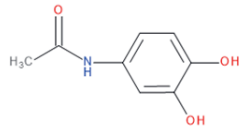
Diclofenac 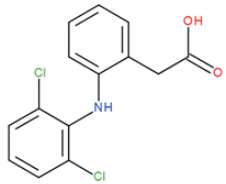	**g/mol** 296.15 **Log $P_{o/w}$** 4.26 **Pk_a** 4.01	-8.508	-0.443	8.065 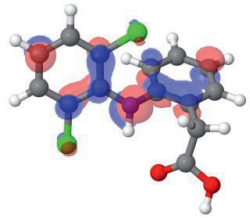	Diclofenac → Hydrxoxylation 4-hydroxy-Diclofenac or 5-hydroxy-Diclofenac 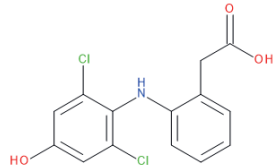

Table 6.4.*Continued*

Phenazone 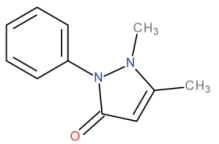	**g/mol** 188.23 **Log $P_{o/w}$** 1.22 **Pk_a** 0.49	-8.637 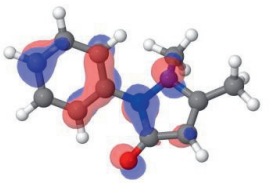	-0.305	8.332	Phenazone → Hydrxoxylation p-Hydroxyantipyrine 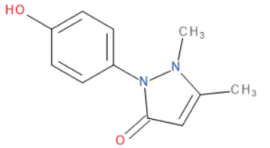
Carbamazepine 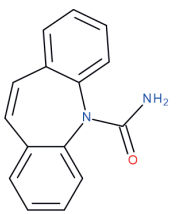	**g/mol** 236.27 **Log $P_{o/w}$** 2.77 **Pk_a** 15.96	-8.712 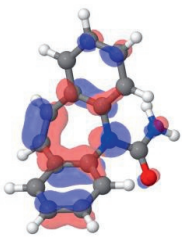	-0.569	8.143	Carbamazepine → Epoxidation Carbamazepine-10,11-epoxide 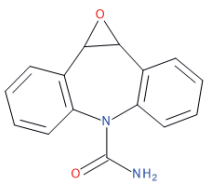
Metoprolol 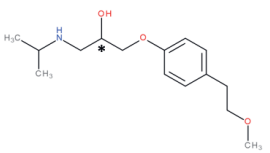	**g/mol** 267.36 **Log $P_{o/w}$** 1.76 **Pk_a** 14.09	-8.764 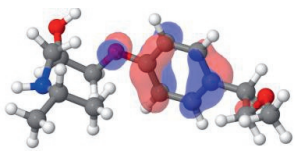	0.177	8.941	Metoprolol → Hydroxylation TP-MET 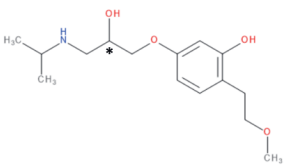

Table 6.4.*Continued*

Metformin 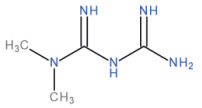	**g/mol** 129.16 **Log $P_{o/w}$** -0.92 **Pk_a** 12.33	-8.824	0.391	9.215 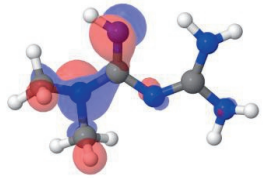	Metformin → dealkylation 1-Methylbiguanide 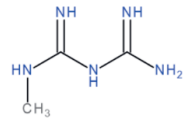
Ciprofloxacin 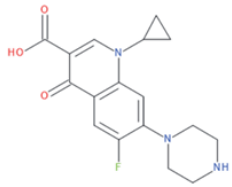	**g/mol** 261.09 **Log $P_{o/w}$** -0.77 **Pk_a** 5.96	-8.920	-0.92	8.000 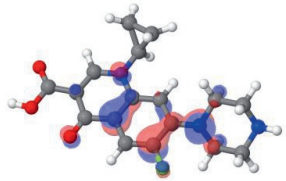	Ciprofloxacin → hydroxylation 8-Hydroxyciprofloxacin 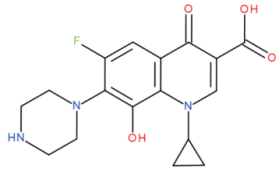
Terbutaline 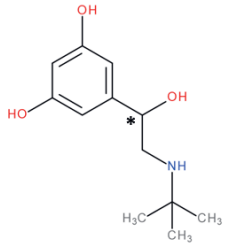	**g/mol** 225.28 **Log $P_{o/w}$** 0.44 **Pk_a** 8.86	-8.976	0.053	9.029 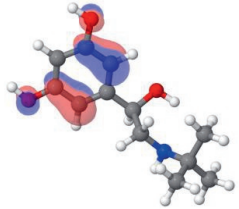	Terbutaline → Hydroxylation TER-intermediate 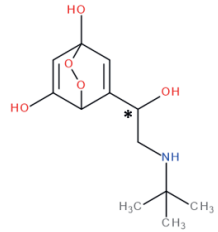

Table 6.4.*Continued*

Fluoxetine 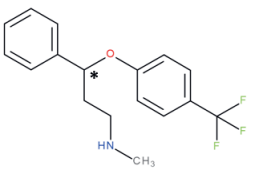	**g/mol** 309.33 **Log $P_{o/w}$** 4.17 **Pk_a** 9.4	-8.976	0.053	9.029 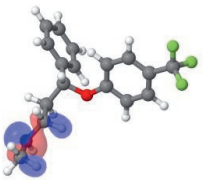	Fluoxetine → Dealkylation (s)-Norfluoxetine 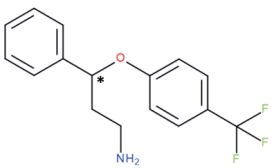
Doxycycline 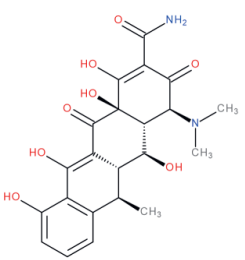	**g/mol** 444.43 **Log $P_{o/w}$** -3.49 **Pk_a** 3.24	-9.320	-1.434	7.886 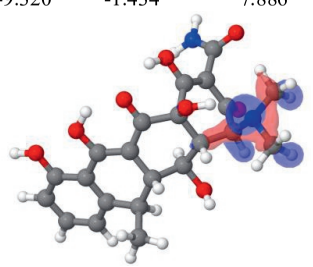	Doxycycline → Dealkylation n-Desmethyl doxycycline 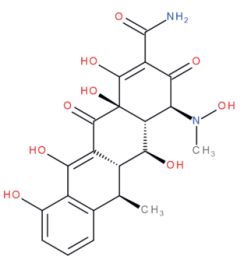
Diatrizoic acid 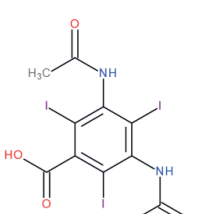	**g/mol** 613.91 **Log $P_{o/w}$** 2.89 **Pk_a** 3.24	-9.323	-1.668	7.655 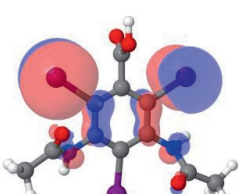	Diatrizoic acid → interaction with Iodide and Hydroxylation DIA-Intermediate 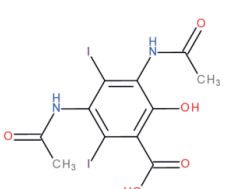

Table 6.4.*Continued*

Cyclophosphamide 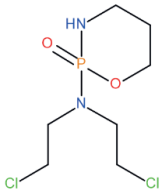	**g/mol** 261.09 **Log $P_{o/w}$** 0.10 **Pk_a** 13.48	-9.744	0.309	10.053 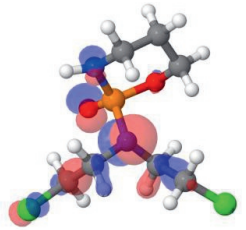	Cyclophosphamide → H-abstraction/hydroxylation next to the N position. 4-Hydroxycyclophosphamide 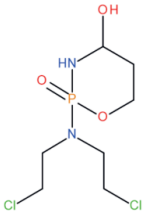
Iopamidol 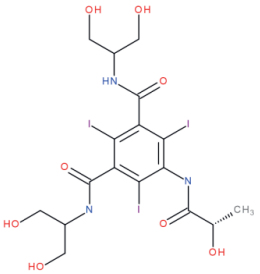	**g/mol** 777.09 **Log $P_{o/w}$** -0.74 **Pk_a** 12.21	-9.933	-2.183	7.750 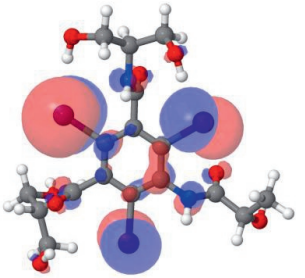	Iopamidol → interaction with Iodide and Hydroxylation IOP-intermediate 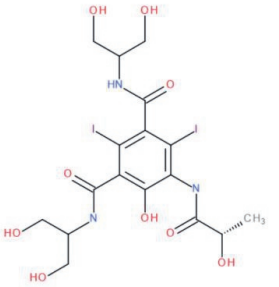

Table 6.4.*Continued*

Iomeprol 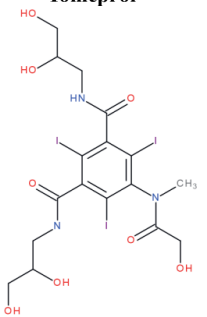	**g/mol** 777.09 **Log $P_{o/w}$** -1.45 **Pk_a** 11.05	-10.264	-2.457	7.807 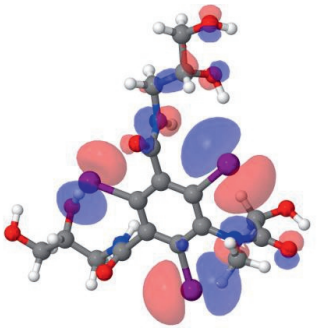	Iomeprol → interaction with I and Hydroxylation IOM intermediate 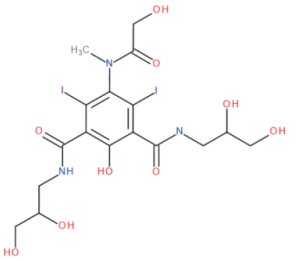

According to the visualised HOMO positions of the pharmaceuticals, structural moieties were denoted that are likely to react with electrophilic species by sharing their electrons. Based on these structural moieties, the expected oxidative transformation products were first shown according to •OH radical attack. Comparing expected degradation intermediates with well-known produced Phase I metabolites, it is clear that oxygenation reactions, listed in **Table 6.1**, result in similar biotransformation products. Although degradation is faster with thermal plasma or UV-C/H_2O_2 treatment, it is clear that any pharmaceutical is degradable. Depending on the AOP applied, matrix composition, concentration and reactivity of a molecular structure, multiple oxidative degradation pathways are possible and many different transformation products are expected over-time (Graumans et al., 2024). As seen in **Table 6.2**, DF, PHE, CB, MET, MF, TER, FLU and DOX all exhibit largely similar degradation characteristics when treated with thermal plasma or UV-C/H_2O_2 (Graumans et al., 2021). Based on their quantum chemical defined descriptors, it is denoted that for these pharmaceuticals hydroxylation and dealkylation reactions occur at structural moieties such as aromatic rings, unsaturated bonds or methyl groups substituted at the N atom (DOX, FLU and MF). Noteworthy is the slow degradation of MF, despite its expected nucleophilic appearance at the tertiary amine backbone. Amines and tertiary amines are considered as nucleophilic moieties, since these groups are capable of donating electrons to form a bond with an electrophile (Lee et al., 2015). However, the nucleophilicity of an amine is decreased when the structural moiety is substituted by electron withdrawing or bulky groups (Lee et al., 2015). The oxidative degradation of MF is further explained in section **6.3.1.1**. It is evident for the compounds APAP, CIP, CP, IOM, IOP and DIA that their degradation efficiency depends on the applied AOP technology. For these compounds it is thought that specifically produced ROS, RNS or photodegradation initiate their chemical abatement.

6.3.1.1 Degradation of metformin

The low degradation kinetics found for MF could be explained by its stability, since the computed 9.215 eV energy gap (ΔE) is the second largest found after that of CP (ΔE; 10.053) (**Table 6.4**). MF is a stable pharmaceutical, which is poorly metabolised, difficult to biodegrade and slowly photolytically altered (Lin et al., 2020; Parra-Marfil et al., 2023; Wols et al., 2013). Based on the physicochemical properties it is anticipated for MF that the protonated *β*- (1) and *γ*- (2) amine (NH_2^+) substituents lower the reactivity. MF (p*K*a 12.33) is primarily protonated within a pH range of 1 – 11 (Graumans et al., 2021), making the structure very water soluble, but also capable of reducing ROS such as •OH and $O_2^{\bullet-}$ (Khouri et al., 2004). Despite the antioxidant properties of MF it is clear that sufficient •OH radical addition eventually leads to

the abatement of the original structure (Khouri et al., 2004; Rossmann et al., 2023). Generated oxidative species can invade MF, showing good conversion levels primarily with thermal plasma treatment in SSW ($\bar{R}$ ~73%; $C_{t(120)}$) and HSW ($\bar{R}$ ~78%; $C_{t(120)}$). Gradual decline was found after UV-C/H_2O_2 application SSW ($\bar{R}$ ~10%; $C_{t(120)}$) and HSW ($\bar{R}$ ~14%; $C_{t(120)}$). In our study it is therefore anticipated that mainly the treatment in complex water matrices, such as SSW and HSW is effective. MF degradation is attributed to the continuous generation of ROS and RONS during thermal plasma treatment but might be also caused by the generation of additional $^{\bullet}$OH. In the presence of other constituents such as dissolved organic matter (DOM), fulvic acid, nitrate, chloride or bicarbonate, $^{\bullet}$OH radical formation might be further promoted (Lin et al., 2020; Wang et al., 2017; Westerhoff et al., 2007). In the presence of nitrate (NO_3^-) it is suggested that $^{\bullet}$OH radical formation is actually boosted by UV-C irradiance (**R2-4**) (Lin et al., 2020).

$$NO_3^- + h\nu \rightarrow NO_3^{-*} \qquad \textbf{(R2)}$$

$$NO_3^{-*} + h\nu \rightarrow NO_2^{-*} + O^{\bullet} \qquad \textbf{(R3)}$$

$$O^{\bullet} \xrightarrow{H_2O} NO_2^- \rightarrow + OH^- + {}^{\bullet}OH \qquad \textbf{(R4)}$$

Due to the continuous plasma discharge in SSW and HSW the formation of reactive species may be promoted further. Increased matrix conductivity can accelerate the formation of reactive species, since the plasma arc current is better facilitated by pre-existing ions (Graumans et al., 2021). A boosted plasma arc will increase chemical activity, stimulating the formation of multiple reactive species and emitting increased UV irradiance (Brisset et al., 2011; Hoeben et al., 2019; Shimizu et al., 2020; Thirumdas et al., 2018). Contrary, UV-C/H_2O_2 application is less likely to be promoted, as organic debris in SSW or HSW will absorb the UV-C irradiance, resulting in less effective formation of $^{\bullet}$OH or the formation of less reactive secondary radical species.

6.3.1.2 Degradation of acetaminophen

The aromatic ring structure of APAP is a reactive position according to the located HOMO. This is also confirmed by the calculated E_{HOMO} energy, indicating that high nucleophilicity is expected for APAP. In an extensive review about APAP degradation initiated by AOPs, the actual reactive positions were quantum-chemically computed (Qutob et al., 2022). The R-C-NH-R position was designated with the highest nucleophilicity, followed by the aromatic ring (Qutob et al., 2022). According to nucleophilicity of the R-C-NH-R moiety, it is indicated that APAP at this position will undergo a cleavage reaction, releasing acetamide and forming a hydroquinone after further hydroxylation (Qutob et al., 2022). This degradation pathway is very

likely to occur, as well as the hydroxylation step forming 3-hydroxyacetaminophen (Qutob et al., 2022). Hydroxyl substitutes in saturated (C-H) or unsaturated (C=C) bonds increase the reactivity of a molecule by donating its electron density in that area (Minakata et al., 2015). That there is a difference in the fast pseudo-first order kinetics between thermal plasma and UV-C/H_2O_2 oxidation is explained by the quantity of produced reactive species and the poor photolytic reactivity of APAP (Pozdnyakov et al., 2014; Wols et al., 2013). The average eV energy gap (ΔE; 8.432) for APAP compared to MF (ΔE; 9.125) or DIA (ΔE; 7.655) further confirms the stability against photolysis. It is found that low pressure (LP) UV-C irradiation at 254 nm is not favoured by APAP, and that the photolysis is likely to be stimulated with polychromatic medium pressure lamps (MP) (Pozdnyakov et al., 2014; Wols et al., 2013). For UV-C/H_2O_2 oxidation it is implied that the observed pseudo-first order kinetics in Milli-Q solely proceeds via hydroxyl radical attack. Regarding the production of reactive species it is found that with UV-C/H_2O_2 only a limited amount of $^{\bullet}$OH species can be formed from the one-time addition of 0.22 mM H_2O_2. Compared to thermal plasma treatment, RONS are continuously produced as long the plasma arc is discharged. The rapid APAP abatement during thermal plasma treatment is therefore mainly attributed to the many different available reactive species (Graumans et al., 2021).

6.3.1.3 Degradation of ciprofloxacin

In contrast to MF and APAP, the degradation of CIP is promoted by photolysis (Babić et al., 2013; Van Doorslaer et al., 2011). In addition to the electrophilic sensitive area, the middle aromatic ring, UV-C 254 nm irradiance can cause direct photolytic cleavage of the n-ethyl-piperazine side chain. CIP has multiple different ionisable groups, which is affecting its reactivity. Direct photolysis of CIP elapses much faster in basic (pH 8) than in acidic conditions (pH 4) (Babić et al., 2013). The UV-C/H_2O_2 observed pseudo-first order rate constant of 1.000 k (min^{-1}) in Milli-Q confirms this reaction mechanism, since UV-C/H_2O_2 treatment was carried out at more neutral pH conditions (pH ~ 7.6) than that of 120 min thermal plasma treatment (pH < 2) (Graumans et al., 2021 and 2022). Despite that CIP degrades very fast under unaffected UV-C irradiance, $^{\bullet}$OH radicals enhance the degradation mechanism. Thermal plasma oxidative treatment confirmed this observation, since in Milli-Q matrix ($\bar{R}$ ~99%; $C_{t(120)}$) also a moderately good pseudo-first order rate constant 0.030 k (min^{-1}) were observed in the absence of a strong UV-C source (Graumans et al., 2021).

6.3.1.4 Degradation of cyclophosphamide

For CP the highest ΔE of 10.053 and a low E_{HOMO} of -9.744 were computed, indicating that the reactivity with electrophilic species is low. Other properties indicate hydrophilicity ($P_{o/w}$: -0.92)

and demonstrate that the molecule in water can withstand direct photolysis (Graumans et al., 2020 and 2021; Wols et al., 2013). In the human body CP is also not directly reactive and needs activation via biotransformation. Despite that during UV-C/H_2O_2 sufficient •OH radicals are produced to initiate CP oxidative degradation, the abatement kinetics are slower than observed with thermal plasma treatment. As previously discussed, CP dissolution is expected to be catalysed by acidic pH, initiating nitration reactions that can assist the oxidative degradation (Graumans et al., 2020 and 2021). The lengthy oxidative degradation via •OH radical attack is further attributed to the structure of CP, demonstrating that the molecule reacts as an electrophile. The high calculated E_{LUMO} energy of 0.309 further confirms this, since the 2-chloroethyl amino side chain is responsible for electrophilic chemical reactions within the body. The LUMO position represents the electrophilic moiety which is the alkylating area that can bind with nucleophilic moieties (amino, phosphate or imidazole groups) in biological systems (LibreTexts; 2023).

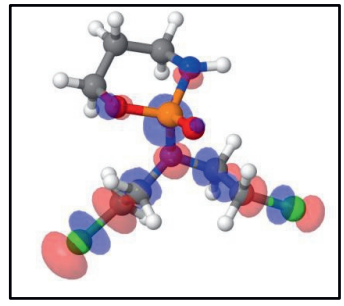

Fig. 6.2. Visualised LUMO positions of cyclophosphamide at the 2-chloroethyl amino side chain.

6.3.1.5 Degradation of X-ray contrast agents

Another remarkable result was observed for the X-ray contrast compounds IOM, IOP and DIA treated with UV-C/H_2O_2. For these compounds also a low nucleophilicity was calculated, suggesting that their reactivity with electrophilic species is expected to be low. For the oxidation with thermal plasma treatment this observation is correct, but on the contrary with UV-C/H_2O_2 treatment, fast abatement kinetics were seen. Poor oxidative degradation is attributed to the molecular structure, since the aromatic ring is fully substituted with large iodine (I) atoms (Zhao et al., 2014). For iopamidol (IOP), iomeprol (IOM) and diatrizoic acid (DIA) this fully substituted aromatic ring in combination with short side chains causes steric hindrance, negatively affecting the biodegradability (Banaschik et al., 2018; Nowak et al., 2020). The computed low nucleophilic E_{HOMO} energy for the X-ray contrast agents further confirms the hypothesis that frontier molecular orbitals play an important role in the oxidative degradation kinetics. Steric hindrance lowers the reactivity of a molecule, mainly when the nucleophilic

group, iodide, in the case of IOP, IOM and DIA, is shielded by interfering amide structures. These bulky groups reduce the reactivity and lower the nucleophilicity of a molecule (Vala et al., 2019; Wade, 2010). For the X-ray contrast agents, oxidative electrophilic species are expected to be hindered, but UV-C photolytic attack on these molecules is very effective (Allard et al., 2016). Compared to other tested pharmaceuticals, the HOMO-LUMO eV energy gaps are the smallest for IOP (ΔE; 7.750), IOM (ΔE; 7.807) and DIA (ΔE; 7.655), suggesting that wavelength absorbance is of influence on the contrast agents stability. UV-C irradiance causes deiodination resulting in an increased reactivity so that active oxygen and even ground state oxygen can better interact at the ipso positions of the aromatic ring (Graumans et al., 2021).

6.3.2 Effectiveness of oxidative treatment

During thermal plasma and UV-C/H_2O_2 oxidation it was found that all pharmaceuticals are affected by either UV-C irradiance, ROS or RONS. Depending on favoured oxidation pathways, deployment of AOPs is demonstrated to be a very effective application to degrade pharmaceuticals into multiple transformation products (Graumans et al., 2020, 2021, 2022 and 2024). Duration of chemical oxidation and the treated matrix composition will determine the overall, reduction in bioactivity and toxicity of unwanted pollutants. AOPs are capable of lowering the overall toxicity of hospital sewage water. It is clear that with hydroxyl radical oxidation, effective treatment can be achieved by ring opening and cleavage reactions, resulting in the formation of smaller aliphatic structures (Banaschik et al., 2018; Hoeben, 2000; Qutob et al., 2022). Organic compounds containing hydroxyl groups attached to a saturated or unsaturated moiety will further increase the electron density in that area (Hoeben, 2000; Minakata et al., 2015), which make the structures prone to further oxidative degradation. Rapid pharmaceutical degradation and the formation of aliphatic compounds is well explained for APAP, as it was found that multiple different oxidation pathways will result in smaller compounds, see **Fig. 6.3** (Qutob et al., 2022).

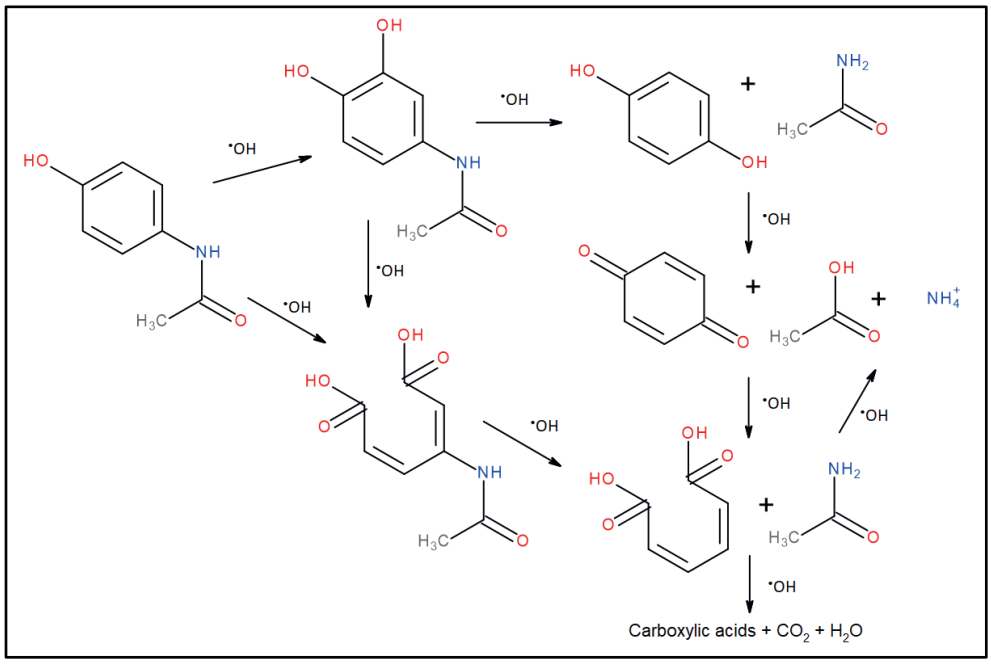

Fig. 6.3. Predicted degradation routes of acetaminophen (APAP) with hydroxylation and ring cleavage reactions as observed in the study of Qutob et al. (2022). Sufficient molecular degradation will result in small aliphatic carboxylic acids (Hoeben, 2000; Qutob et al., 2022).

Substituted carboxylic acids (RCOOH) or carboxylate (COO^-) functional groups decrease the reactivity of molecules (e.g. IOM, IOP, DIA) (Minakata et al., 2015; Puhlmann et al., 2021). These functional groups do have electron withdrawing effects, making molecules less prone to •OH radical invasion. Based on this molecular interaction it is expected that the smaller aliphatic compounds become the termination products of oxidatively treated pharmaceuticals. Carboxylic acids are relatively stable and are capable of forming hydrogen bridges in the water matrix, making them less reactive. Further degradation of carboxylic acids will eventually lead into mineralisation having CO_2 and H_2O as end products.

6.4 Conclusion

Usage of quantum chemical software packages for the localisation of molecular frontier orbitals is a valuable tool to indicate the reactivity and stability of a pharmaceutical. The energy of the determined highest occupied molecular orbital is used to demonstrate nucleophilicity. Specific nucleophilic functional groups can donate their electrons to an electrophile to form a chemical bond. The energy gap between the highest and lowest occupied molecular orbital (HOMO-LUMO) is a measure for a compound its stability. Molecular quantum chemical parameters were calculated and subsequently compared to thermal plasma technology and UV-C/H_2O_2 oxidative chemical abatement kinetics. For the pharmaceuticals APAP, DF and PHE treated with thermal plasma oxidation it was indicated that specific structure moieties are vulnerable for •OH electrophilic attack. In contrast, for the compounds DIA, CP, IOP and IOM it was found that reactivity with •OH radicals is lower, indicating that their chemical abatement is initiated by other reactive species. Due to the limited tested number of pharmaceuticals no direct statistical correlation was found between pseudo-first order degradation kinetics and the calculated quantum chemical HOMO positions. However, the currently determined quantum chemical parameters indicate that chemical abatement is initiated by either UV-C irradiance, ROS or RNS generated species. It is expected that the usage of quantum chemical calculations can be beneficial to determine the reactivity of micropollutants prior to oxidative treatment.

Literature

Asghar, A., Bello, M. M., Raman, A. A. A., Daud, W. M. A. W., Ramalingam, A., & Zain, S. B. M. (2019). Predicting the degradation potential of Acid blue 113 by different oxidants using quantum chemical analysis. *Heliyon*, *5*(9), e02396. https://doi.org/10.1016/j.heliyon.2019.e02396

Babić, S., Periša, M., & Škorić, I. (2013). Photolytic degradation of norfloxacin, enrofloxacin and ciprofloxacin in various aqueous media. *Chemosphere*, *91*(11), 1635–1642. https://doi.org/10.1016/j.chemosphere.2012.12.072

Banaschik, R., Jablonowski, H., Bednarski, P. J., & Kolb, J. F. (2018). Degradation and intermediates of diclofenac as instructive example for decomposition of recalcitrant pharmaceuticals by hydroxyl radicals generated with pulsed corona plasma in water. *Journal of Hazardous Materials*, *342*, 651–660. https://doi.org/10.1016/j.jhazmat.2017.08.058

Bartberger, M. D., Liu, W., Ford, E., Miranda, K. M., Switzer, C., Fukuto, J. M., Farmer, P. J., Wink, D. A., & Houk, K. N. (2002). The reduction potential of nitric oxide (NO) and its importance to NO biochemistry. *Proceedings of the National Academy of Sciences*, *99*(17), 10958–10963. https://doi.org/10.1073/pnas.162095599

Brisset, J.-L., Benstaali, B., Moussa, D., Fanmoe, J., & Njoyim-Tamungang, E. (2011). Acidity control of plasma-chemical oxidation: applications to dye removal, urban waste abatement and microbial inactivation. *Plasma Sources Science and Technology*, *20*(3), 034021. https://doi.org/10.1088/0963-0252/20/3/034021

Cuerda-Correa, E. M., Alexandre-Franco, M. F., & Fernández-González, C. (2019). Advanced Oxidation Processes for the Removal of Antibiotics from Water. An Overview. *Water*, *12*(1), 102. https://doi.org/10.3390/w12010102

Edward B. Walker. (n.d.). *LibreTexts Chemistry: Anticancer Drugs*. Retrieved November 1, 2023, from https://chem.libretexts.org/Bookshelves/Biological_Chemistry/Supplemental_Modules_(Biological_Chemistry)/Medicinal_Chemistry/Anticancer_Drugs

Engel, T. , & H. W. J. (2006). *Quantum chemistry and spectroscopy*. Pearson/Benjamin Cummings.

Fukui, K., Kato, H., & Yonezawa, T. (1961). A New Quantum-mechanical Reactivity Index for Saturated Compounds. *Bulletin of the Chemical Society of Japan*, *34*(8), 1111–1115. https://doi.org/10.1246/bcsj.34.1111

Fukui, K., Yonezawa, T., & Shingu, H. (1952). A Molecular Orbital Theory of Reactivity in Aromatic Hydrocarbons. *The Journal of Chemical Physics*, *20*(4), 722–725. https://doi.org/10.1063/1.1700523

Graumans, M. H. F., Hoeben, W. F. L. M., Ragas, A. M. J., Russel, F. G. M., & Scheepers, P. T. J. (2024). In silico ecotoxicity assessment of pharmaceutical residues in wastewater following oxidative treatment. *Environmental Research*, *243*, 117833. https://doi.org/10.1016/j.envres.2023.117833

Graumans, M. H. F., Hoeben, W. F. L. M., Russel, F. G. M., & Scheepers, P. T. J. (2020). Oxidative degradation of cyclophosphamide using thermal plasma activation and UV/H_2O_2 treatment in tap water. *Environmental Research*, *182*. https://doi.org/10.1016/j.envres.2019.109046

Graumans, M. H. F., Hoeben, W. F. L. M., van Dael, M. F. P., Anzion, R. B. M., Russel, F. G. M., & Scheepers, P. T. J. (2021). Thermal plasma activation and UV/H_2O_2 oxidative degradation of pharmaceutical residues. *Environmental Research*, *195*. https://doi.org/10.1016/j.envres.2021.110884

Graumans, M. H. F., van Hove, H., Schirris, T., Hoeben, W. F. L. M., van Dael, M. F. P., Anzion, R. B. M., Russel, F. G. M., & Scheepers, P. T. J. (2022). Determination of cytotoxicity following oxidative treatment of pharmaceutical residues in wastewater. *Chemosphere*, *303*. https://doi.org/10.1016/j.chemosphere.2022.135022

Hoeben, W. F. L. M. (2000). *Pulsed corona-induced degradation of organic materials in water*. Technische Universiteit Eindhoven. ISBN: 90-386-1549-3

Hoeben, W. F. L. M., van Ooij, P. P., Schram, D. C., Huiskamp, T., Pemen, A. J. M., & Lukeš, P. (2019). On the Possibilities of Straightforward Characterization of Plasma Activated Water. *Plasma Chemistry and Plasma Processing*, *39*(3), 597–626. https://doi.org/10.1007/s11090-019-09976-7

Kar, S., Sanderson, H., Roy, K., Benfenati, E., & Leszczynski, J. (2020). Ecotoxicological assessment of pharmaceuticals and personal care products using predictive toxicology approaches. *Green Chemistry*, *22*(5), 1458–1516. https://doi.org/10.1039/C9GC03265G

Karelson, M., Lobanov, V. S., & Katritzky, A. R. (1996). Quantum-Chemical Descriptors in QSAR/QSPR Studies. *Chemical Reviews*, *96*(3), 1027–1044. https://doi.org/10.1021/cr950202r

Khan, K., Baderna, D., Cappelli, C., Toma, C., Lombardo, A., Roy, K., & Benfenati, E. (2019). Ecotoxicological QSAR modeling of organic compounds against fish: Application of fragment based descriptors in feature analysis. *Aquatic Toxicology*, *212*, 162–174. https://doi.org/10.1016/j.aquatox.2019.05.011

Khouri, H., Collin, F., Bonnefont-Rousselot, D., Legrand, A., Jore, D., & Gardès-Albert, M. (2004). Radical-induced oxidation of metformin. *European Journal of Biochemistry*, *271*(23–24), 4745–4752. https://doi.org/10.1111/j.1432-1033.2004.04438.x

Klaassen, C. D. , C. L. J. , & D. J. (2013). *Casarett and doull's toxicology : the basic science of poisons (8th ed.). McGraw-Hill Education* (8th ed.).

Kostal, J., Voutchkova-Kostal, A., Anastas, P. T., & Zimmerman, J. B. (2015). Identifying and designing chemicals with minimal acute aquatic toxicity. *Proceedings of the National Academy of Sciences*, *112*(20), 6289–6294. https://doi.org/10.1073/pnas.1314991111

Lee, M., Zimmermann-Steffens, S. G., Arey, J. S., Fenner, K., & von Gunten, U. (2015). Development of Prediction Models for the Reactivity of Organic Compounds with Ozone in Aqueous Solution by Quantum Chemical Calculations: The Role of Delocalized and Localized Molecular Orbitals. *Environmental Science & Technology*, *49*(16), 9925–9935. https://doi.org/10.1021/acs.est.5b00902

Lin, W., Zhang, X., Li, P., Tan, Y., & Ren, Y. (2020). Ultraviolet photolysis of metformin: mechanisms of environmental factors, identification of intermediates, and density functional theory calculations. *Environmental Science and Pollution Research*, *27*(14), 17043–17053. https://doi.org/10.1007/s11356-020-08255-9

Minakata, D., Li, K., Westerhoff, P., & Crittenden, J. (2009). Development of a Group Contribution Method To Predict Aqueous Phase Hydroxyl Radical (HO•) Reaction Rate Constants. *Environmental Science & Technology*, *43*(16), 6220–6227. https://doi.org/10.1021/es900956c

Murrel, J. N. , K. S. F. A. , & T. J. M. (1985). *The chemical bond* (2nd ed.). Wiley.

Nolte, T. M., Chen, G., van Schayk, C. S., Pinto-Gil, K., Hendriks, A. J., Peijnenburg, W. J. G. M., & Ragas, A. M. J. (2020). Disentanglement of the chemical, physical, and biological processes aids the development of quantitative structure-biodegradation relationships for aerobic wastewater treatment. *Science of The Total Environment*, *708*, 133863. https://doi.org/10.1016/j.scitotenv.2019.133863

Nolte, T. M., & Peijnenburg, W. J. G. M. (2017). Aqueous-phase photooxygenation of enes, amines, sulfides and polycyclic aromatics by singlet (a1Δg) oxygen: prediction of rate constants using orbital energies, substituent factors and quantitative structure–property relationships. *Environmental Chemistry*, *14*(7), 442. https://doi.org/10.1071/EN17155

Nowak, A., Pacek, G., & Mrozik, A. (2020). Transformation and ecotoxicological effects of iodinated X-ray contrast media. *Reviews in Environmental Science and Bio/Technology*, *19*(2), 337–354. https://doi.org/10.1007/s11157-020-09534-0

Önlü, S., & Saçan, M. T. (2017). An in silico approach to cytotoxicity of pharmaceuticals and personal care products on the rainbow trout liver cell line RTL-W1. *Environmental Toxicology and Chemistry*, *36*(5), 1162–1169. https://doi.org/10.1002/etc.3663

Pandit, N. K. , S. R. , P. B. S. (2012). *Introduction to the pharmaceutical sciences: an integrated Approach* (2nd edtion). Lippincott Williams & Wilkins, a Wolters Kluwer business.

Parra-Marfil, A., López-Ramón, M. V., Aguilar-Aguilar, A., García-Silva, I. A., Rosales-Mendoza, S., Romero-Cano, L. A., Bailón-García, E., & Ocampo-Pérez, R. (2023). An efficient removal approach for degradation of metformin from aqueous solutions with sulfate radicals. *Environmental Research*, *217*, 114852. https://doi.org/10.1016/j.envres.2022.114852

Pozdnyakov, I. P., Zhang, X., Maksimova, T. A., Yanshole, V. V., Wu, F., Grivin, V. P., & Plyusnin, V. F. (2014). Wavelength-dependent photochemistry of acetaminophen in aqueous solutions. *Journal of Photochemistry and Photobiology A: Chemistry*, *274*, 117–123. https://doi.org/10.1016/j.jphotochem.2013.10.006

Puhlmann, N., Mols, R., Olsson, O., Slootweg, J. C., & Kümmerer, K. (2021). Towards the design of active pharmaceutical ingredients mineralizing readily in the environment. *Green Chemistry*, *23*(14), 5006–5023. https://doi.org/10.1039/D1GC01048D

Qutob, M., Hussein, M. A., Alamry, K. A., & Rafatullah, M. (2022). A review on the degradation of acetaminophen by advanced oxidation process: pathway, by-products,

biotoxicity, and density functional theory calculation. *RSC Advances*, *12*(29), 18373–18396. https://doi.org/10.1039/D2RA02469A

Rossmann, C., Ranz, C., Kager, G., Ledinski, G., Koestenberger, M., Wonisch, W., Wagner, T., Schwaminger, S. P., Di Geronimo, B., Hrzenjak, A., Hallstöm, S., Reibnegger, G., Cvirn, G., & Paar, M. (2023). Metformin Impedes Oxidation of LDL In Vitro. *Pharmaceutics*, *15*(8), 2111. https://doi.org/10.3390/pharmaceutics15082111

Royal Society of Chemistry. (n.d.). *Concepts from Quantum Mechanics* . Royal Society of Chemistry .

Shimizu, T., Kishimoto, N., & Sato, T. (2020). Effect of electrical conductivity of water on plasma-driven gas flow by needle-water discharge at atmospheric pressure. *Journal of Electrostatics*, *104*, 103422. https://doi.org/10.1016/j.elstat.2020.103422

Rumble, J. (2023). *104th Edition CRC Handbook of Chemistry and Physics* (104th ed.). Taylor & Francis Group.

Thirumdas, R., Kothakota, A., Annapure, U., Siliveru, K., Blundell, R., Gatt, R., & Valdramidis, V. P. (2018). Plasma activated water (PAW): Chemistry, physico-chemical properties, applications in food and agriculture. *Trends in Food Science & Technology*, *77*, 21–31. https://doi.org/10.1016/j.tifs.2018.05.007

Vala, R. M., Patel, D. M., Sharma, M. G., & Patel, H. M. (2019). Impact of an aryl bulky group on a one-pot reaction of aldehyde with malononitrile and *N* -substituted 2-cyanoacetamide. *RSC Advances*, *9*(49), 28886–28893. https://doi.org/10.1039/C9RA05975J

Van Doorslaer, X., Demeestere, K., Heynderickx, P. M., Van Langenhove, H., & Dewulf, J. (2011). UV-A and UV-C induced photolytic and photocatalytic degradation of aqueous ciprofloxacin and moxifloxacin: Reaction kinetics and role of adsorption. *Applied Catalysis B: Environmental*, *101*(3–4), 540–547. https://doi.org/10.1016/j.apcatb.2010.10.027

Voutchkova-Kostal, A. M., Kostal, J., Connors, K. A., Brooks, B. W., Anastas, P. T., & Zimmerman, J. B. (2012). Towards rational molecular design for reduced chronic aquatic toxicity. *Green Chemistry*, *14*(4), 1001. https://doi.org/10.1039/c2gc16385c

Wade, L. G. (2010). *Organic chemistry* (7th ed.). Pearson Prentice Hall.

Wang, Y., Roddick, F. A., & Fan, L. (2017). Direct and indirect photolysis of seven micropollutants in secondary effluent from a wastewater lagoon. *Chemosphere*, *185*, 297–308. https://doi.org/10.1016/j.chemosphere.2017.06.122

Westerhoff, P., Mezyk, S. P., Cooper, W. J., & Minakata, D. (2007). Electron Pulse Radiolysis Determination of Hydroxyl Radical Rate Constants with Suwannee River Fulvic Acid and Other Dissolved Organic Matter Isolates. *Environmental Science & Technology*, *41*(13), 4640–4646. https://doi.org/10.1021/es062529n

Wols, B. A., Hofman-Caris, C. H. M., Harmsen, D. J. H., & Beerendonk, E. F. (2013). Degradation of 40 selected pharmaceuticals by UV/H2O2. *Water Research*, *47*(15), 5876–5888. https://doi.org/10.1016/j.watres.2013.07.008

Zhang, Z., & Tang, W. (2018). Drug metabolism in drug discovery and development. *Acta Pharmaceutica Sinica B*, *8*(5), 721–732. https://doi.org/10.1016/j.apsb.2018.04.003

Zhao, C., Arroyo-Mora, L. E., DeCaprio, A. P., Sharma, V. K., Dionysiou, D. D., & O'Shea, K. E. (2014). Reductive and oxidative degradation of iopamidol, iodinated X-ray contrast media, by Fe(III)-oxalate under UV and visible light treatment. *Water Research*, *67*, 144–153. https://doi.org/10.1016/j.watres.2014.09.009

Chapter 7

General Discussion

7.1 Introduction

It is undisputable that action is needed to keep our aquatic environment and drinking water safe for the future. Usage of tertiary treatment steps to support conventional wastewater treatment can result in better removal of micropollutants. However, too diluted concentrations of pharmaceuticals and the presence of other organic pollutants that quench ROS or RONS might hamper the effective removal of unwanted pollutants. Deployment of available technology such as AOPs, reverse osmosis or PACAS adding need to be carefully considered since certain techniques require additional chemicals, filtration beds or UV sources. Additionally, the operational costs will increase and the waste production as well. It is therefore expected that the implementation of tertiary treatment techniques, such as advanced oxidation processes at the WWTP is still a challenge. In addition to the currently applied end-of-pipe WWTP solutions, it is therefore proposed to introduce AOPs at the contamination source.

In the studies described in this thesis, bench-scale thermal plasma technology has been extensively tested, indicating that this oxidation technique has the applicability to degrade pharmaceutical residues in complex matrices. Our work demonstrates that there is an opportunity for scale-enlargement and technology optimisation leading to an application that could be deployed as on-site sewage water treatment facility at the source. On-site thermal plasma treatment will lower the concentrated amounts of specific pharmaceuticals, metabolites and their transformation products before they enter conventional WWTPs at very low concentrations due to dilution.

7.2 Mitigation of unwanted substances is needed

To contribute to the mitigation of pharmaceutical emissions in sewage water it was aimed to demonstrate the effectiveness of on-site oxidative treatment. The following research objectives were explored in **Chapters 2** – **6**:

- **Chapter 2:** Does plasma activation of water degrade pharmaceuticals in (waste)water?
- **Chapter 3:** What is the effect of plasma treatment on complex water matrices containing multiple pharmaceutical residues?
- **Chapter 4:** Does plasma-induced oxidative degradation decrease the toxicity of treated water matrices?
- **Chapter 5:** Are predictive models applicable in providing indicative (eco)toxicity data by completing actual measured results?

- **Chapter 6:** How can quantum chemical calculations support the understanding of oxidative chemical degradation?

For this thesis 14 different substances were selected ranging from antibiotics, anti-epileptic, cytostatic, contrast agents, analgesic and anti-diabatic. Compounds selected were related to the MEDUWA-Vecht(e) project. Therapeutic classes relevant for the MEDUWA project had to comply with multiple selection criteria such as their measurement in surface water (the Vecht catchment NL-DE), consumption rate, biodegradability and expected ecotoxicity (Duarte, et al., 2022a; Duarte et al., 2022b).

An additional selection criterium included use frequency in the healthcare sector. The 14 selected compounds; iomeprol, iopamidol, diatrizoic acid, doxycycline, ciprofloxacin, fluoxetine, diclofenac, metoprolol, cyclophosphamide, carbamazepine, terbutaline, phenazone, acetaminophen and metformin aim to represent a wide range of multiple pharmaceutical classes.

All chapters (**1** – **6**) provided data regarding pharmaceutical degradation and their potential (eco)toxicity prior and after thermal plasma and UV-C/H_2O_2 (waste)water treatment. Despite the extensive dataset obtained for the 14 selected pharmaceuticals, it is difficult to directly implement and scale-up plasma technology. The currently presented information is retrieved by laboratory scale experiments and therefore it is advisable to start with manageable pilot-scale source-oriented treatment experiments. The currently presented data can act as guidance to demonstrate the effectiveness of scaling-up AOP technology. Based on **Chapter 5** and **6** it is anticipated that usage of *in silico* tools in combination with measured data can result in better targeted experiments (**Fig. 7.1.**).

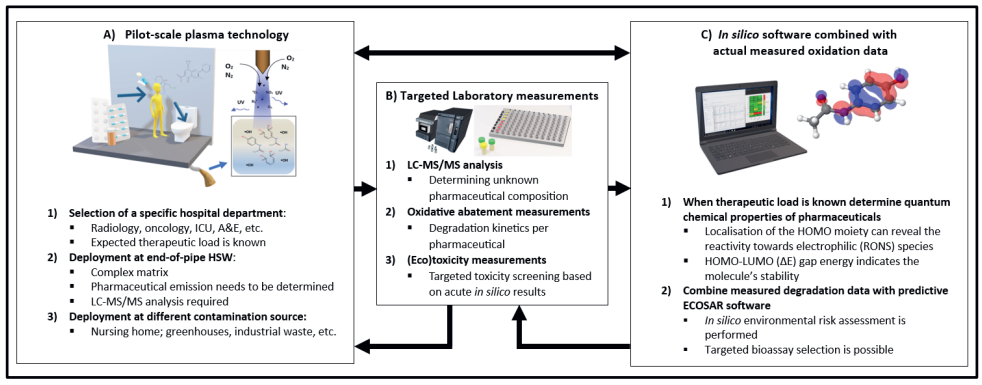

Fig 7.1. Based on the **Chapters 2-6**, it is expected that the combination of measured data and computer software will result in target specific evaluations and further AOP development. For the deployment of on-site plasma technology multiple pilot-scale experiments are possible (**A**). Data evaluation using analytical measurement or bioassays (**B**) will show the technique its efficiency. To optimise the pilot-scale set up, it is encouraged to use quantum chemical calculations and *in silico* environmental risk assessment tools (**C**).

7.3 Comparable expected degradation kinetics for similar pharmaceutical classes

Despite that the focus of this research is on the removal of a selection of 14 pharmaceuticals it was expected to find some generic principles that could be applied to the oxidative treatment for other chemical substances. Previous studies on AOP have demonstrated benefits of this technology for other chemicals than pharmaceuticals, such as dyes and pesticides (Magureanu et al., 2015, 2018). Based on the distinctively treated chemical structures it was attempted to interpret the differences in obtained pseudo-first order kinetics. Only for the structurally similar X-ray contrast agents, a class-comparable oxidative degradation could be confirmed. IOM and IOP are structurally nearly identical (IOM, $C_{17}H_{22}I_3N_3O_8$; 777.085 g/mol and IOP, $C_{17}H_{22}I_3N_3O_8$; 777.085 g/mol, see **Table 6.4**, **Chapter 6**), demonstrating comparable chemical abatement kinetics k min^{-1} 0.009 ($\bar{R}$%: 67) and k min^{-1} 0.008 ($\bar{R}$%: 63) after 120 min plasma treatment. UV-C/H_2O_2 oxidative degradation resulted in k min^{-1} 0.477 ($\bar{R}$%: 100) and k min^{-1} 0.587 ($\bar{R}$%: 100). Despite that IOM and IOP are structure isomers, they have distinct arrangements, which may cause deviation in physicochemical properties (Loftsson, 2014). When the structural arrangement is nearly similar, chemical abatement kinetics for structurally comparable substances are expected to be similar. It may be assumed that this is also true for the NSAIDs diclofenac (DF), ibuprofen (IBP), naproxen (NPX), and ketoprofen (KP). Identification of quantum chemical parameters provide for DF and NPX analogous E_{HOMO} (eV)

energies (-8.508 and -8.520) which might be linked to the aromatic ring structure where the HOMO frontier orbital mainly is found, see **Table 7.1**.

Table 7.1.

NSAIDs structures and their quantum chemical properties

2D structures	Physico-chemical properties	3D structures with highest occupied molecular orbital (HOMO)		
		E_{HOMO} (eV)	E_{LUMO} (eV)	Energy gap EΔ (eV)
Diclofenac 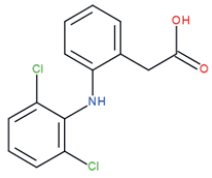	**g/mol** 296.15 **Log $P_{o/w}$** 4.26 **Pk_a** 4.01	-8.508	-0.443	8.065 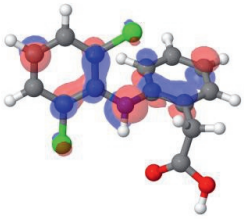
Naproxen 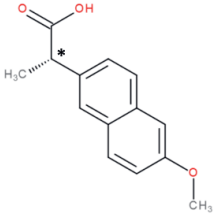	**g/mol** 230.26 **Log $P_{o/w}$** 2.99 **Pk_a** 4.24	-8.520	-0.543	7.977 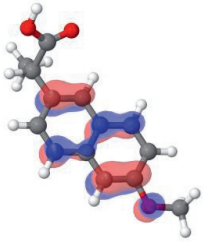
Ibuprofen 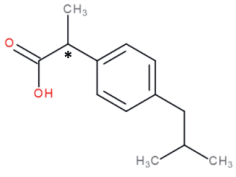	**g/mol** 206.29 **Log $P_{o/w}$** 3.84 **Pk_a** 4.85	-9.245	0.226	9.471 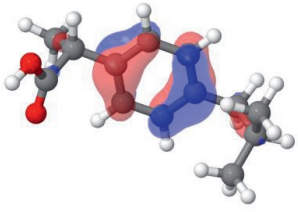
Ketoprofen 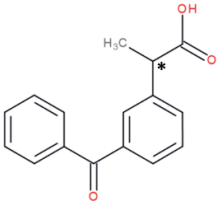	**g/mol** 254.26 **Log $P_{o/w}$** 3.61 **Pk_a** 4.00	-9.924	-0.621	9.303 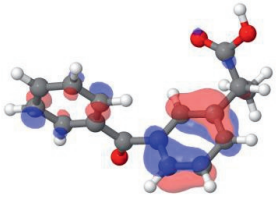

Higher expected reactivity for DF compared to KP is attributed to the tertiary amine coupled to the aromatic ring. The localised HOMO for DF is also seen at the R-NH-R position and is expected to increase the nucleophilicity. Non-bulky tertiary amines are considered as high nucleophilic moieties capable of donating a lone pair to form bonds (Ashenhurst, 2022).

Rapid conversion seen for DF using both thermal plasma and UV-C/H_2O_2 oxidation (**Chapter 3**), indicate that the molecular similarities for IBP, NPX and KF lead to comparable degradation reactions. Based on previous studies it is suggested that 500 µg/L DF in Milli-Q demonstrated a comparable exponential decay rate after immersed non-thermal plasma (80 kV high voltage pulse, 20 Hz repetition rate) application. In the study of Banaschik and co-workers hydroxyl radical reactions were designated as the main oxidative pathway. The degradation kinetics for IBP was slower, but with still a good conversion ratio ($\bar{R}$%: 80%) after 60 min of treatment (Banaschik et al., 2018). Slower degradation for IBP (ΔE 9.471) can be explained, based on its computed stability compared to DF (ΔE 8.065) and NPX (ΔE 7.977). Usage of non-thermal dielectric barrier discharge (DBD; 21 kV at 5-20 kHz) in deionised water, resulted in a complete conversion of 50.000 µg/L DF and IBP within 20 min (Hama Aziz et al., 2019). A similar result was seen for 50.000 µg/L KP in tap water, which was completely mineralised within 120 min using electro-Fenton and anodic oxidation processes (Feng et al., 2014). Degradation kinetics of KP in tap water including a Fe^{2+} catalyst for electro-Fenton or Na_2SO_4 as supporting electrolyte, elapsed via pseudo first-order kinetics initiated by $^{\bullet}OH$ radical attack. Also 100.000 µg/L NPX decomposed well via pseudo-first-order degradation kinetics after plasma discharges in liquid (200 – 250V at 21 – 30 kHz). (Park et al., 2021). Multiple hydroxyl radical reactions were proposed, indicating the mineralisation possibilities via decarboxylation, dehydration, demethylation and hydroxylation (Park et al., 2021). Based on these abatement kinetics of multiple separate AOP studies, it is clear that the NSAID pharmaceuticals DF, IBP, KP and NPX are susceptible to degradation via comparable $^{\bullet}OH$ radical degradation pathways.

7.4 Lowered toxicity

Sufficient oxidative degradation of a contaminated water matrix will eventually lead to reduced toxicity (**Chapter 4** and **5**). Hospital sewage is defined as a toxic matrix containing pathogens and related toxins, hormones, detergents, disinfectants, pharmaceuticals and metabolites. Acute toxicity of untreated HSW was found after 24h and 48h exposed to HeLa cells (**Chapter 4**). Comparable results were found in ecotoxicity studies showing that unfiltered and filtered HSW effluent can cause mortality in *Daphnia magna, Vibrio fisheri* and *Pseudokirchneriella subcapitata* species (LC_{50}), ranging from 0.7 up to 90% (Orias & Perrodin, 2013). In our

cytotoxicity study we observed reduced toxicity by direct oxidative treatment in hospital effluent (**Chapter 4**). Insufficient pharmaceutical degradation can result in the formation of unwanted transformation products. Spiked surrogate matrices like Milli-Q and synthetic sewage were also oxidatively treated and directly exposed to HeLa cells. From these results it was concluded that too short or too long AOP treatment might cause undesired effects. Too short treatment can result in partial conversion of unwanted pharmaceuticals. Primarily, after 5 - 15 min plasma treatment, Milli-Q demonstrated increased oxidative stress in HeLa cells, which was attributed to the potentially formed degradation intermediates. Despite the elevated levels of oxidative stress measured, a minimal reduction of viability was observed. Too long treatment might result in residual reactive oxygen species or the formation of an acid cell-irritating environment. Prolonged plasma treatment in Milli-Q resulted in a decline in viability, which is expected to derive from plasma activated water itself and to a lesser extent from the degraded pharmaceuticals. Comparable elevated oxidative stress levels after UV-C/H_2O_2 treatment were seen, indicating that the degradation intermediates caused this effect in treated Milli-Q. Less erratic effects were found after oxidative treatment in synthetic sewage water, indicating that organic matter and minerals in the matrix neutralised produced RNS and ROS (**Chapter 4**). This buffer capacity is even higher for real sewage water since UV-H_2O_2 treatment showed much slower pharmaceutical degradation kinetics compared to thermal plasma oxidation (**Chapter 3**). Thermal plasma is therefore still preferred over UV-C/H_2O_2 treatment, as inhibiting constituents present in sewage water will lower the effectiveness of this AOP application (**Chapter 3**). Sufficient AOP treatment capacity is beneficial to lower the overall toxicity, but further dilution with non-toxic sewage water is required.

To achieve adequate degradation of metabolites, pharmaceuticals, hormones and other organic micropollutants the purpose is to reduce toxicity by the formation of smaller and less reactive degradation intermediates. It is expected that with oxidative treatment at the source this can be achieved, because high concentrations are more rapidly and effectively broken down into smaller transformation products such as aliphatic compounds (Banaschik et al., 2018; Hoeben et al., 2000; Isarain-Chávez et al., 2011; Qutob et al., 2022; Tisler et al., 2019; Tisler & Zwiener, 2019; Yang et al., 2018). Further analysis with QSAR-based predictions shows that certain oxidative transformation products are less toxic to aquatic species such as fish, Daphnia and green algae. High hydrophobicity (>0 Log $P_{o/w}$) and increased nucleophilic properties are both correlated with toxicity (Kar et al., 2020; Kostal et al., 2015; Voutchkova-Kostal et al., 2012). On the opposite, hydrophilic properties and compounds with increased number of RCOOH

groups are identified as QSAR predictors of reduced toxicity (Önlü & Saçan, 2017). Further elaboration on these parameters can depict that toxicity is decreased when pharmaceuticals are oxidatively treated by increasing the hydrophilicity and eventually degrade to carboxylic acids (**Fig. 7.2**).

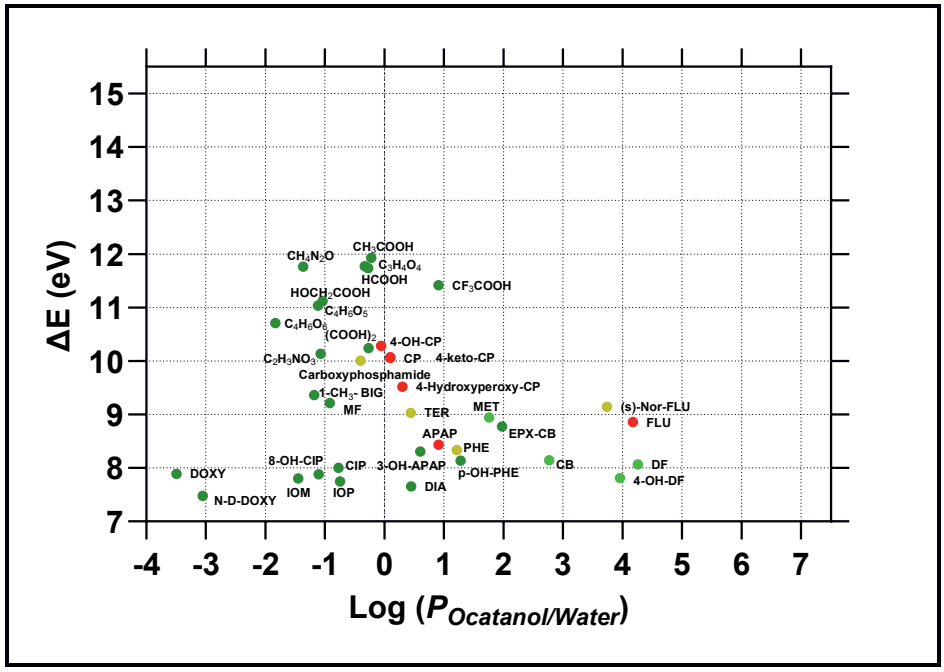

Fig 7.2. ECOSAR LC_{50} (mg/L) predictions were determined for pharmaceuticals (iomeprol (**IOM**), iopamidol (**IOP**), diatrizoic acid (**DIA**), doxycycline (**DOXY**), ciprofloxacin (**CIP**), fluoxetine (**FLU**), diclofenac (**DF**), metoprolol (**MET**), cyclophosphamide (**CP**), carbamazepine (**CB**), terbutaline (**TER**), phenazone (**PHE**), acetaminophen (**APAP**), metformin (**MF**)) their expected hydroxylation transformation products ((8-Hydroxyciprofloxacin (**8-OH-CIP**), n-Desmethyl-doxycycline (**N-D-DOXY**), (s)-Norfluoxetine (**(s)-Nor-FLU**), 4-Hydroxydiclofenac (**4-OH-DF**), 4-Hydroxycyclophosphamide (**4-OH-CP**), 4-keto-cyclophosphamide (**4-keto-CP**) Carbamazepine-10,11-epoxide (**EPX-CB**), p-Hydroxyantipyrine (**p-OH-PHE**), 3-Hydroxyacetaminophen (**3-OH-APAP**), 1-Methylbiguanide (**1-CH_3-BIG**)) and eventually the potential formed carboxylic acids (Acetic acid (**CH_3COOH**), Formic acid (**HCOOH**), Glycolic acid (**$HOCH_2COOH$**), Malic acid (**$C_4H_4O_4$**), Malonic acid (**$C_3H_4O_4$**) Oxalic acid (**$(COOH)_2$**), Oxamic acid (**$C_2H_3NO_3$**), Tartaric acid (**$C_4H_6O_6$**), Trifluoroacetic acid (**CF_3COOH**), Urea (**CH_4N_2O**). LC_{50} values were plotted for each compound according to their calculated energy gap (**ΔE**) and Log $P_{o/w}$ values. Daphnia 48h LC_{50} predictions were used classified as; ■ *not harmful* (>100 mg/L); ■ *harmful* (10-100 mg/L); ■ *toxic* (1-10 mg/L) and ■ *very toxic* (<1 mg/L) (European Chemicals Bureau, 2003; Commission Directive 93/67/EEC; Notified in Accordance with Council Directive 67/548/EEC, 1993 **Chapter 5**).

Based on the QSAR results presented in **Chapter 5**, Daphnia was found to be the most vulnerable test organism when exposed to environmental contaminants. Earlier estimated risk

quotients (RQ) for APAP (RQ; *toxic*) and CP (RQ; *moderate*) indicated ecotoxic levels characterised in untreated HSW. The currently plotted LC_{50} values for APAP, FLU and CP demonstrate that these substances are all likely to be *very toxic* for Daphnia. Other pharmaceuticals were predicted to be potentially *toxic*, based on their structural appearance are PHE and TER. Oxidative treatment will result in lowered toxicity since for the majority of the hydroxylated structures (CB-epoxide; p-hydroxy-PHE; 3-hydroxy-APAP and (s)-Nor-FLU) and for a ring opened structure, lower toxicity of carboxyphosphamide (**Chapter 2**) was determined. Adequate oxidative treatment will therefore result in more hydrophilic products, which in some cases (4-hydroxy-DF; p-hydroxy-PHE; 8-hydroxy-CIP; n-desmethyl-DOXY; 4-hydroperoxy-CP and 3-hydroxy-APAP) are indicated to be more reactive compared to the parent pharmaceutical ingredient, making them more prone for further break down, which results in even smaller fragments. This observation is in line with the details presented in **Chapter 5** and paragraph 3.2 of **Chapter 6**, leading to favoured carboxylic acids. These relatively small degradation products have hydrophilic properties Log $P_{o/w}$ <0, and indicate increased stability >10 ΔE (**Fig. 7.2.**). According to our results it is assumed that incomplete mineralisation will be already beneficial to lower the aquatic toxicity. It is therefore expected that incomplete mineralisation is also favourable for conventional wastewater treatment plants, because hydroxylated and carboxylic degradation products become better biodegradable.

7.5 Increased biodegradation

With the deployment of AOPs at the wastewater treatment plants, combined with conventional wastewater treatment options, it is presumed that certain unwanted organic micropollutant levels are too low to be effectively eliminated. Some of these limitations complicate the scaling-up of AOPs (see **Chapter 1**, **table 1.2** for details). It is expected that oxidative treatment at the contamination source will be more feasible. In the case of specialised hospital departments, such as accident and emergency (A&E); cardiology, intensive care unit (ICU), oncology or radiology, plasma technology can be introduced at toilet facilities for the oxidative degradation of specific unwanted pharmaceuticals. Depending on the type of healthcare provided, it is supposed that the plasma technology could be integrated in the current workflow of disposal of patient urine. According to HSW matrix we characterised, an antibiotic (CIP), painkillers (DF, APAP), a cytostatic drug (CP), beta-blockers (MET) and X-ray contrast agents (IOM and DIA) are found in the effluent (**Chapter 3**). Their constant presence contributes prominently to the medicinal load discharged into the sewer system. Observed critical pharmaceutical residues present in HSW need to be inactivated and degraded to lower their chemical reactivity or

toxicity (**Chapter 4**). Despite further dilution through the sewer system, the continuous load of pharmaceutical residues and fluctuating concentrations might cause inhibition of WWTP biofilm activity. Glucuronide-containing metabolites (**Chapter 4** and **Chapter 5**), are possibly converted back into the parent compound by WWTP biofilm (**Chapter 1**; Ajo et al., 2018). Microorganisms utilise organic matter to serve as nutrients, such as amino acids, fatty acids and carbohydrates (Peake et al., 2016; Puhlmann et al., 2021). Conjugated metabolites often have a glucuronide containing moiety, which is unfortunately the preferred area that serves as nutrient. In the presence of oxygen, biodegradation primarily occurs by oxygenase reactions. Molecular structures are usually degraded by the insertion of oxygen. In the biodegradability of molecules it is well established that less complex moieties are preferred by microorganisms. Highly substituted and branched alkanes are more difficult to be converted by biodegradation. Other complex features are steric hindrance, multiple combined aromatic rings, electron withdrawing substituents (I, Cl, F or R-O-R) or nitrogen, sulphur and phosphorus containing compounds (Puhlmann et al., 2021). Generally, compounds with hydroxy groups and medium polarity demonstrate good biodegradability as hydroxy groups are ascribed as a good starting point for further degradation. Another feature which is beneficial for biodegradation is improved hydrolysis of bonds such as amides (R-C=O-N-R) and esters (R-C=O-OR). Lowered nucleophilicity and increased hydrophilicity are preferred structural requirements to reduce the (eco)toxicity. Structural changes obtained after oxidative treatment will enhance the possibilities of further biodegradation. Oxidative treatment of pharmaceuticals resulted in the alteration of specific physicochemical parameters, such as increase in polarity by hydroxylation (**Fig. 7.2**), ring opening and dealkylation, all lowered the molecular complexity. Not only decreasing the Log $P_{o/w}$ is beneficial for improved biodegradation, but also reduced hydrophobicity of the oxidative intermediate lowers the sorption potential towards the active sludge. Prolonged thermal plasma treatment might result in a too low pH (< 2.0) of the matrix (**Chapter 3** and **4**). However, when the oxidatively treated sewage water is mixed and further diluted with other wastewater streams there will be minimal consequences for conventional WWTPs. Furthermore, it is supposed that optimal treatment times could be determined, with only minimal effect on pH. An additional advantage of thermal plasma treatment is that pathogens and virus particles are also deactivated. The ROS and RNS species produced, such as H_2O_2 and ONOOH, contribute to disinfection of *Escherichia coli* (Perinban et al., 2022). Therefore, not only the removal of medicinal residues is beneficial but also the potential of removing unwanted pathogens, lowering indirectly the problem of AMR.

7.6 Safe and sustainable by design

Not only the focus on additional water purification steps is required for the removal of unwanted chemicals from the hydrosphere, but also the design towards better degradable chemicals is preferred. Following this principle, EU policy attempts to stimulate the design of green chemicals which could be better mineralised in the environment (Puhlmann et al., 2021). An example of the benign by design principle is the candidate ciprofloxacin-Hemi (CIP-Hemi) which is an analogue of the antibiotic ciprofloxacin (CIP) (Leder et al., 2021). The antibiotic and metabolic properties of CIP-Hemi are maintained while the environmental properties are improved compared to CIP (**Fig. 7.3**).

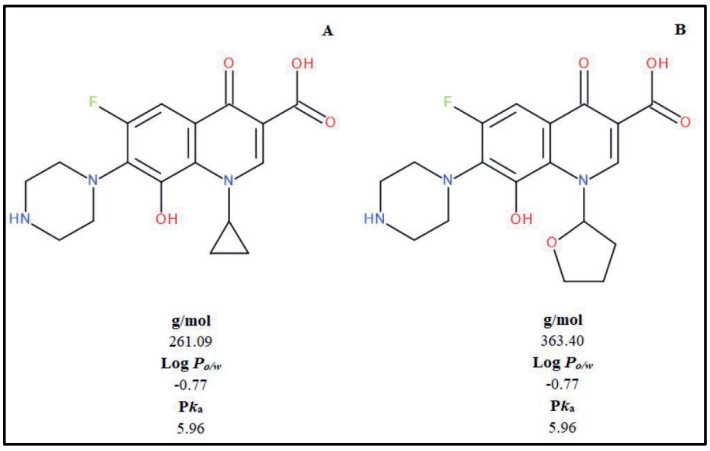

Fig 7.3. Ciprofloxacin (**A**) in poorly biodegradable and certain bacteria developed resistance to this pharmaceutical. With the usage of *in silico* and *in vitro* tools CIP-Hemi (**B**) was designed to be better degradable in the environment but preserving the antibiotic activity in humans (Leder et al., 2021). Environmental emission of CIP-Hemi results in biodegradability by hydrolytic cleavage of the tetrahydrofuranyl. The tetrahydrofuranyl is completely mineralised by 3 reaction steps via 1) hydrolysis into 4-hydroxybutanal and 2) oxidation into γ-hydroxybutanoic acid which 3) eventually mineralises into H_2O and CO_2. The remaining persistent fluoroquinolone fragment after the loss of the tetrahydrofuranyl moiety has reduced antibacterial activity making the compound less reactive in the environment (Castiello et al., 2023; Leder et al., 2021; Puhlmann et al., 2021).

For the prevention and treatment of diseases, several thousand APIs are available on the market (Pandit, 2012; Puhlmann et al., 2021) and annually a varying number of new therapeutic compounds are by the European Medicine Agency (EMA) recommended for marketing authorisation within the European Union. In the year 2022, *41* new active substances were proposed and in 2023, *39* compounds were suggested for authorisation (European Medicine Agency, 2023; European Medicines Agency, 2024). With the EU's chemicals strategy for sustainability towards a toxic-free environment, the innovation for safe and sustainable chemicals is promoted (European Commission, Chemicals strategy). The safe and sustainable

by design (SSbD) concept is promoted in addition to lowering the pharmaceutical emission and encouraging appropriate disposal, (Kümmerer et al., 2018; Puhlmann et al., 2021). With SSbD it is stimulated that pharmaceuticals in their developmental stage require a design which allows biodegradation that result in H_2O, CO_2 and minerals (Kümmerer et al., 2018). Joining the forces of *in silico* predictions with *in vitro* biodegradation studies, new chemical structures can be designed and tested. Alterations in the chemical structure should result in changes of physicochemical properties improving the biodegradability. Structure changes are attempted at molecular positions without comprising the pharmaceutical its activity (Puhlmann et al., 2021). AOPs placed at the contamination source integrated with other available technologies are expected to be more effective than stand-alone solutions or than techniques placed further downstream after conventional applications. A combination of SSbD pharmaceuticals, greener API production and behavioural changes will eventually lead to the most prominent pharmaceutical discharge reduction (Puhlmann et al., 2021). Our increased knowledge about pharmaceutical residues, their biological interactions and the risks towards organisms and the environment can be used to design less harmful and better (bio)degradable substances (Puhlmann et al., 2021). It is therefore anticipated that with new insights, behavioural change, valuable monitoring information and applicable AOPs prior to WWTP deployment, will contribute to an integrated solution to attain a sustainable and clean aquatic environment.

7.7 Further development and recommended research for plasma oxidation

The discharge of many different substances via industrial, domestic and hospital sewage water could be minimised and regulated by public awareness, design of better (bio)degradable chemicals and good monitoring. Advanced oxidation processes could be part of this comprehensive approach. Suspect-screening and targeted monitoring data could serve as an early warning system for emerging risks (Egli et al., 2023). In addition to pharmaceuticals, antibiotics and microplastics have recently been found in the hydrosphere as well as in human blood (Leslie et al., 2022). It is expected that the presence of microplastics in the aquatic environment serves as a host for biofilms. Accumulation of plastic micropollutants together with unwanted pharmaceutical substances can result in increased antimicrobial resistance (Pham et al., 2022). Additionally, we need to be aware of the extensive use of drugs of abuse (DoA) and legal highs. Similar as pharmaceuticals, DoA have also very specific bioactive effects (Gomez Cortes et al., 2022). When using reliable monitoring data combined with *in silico* predicative tools and bioassays, it is expected that immediate action can be taken to assess

a potential aquatic toxicity risk. Small scale AOP applications could become part of a remediation plan. An example is the use of plasma technology integrated in toilet facilities at crowded locations with clusters of individuals with an average higher intake of pharmaceuticals such as hospitals or use of synthetic drugs at music festivals. Additionally, in the case of specific contaminated locations direct AOP deployment can be suggested for greenhouse sewage water after pesticide usage or at sewer overflow points causing the direct emission of pollutants into surface waters, see **Fig 7.4**.

To further develop plasma oxidation into a technique suitable for treatment-at-the-source additional research is advisable. To overcome certain limitations of this study it is recommended to know the complete wastewater composition (**Chapter 3**). The limited number of identified pharmaceuticals in hospital sewage do not represent the entire composition. The current study presented primarily the degradation of pharmaceuticals, but it is expected that the high concentrations of produced H_2O_2, HNO_3 and RONS will also inactivate bacteria such as *E.coli* or other pathogens (**Chapter 4**). Other components present in sewage water can inhibit or stimulate the oxidative treatment process. Furthermore, there is a great uncertainty regarding the infinite complexity of potentially formed transformation and oxidative termination products. With better knowledge of the complete composition of sewage water it is expected that an increased removal efficiency could be determined. In addition to the degradation effectiveness, it is also important to determine the operational costs of a pilot-scale technology. Many different parameters must be taken into account when determining costs, but this estimation was beyond the scope of this thesis. Nonetheless, it is presumed that with a much more powerful plasma technology, the desired oxidative effects could be achieved readily and rapidly. A futuristic example could be data (Artificial Intelligence) and (bio)sensor-driven AOP technology. It is assumed that the oxidative generation of reactive species could be adjusted for specific contaminants.

The results presented in this thesis can be used for the further development of a small and dedicated plasma unit that can be applied at the source. The laboratory scale experiments have shown that thermal plasma treatment is a promising technology for the rapid degradation of pharmaceuticals that leads to a reduction of toxicity of HSW. The results further indicate that the deployment of plasma technology is not limited to the abatement of pharmaceuticals but could also be a useful for the oxidative treatment of other contaminants such as dyes, plant protection products, pathogens, chemical spill or illegal drugs present in an aqueous matrix.

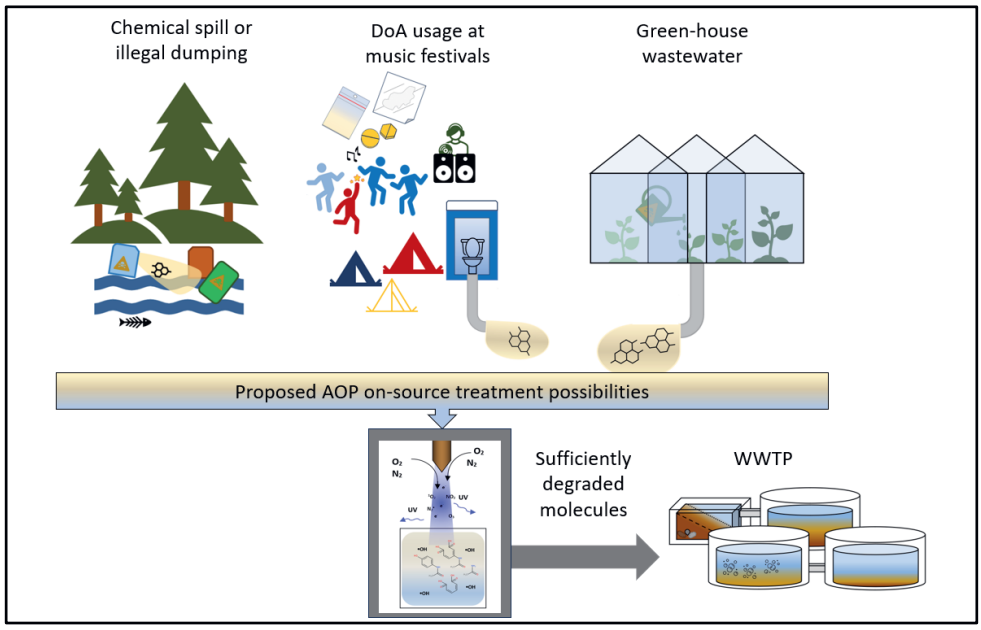

Fig 7.4. Proposed AOP deployment with on-source plasma technology for the treatment of chemical spills, remediate contaminated groundwater, pre-treatment music festivals or greenhouse wastewater.

7.8 Conclusions

AOP treatment is a promising technology for the removal of unwanted pharmaceutical residues found in the (waste)water stream. With a changing environment, population growth, increase of aging adults needing care and the continuous introduction of new chemical substances, it is important that the aquatic environment and drink water sources are kept safe for future generations. With this thesis it was aimed to prepare a guidance to demonstrate the degradation of 14 different pharmaceuticals studied in different complex water matrices. Chemical abatement data was obtained showing the potential of UV-C/H_2O_2 treatment and plasma technology.

The main findings are:

- Distinct chemical kinetics were observed for UV-C/H_2O_2 treatment and plasma oxidation, which were confirmed by the production of identified oxidative degradation intermediates derived from CP spiked in tap water (**Chapter 2**).
- Advanced oxidation is possible in complex matrices and indicates that each AOP has added value towards specific contaminants (**Chapter 3**).

- The continuous introduction of ROS and RNS during plasma treatment make the plasma technology AOP a very suitable application for the treatment of hospital sewage water and similar complex matrices (**Chapter 3** and **4**).
- Cytotoxicity of the degradation products is determined by the initial pharmaceutical concentration, matrix composition, the period of oxidative treatment and the ability of the cellular system to recover (**Chapter 4**).
- Direct oxidative treatment of hospital sewage water leads to an overall reduction in toxicity. Showing that plasma technology is an effective pre-treatment step to reduce mixture toxicity (**Chapter 4** and **5**).
- The combination of laboratory measured degradation data and software-based *in silico* predictions serve as a valuable screening to estimate ecotoxic risk for the aquatic compartment (**Chapter 5**).
- It was found with *in silico* environmental risk assessment that untreated HSW contains environmentally unwanted pharmaceutical levels. *In silico* extrapolation of the advanced oxidation results indicates that treatment techniques such as thermal plasma and UV-C/H_2O_2 application are beneficial for lowering the ecotoxicity of HSW (**Chapter 5**).
- Determination of quantum chemical parameters such as E_{HOMO} (eV), E_{LUMO} and ΔE (eV) showed their usefulness in understanding the oxidative degradation kinetics. With the computed parameters nucleophilicity was localised and the potential stability of a substance was determined (**Chapter 6**).

It is clear that many different factors such as matrix composition, pollutant concentration, molecular structure and AOP produced reactive species will influence the efficiency of pharmaceutical removal. Similar as for other AOPs (**Table 1.2**) UV-C/H_2O_2 and thermal plasma technology each have their own specific advantages and limitations. Nonetheless, it is advised to continue laboratory-scale experiments described in this thesis with a pilot demonstration. By combining the *in silico* quantum chemical estimations hand-in-hand with analytical and toxicological assays we see opportunities for further development of this technology to complement current WWTP practice. Interdisciplinary collaboration between academics, government, industry, healthcare professionals, patients and the water sector will further lead to improvement of the overall water quality. With the right vision and strategy, water pollution can be further reduced!

Literature

Ajo, P., Preis, S., Vornamo, T., Mänttäri, M., Kallioinen, M., & Louhi-Kultanen, M. (2018). Hospital wastewater treatment with pilot-scale pulsed corona discharge for removal of pharmaceutical residues. *Journal of Environmental Chemical Engineering*, *6*(2), 1569–1577. https://doi.org/10.1016/j.jece.2018.02.007

Banaschik, R., Jablonowski, H., Bednarski, P. J., & Kolb, J. F. (2018). Degradation and intermediates of diclofenac as instructive example for decomposition of recalcitrant pharmaceuticals by hydroxyl radicals generated with pulsed corona plasma in water. *Journal of Hazardous Materials*, *342*, 651–660. https://doi.org/10.1016/j.jhazmat.2017.08.058

Castiello, C., Junghanns, P., Mergel, A., Jacob, C., Ducho, C., Valente, S., Rotili, D., Fioravanti, R., Zwergel, C., & Mai, A. (2023). GreenMedChem: the challenge in the next decade toward eco-friendly compounds and processes in drug design. *Green Chemistry*, *25*(6), 2109–2169. https://doi.org/10.1039/D2GC03772F

Duarte, D. J., Niebaum, G., Lämmchen, V., van Heijnsbergen, E., Oldenkamp, R., Hernández-Leal, L., Schmitt, H., Ragas, A. M. J., & Klasmeier, J. (2022). Ecological Risk Assessment of Pharmaceuticals in the Transboundary Vecht River (Germany and The Netherlands). *Environmental Toxicology and Chemistry*, *41*(3), 648–662. https://doi.org/10.1002/etc.5062

Duarte, D. J., Oldenkamp, R., & Ragas, A. M. J. (2022). Human health risk assessment of pharmaceuticals in the European Vecht River. *Integrated Environmental Assessment and Management*, *18*(6), 1639–1654. https://doi.org/10.1002/ieam.4588

Egli, M., Rapp-Wright, H., Oloyede, O., Francis, W., Preston-Allen, R., Friedman, S., Woodward, G., Piel, F. B., & Barron, L. P. (2023). A One-Health environmental risk assessment of contaminants of emerging concern in London's waterways throughout the SARS-CoV-2 pandemic. *Environment International*, *180*, 108210. https://doi.org/10.1016/j.envint.2023.108210

European Chemicals Bureau, I. for H. and C. P. (Joint R. C. (2003). *Technical Guidance Document on risk assessment in support of Commission Directive 93/67/EEC on risk assessment for new notified substances, Commission Regulation (EC) No 1488/94 on risk assessment for existing substances, Directive 98/8/EC of the European Parliament and of the Council concerning the placing of biocidal products on the market. Part II*.

European Commission. (n.d.). *The EU's chemicals strategy for sustainability towards a toxic-free environment*. Retrieved November 1, 2023, from https://environment.ec.europa.eu/strategy/chemicals-strategy_en

Commission Directive 93/67/EEC of 20 July 1993 laying down the principles for assessment of risks to man and the environment of subtances notified in accordance with Council Directive 67/548/EEC, Pub. L. No. Directive 93/67/EEC (1993).

European Medicine Agency. (2023). *Human medicines highlights 2022*.

European Medicines Agency. (2024). *Human medicines highlights 2023*.

Feng, L., Oturan, N., van Hullebusch, E. D., Esposito, G., & Oturan, M. A. (2014). Degradation of anti-inflammatory drug ketoprofen by electro-oxidation: comparison of electro-Fenton and anodic oxidation processes. *Environmental Science and Pollution Research*, *21*(14), 8406–8416. https://doi.org/10.1007/s11356-014-2774-2

Gomez Cortes, L., Marinov, D., Sanseverino, I., Navarro Cuenca, A., Niegowska Conforti, M., Porcel Rodriguez, E., Stefanelli, F., & Lettieri, T. (2022). *Selection of substances for the 4th Watch List under the Water Framework Directive*. *KJ-NA-31-148-EN-N (online),KJ-NA-31-148-EN-C (print)*. https://doi.org/10.2760/01939 (online),10.2760/909608 (print)

Hama Aziz, K. H., Omer, K. M., Mahyar, A., Miessner, H., Mueller, S., & Moeller, D. (2019). Application of Photocatalytic Falling Film Reactor to Elucidate the Degradation Pathways of Pharmaceutical Diclofenac and Ibuprofen in Aqueous Solutions. *Coatings*, *9*(8), 465. https://doi.org/10.3390/coatings9080465

Hoeben, W. F. L. M. (2000). *Pulsed corona-induced degradation of organic materials in water*. Technische Universiteit Eindhoven.

Isarain-Chávez, E., Rodríguez, R. M., Cabot, P. L., Centellas, F., Arias, C., Garrido, J. A., & Brillas, E. (2011). Degradation of pharmaceutical beta-blockers by electrochemical advanced oxidation processes using a flow plant with a solar compound parabolic collector. *Water Research*, *45*(14), 4119–4130. https://doi.org/10.1016/j.watres.2011.05.026

James Ashenhurst. (2022, September 20). *Nucleophilicity of Amines*. MASTER ORGANIC CHEMISTRY.

Kar, S., Sanderson, H., Roy, K., Benfenati, E., & Leszczynski, J. (2020). Ecotoxicological assessment of pharmaceuticals and personal care products using predictive toxicology approaches. *Green Chemistry*, *22*(5), 1458–1516. https://doi.org/10.1039/C9GC03265G

Kostal, J., Voutchkova-Kostal, A., Anastas, P. T., & Zimmerman, J. B. (2015). Identifying and designing chemicals with minimal acute aquatic toxicity. *Proceedings of the National Academy of Sciences*, *112*(20), 6289–6294. https://doi.org/10.1073/pnas.1314991111

Kümmerer, K., Dionysiou, D. D., Olsson, O., & Fatta-Kassinos, D. (2018). A path to clean water. *Science*, *361*(6399), 222–224. https://doi.org/10.1126/science.aau2405

Leder, C., Suk, M., Lorenz, S., Rastogi, T., Peifer, C., Kietzmann, M., Jonas, D., Buck, M., Pahl, A., & Kümmerer, K. (2021). Reducing Environmental Pollution by Antibiotics through Design for Environmental Degradation. *ACS Sustainable Chemistry & Engineering*, *9*(28), 9358–9368. https://doi.org/10.1021/acssuschemeng.1c02243

Leslie, H. A., van Velzen, M. J. M., Brandsma, S. H., Vethaak, A. D., Garcia-Vallejo, J. J., & Lamoree, M. H. (2022). Discovery and quantification of plastic particle pollution in human blood. *Environment International*, *163*, 107199. https://doi.org/10.1016/j.envint.2022.107199

Loftsson T. (2014). *Drug Stability for Pharmaceutical Scientists*.

Magureanu, M., Bradu, C., & Parvulescu, V. I. (2018). Plasma processes for the treatment of water contaminated with harmful organic compounds. *Journal of Physics D: Applied Physics*, *51*(31), 313002. https://doi.org/10.1088/1361-6463/aacd9c

Magureanu, M., Mandache, N. B., & Parvulescu, V. I. (2015). Degradation of pharmaceutical compounds in water by non-thermal plasma treatment. *Water Research*, *81*, 124–136. https://doi.org/10.1016/j.watres.2015.05.037

Önlü, S., & Saçan, M. T. (2017). An in silico approach to cytotoxicity of pharmaceuticals and personal care products on the rainbow trout liver cell line RTL-W1. *Environmental Toxicology and Chemistry*, *36*(5), 1162–1169. https://doi.org/10.1002/etc.3663

Orias, F., & Perrodin, Y. (2013). Characterisation of the ecotoxicity of hospital effluents: A review. *Science of The Total Environment*, *454–455*, 250–276. https://doi.org/10.1016/j.scitotenv.2013.02.064

Pandit, N. K. , S. R. , P. B. S. (2012). *Introduction to the pharmaceutical sciences: an integrated Approach* (2nd edtion). Lippincott Williams & Wilkins, a Wolters Kluwer business.

Park, Y.-K., Kim, B.-J., Kim, S.-C., You, C.-S., Choi, J., Park, J., Lee, H., & Jung, S.-C. (2021). Decomposition of naproxen by plasma in liquid process with TiO2 photocatslysts and hydrogen peroxide. *Environmental Research*, *195*, 110899. https://doi.org/10.1016/j.envres.2021.110899

Peake, B. M., Braund, R., Tong, A. Y. C., & Tremblay, L. A. (2016). *The Life-cylce of pharmaceuticals in the environment*. Woodhead Publishin, Elsevier.

Perinban, S., Orsat, V., Lyew, D., & Raghavan, V. (2022). Effect of plasma activated water on Escherichia coli disinfection and quality of kale and spinach. *Food Chemistry*, *397*, 133793. https://doi.org/10.1016/j.foodchem.2022.133793

Pham, T. H., Myung, Y., Van Le, Q., & Kim, T. (2022). Visible-light photocatalysis of Ag-doped graphitic carbon nitride for photodegradation of micropollutants in wastewater. *Chemosphere*, *301*, 134626. https://doi.org/10.1016/j.chemosphere.2022.134626

Puhlmann, N., Mols, R., Olsson, O., Slootweg, J. C., & Kümmerer, K. (2021). Towards the design of active pharmaceutical ingredients mineralizing readily in the environment. *Green Chemistry*, *23*(14), 5006–5023. https://doi.org/10.1039/D1GC01048D

Qutob, M., Hussein, M. A., Alamry, K. A., & Rafatullah, M. (2022). A review on the degradation of acetaminophen by advanced oxidation process: pathway, by-products, biotoxicity, and density functional theory calculation. *RSC Advances*, *12*(29), 18373–18396. https://doi.org/10.1039/D2RA02469A

93/67/EEC, Pub. L. No. 93/67/EEC, Commission Directive 93/67/EEC (1993).

Tisler, S., Zindler, F., Freeling, F., Nödler, K., Toelgyesi, L., Braunbeck, T., & Zwiener, C. (2019). Transformation Products of Fluoxetine Formed by Photodegradation in Water and Biodegradation in Zebrafish Embryos (*Danio rerio*). *Environmental Science & Technology*, *53*(13), 7400–7409. https://doi.org/10.1021/acs.est.9b00789

Tisler, S., & Zwiener, C. (2019). Aerobic and anaerobic formation and biodegradation of guanyl urea and other transformation products of metformin. *Water Research*, *149*, 130–135. https://doi.org/10.1016/j.watres.2018.11.001

Voutchkova-Kostal, A. M., Kostal, J., Connors, K. A., Brooks, B. W., Anastas, P. T., & Zimmerman, J. B. (2012). Towards rational molecular design for reduced chronic aquatic toxicity. *Green Chemistry*, *14*(4), 1001. https://doi.org/10.1039/c2gc16385c

Yang, B., Wei, T., Xiao, K., Deng, J., Yu, G., Deng, S., Li, J., Zhu, C., Duan, H., & Zhuo, Q. (2018). Effective mineralization of anti-epilepsy drug carbamazepine in aqueous solution by simultaneously electro-generated H2O2/O3 process. *Electrochimica Acta*, *290*, 203–210. https://doi.org/10.1016/j.electacta.2018.09.067

Summary & Samenvatting

Summary

Pharmaceuticals are extensively used and cause a continuous discharge of active substances into the sewer system directed to the wastewater treatment plants. Wastewater effluents are treated with conventional treatment steps to prepare it for return into the aquatic environment. Due to insufficient removal efficiency, persistent and complex bioactive contaminants end up in surface waters. The presence of unwanted medicinal residues in surface water will cause a potential risk for the aquatic ecosystem.

The aim of this thesis is to lower pharmaceutical discharge in sewage water by testing the effectiveness of on-site oxidative treatment. With multiple specific research objectives the chemical abatement for 14 pharmaceuticals in complex water matrices was analysed using bench-scale advanced oxidation processes. 14 selected pharmaceuticals were used to represent a wide range of multiple therapeutic classes and consisted of iopamidol, iomeprol, diatrizoic acid, fluoxetine, diclofenac, metoprolol, carbamazepine, terbutaline, phenazone, acetaminophen, ciprofloxacin, doxycycline and metformin.

Chapter 1 provides theoretical information to support the research presented in this thesis. The introduction section defines the multiple aquatic contamination routes, pharmaceuticals of concern, conventional wastewater treatment steps and the functioning of advanced oxidation processes.

Chapter 2 describes the oxidative degradation of cyclophosphamide in simulated tap water. Evaluation of thermal plasma activation compared to UV/H_2O_2 treatment resulted in optimised parameters for both techniques to degrade pharmaceuticals. Both applied techniques initiated different structural changes indicating that AOP technology is useful for the degradation of unwanted medicine residues.

Chapter 3 continues the research on oxidative degradation kinetics of multiple pharmaceuticals simulated in complex water matrices. The 14 selected pharmaceuticals were spiked in surrogate matrices Milli-Q, tap water, synthetic urine, diluted urine and synthetic sewage water and treated with thermal plasma and UV-C/H_2O_2. Untreated hospital sewage water was also oxidatively activated. In hospital sewage water 10 pharmaceutical compounds were quantified ranging from 0.08 up to 2400 µg/L. Next to the influence of the matrix complexity, thermal plasma and UV-C/H_2O_2 treatment have their own degradation capability for specific pharmaceutical classes.

Chapter 4 provides insight into the acute cytotoxicity prior to and after oxidative treatment of contaminated water matrices. Despite that advanced oxidation processes are very powerful techniques for the rapid decay of pharmaceuticals, too short reaction times or inhibitory influences of matrix constituents might result in the production of toxic by-products. To demonstrate cytotoxicity derived from oxidative treatment, thermal plasma and UV-C/H_2O_2 activation were applied on surrogate matrices containing concentrations of the 10 identified pharmaceuticals in hospital sewage water. Test matrices were 180 minutes oxidatively treated and added to cultured HeLa cells. Regarding oxidative treatment of untreated hospital sewage water, the main findings demonstrate that oxidative pre-treatment of wastewater with high pharmaceutical concentrations is beneficial for a cellular system.

Chapter 5 demonstrates an *in silico* environmental risk assessment to estimate ecotoxicity. Quantitative structure-activity relationship software was used to predict the ecotoxicity. The molecular structures of 10 identified pharmaceuticals and their expected oxidative transformation products were assessed individually and as a mixture using ECOSAR software. In line with the previously tested cytotoxicity results presented in chapter 4, our findings indicated that untreated hospital sewage water contains substances that could negatively affect the aquatic environment. AOPs such as thermal plasma and UV/H_2O_2 treatment lowers the ecotoxicity risk levels of original products.

Chapter 6 explains the usage of quantum chemical parameters to support the understanding about the reactivity of pharmaceuticals. The nucleophilic molecular frontier orbitals were localised using quantum chemical calculations. The localised nucleophilic areas of the tested pharmaceuticals were compared with previously obtained oxidative degradation data. Based on the determined reactive molecular moieties it is found that the usage of quantum chemical software is a useful predictor to support the understanding of chemical abatement kinetics.

Chapter 7 evaluates the overall aim of this thesis. It is clearly demonstrated that advanced oxidation processes are very powerful techniques to pre-treat sewage water for the removal of pharmaceuticals and lowering the (eco)toxicity. The currently presented laboratory data reveal that there is an opportunity for scale-enlargement and technology optimisation. Integration of AOPs with other available techniques prior to conventional treatment is expected to enlighten pharmaceutical discharge. A combination of wastewater treatment techniques, greener pharmaceutical production and the development of better (bio)degradable therapeutics will eventually lead to a reduction in the emission of pharmaceuticals into the aquatic environment.

Samenvatting

Door het grootschalige gebruik van geneesmiddelen is er een constante lozing van actieve stoffen via het riool naar de waterzuiveringsinstallaties. De huidige afvalwaterstromen worden behandeld met conventionele zuiveringstappen om het water voor te bereiden op terugkeer in het aquatische milieu. Door onvoldoende verwijderingsrendement komen persistente en complexe bioactieve stoffen in het oppervlaktewater terecht. De aanwezigheid van ongewenste medicijnresten in oppervlaktewater vormt een potentieel risico voor ons aquatische ecosysteem.

Het doel van dit proefschrift is om een bijdrage te leveren aan het verminderen van geneesmiddelen emissie in het afvalwater. Er wordt verwacht dat met de inzet van oxidatieve behandeling bij de contaminatiebron kan resulteren in een effectieve afbraak van geneesmiddelen. Middels meerdere specifiek gedefinieerde onderzoeksdoelstellingen is de oxidatieve chemie van 14 geneesmiddelen in complexe watermatrices onderzocht. 14 geneesmiddelen zijn geselecteerd om een breed scala van meerdere therapeutische klassen te vertegenwoordigen en bestaan uit iopamidol, iomeprol, amidotroide zuur, fluoxetine, diclofenac, metoprolol, carbamazepine, antipyrine, paracetamol, ciprofloxacine, doxycycline en metformine.

Hoofdstuk 1 is een inleidende sectie die dient ter ondersteuning van het onderzoek gepresenteerd in dit proefschrift. De theoretische achtergrond definieert verschillende routes van waterverontreiniging, potentiële gevaarlijke farmaceutische stoffen, conventionele waterzuiveringsstappen en de werking van geavanceerde oxidatieprocessen.

Hoofdstuk 2 beschrijft een optimalisatiestudie waarbij de chemische degradatiekinetiek voor cyclofosfamide is gesimuleerd in kraanwater. Evaluatie van thermische plasma-activatie in vergelijking met UV/H_2O_2-oxidatie resulteerde in geoptimaliseerde parameters voor beide technieken om geneesmiddelen effectief af te breken. Beide onderzochte technieken tonen verschillende afbraakroutes. Hiermee is aangetoond dat geavanceerde oxidatieprocessen een bruikbare technologie vormen voor de degradatie van ongewenste medicijnresten.

Hoofdstuk 3 is een vervolgstudie naar de chemische degradatiekinetiek van verschillende geneesmiddelen in complexe watermatrices. De 14 geselecteerde geneesmiddelen werden in de matrices Milli-Q water, kraanwater, synthetische urine, verdunde urine en synthetisch afvalwater gebracht. Onbehandeld ziekenhuisafvalwater werd ook oxidatief geactiveerd. In het ziekenhuisafvalwater werden 10 geneesmiddelen gekwantificeerd met een concentratiebereik van 0.08 tot 2400 µg/L. Ondanks de complexiteit van de matrix hebben de behandeling met

thermisch plasma en UV-C/H_2O_2 ieder hun eigen specifieke afbraakvermogen voor verschillende farmaceutische klassen.

Hoofdstuk 4 geeft inzicht in de acute cytotoxiciteit voor en na oxidatieve behandeling van verontreinigde watermatrices. Hoewel oxidatieve behandeling een zeer krachtige techniek is voor de snelle afbraak van geneesmiddelen, kan een te korte behandelingstijd of de remmende werking van bestanddelen uit de watermatrix resulteren in de vorming van giftige bijproducten. Om de cytotoxiciteit voor en na oxidatieve behandeling aan te tonen zijn thermisch plasma en UV-C/H_2O_2 behandeling toegepast op surrogaatmatrices die concentraties van 10 verschillende geneesmiddelen bevatten. De testmatrices werden 180 minuten oxidatief behandeld en vervolgens toegevoegd aan HeLa-cellen. Oxidatieve activatie van afvalwater met hoge geneesmiddelen concentraties tonen daarentegen aan dat voorbehandeling van afvalwater gunstig is voor een cellulair systeem.

Hoofdstuk 5 presenteert een *in silico* milieurisicobeoordeling studie voor het schatten van de ecotoxiciteit. Software voor kwantitatieve structuur-actviteitsrelaties is gebruikt voor biologische-chemische toxiciteit berekening. De molecuulstructuren van de 10 geneesmiddelen en hun verwachte oxidatieve transformatieproducten werden afzonderlijk en als een mengsel beoordeeld door gebruik te maken van ECOSAR software. Vergelijkbare resultaten zoals eerder in hoofdstuk 4 verkregen met de cytotoxiciteitstudie demonstreren dat onbehandeld ziekenhuisafval water medicijnresten bevat die negatieve effecten kunnen hebben op waterorganismen. Door gebruik te maken van geavanceerde oxidatieve processen, zoals thermisch plasma en UV-C/H_2O_2 behandeling, kunnen de ecotoxische risiconiveaus van geneesmiddelen worden verminderd.

Hoofdstuk 6 legt het gebruik van kwantumchemische parameters uit om de reactiviteit van geneesmiddelen te begrijpen. Nucleofiele moleculaire grensorbitalen werden gelokaliseerd met behulp van kwantumchemische berekeningen. De gelokaliseerde nucleofiele gebieden van de geteste geneesmiddelen werden vervolgens vergeleken met de eerder verkregen oxidatieve degradatie kinetiek. Op basis van de gepresenteerde resultaten wordt verwacht dat het aantonen van mogelijke reactieve moleculaire gebieden kan resulteren in het beter begrijpen van chemische afbraak kinetiek.

Hoofdstuk 7 evalueert het doel van dit proefschrift. Geavanceerde oxidatie processen zijn zeer krachtige technieken voor de verwijdering van ongewenste medicijnresten in afvalwater. Uit de gepresenteerde laboratoriumgegevens blijkt dat er kansen zijn voor schaalvergroting en technologische optimalisatie. De integratie van oxidatieve technieken gecombineerd met

andere beschikbare oplossingen voorafgaand aan conventionele rioolwaterzuivering zal naar verwachting de emissie van medicijnresten kunnen verlichten. Een combinatie van afvalwaterzuiveringstechnieken, een groenere farmaceutische productie en ontwikkeling van beter (biologisch) afbreekbare geneesmiddelen zal uiteindelijk leiden tot een vermindering van geneesmiddelen in het aquatisch milieu.

Research data management

Research for this dissertation has been carried out under the research Data Management policy of the former Radboud Institute for Health Sciences (Radboud University Medical Center) and the Radboud Institute for Biological and Environmental Sciences (Radboud University). Data is stored according to the findable, accessible, interoperable and reusable (FAIR) principle. The produced and archived data for this thesis is specified below:

Chapter 1: No new data was generated for this section.

Chapter 2: Graumans, M. H. F., Hoeben, W. F. L. M., Russel, F. G. M., & Scheepers, P. T. J. (2020). Oxidative degradation of cyclophosphamide using thermal plasma activation and UV/H_2O_2 treatment in tap water. Environmental Research, 182. https://doi.org/10.1016/j.envres.2019.109046. All data for this chapter can be found in the published research article or corresponding supplementary information.

Chapter 3: Graumans, M. H. F., Hoeben, W. F. L. M., van Dael, M. F. P., Anzion, R. B. M., Russel, F. G. M., & Scheepers, P. T. J. (2021). Thermal plasma activation and UV/H_2O_2 oxidative degradation of pharmaceutical residues. Environmental Research, 195. https://doi.org/10.1016/j.envres.2021.110884. All data for this chapter can be found in the published research article or corresponding supplementary information.

Chapter 4: Graumans, M. H. F., van Hove, H., Schirris, T., Hoeben, W. F. L. M., van Dael, M. F. P., Anzion, R. B. M., Russel, F. G. M., & Scheepers, P. T. J. (2022). Determination of cytotoxicity following oxidative treatment of pharmaceutical residues in wastewater. Chemosphere, 303. https://doi.org/10.1016/j.chemosphere.2022.135022. All data for this chapter can be found in the published research article or corresponding supplementary information.

Chapter 5: Graumans, M. H. F., Hoeben, W. F. L. M., Ragas, A. M. J., Russel, F. G. M., & Scheepers, P. T. J. (2024). In silico ecotoxicity assessment of pharmaceutical residues in wastewater following oxidative treatment. Environmental Research, 243, 117833. https://doi.org/10.1016/j.envres.2023.117833. All data for this

chapter can be found in the published research article or corresponding supplementary information.

Chapter 6: All quantum chemical determined data for this chapter is provided in the main text.

Chapter 7: No new data was generated for this section.

About the author

Martinus Hendrik Franciscus Graumans, born on 31st of January 1991 in Tilburg, the Netherlands. He has always been interested in solving complex questions using chemistry and biology. After high school (2008) he started with his Bachelor of Applied Sciences in Chemistry at Avans University of Applied Sciences Breda (The Netherlands). During this study Martien became intrigued in the versatility of analytical chemical detection techniques. In 2010 Martien performed a work experience internship at the drug laboratory of the Police Force Amsterdam-Amstelland, where he was responsible for qualitative and quantitative laboratory analysis of potentially submitted illicit drugs. Subsequently he started with his Major in Forensic Chemistry further specialising in analytical chemistry for the detection of small molecules. In 2011 he started an internship at Staffordshire University, Stoke-on-Trent (United Kingdom). During this internship Martien further developed his research laboratory skills by working on a project to develop a fingerprint proficiency testing scheme. After this placement he moved to London where he started his graduation internship at King's College London (United Kingdom). During this project Martien specialised in working with analytical techniques such as solid phase extraction, HPLC-UV and LC-MS/MS analysis for the detection of legal and illegal drugs in the river Thames. Martien graduated in 2012 and started in September of that year with a Master's of Research in Forensic Science at King's College London (United Kingdom). He graduated in 2014 after working on an academic research project for the validation of determining the shooting distance of gunshot residues. After that, Martien moved back to the Netherlands and started his work for a second Master degree in Toxicology and Environmental Health at the University of Utrecht (the Netherlands). During his major research project Martien worked on solid phase microextraction combined with HPLC-UV for the detection of medicines in post-mortem tissue. At the end of 2016 Martien obtained a Master of Science degree after completing a project on the development of a detection technique for therapeutic antibodies using UPLC-MS/MS at Charles River Laboratories, 's-Hertogenbosch (the Netherlands). Early 2017 he started working on his PhD research at Radboud University Medical Center. From 2017 till 2022 Martien was affiliated with the Research Laboratory for Molecular Epidemiology at the Department for Health Evidence. Since 2022 the Research Laboratory for Molecular Epidemiology is part of the Department of Environmental Science of

Radboud University. Martien is currently a post-doctoral researcher involved in multiple research projects in the field of risk assessment and toxicology. Analytical chemistry techniques are used for the analysis of environmental contaminants, using liquid chromatography tandem mass spectrometry (LC-MS/MS) and thermal desorption gas chromatography mass spectrometry (TD-GC-MS). Additionally, Martien is responsible for project coordination, method development, reporting and service projects.

List of publications

Graumans, M. H. F., van der Heijden, T. C. W., Kosinska, A., Blom, M. J., & de Rooij, B. M. (2016). *Filter Paper Adsorption and Ninhydrin Reagent as Presumptive Test for Gravesoil* (pp. 229–240). https://doi.org/10.1007/978-3-319-33115-7_15

Peltenburg, H*., **Graumans, M. H. F***., Droge, S. T. J., Hermens, J. L. M., & Bosman, I. J. (2016). Direct tissue sampling of diazepam and amitriptyline using mixed-mode SPME fibers: A feasibility study. *Forensic Chemistry*, *1*. https://doi.org/10.1016/j.forc.2016.07.006 (*Joint first authorship)

Scheepers, P. T. J., **Graumans, M. H. F**., Beckmann, G., van Dael, M., Anzion, R. B. M., Melissen, M., Pinckaers, N., van Wel, L., de Werdt, L. M. A., Gelsing, V., & van Linge, A. (2018). Changes in work practices for safe use of formaldehyde in a university-based anatomy teaching and research facility. *International Journal of Environmental Research and Public Health*, *15*(9). https://doi.org/10.3390/ijerph15092049

Scheepers, P. T. J., **Graumans, M. H. F**., van Dael, M., de Werdt, L., Pinckaers, N., Beckmann, G., & Anzion, R. (2019). Intrusion of chlorinated hydrocarbons and their degradation products from contaminated soil. Measurement of indoor air quality and biomonitoring by analysis of end-exhaled air. *Science of the Total Environment*, *653*. https://doi.org/10.1016/j.scitotenv.2018.10.365

Graumans, M. H. F., Hoeben, W. F. L. M., Russel, F. G. M., & Scheepers, P. T. J. (2020). Oxidative degradation of cyclophosphamide using thermal plasma activation and UV/H_2O_2 treatment in tap water. *Environmental Research*, *182*. https://doi.org/10.1016/j.envres.2019.109046

Graumans, M. H. F., Hoeben, W. F. L. M., van Dael, M. F. P., Anzion, R. B. M., Russel, F. G. M., & Scheepers, P. T. J. (2021). Thermal plasma activation and UV/H_2O_2 oxidative degradation of pharmaceutical residues. *Environmental Research*, *195*. https://doi.org/10.1016/j.envres.2021.110884

Silva, V., Alaoui, A., Schlünssen, V., Vested, A., **Graumans, M**., van Dael, M., Trevisan, M., Suciu, N., Mol, H., Beekmann, K., Figueiredo, D., Harkes, P., Hofman, J., Kandeler, E., Abrantes, N., Campos, I., Martínez, M. Á., Pereira, J., Goossens, D., … Scheepers, P. T. J. (2021). Collection of human and environmental data on pesticide use in Europe and

Argentina: Field study protocol for the SPRINT project. *PLoS ONE*, *16*(11 November). https://doi.org/10.1371/journal.pone.0259748

van Bergen, T. J. H. M., Rios-Miguel, A. B., Nolte, T. M., Ragas, A. M. J., van Zelm, R., **Graumans, M**., Scheepers, P. T. J., Jetten, M. S. M., Hendriks, A. J., & Welte, C. U. (2021). Do initial concentration and activated sludge seasonality affect pharmaceutical biotransformation rate constants? *Applied Microbiology and Biotechnology*, *105*(16–17). https://doi.org/10.1007/s00253-021-11475-9

Graumans, M. H. F., van Hove, H., Schirris, T., Hoeben, W. F. L. M., van Dael, M. F. P., Anzion, R. B. M., Russel, F. G. M., & Scheepers, P. T. J. (2022). Determination of cytotoxicity following oxidative treatment of pharmaceutical residues in wastewater. *Chemosphere*, *303*. https://doi.org/10.1016/j.chemosphere.2022.135022

Cleys, P., Hardy, E., Ait Bamai, Y., Poma, G., Cseresznye, A., Malarvannan, G., Scheepers, P. T. J., Viegas, S., Porras, S. P., Santonen, T., Godderis, L., Verdonck, J., Poels, K., Martins, C., João Silva, M., Louro, H., Martinsone, I., Akūlova, L., van Nieuwenhuyse, A., **Graumans, M.H.F**., Mahiout, S., Duca, Covaci, A. (2024). HBM4EU e-waste study: Occupational exposure of electronic waste workers to phthalates and DINCH in Europe. *International Journal of Hygiene and Environmental Health*, *255*, 114286. https://doi.org/10.1016/j.ijheh.2023.114286

Graumans, M. H. F., Hoeben, W. F. L. M., Ragas, A. M. J., Russel, F. G. M., & Scheepers, P. T. J. (2024). In silico ecotoxicity assessment of pharmaceutical residues in wastewater following oxidative treatment. *Environmental Research*, *243*, 117833. https://doi.org/10.1016/j.envres.2023.117833

Portfolio

Year	Courses	
2017	Certificate of attendance Acuity UPLC-Xevo TQ-S micro Operator training	*Waters Chromatography*
2017	Pathobiology	*Postgraduate Education in Toxicology*
2018	Introduction course for PhD candidates	*RIHS, RUMC*
2019	Cell Toxicology	*Postgraduate Education in Toxicology*
2019	Molecular Toxicology	*Postgraduate Education in Toxicology*
2020	Scientific integrity	*RIHS, RUMC*
2021	Organ Toxicology	*Postgraduate Education in Toxicology*
2021	Ecotoxicology I and II	*Postgraduate Education in Toxicology*
2021	Adverse outcome pathways (AOPs) – principles and applications in toxicology and health risk assessment (online)	*Karolinska Insitutet, Sweden*
2021	Laboratory Animal Science	*Postgraduate Education in Toxicology*
2024	Pharmaceutical Toxicology	*Postgraduate Education in Toxicology*

Year	Conferences and meetings	
2017	Green Pharmacy conference 2017 *Utrecht, the Netherlands*	*Poster presentation*
2018	Nederlandse Vereniging voor Toxicologie (NVT) Jaarvergadering *Hilversum, the Netherlands*	*Poster presentation*
2018	EUROTOX 2018 – 54th Congress of the European Societies of Toxicology *Brussels, Belgium*	*Poster presentation*
2018	CleanMed Europe 2018 *Nijmegen, the Netherlands*	*Oral presentation*
2019	28ste Nederlandse Vereniging voor Arbeidshygiëne (NVvA) symposium *Zeist, the Netherlands*	*Oral presentation*
2019	Care days 2019 *Eindhoven, the Netherlands*	*Oral presentation*

2019	Nederlandse Vereniging voor Toxicologie (NVT) Jaarvergadering *Ede, the Netherlands*	*Oral presentation*
2022	Symposium Medicijnresten uit Water *Tilburg, the Netherlands*	*Poster presentation and networking with a stand*
2023	Heath Care Without Harm Europe Annual General Meeting 2023 *Brussels, Belgium*	*Oral presentation*
2023	RIBES Day 2023 *Nijmegen, the Netherlands*	*Oral presentation*
2024	Nederlandse Vereniging voor Toxicologie (NVT) Jaarvergadering *Ede, the Netherlands*	*Poster presentation*

Year	**Teaching activities**	
2017	BMS60 master course Human Health Risk Assessment	*Assisted during computer practical and student supervision*
2018	BMS60 master course Human Health Risk Assessment	*Assisted during computer practical and student supervision*
2019	Q7 Biomedical evidence in practice	*Assisted with student supervision*
2019	BMS60 master course Human Health Risk Assessment	*Assisted during computer practical and student supervision*
2020	Q7 Biomedical evidence in practice	*Assisted with student supervision*
2021	Q7 Biomedical evidence in practice	*Assisted with student supervision*
2021	BMS60 master course Human Health Risk Assessment	*Assisted during computer practical and student supervision*
2022	BMS60 master course Human Health Risk Assessment	*Assisted during computer practical and student supervision*
2023	NWI-BB096 bachelor course Environmental Toxicology	*Involved in the design of a laboratory experiment*

Year	**Supervision of internships and other**
2018	Supervised Master student (Veronique Peerbooms)
2021	Second thesis assessor Bachelor student (Laurie Novák)
2022	Supervised Master student (Irati Fernandez de Mendiola Peña)
2022	Supervised Master student (Leonie Czernik)

2023 Supervised Thesis (Jan-Pieter Bakker)

2023 Supervised Bachelor student Avans University of applied sciences (Birte van Alfen)

2024 Supervised Bachelor graduation internship Avans University of applied sciences (Celina Havers)

Recognised Reviewer Certificates

Environmental Research

Awarded for 11 reviews between May 2019 and March 2024

Desalination and Water Treatment

Awarded for 1 review in June 2024

Elsevier certificate

1 open access published article linked to the UN SDGs

Acknowlegdements

This manuscript is written with the help of many other persons. I would like to thank you all!

First of all, my gratitude goes to my great supervisors Wilfred Hoeben, Paul Scheepers and Frans Russel for all their advice, commitments, critical discussions, guidance, knowledge and supervision of course. I would like to thank you all for offering me this PhD position. It was a great pleasure working together!

A special thanks to Paul Leenders, who provided the plasma technology and UV-C source. Great to see how you appreciate our work. Your support, collaboration and knowledge has been very valuable. I also would like to express my appreciation to all other MEDUWA colleagues and especially Alfons Uijtewaal who brought this consortium together.

A special thanks for Maurice van Dael and Rob Anzion! It was great learning from you both, but also our coffee and lunch breaks were spot on. Next to our scientific discussions, I loved the daily chat, thank you for that! Also a special thanks to Hedwig van Hove and Petra van den Broek. I valued our collaboration and lunchbreaks together.

I really would like to thank Ben de Rooij for providing me with the great opportunity to develop myself within the academic world. Leon Barron, a special thanks for you, your way of supervision and teaching taught me well how to perform academic research!

Thank you colleagues from the department for Health Evidence Radboudumc, it was a pleasure working together. A special appreciation for Bart Bloemen, Martilord Ifeanychi, Arné Oerlemans and Nel Roeleveld, who always showed their interest in my progress. All colleagues from the Environmental Science department, thank you all very much for your warm welcome at the department, it has been a great pleasure meeting you all.

Of course, I also would like to acknowledge all my friends and family, without your encouragement the completion of this thesis would not have been possible.

Dear mother Josien Graumans-Jong, father Frans Graumans and brother Hendrik Graumans, without your unconditional support, love and good advice my thesis would never have been written. Thank you for that!

Last but not least, my dear Ilse Krikken, I'm really grateful you came into my life, your love and support means a lot to me. You really motivated me during this PhD trajectory, it was great discussing this thesis topic together. I'm looking forward to the future!

Radboudumc
university medical center
IN DEI NOMINE FELICITER
Radboud University